Acknowledgements

First and foremost, I would like to thank my guide, Professor Catherine Godfraind for giving me an opportunity to work on this project. I am grateful for her contributions of time, advice, ideas and funding throughout this work. I am also thankful to my co-guide, Professor Miikka Vikkula for his guidance and useful discussions during the course of this Ph.D.

I wish to express my gratitude to all members of GEHU for their contribution to my work, as well as personal time in Brussels. Amongst them, special thanks to Professor Nisha Limaye for her advice, support and help in both professional and personal matters. Also, thanks to Drs. Monika and Sandhya for their company and friendship.

My sincere thanks to: Ludwig Institute of Cancer Research, Brussels branch for snap-frozen uveal melanoma samples; Professor Catherine Legrand and Dr Marco Munda for guidance with statistical analyses; Professor Diane Damotte and team for useful discussions and help with immunohistochemistry; all physicians in Belgium who responded to my request for patient follow-up information.

I would like to thank the members of the Jury: Professor Pierre Coulie, Professor Hélène Antoine-Poirel, Professor André Goffinet, Professor Patrick De Potter, Professor Diane Damotte and Professor Bart Neyns for their helpful comments and recommendations.

I gratefully acknowledge the funding sources that made my Ph.D. possible. I was funded by Centre du cancer, Cliniques universitaires Saint-Luc, Brussels during the first year and by Télévie, Belgium for the remaining four years. The project was also supported by Le Fonds Joseph Maisin from Centre du cancer, Cliniques universitaires Saint-Luc, Brussels and F.R.S-FNRS, Belgium.

Finally, and most importantly, I wish to thank my family: my parents, Appa and Amma; sisters, Jyothi and Arathi; brothers-in-law Kusha and Dilip; niece, Anusha and nephew, Aditya for their love and encouragement. I dedicate this thesis to my parents who have supported me in all my endeavors.

Deepti

Jury

Professor Pierre COULIE (President of the jury)
Human Tumor Immunology Unit, de Duve Institute
Université catholique de Louvain, Brussels, Belgium

Professor Catherine GODFRAIND (Promoter)
Laboratory of Human Molecular Genetics, de Duve Institute, Université catholique de Louvain, Brussels, Belgium & Department of Pathology, Hôpital Albert Michallon, CHU, Grenoble

Professor Miikka VIKKULA (Co-Promoter)
Laboratory of Human Molecular Genetics, de Duve Institute
Université catholique de Louvain, Brussels, Belgium

Professor Hélène ANTOINE-POIREL
Center for Medical Genetics
Université catholique de Louvain, Brussels, Belgium

Professor André GOFFINET
Institute of Developmental Neurobiology
Université catholique de Louvain, Brussels, Belgium

Professor Patrick DE POTTER
Department of Ophthalmology
Université catholique de Louvain, Brussels, Belgium

Professor Diane DAMOTTE
INSERM U1138, Team <Cancer, Immune control, and Escape>
Centre de Recherche des Cordeliers, Paris, France

Professor Bart NEYNS
Medical Oncology, Universitair Ziekenhuis Brussel
Laarbeeklaan 101, 1090 Brussel

Table of contents

Abbreviations

2-HG	2-hydroxyglutaric acid
5hmC	5-hydroxymethylcytosine
5mC	5-methylcytosine
ABCC5	ATP-binding cassette, sub-family C (CFTR/MRP), member 5
ACAID	Anterior Chamber Associated Immune Deviation
ANLN	Anillin, actin binding protein
ALCAM	Activated leukocyte cell adhesion molecule
AP-1	/JUN; Jun proto-oncogene
ASAP1 (DDEF1)	ArfGAP with SH3 domain, ankyrin repeat and PH domain 1 (Development and differentiation enhancing factor 1)
ATP	Adenosine triphosphate
ATP6V1A	ATPase, H+ transporting, lysosomal 70kDa, V1 subunit A
ATRA	All-trans retinoic acid
ATRX	Alpha-thalassemia X-linked mental retardation syndrome, X-linked
BAGE	B melanoma antigen
BAP1	BRCA1 associated protein-1 (ubiquitin carboxy-terminal hydrolase)
BCL2	B-cell CLL/lymphoma 2
BRAF	B-Raf proto-oncogene, serine/threonine kinase
BRCA2	Breast cancer 2, early onset
C	Cysteine
CCL2	Chemokine (C-C motif) ligand 2
CCL21	Chemokine (C-C motif) ligand 21
CCL22	Chemokine (C-C motif) ligand 22
CCL28	Chemokine (C-C motif) ligand 28
CCL5	Chemokine (C-C motif) ligand 5
CCL7	Chemokine (C-C motif) ligand 7
CCND1	Cyclin D1
CCR2	Chemokine (C-C motif) receptor 2
CCR4	Chemokine (C-C motif) receptor 4
CCR5	Chemokine (C-C motif) receptor 5 (gene/pseudogene)
CCR7	Chemokine (C-C motif) receptor 7
CD	Cluster of differentiation
CDK4	Cyclin-dependent kinase 4
CDKN1A	Cyclin-dependent kinase inhibitor 1A (p21, Cip1)
CDKN2A	Cyclin-dependent kinase inhibitor 2A
CKAP5	Cytoskeleton associated protein 5
CNA	Copy number alteration
CNS	Central nervous system
CpG	C-phosphate-G
CpG-ODN	CpG oligodeoxynucleotides
CSC	Cancer stem cells
CTLA4	Cytotoxic T-lymphocyte-associated protein 4
CTNNB1	Catenin (cadherin-associated protein), beta 1, 88kDa
CX3CL1	Chemokine (C-X3-C motif) ligand 1
CXCL1	Chemokine (C-X-C motif) ligand 1 (melanoma growth stimulating activity, alpha)

CXCL10	Chemokine (C-X-C motif) ligand 10
CXCL12	Chemokine (C-X-C motif) ligand 12
CXCL12	Chemokine (C-X-C motif) ligand 12
CXCL3	Chemokine (C-X-C motif) ligand 3
CXCL6	Chemokine (C-X-C motif) ligand 6
CXCL8	Chemokine (C-X-C motif) ligand 8
CXCL9	Chemokine (C-X-C motif) ligand 9
CXCR2	Chemokine (C-X-C motif) receptor 2
CXCR3	Chemokine (C-X-C motif) receptor 3
CXCR4	Chemokine (C-X-C motif) receptor 4
D	Dexter
DCT	Dopachrome tautomerase
DLC1	DLC1 Rho GTPase activating protein
DNA	Deoxyribonucleic acid
E	Glutamic acid
ECM	Extracellular matrix
EGF	Epidermal growth factor
EGFR	Epidermal growth factor receptor
EGLN1	Egl-9 family hypoxia-inducible factor 1
EGLN2	Egl-9 family hypoxia-inducible factor 2
EGLN3	Egl-9 family hypoxia-inducible factor 3
EIF1AX	Eukaryotic translation initiation factor 1A, X-linked
EMT	Epithelial-to-mesenchymal transition
EPB41L3	Erythrocyte membrane protein band 4.1-like 3
ERK1	Extracellular signal-regulated kinase 1 (MAPK3-Mitogen-activated protein kinase 3)
ERK2	Extracellular signal-regulated kinase 2 (MAPK1-Mitogen-activated protein kinase 1)
ET2	/EDN2; Endothelin 2
FBLN2	Fibulin 2
FDA	Food and Drug Administration
FGF	Fibroblast growth factors
FH	Fumarate hydratase
FHIT	Fragile histidine triad
FNAB	Fine needle aspiration biopsy
Foxp3	Forkhead box P3
GAGE	G antigen
GBA	Glucosidase, beta, acid
GBM	Glioblastoma multiforme
GBP1	Guanylate binding protein 1, interferon-inducible
GC	Gliomatosis cerebri
GDP	Guanosine diphosphate
GLUL	Glutamate-ammonia ligase
GNA11	Guanine nucleotide binding protein (G protein), alpha 11 (Gq class)
GNAQ	Guanine nucleotide binding protein, q polypeptide
GNLY	Granulysin
gp100 (PMEL)	Premelanosome protein
GTP	Guanosine-5'-triphosphate
GZMB	Granzyme B (granzyme 2, cytotoxic T-lymphocyte-associated serine esterase 1)

H	Histidine
HDAC	Histone deacetylase
HES2	Hes family bHLH transcription factor 2
HES5	Hes family bHLH transcription factor 5
HIF-1	Hypoxia inducible factor 1
HLA-A	Major histocompatibility complex, class I, A
HLA-B	Major histocompatibility complex, class I, B
HLA-C	Major histocompatibility complex, class I, C
HLA-E	Major histocompatibility complex, class I, E
HLA-F	Major histocompatibility complex, class I, F
HLA-G	Major histocompatibility complex, class I, G
IDH	Isocitrate dehydrogenase
IDH1	Isocitrate dehydrogenase 1 (NADP+), soluble
IDH2	Isocitrate dehydrogenase 2 (NADP+), mitochondrial
IDH3A	Isocitrate dehydrogenase 3 (NAD+) alpha
IDH3B	Isocitrate dehydrogenase 3 (NAD+) beta
IDH3G	Isocitrate dehydrogenase 3 (NAD+) gamma
IDO	Indoleamine 2,3-dioxygenase
IFNG	Interferon -gamma
IGF	Insulin-like growth factor
IHC	Imunohistochemistry
IIC	Infiltrating immune cells
IL-1	Interleukin-1
IL-10	Interleukin-10
IL-13	Interleukin-13
IL-6	Interleukin-6
IL-8	Interleukin-8
IRF1	Interferon regulatory factor 1
ITGA6	Integrin, alpha 6
JmjC	Jumonji C
JNK	c-Jun N-terminal kinase
KIT	v-kit Hardy-Zuckerman 4 feline sarcoma viral oncogene homolog
KDR (VEGFR2)	Kinase insert domain receptor (a type III receptor tyrosine kinase)
L	Laevus
L	Leucine
LAMR1	/RPSA; Ribosomal protein SA
LOH	Loss of heterozygosity
LZTS1	Leucine zipper, putative tumor suppressor 1
M3	Monosomy 3
MAGE	Melanoma antigen family
MAPK	Mitogen-activated protein kinase
Mb	Megabase
MBAIT	Melanocytic *BAP1*-mutated atypical intradermal tumors
MCAM	Melanoma cell adhesion molecule
MCL1	Myeloid cell leukemia 1
MDM2	MDM2 proto-oncogene, E3 ubiquitin protein ligase
MDSC	Myeloid-derived suppressor cells
MEK	Mitogen-activated protein kinase kinase
MGMT	O-6-methylguanine-DNA methyltransferase

MHC	Major histocompatibility complex
MIF	Macrophage migration inhibitory factor
miRNA	Micro RNA
MITF	Microphthalmia-associated transcription factor
MMP	Matrix-metalloproteinases
MMR	Mismatch repair
MRI	Magnetic resonance imaging
mRNA	Messenger RNA
MYC	v-myc avian myelocytomatosis viral oncogene homolog
NADPH	Nicotinamide adenine dinucleotide phosphate
NBN	Nibrin
NF1	Neurofibromin 1
NF-κB	Nuclear factor of kappa light polypeptide gene enhancer in B-cells 1
NGS	Next-generation sequencing
NK cell	Natural-killer cell
NRAS	Neuroblastoma RAS viral (v-ras) oncogene homolog
NY-ESO-1 (CTAG1B)	Cancer/testis antigen 1B
PD-1	Programmed cell death 1
PDGF	Platelet-derived growth factor
PD-L1	Programmed death ligand-1
PIK3	Phosphatidylinositol-4,5-bisphosphate 3-kinase
PPP6C	Protein phosphatase 6, catalytic subunit
PRF1	Perforin 1 (pore forming protein)
PTEN	Phosphatase and tensin homolog
Q	Glutamine
R	Arginine
RAB27A	RAB27A, member RAS oncogene family
RAC1	Ras-related C3 botulinum toxin substrate 1 (rho family, small GTP binding protein Rac1)
Ras	Rat sarcoma
RASSF1A	Ras association (RalGDS/AF-6) domain family member 1
RB1	Retinoblastoma 1
RNA	Ribonucleic acid
ROBO1	Roundabout, axon guidance receptor, homolog 1 (Drosophila)
RUNX2	Runt-related transcription factor 2
S	Serine
SDH	Succinate dehydrogenase
SF3B1	Splicing factor 3b, subunit 1, 155kDa
SLC16A6	Solute carrier family 16, member 6
SNX31	Sorting nexin 31
STAT1	Signal transducer and activator of transcription 1, 91kDa
STAT3	Signal transducer and activator of transcription 3 (acute-phase response factor)
STK19	Serine/threonine kinase 19
TAA	Tumor-associated antigens
TACC1	Transforming, acidic coiled-coil containing protein 1
TAM	Tumor-associated macrophages
TAP1	Transporter 1, ATP-binding cassette, sub-family B (MDR/TAP)
TAP2	Transporter 2, ATP-binding cassette, sub-family B (MDR/TAP)
TERT	Telomerase reverse transcriptase

TERT	Telomerase reverse transcriptase
TET	Ten-eleven translocation
TET1	Ten-eleven translocation methylcytosine dioxygenase 1
TET2	Ten-eleven translocation methylcytosine dioxygenase 2
TET3	Ten-eleven translocation methylcytosine dioxygenase 3
TF	Transcription factor
TGF-β	Transforming growth factor- beta
Th1	Type 1 helper T-cell
Th2	Type 2 helper T-cell
TIE2	TEK tyrosine kinase, endothelial
TIL	Tumor-infiltrating lymphocyte
TME	Tumor microenvironment
TMZ	Temozolomide
TNF-α	Tumor necrosis factor-alpha
TOP2A	Topoisomerase (DNA) II alpha 170kDa
TP53	Tumor protein p53
TP73	Tumor protein p73
TRAIL	TNF-related apoptosis-inducing ligand
Treg	Regulatory T-cell
tRNA	Transfer RNA
TRPM1	Transient receptor potential cation channel, subfamily M, member 1
TSG	Tumor suppressor gene
TYR	Tyrosinase
UM	Uveal melanoma
V	Valine
VEGF	Vascular endothelial growth factor
VHL	Von Hippel-Lindau tumor suppressor, E3 ubiquitin protein ligase
WHO	World Health Organization
WNT7A	Wingless-type MMTV integration site family, member 7A
XPC	Xeroderma pigmentosum, complementation group C
α-KG	Alpha-ketoglutarate

Summary

The advances in understanding the genetic basis of cancer have focused largely on cancer cell *per se*. However, in the last few decades, this interest has extended to include the 'tumor microenvironment' (TME). Amongst the spectrum of constituents in the microenvironment, immune component has received much attention. Together, these data have led to identification of novel biomarkers in cancer, from both genetic and immune perspectives. Of course, one should not forget the time honoured clinical and pathological risk factors. An integrated analysis of all these different aspects may lead to improved delineation of prognostic groups and development of cost-effective biomarkers for routine clinical use.
With this objective in mind, the present work on gliomatosis cerebri and uveal melanoma was carried out.

Gliomatosis cerebri (GC) is an extensively infiltrative glial tumor occurring in adults and children. Its histogenesis had long been controversial and only lately it has been regarded as a glioma subtype. Recently, mutations in isocitrate dehydrogenase genes 1 and 2 (*IDH1/2*) have been identified as early events in gliomas of mainly adults.

In this work, 15 GC (12 adult, 3 pediatric) were tested for *IDH1/2* mutations as there was no data available at that point. Only *IDH1* mutations were identified in adult GC (40%), but not in pediatric ones. The median overall survival was longer in *IDH1*-mutant GC than *IDH1*-wild-type one. These results made the final histogenetic link between GC and diffuse gliomas and emphasized the

relevance of *IDH* mutation testing in GC prognostication (*Publication I – Narasimhaiah D, et al. Neuropathology 2012; 32:30-7*).

Uveal melanomas (UM) are the most common primary, intra-ocular malignant tumors in adults. About 50% of these tumors disseminate, mostly to liver and metastatic disease is a major cause of mortality. Monosomy 3 (M3) is a well-recognized marker of poor prognosis in these tumors. In addition, unlike in most other solid tumors, lymphocytic infiltration is a marker of poor clinical outcome in UM. When this work was started, using single biomarkers, UM were stratified in two groups. The fact that there has been no improvement in their survival over the last three decades indicates a need for better definition of risk-groups.

With this aim, we assessed genetic, immune and clinic-pathological features of 89 primary, untreated UM. Using these variables, five multivariate Cox models to predict disease-free survival (DFS) were constructed, compared and validated. Amongst them, three performed better (CNA, immune-CNA and combined) and independently delineated presence of three prognostic groups (all, $p < 0.001$). Of these, copy number alteration (CNA) model based on M3, 8q gain, *LZTS1* deletion and *NBL1* deletion emerged as the strongest one. Another, combining immune and CNA, demonstrated that UM with high degree of immune infiltrate (immune-high) stratified more frequently to high risk-group (73.7%), than to intermediate (21%) and low (5.3%). This suggested a possible reason for the paradoxical association between immune infiltration and poor clinical outcome in UM. Furthermore, the prognostic impact of immune-high varied between risk-groups, with no survival effect in high risk-group, but with a poorer outcome in intermediate risk-group. This indicated

that impact of immune on outcome is dependent on associated chromosomal alteration. These findings are relevant for designing clinical trials and application of risk-tailored adjuvant therapies to improve survival. Furthermore, they emphasize the need for innovative strategies to target immune-high UM (*Publication II - manuscript in preparation*).

In the other part of UM work, transcriptomic profile analysis, led to identification of two molecular subgroups based on a gene signature. The latter comprised of immune genes of IFNG/STAT1-IRF1 axis and its presence was correlated with intra-tumoral infiltrate of lymphocytes and macrophages. From prognostic point of view, this signature was associated with poor clinical outcome; which was also validated on two independent datasets. These findings provide an insight into the immune profile of UM; a better understanding of the underlying immunological processes through the elucidated network of genes and pathways and could have implications for designing target-based therapies (*Publication III - manuscript in preparation*).

Résumé

Les progrès dans la compréhension des bases génétiques du cancer ont porté en grande partie sur des cellules cancéreuses elles-mêmes. Toutefois, au cours des dernières décennies, cet intérêt s'est étendu au microenvironnement de la tumeur (TME). Parmi les constituants du microenvironnement, la composante immunitaire a reçu beaucoup d'attention. Ces données ont permis d'identifier de nouveaux biomarqueurs dans le cancer, en combinant des approches génétiques et immunitaires. Bien sûr, il ne faut pas négliger l'importance des facteurs de risque cliniques et pathologiques. Une analyse intégrée de ces différents aspects peut conduire à une meilleure délimitation des groupes pronostiques et le développement de biomarqueurs rentables pour l'utilisation clinique de routine. Avec cet objectif à l'esprit, le présent travail a été réalisé sur la gliomatose cérébrale et le mélanome de l'uvée.

La gliomatose cérébrale (GC) est une tumeur gliale largement infiltrante chez les adultes et les enfants. Son histogenèse a longtemps été controversée et ce n'est que dernièrement qu'elle a été considérée comme un sous-type de gliome. Récemment, des mutations dans les gènes de l'isocitrate déshydrogénase 1 et 2 (*IDH1/2*) ont été identifiés comme des événements précoces dans les gliomes, surtout des adultes. Dans ce travail, 15 GC (12 adultes, 3 enfants) ont été testés pour des mutations dans *IDH1/2* car on ne possédait aucune donnée à ce sujet. Des mutations ont seulement été identifiées dans *IDH1* chez les GC de l'adulte (40%), mais pas dans celles pédiatriques. La survie globale médiane était plus élevée pour les GC mutées dans *IDH1* que dans celles non mutées. Ces résultats confirment donc le lien histogénétique entre la GC et les gliomes diffus et soulignent la pertinence de rechercher des mutations dans *IDH pour le*

pronostique des GC (*Publication I - Narasimhaiah D, et al. Neuropathology 2012;32 :30-7).*

Les mélanomes de l'uvée (UM) sont les tumeurs malignes primaires intra-oculaires les plus courantes chez les adultes. Environ 50% de ces tumeurs métastasent, principalement dans le foie, et sont une cause majeure de mortalité. La monosomie 3 (M3) est un marqueur bien connu de pronostic défavorable dans ces tumeurs. En outre, contrairement à la plupart des autres tumeurs solides, l'infiltration lymphocytaire est aussi un marqueur de mauvais pronostic des UM. Lorsque ce travail a commencé, les UM ont été stratifiés en deux groupes en utilisant des biomarqueurs simples. Le fait qu'il n'y a eu aucune amélioration dans leur survie au cours des trois dernières décennies renforce la nécessité d'une meilleure définition des groupes à risque.

Dans ce but, nous avons évalué les caractéristiques génétiques, immunitaires et clinico-pathologiques de 89 UM primaires, non traitées. En utilisant ces variables, cinq modèles de Cox multivariés ont été construits pour prédire la survie sans maladie (DFS), comparés et validés. Parmi ceux-ci, trois ont mieux réussi (l'altération du nombre de copies (CNA), la combinaison infiltration immunitaire/CNA et un modèle combinées 3 caractéristiques) et ont défini la présence de trois groupes pronostiques indépendants ($p < 0,001$ pour tous). Le modèle CNA, basé sur les monosomies 3 ainsi que le gain de 8q et les délétions de *LZTS1* et de *NBL1,* est apparu comme le plus fort. Celui combinant aspect immunitaire et CNA a démontré que le mélanome de l'uvée avec un haut degré d'infiltration immunitaire (immune-haut) se trouve le plus souvent dans le groupe à haut risque (73.7%) que ceux de risque intermédiaire (21%) ou faible (5.3%). Cela suggère une raison possible pour l'association paradoxale entre

infiltration immunitaire et une réponse clinique insuffisante des UM. En outre, l'impact pronostique d'immune-haut varie entre les groupes de risque, sans modifier la survie du groupe à haut risque, mais avec un moins bon pronostic dans des groupes à risque intermédiaire. Cela indique que l'impact de la réponse immunitaire sur le pronostic dépend de l'altération chromosomique associée. Ces résultats sont importants pour la conception d'essais cliniques et l'application de thérapies complémentaires basées sur le niveau de risque et destinées à améliorer la survie. En outre, ils soulignent la nécessité de stratégies innovantes pour cibler les mélanomes de l'uvée avec infiltration immunitaire (*Publication II - manuscrit en préparation*).

Dans l'autre partie du travail sur les UM, l'analyse du profil transcriptomique a conduit à l'identification de deux sous-groupes moléculaires sur la base d'une signature génique. Celle-ci est composée de gènes immunitaires de l'axe IFNG / STAT1-IRF1 et sa présence a été corrélée avec l'infiltration intra-tumorale de lymphocytes et de macrophages. Du point de vue pronostique, cette signature a été associée avec une évolution clinique défavorable; ce qui a également été validé sur deux séries de données indépendantes. Ces résultats donnent un aperçu du profil immunitaire des UM; une meilleure compréhension des processus immunologiques sous-jacents au réseau de gènes et de voies de signalisation découverts, ce qui pourrait avoir des implications pour la conception de thérapies ciblées (*Publication III - manuscrit en préparation*).

Objective of the thesis

This work was carried out with the aim of improving tumor prognostication through identification of risk-groups by co-analyses of genetic features and immune infiltrate, along with clinical and pathological aspects. This approach was applied to two tumor types: gliomatosis cerebri and uveal melanoma.

Sections

The thesis comprises of two parts:

Part A. Gliomatosis cerebri (GC)

This section is divided into:

- Introduction describes the clinico-pathological and genetic features of GC and about isocitrate dehydrogenase (IDH) mutations in gliomas, including their prevalence, role in gliomagenesis and clinical relevance
- Results includes a brief synopsis about publication I describing the objective of the work and its contribution towards the current understanding of GC
- Discussion deals with future work that can be undertaken to improve the understanding of pathobiology of GC

Part B. Uveal melanoma (UM)

This section is also divided into three parts:

- Introduction focuses on the genetics of uveal and other melanomas and on role of immune microenvironment in cancer *per se* and specifically in UM
- Results includes a brief synopsis about publications II and III describing the objective of the work and its contribution towards improvement of prognostication in UM
- Discussion highlights the important findings and future perspectives

A.GLIOMATOSIS CEREBRI

INTRODUCTION

I. Gliomatosis cerebri

I.1. Background

Primary brain tumors comprise a diverse variety of neoplasms which can be distinguished at both histological and molecular levels {Swartling et al, 2013}. The annual average incidence of primary brain tumors is 21 per 100,000 and they are the most common solid tumors in the pediatric age group {Ostrom et al, 2013}. The current 2007 World Health Organization (WHO) classification of tumors of the central nervous system distinguishes tumors based on histological criteria with the nomenclature based on the presumed cell of origin {Louis 2007}. Gliomas originate from glial cells (astrocytes, oligodendrocytes and ependymal cells) and account for 28% of all primary brain tumors, as well as 80% of malignant ones {Ostrom et al, 2013}.

I.2. Definition

The term gliomatosis cerebri (GC) was first coined by Nevin S in 1938 {Nevin 1938}. It is defined as "a diffuse glioma, growth pattern consisting of exceptionally extensive infiltration of the central nervous system (CNS) with involvement of at least three cerebral lobes, usually with bilateral involvement of the cerebral hemispheres and/or deep gray matter"{Louis 2007}.

I.3. Clinical features and imaging

GC affects mainly adults, but can also occur in children. The age at presentation is widely variable, ranging from 1 month to 85 years (median ~ 42 years), with male to female ratio of 1.3 {Taillibert et al, 2006}. They usually present with seizures, focal neurological deficits, cognitive dysfunction and signs of raised intracranial pressure {Taillibert et al, 2006}.

There are two radiologic subtypes of GC: type 1 and type 2. Type 1 is the classical form, in which no tumor mass is present at initial clinical presentation and type 2 demonstrates a tumor mass in addition to extensive CNS involvement {Louis 2007}. Magnetic resonance imaging (MRI) is the imaging modality of choice for diagnosis and follow-up of GC {Desclee et al, 2010}. On T1-weighted images, they are poorly defined, iso- to hypointense lesions {Freund et al, 2001}. Contrast enhancement is absent in type 1 and present in type 2.

I.4. Histopathology

GC mostly displays an astrocytic morphology, though oligodendroglial and mixed oligoastrocytic phenotypes can also be present {Louis 2007}. In a large meta-analysis, 60% were astrocytic, 30% were oligodendroglial and 10% were mixed {Taillibert et al, 2006}. Mitotic activity is variable, but is typically low. Microvascular proliferation and necrosis are usually absent. There can be histological heterogeneity within the same neoplasm {Louis 2007}.

These tumors are graded using the same criteria as for diffuse gliomas (grade II – with anaplasia, III – increased mitotic activity and IV – microvascular proliferation and necrosis). Even though WHO grades II-IV may be applicable to GC, the overall biologic behavior corresponds to grade III tumors {Louis 2007; Romeike et al, 2008}. However, since diagnosis is confirmed through limited tissue biopsy of this extensive tumor, the grading has to be performed in correlation with clinical and imaging information {Romeike et al, 2008}.

I.5. Treatment, survival and prognosis

Treatment modalities for GC are controversial, with some of them not receiving any treatment at all {Taillibert et al, 2006}. Surgical resection is

usually limited to relieve local mass effect {Romeike et al, 2008}. Radiotherapy is considered beneficial in some {Chen et al, 2013}, but not in others {Romeike et al, 2008}. It is likewise for chemotherapy {Romeike et al, 2008}.

The median overall survival was 14.5 months in a large meta-analysis of nearly 300 tumors, with the survival ranging from 1 month to 200 months {Taillibert et al, 2006}. The grade-specific survival was 20 months, 11.5 months and 8.5 months for grade II, III and IV tumors, respectively. Likewise, the median survival was 36 months in oligodendroglial GC and 11 months for astrocytic GC {Taillibert et al, 2006}.

The poor prognostic indicators in GC are: higher patient age, lower Karnofsky performance status, higher WHO grade and astrocyte phenotype {Louis 2007}.

I.6. Genetic features

Identification of molecular pathology of GC has lagged behind those of diffuse gliomas in view of limited amount of lesional tissue available, as large surgical resections are usually not performed and fresh-frozen tissue samples are not readily available {Louis 2007; Romeike et al, 2008}.

I.6.1. Mutations

TP53 and *PTEN*

About 30-50% of astrocytomas show mutations in *TP53*, the well-known tumor suppressor gene. *TP53* mutations have been reported in 21/85 (25%) GC in literature {Herrlinger et al, 2002; Kros et al, 2002; Mawrin et al, 2003; D'Urso et al, 2009}. Likewise, *PTEN* mutations are present in 12/82 (15%) of GC {Herrlinger et al, 2002; Mawrin et al, 2003; D'Urso et al, 2009}. They are

considered mutually exclusive as their co-occurrence is reported in 3/42 (7%) GC {D'Urso et al, 2009}.

IDH1* and *IDH2

Mutations in isocitrate dehydrogenases 1 and 2 (*IDH1/2*) have been recently identified in gliomas of adults {Parsons et al, 2008} and are considered early events in gliomagenesis {Ohgaki et al, 2009}.

At the beginning of the present work, there were no reports of *IDH1/2* status in gliomatosis cerebri. When the work was ongoing, Seiz, et al demonstrated the presence of *IDH1* mutations in GC {Seiz et al, 2010}. The present work was the second study on the topic. Since then, there have been additional reports on the same {Desestret et al, 2011; Buccoliero et al, 2012; Kwon et al, 2012; Chen et al, 2013}.

IDH1/2 mutations have also been analyzed in adult and pediatric GC. Only *IDH1* mutations are observed in 61/175 (35%) of patients. In all of them, with the exception of one tumor arginine is replaced by histidine in codon 132 (R132H), {Seiz et al, 2010; Desestret et al, 2011; Buccoliero et al, 2012; Kwon et al, 2012; Chen et al, 2013}. Both type 1 and type 2 GC show mutations {Kwon et al, 2012}. Rarely, mutations have been reported in patients < 18 years old (although the exact age is not available) {Kwon et al, 2012}.

Patients with *IDH1*-mutant GC have longer overall survival than *IDH*-wild-type GC (***Figure 1***). Also, when considering the subtype, *IDH* mutation confers a survival advantage only in type 2 GC, but not in type 1 GC {Kwon et al, 2012}.

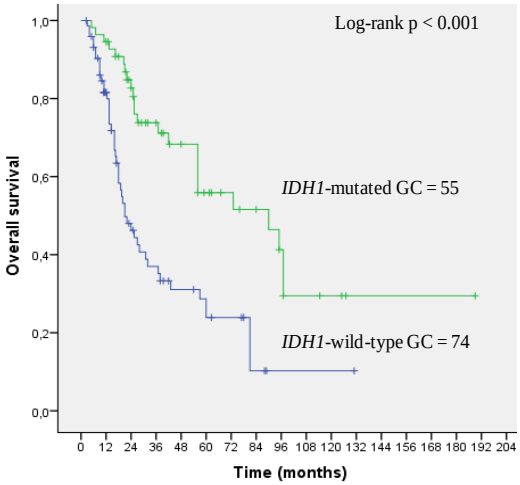

Figure1. Kaplan-Meier plots comparing overall survival in *IDH1*-mutant and *IDH1*-wild-type GC
(Survival data collated from: present study and {Desestret et al, 2011; Kwon et al, 2012})

TERT

Telomerase reverse transcriptase (TERT) plays an important role in telomere extension. Mutations in *TERT* promoter have been identified in 508/1342 (38%) of gliomas {Koelsche et al, 2013; Killela et al, 2014}.

In GC, *TERT* promoter mutations have been reported in 7/10 tumors (6 adult, 1 pediatric) {Koelsche et al, 2013}.

Others

No significant alterations in other astrocytoma genes such as, *EGFR*, *CDKN2A* and *MDM2* have been reported in GC {Mawrin et al, 2003; Romeike et al, 2008}.

I.6.2. Copy number alterations

There are few studies that have analyzed chromosomal aberrations in astrocytic GC at genome-wide level {Ware et al, 2007; Min et al, 2008}. Losses were more frequent and observed on 1p, 1q, 5q, 6q and 14q; whereas gains were infrequent and involved 3p, 17q and 22q {Min et al, 2008}. 1p/19q co-deletion is another alteration observed in GC with oligodendroglial morphology as demonstrated in the present work, as well as by others {Seiz et al, 2010}. This provides an additional genetic link between GC and gliomas, besides *IDH1* and *TP53* mutations. Moreover, 1p/19q co-deletion is a prognostic, as well as predictive marker in oligodendroglial GC {Taillibert et al, 2006}.

I.6.3. Gene expression profiling

There is only one study which has analyzed the expression profiles of GC {D'Urso et al, 2009}. Based on a signature of 23 genes, there were two sub-groups of GC corresponding to poor (n = 15) and good (n = 8) prognosis, respectively {D'Urso et al, 2009}. The pathways associated with this signature were: pathways in cancer; melanoma; prostate cancer; focal adhesion and regulation of actin cytoskeleton. The associated gene ontology terms were: regulation of cell cycle; positive regulation of cell proliferation; chromatin remodeling and response to ultraviolet light.

I.6.4. Methylation

The *MGMT* gene encodes a DNA-repair protein that removes alkyl groups from O^6 position of guanine, rendering the tumor cell resistant to chemotherapeutic agent temozolomide (TMZ). In gliomas, methylation of *MGMT* promoter decreases its expression and increases TMZ sensitivity {Hegi

et al, 2005}. In addition, *IDH* mutations in gliomas are associated with *MGMT* promoter methylation {Sanson et al, 2009}.

In GC, there is not much data available regarding *MGMT* promoter methylation. It has been reported in 20/87 (23%) tumors. Its association with *IDH* mutation is variable, requiring additional studies {Glas et al, 2011; Kwon et al, 2012}.

I.7. Clonality

The hypotheses of GC origin were: whether it is a single tumor clone with extensive infiltration or if it was the result of simultaneous neoplastic transformation of multiple foci (field cancerization) {Louis 2007}. Data from limited number of studies support a monoclonal origin {Hecht et al, 1995; Kros et al, 2002}. Kros, et al, demonstrated the presence of identical *TP53* mutations and copy number changes in tumor tissue sampled from different sites infiltrated by GC {Kros et al, 2002}.

I.8. Histogenesis

Over the years, the origin of GC has been unclear, as indicated by its inclusion under different categories in previous WHO classifications. It has been categorized under "undifferentiated and embryonic tumors" and "neuroepithelial tumors of uncertain origin"{Romeike et al, 2008}. It was only in 2007 WHO classification that GC was defined as a 'diffuse glioma' and classified under 'astrocytic neoplasm' {Louis 2007}. However, the latter still does not solve the issue of GC with oligodendroglial phenotype.

GC shares with diffuse gliomas, genetic alterations such as, *TP53* and *IDH1* mutations, even though they occur at much lower frequency in the former. The demonstration of *IDH1* mutations in GC, even in type 1, non-mass forming

phenotype strengthens this histogenetic link. As *IDH* mutations are considered to be early events in gliomagenesis, their occurrence in GC justifies their inclusion under gliomas in the WHO classification.

II. *IDH1/2* mutations in gliomas

II.1. Background

Mutations in isocitrate dehydrogenases 1 and 2 (*IDH1/2*) were first reported in gliomas in 2008 by Parsons, et al {Parsons et al, 2008}. Since then, a large volume of data has accumulated about these mutations, not only in gliomas, but also in other cancer types. This 'new kid on the block' in molecular pathology of brain tumors has become an integral part of molecular analysis of gliomas, along with well-established markers such as, *TP53* mutations, 1p/19q co-deletion and *MGMT* methylation {von Deimling et al, 2011}.

II.2. Physiological role of wild-type isocitrate dehydrogenases

IDH is an enzyme that catalyzes oxidative decarboxylation of isocitrate to alpha-ketoglutarate (α-KG). There are three isoforms of this enzyme: IDH1, IDH2 and IDH3. IDH1 and IDH2 are encoded by isocitrate dehydrogenase 1 (NADP+), soluble (2q33) and isocitrate dehydrogenase 2 (NADP+), mitochondrial (15q26), respectively; whereas, IDH3 is encoded by isocitrate dehydrogenase 3 (NAD^+) alpha (*IDH3A*; 15q25), beta (*IDH3B*; 20p13) and gamma (*IDH3G*; Xq28). IDH1/2 reduce NADP+ to NADPH and are involved in cellular protection from oxidative stress {Weller et al, 2011}. IDH1 is in cytoplasm and peroxisomes; IDH2 and 3 are in mitochondria. Only *IDH1* and *IDH2* are mutational targets in human cancers (**Figure 2**).

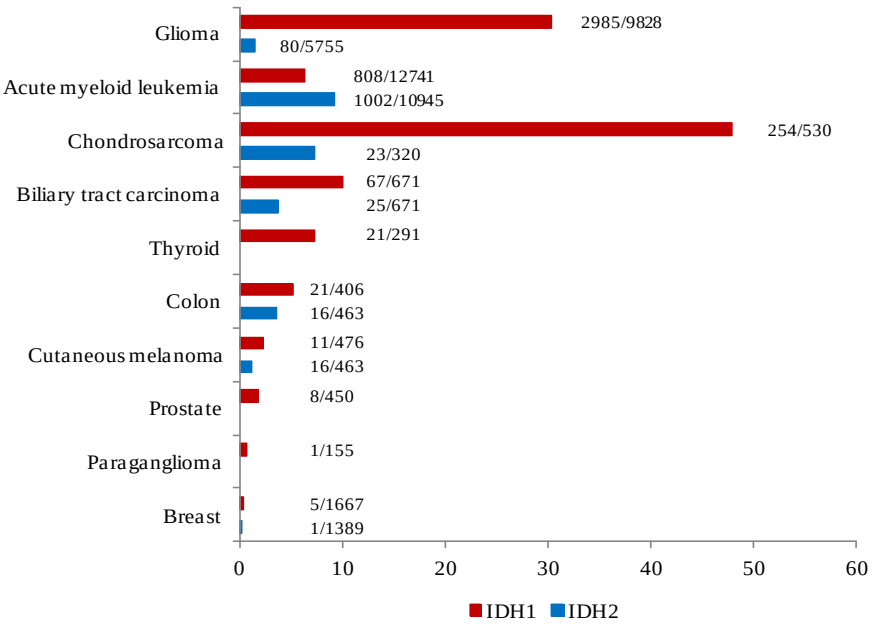

Figure 2. Distribution of *IDH1/2* mutations in different types of cancers (numbers adjacent to the bars indicate tumors mutated vs. tested)
Source: http://cancer.sanger.ac.uk/cancergenome/projects/cosmic

II.3. Features, frequency and distribution

IDH1/2 mutations in gliomas are somatic missense mutations and are heterozygous, with the tumor retaining the wild-type allele {Horbinski 2013}. They predominantly involve the catalytic sites on codons 132 (*IDH1*) and 172 (*IDH2*). Rarely, other codons such as, 49, 97 and 100 on *IDH1* and 140 on *IDH2* are affected {Pusch et al, 2011; Ward et al, 2012}. Concurrent *IDH1/2* mutations are extremely rare; as are double mutations {Horbinski 2013}.

They usually occur in adults (20-60 year age group); occurrence in the pediatric population involves adolescents.

About 60-80% of grade II and III astrocytomas, oligodendrogliomas and oligoastrocytomas are mutated. Amongst glioblastomas (GBM; WHO grade IV), mutations are mostly observed in secondary GBMs (arising from lower grade gliomas) and are infrequent in primary GBMs {Horbinski 2013}. The frequency of *IDH1/2* mutations in gliomas in COSMIC v69 database {http://cancer.sanger.ac.uk/cancergenome/projects/cosmic} is indicated in **figure 3**.

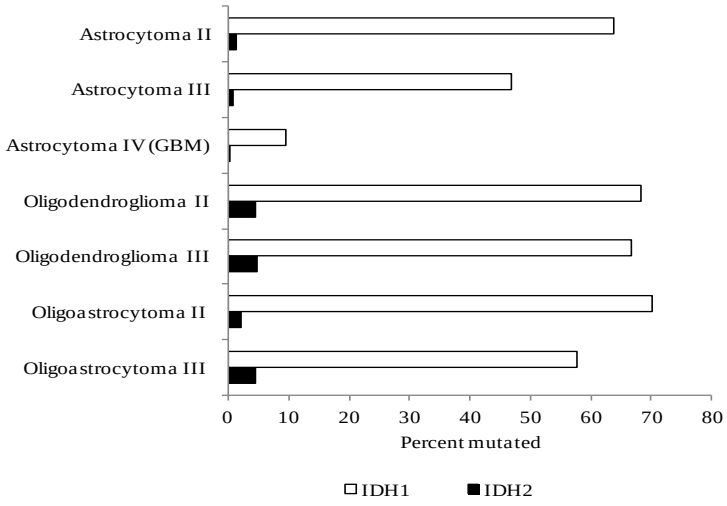

Figure 3. Distribution of *IDH1/2* mutations in glioma subtypes
Source: http://cancer.sanger.ac.uk/cancergenome/projects/cosmic

Over 90% of the mutations involve *1DH1* and about 90% of these mutations are CGT > CAT transitions in codon 132, replacing arginine with histidine (R132H). Rarely, other substitutions such as, cysteine (R132C) and serine (R132S) occur. *IDH2* mutations that occur in codon 172 do not show the same predilection for histidine {Horbinski 2013} (**Figure 4**). In other malignancies

such as cholangiocarcinoma and chondrosarcoma, *IDH1* R132C variant is more frequent {Amary et al, 2011; Molenaar et al, 2014}.

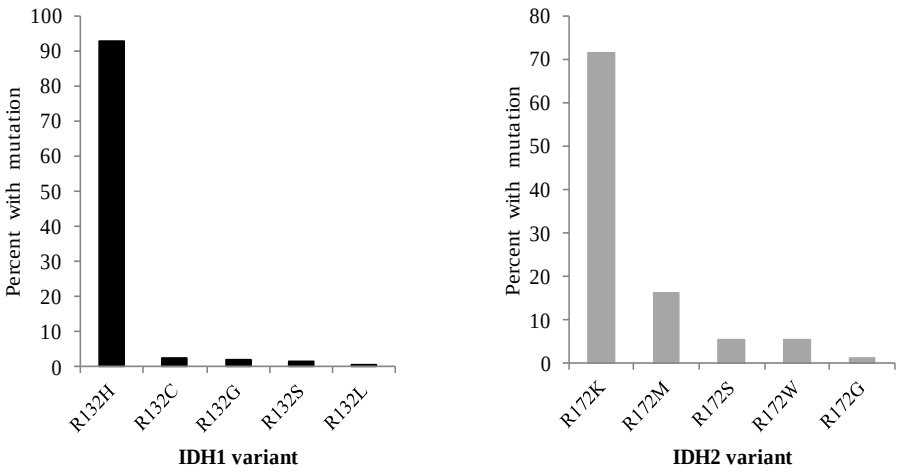

Figure 4. Distribution of *IDH1/2* variants in gliomas
Source*: http://cancer.sanger.ac.uk/cancergenome/projects/cosmic*

II.4. Role of mutant enzyme

The loss-of-function effect of mutation leads to reduction of *IDH1/2* facilitated production of NADPH by about 50%. In addition, the mutant allele causes loss-of-function through a dominant negative inhibition of the wild-type allele {Molenaar et al, 2014}.

These mutations also have a gain-of-function effect which confers 'neoenzymatic activity' on IDH1/2. This is a novel aspect in mutation of metabolic enzymes, as others (SDH and FH) function as tumor suppressors {Mullen et al, 2012}.

The functional gain leads to the mutant enzyme reducing α-KG to D isomer of 2-hydroxyglutaric acid (D-2-HG) {Dang et al, 2009}. Mutant gliomas have 10-

100 fold higher levels of D-2-HG. The amount of 2-HG produced varies with the type of amino acid substitution. Amongst the *IDH1* mutants, the R132H is the weakest 2-HG producer. It has been hypothesized that the amount of 2-HG required for oncogenesis varies with tumor type. Hence, each tumor type shows proclivity for the *IDH1/2* mutants that can provide the optimal amount of 2-HG {Horbinski 2013; Molenaar et al, 2014}.

II.5. Effect of *IDH1/2* mutations

The impact of *IDH1/2* mutations has been attributed to their neoenzymatic function leading to production of D-2-HG. Mammalian cells have several dioxygenases involved in a variety of biologic processes whose activity is dependent on physiological concentrations of α-KG {Xu et al, 2011}. D-2-HG acts as a competitive inhibitor of these dioxygenases by binding to the active site of α-KG.

The dioxygenases which have received most attention as potential targets of 2-HG are: prolyl hydroxylases involved in hypoxia-inducible factor signaling; JumonjiC domain-containing histone demethylases and TET family of DNA demethylases; lysine and proline hydroxylases involved in collagen synthesis {Xu et al, 2011; Koivunen et al, 2012; Cairns et al, 2013; Molenaar et al, 2014}.

II.5.1. Hypoxia-inducible factor (HIF) signaling

HIF-1 is a transcription factor complex that functions as a master regulator of cellular and systemic homeostatic response to hypoxia by activating transcription of many genes involved in energy metabolism, angiogenesis and apoptosis among others. In cancer, HIF-1α is typically considered as an oncoprotein, though it can also act as a tumor suppressor {Koivunen et al,

2012}. According to Koivunen, et al, 2-HG diminishes HIF-1 levels by stimulating the activity of HIF prolyl hydroxylases, egl-9 family hypoxia-inducible factors (*EGLN1-3*) {Koivunen et al, 2012}. Also, *EGLN1* over-expression or HIF-1 depletion leads to astrocyte proliferation. On the other hand, Xu et al, report that 2-HG increases HIF-1 levels {Xu et al, 2011}. The explanation for these ambiguous findings is yet to be elucidated. However, it has been hypothesized that in *IDH*-mutant tumors, *HIF-1* levels are initially decreased, but tumor growth with resulting hypoxia, increases *HIF-1* levels {Molenaar et al, 2014}.

II.5.2. Epigenetic effects

Epigenetic modification of gene expression is known to play a role in cancer. *IDH* mutations are associated with hypermethylated phenotype. Here again, they involve the α-KG-dependent dioxygenases which regulate DNA and histone protein methylation {Cairns et al, 2013}.

TET

The ten-eleven translocation (TET1-3) family of dioxygenases are involved in demethylation of cytosine residues in α-KG-dependent manner. They convert 5-methylcytosine (5mC) to 5-hydroxymethylcytosine (5hmC) {Xu et al, 2011}. *In vitro* studies have demonstrated that mutant *IDH1/2* inhibit *TET*-mediated hydroxylation through 2-HG and 5hmC levels are relatively lower in *IDH*-mutant gliomas, as compared to *IDH*-wild-type ones {Xu et al, 2011}.

Histone demethylases

Methylation of histone proteins contributes to chromatin structure alteration and transcriptional regulation. It is regulated mainly by the Jumonji C (JmjC)-domain containing family of demethylases {Cairns et al, 2013}. *In vitro* and *in*

vivo studies have demonstrated that increased 2-HG inhibits histone demethylases {Chowdhury et al, 2011; Xu et al, 2011; Lu et al, 2012}. In addition, inhibition of histone demethylation also prevents differentiation of lineage-specific progenitor cells into differentiated cells {Lu et al, 2012}. This is also supported by the fact that *IDH*-mutant gliomas demonstrate a proneural phenotype and increased histone methylation {Verhaak et al, 2010; Lu et al, 2012}.

II.6. Oncogenesis

Based on the accumulated evidence, *IDH1/2* mutations are considered important events in glioma development. However, the issue of them being 'driver mutations' in gliomas is debatable; with the growing consensus being that these mutations are insufficient to drive oncogenesis. To better understand the effects of mutant *IDH1* in CNS, transgenic mouse models have been generated. They demonstrated intracranial hemorrhage and perinatal lethality; but did not develop brain tumors {Sasaki et al, 2012}. In addition, D-2-hydroxyglutaric aciduria, a neurometabolic disorder associated with elevated D-2-HG levels is not associated with increased incidence of cancer {Kranendijk et al, 2010}. On the other hand, it is L-2-hydroxyglutaric aciduria producing the L-isomer of 2-HG which is associated with brain tumors {Aghili et al, 2009}. As described previously, mutant *IDH1/2* produce only the D-isomer of 2-HG. As of now, our understanding of the significance of these mutations in gliomagenesis is still incomplete.

II.7. Correlation between *IDH* mutations and other genetic alterations in gliomas

The well-established markers of gliomas are *TP53* mutations, 1p/19q co-deletion and *MGMT* promoter methylation. In low grade astrocytomas, *IDH* mutations are associated with *TP53* mutations and in oligodendrogliomas, they are associated with 1p/19q co-deletion. Likewise, methylation of *MGMT* promoter is associated with *IDH* mutation {Ohgaki et al, 2009} {Sanson et al, 2009}.

Amongst the newly identified mutations, histone H3.3 mutations and *IDH1/2* mutations are mutually exclusive {Sturm et al, 2012}. Likewise, there is an inverse association between presence of *TERT* promoter mutations and *IDH1/2* mutations in gliomas {Koelsche et al, 2013; Killela et al, 2014}, except in oligodendrogliomas {Killela et al, 2014}. On the other hand, *ATRX* (α-thalassemia X-linked mental retardation syndrome, X-linked) alterations are associated with *IDH* mutations in tumors of astrocytic lineage {Jiao et al, 2012; Liu et al, 2012}.

II.8. Relevance of *IDH1/2* mutations

II.8.1. Diagnostic

Screening for *IDH1/2* mutations has become *de rigeur* in diagnostic neuropathology. Demonstration of *IDH* mutations is useful in the following instances:

- To differentiate diffuse tumor infiltration from reactive astrocytosis
- In a histologically equivocal biopsy, presence of mutation is evidence of a glioma

- To distinguish WHO grade I pilocytic astrocytomas (lack *IDH* mutations) from diffuse grade II astrocytomas
- In differential diagnosis of oligodendrogliomas from other histological mimics such as, dysembryoplastic neuroepithelial tumors and clear cell ependymomas

In addition, D-2-HG can also be detected in gliomas using magnetic resonance spectroscopy. This offers a non-invasive method of mutation detection when it is difficult to obtain biopsies {Choi et al, 2012}.

II.8.2. Prognostic and predictive

IDH mutation is considered a marker of good prognosis in grade III and IV gliomas. Mutant tumors have better clinical outcome than their WHO grade matched wild-type counterparts {Parsons et al, 2008; Nobusawa et al, 2009; Sanson et al, 2009; Weller et al, 2009; Wick et al, 2009; van den Bent et al, 2010; Zhang et al, 2014}. Their prognostic value in grade II gliomas remains ambiguous. Some have suggested better prognosis {Houillier et al, 2010; Metellus et al, 2010}, while others indicate there is no difference {Ahmadi et al, 2012; Juratli et al, 2012}.

As the reports regarding it being a predictive marker have been conflicting {Weller et al, 2009; van den Bent et al, 2010; Cairncross et al, 2014}, the role of *IDH* mutation in this context requires additional studies.

II.8.3. Therapeutic

The therapeutic strategies to target *IDH* mutations can be both direct and indirect.

The direct method involves inhibition of mutant *IDH1/2*. The efficacy of small molecule IDH inhibitors has been demonstrated by *in vitro* and *in vivo*

studies. The first clinical trial based on *IDH2*-mutant inhibitor is ongoing in acute myeloid leukemias {Molenaar et al, 2014}.

The indirect approaches involve:

- Inhibition of IDH mutabolism {Molenaar et al, 2014}

In mutant tumors, the source of D-2-HG is glutamine. Glutamine is hydrolyzed by glutaminase to glutamate which is subsequently converted to α-KG {Seltzer et al, 2010}. *In vitro* studies have demonstrated that use of glutaminase inhibitor reduces growth of *IDH1*-mutant cells {Seltzer et al, 2010}.

- Targeting the epigenetic effects

It is not clear if the DNA and histone methylation changes in *IDH*-mutant cells drive oncogenesis. If that is the case, use of demethylating agents such as 5-azacytidine could be a therapeutic option as it has been demonstrated to reduce tumor growth, proliferation and methylation; and induce glial differentiation {Borodovsky et al, 2013; Turcan et al, 2013}.

II.9. Future directions

IDH mutations are considered important events in gliomagenesis through 2-HG mediated effects on α-KG dependent dioxygensases. Even though these mechanisms are still being elucidated, mutation detection has been incorporated into clinical practice, mainly in diagnostic settings. In addition, the mutation status has become one of the frequently evaluated markers in glioma survival studies. Their role as therapeutic targets in glioma management is under evaluation.

As of now, it is not known why gliomas have *IDH* mutations. Certain inherited single nucleotide polymorphisms (SNPs) on 8q24.21 {Jenkins et al, 2012} and 11q23 {Rice et al, 2013} are associated with increased risk of *IDH*-mutant gliomas. Again, how or why they increase this risk in not known at present

{Horbinski 2013}. The large amount of data generated so far has set the stage to address these and many other questions in the years to come.

RESULTS

Synopsis for publication I

Neuropathology. 2012 Feb;32(1):30-7.

IDH1 mutation, a genetic alteration associated with adult gliomatosis cerebri

Narasimhaiah D, Miquel C, Verhamme E, Desclée P, Cosnard G, Godfraind C

Ever since the identification of *IDH1/2* mutations in gliomas, different types of brain tumors have been tested for these mutations. We decided to analyze the *IDH* status in 15 gliomatosis cerebri (GC) as there was no data available in the literature at that point.

New information obtained from this work:

- Both type 1 and type 2 GC have *IDH1* mutations
- *IDH1* mutation is associated with better prognosis in GC also

The author carried out: data collection, histopathological examination, FISH experiments and interpretation; and data analysis.

NEUROPATHOLOGY

Neuropathology 2012; **32**, 30–37 doi:10.1111/j.1440-1789.2011.01216.x

Original Article

IDH1 mutation, a genetic alteration associated with adult gliomatosis cerebri

Deepti Narasimhaiah,[1] Catherine Miquel,[3] Elisabeth Verhamme,[1] Paul Desclée,[2] Guy Cosnard[2] and Catherine Godfraind[1]

[1]Laboratory of Pathology, [2]Department of Radiology and Medical Imaging, Cliniques Universitaires Saint-Luc, Université catholique de Louvain, Brussels, Belgium, and [3]Department of Neuropathology, Centre Hospitalier Sainte-Anne, Paris, France

Recently, mutations in *IDH1* and *IDH2* have been reported as an early and common genetic alteration in diffuse gliomas, being possibly followed by *1p/19q* loss in oligodendrogliomas and *TP53* mutations in astrocytomas. Lately, *IDH1* mutations have also been identified in adult gliomatosis cerebri (GC). The aim of our study was to test the status of *IDH1/2*, p53 and of chromosomes 1 and 19 in a series of 12 adult and three pediatric GC. For all tumors, clinico-radiologic characteristics, histopathologic features, status of *IDH1/2*, p53 and of chromosomes 1 and 19 were evaluated. *IDH1* mutations were detected only in GC of adult patients (5/12). They all corresponded to R132H. Additional *1p/19q* losses were observed in two of them with histological features of oligodendroglial lineage. Other copy number alterations of chromosomes 1 and 19 were also noticed. The median overall survival in adults was 10.5 months in non-mutated GC and 43.5 months in mutated GC. *IDH1* mutations were present in GC of adult patients, but not in those of children. There was a trend toward longer overall survival in mutated GC when compared to non-mutated ones. Concomitant *1p/19q* loss was observed in *IDH1*-mutated GC with oligodendroglial phenotype. These observations contribute toward establishing a stronger link between GC and diffuse glioma. In addition, these results also emphasize the importance of testing for *IDH1/2* mutations and *1p/19q* deletions in GC to classify them better and to allow the development of targeted therapy.

Correspondance: Catherine Godfraind, MD, PhD, Laboratory of Pathology, Cliniques Universitaires Saint-Luc, Université catholique de Louvain, Avenue Hippocrate 10, 1200 Brussels, Belgium. Email: catherine.godfraind@uclouvain.be

Received 10 February 2011; revised and accepted 21 February 2011; published online 11 April 2011.

Key words: *1p/19q* deletion, glioma, gliomatosis cerebri, *IDH1*, pediatric.

INTRODUCTION

Gliomatosis cerebri (GC) is defined as an extensively infiltrating glioma with involvement of at least three cerebral lobes. The diagnosis is based on radiology. Histologically, this lesion commonly displays an astrocytic phenotype, although oligodendroglial differentiation has also been reported.[1–3] The World Health Organization (WHO) considers it as malignant and refers to it as grade III. This tumor has been divided into primary and secondary GC. The former exhibits extensive involvement of the CNS at the time of clinical presentation; the latter consists of progressive infiltration of the brain by an initial diffuse glioma. Primary GC is further subcategorized into type 1 or classical form and type 2. This subdivision is based on the absence (type 1) or presence (type 2) of a tumor mass at initial clinical presentation.[1,4] However, these subgroups are referred to, but not included in, the 2007 WHO classification of tumors of the CNS. GC affects patients of all ages with peak incidence between the fourth and fifth decades,[1,4] with fewer cases being reported in children.[4–6]

Recently, recurrent mutations in isocitrate dehydrogenase 1 (*IDH1*) were identified in adult glioblastomas (GBM) with better prognosis.[7] Such mutations are infrequently observed in pediatric populations.[8–12] They affect arginine at position 132, an evolutionarily conserved residue within the active substrate-binding site.[7] Subsequently, mutations in R172 residue of isocitrate dehydrogenase 2 (*IDH2*) were detected in gliomas not mutated for *IDH1*.[8] *IDH1* and *IDH2* mutations were shown in astrocytomas of WHO grades II and III, secondary GBM, oligodendrogliomas and oligoastrocytomas.[8,9,13,14] These mutations appear early in tumorigenesis and can

subsequently be associated with *TP53* mutations in low-grade diffuse astrocytomas or with *1p/19q* loss in oligodendrogliomas.[13] Lately, adult primary GC have been reported to harbor mutations in the *IDH1* gene.[15]

In the present study, we analyzed a series of adult and pediatric primary GC for *IDH1/2* mutations. All identified mutations involved *IDH1* and adult patients. Concurrent *1p/19q* deletions were seen in GC exhibiting an oligodendroglial phenotype. These data linked diffuse glioma and GC in adults through an early genetic event. This was further reinforced while observing GC with oligodendroglial aspects to be associated with *1p/19q* loss. Also, similar to their diffuse glioma counterpart, pediatric GC did not show *IDH1* mutation.

MATERIALS AND METHODS

Tumor series

Our series included 15 cases of primary GC (5 males and 10 females). The diagnosis was based on radiological criteria as previously described.[16] They were further subcategorized, independently by two experienced neuroradiologists (PD and GC), as type 1 ($n = 9$) and type 2 ($n = 6$). Patients' ages varied between 3 to 75 years (mean: 45.6 years; median: 51.5 years) with three patients younger than 18 years included in the pediatric group. The clinical information, radiologic findings and follow-up data were obtained from the hospital records. The overall survival (OS) was calculated from the date of onset of symptoms to the date of death or last follow-up. The study was carried out in compliance with our institutional ethics committee guidelines.

Pathology

The haematoxylin and eosin (HE) slides and paraffin blocks of the cases were retrieved from the archives of the Laboratory of Anatomie Pathologique, St.Luc Hospital, Belgium. The examined material comprised of stereotactic biopsies (11 cases) and partial resections (4 cases). In addition, two cases had resections from both the initial and recurrent/progressive lesion. The diagnosis was independently assessed by two neuropathologists.

The clinical, radiological and pathological features have been summarized in Tables 1 and 2.

Immunohistochemistry

The expression of mutant IDH1 protein variant R132H was assessed on formalin-fixed paraffin-embedded sections (FFPE) using the mouse monoclonal antibody, anti-human IDH1 R132H (clone H09, dilution 1:100, Cat.# DIA H09 L, Dianova GmbH, Hamburg, Germany). The slides were stained using the Benchmark Ventana system (Roche, Basel, Switzerland). The Ventana staining procedure included pre-treatment with cell conditioner # 1 (CC1, pH 9) for 60 min, incubation with IDH1 R132H antibody for 72 min at 37°C followed by amplification, ultrawash, counterstaining with hematoxylin for 8 min and bluing reagent for 4 min. Antigen detection was performed using UltraView diaminobenzidine chromogen step (Ventana Medical

Table 1 Clinical and imaging features in cases of primary gliomatosis cerebri

Case	Age/sex	Symptoms	Subtype	Localization	Imaging	Treatment	OS†	Status at last contact
1	3/M	AS	Type 1	R CC,SFG,bilat CG	T1 hypo,T2 hyper,CE –,ME +	NT	5	Alive
2	10/M	GCT	Type 1	R F,T,O,BG,MB,pons	T1 hypo,T2 hyper,CE –,ME +	RT	18	Dead
3	16/F	HP	Type 1	L F,P,T	T1 hypo,T2 hyper,CE –,ME +	S,CT	11	Alive
4	32/F	GD	Type 1	MCP,pons to C6-C7	T1 hypo,T2 hyper, CE –,ME+	RT,CT	90	Dead
5	40/F	HP,VD	Type 1	Bilat Th,BS,PVWM	Infiltrative	NT	2.5	Dead‡
6	51/F	GCT	Type 1	R F,T,BG	T1 hypo,T2 hyper,CE–,ME–	S,RT,CT	56	Alive
7	59/F	GCT	Type 1	L F,P,T,CC,Th	Extensively infiltrative,CE –,ME–	CT	13	Alive
8	61/F	VD	Type 1	Bilat T,Th,BS	Expansile, CE –	NT	4	Dead
9	75/F	CD	Type 1	L F,P,T,BG	Expansile, CE focal,ME+	S	12	Dead§
10	23/F	GCT	Type 2	R F,P,L F,ins	T1 hypo, T2 hyper,CE –,ME –	CT	31	Alive
11	44/F	GCT	Type 2	RF,L CC	T1 hypo,T2 hyper,CE+,ME+	S,RT,CT	57	Dead
12	52/M	CD	Type 2	Bilat P,T,L F,O,CC,pons	T2 hyper,CE focal,ME –	NA	11	Alive
13	59/M	Aphasia	Type 2	L F,P,T	T2 hyper,CE focal,ME –	S,RT,CT	8	Alive
14	62/M	HP	Type 2	L F,P,T,BG,Th	Infiltrative CE focal,ME +	CT	10	Alive
15	74/F	GD	Type 2	Bilat O,L CC	T1 iso,T2 hyper,CE focal,ME –	NT	12	Alive

– absent, + present, † months, ‡ died of unrelated cause, § died post-surgery. AS, altered sensorium; BG, basal ganglia; Bilat, bilateral; BS, brainstem; CC, corpus callosum; CD, cognitive dysfunction; CE, contrast enhancement; CG, cingulate gyrus; CT, chemotherapy; F, frontal; GCT, generalized tonic clonic seizures; GD, gait disturbances; HP, hemiparesis; Hyper, hyperintense; Hypo, hypointense; Ins, insula; Iso, isointense; L, left; MB, midbrain; MCP, middle cerebellar peduncle; ME, mass effect,; NA, not available; NT, not treated; O, occipital; OS, overall survival; p, parietal; PVWM, periventricular white matter; R, right; RT, radiotherapy; S, surgery; SFG, superior frontal gyrus; T, temporal; Th, thalamus; VD, visual disturbances.

Table 2 Pathologic and genetic features in cases of primary gliomatosis cerebri

Case	Histology	Necrosis	MVP	Ki-67	p53	α IN	IDH1 IHC	*IDH1* seq	*IDH2* seq	Chr 1& Chr 19 status
1	A	–	–	2%	–	ND	–	–	–	Pol Chr 19
2	A	–	–	7%	–	–	–	–	–	No alt
3	A	–	–	10%	–	–	–	–	–	Pol Chr 19
4	A	–	–	7%	+	–	+	R132H	–	Pol Chr 19
5	A	–	–	2%	–	–	–	–	–	No alt
6	A	–	–	5%	+	–	+	R132H	–	No alt
7	A	–	–	8%	+	–	+	R132H	–	Pol Chr 1
8	A	–	–	7%	+	–	–	–	–	No alt
9	OA	–	–	7%	–	+	+	R132H	–	Del 1p/19q
10	O	–	–	10%	–	–	+	R132H	–	Del 1p/19q
11	A	+¶	+	20%	+	–	–	–	–	No alt
12	A	–	–	20%	+	–	–	–	–	1q del
13	A	+	+	15%	+	–	–	–	–	No alt
14	A	+	+	15%	+	–	–	–	–	No alt
15	A	–	–	1%	+	–	–	–	–	Pol Chr 1 & 19

– absent, + present, ¶ necrosis present only in second resection. A, astrocytoma; α IN, alpha-internexin; Alt, alteration; Chr, chromosome; Del, deletion; F, female; IHC, immunohistochemistry; M, male; MVP, microvascular proliferation; ND, not done; O, oligodendroglioma; OA, oligoastrocytoma; Pol, polysomy; Seq, sequencing.

Systems, Roche). Cases with cytoplasmic expression of the mutant IDH1 R132H protein by tumor cells were scored as positive; absence of staining was scored as negative. A weak diffuse staining was interpreted as negative.

Immunohistochemistry for Ki-67 (clone MIB-1, dilution 1:150, Code no. M7240, Dako, Glostrup, Denmark), p53 (clone DO7, dilution 1v1000, Cat.#CM042C, Biocare Medical, Concord, CA, US) and Alpha-internexin (clone 2E3, dilution 1:300, Cat#MAB5224, Millipore Corporation, Billerica, MA, US) were performed using the Benchmark Ventana system (Roche) as per the manufacturer's recommendations.

Analysis of chromosomes 1 and 19 by fluorescence in situ hybridization (FISH)

The FISH technique was adapted from Perry *et al*.[17] The sections stained with HE were used to determine the area to be targeted for hybridization: 4 µm FFPE sections were deparaffinized in xylene, dehydrated in graded isopropanol (absolute, 90%, 70%) and denatured in 0.2 N hydrochloric acid for 10 min. Target retrieval was done using citrate buffer (0.01 mol, pH 5.7) at 100°C for 40 min. The slides were digested for 85 min in a tissue digest solution (Cat#T101&102, Insitus Biotechnologies, Albuquerque, NM, US) using the manufacturer's protocol. The probes used were: Locus specific identifier (LSI) 1p36/LSI 1q25 and LSI 19q13/LSI 19p13 (Vysis, Abbott Molecular, Des Plaines, IL, US) diluted to 1:3 in tissue DenHyb-2 (tDenHyb-2) (Cat#D102, Insitus Biotechnologies). The target and probe DNA were co-denatured at 90°C for 13 min and the slides were hybridized overnight at 37°C in a humidified chamber. Post-hybridization, the slides were washed with 1.5× saline-sodium citrate (SSC) (S6639, Sigma-Aldrich, Munich, Germany) and 50% formamide and counterstained with 4′,6′-diamidino-2-phenylindole (Cat#F202, Insitus Biotechnologies). The fluorescent signals were analyzed using Zeiss Axioplan 2 microscope equipped with an appropriate filter set. For each hybridization, 100–200 non-overlapping nuclei with unequivocal signals were enumerated. Target/reference signal ratios without (1/2) and with disproportion (2/3, 2/4) were interpreted as deletions. The cut-off used for deletion was 51.7% and 48% for 1p and 19q, respectively. This criterion is used in our lab for assessment of *1p/19q* status in clinical cases. The cut-off was set by FISH analysis of a series of glial tumors with confirmed non-deleted *1p/19q* status based on microsatellite analysis using the average number of cells with deletion plus four standard deviations (mean+4SD). Polysomy was defined as ≥3 signals for both target and reference.

Microsatellite analysis

The microsatellite analysis for detection of loss of heterozygosity for *1p* and *19q* was performed as described previously.[18]

IDH1/2 sequencing

Target DNA was extracted from FFPE tissue using DNA extraction kit (Promega Corporation, Madison, WI, US). The percentage of tumor cells in the FFPE sections ranged from 40% to 90%. DNA concentration was then assessed using a NanoDrop 1000 spectrophotometer (Thermo Scientific, Wilmington, DE, US). For PCR amplification of exon 4 of both genes, previously reported forward and reverse primer sequences were used.[19] PCR amplification was performed using 37 to 50 ng of DNA, 0.5 µL of 10 mmol of each primer and PCR mix. The reaction

mixture was subjected to initial denaturation at 94°C for 10 min, followed by 35 cycles of PCR comprising of denaturation at 94°C for 30 s, annealing at 55°C for 30 s and extension at 72°C for 60 s concluded by final extension at 72°C for 7 min in a total volume of 23 μL. The PCR products were then sequenced in both sense and antisense directions using the forward and reverse primers utilizing the BigDye terminator v3.1 cycle sequencing kit (Applied Biosystems Inc, Foster City, CA, US). The sequencing reaction mixture was subjected to initial denaturation at 96°C for 1 min followed by 24 cycles of amplification consisting of denaturation at 96°C for 10 s, annealing at 50°C for 5 s and extension at 60°C for 120 s in a total volume of 9 μL. The sequencing products were then purified using Sephadex columns (GE Healthcare, Buckinghamshire, UK) and analyzed by capillary gel electrophoresis on ABI 3130xl/ Genetic Analyzer (Applied Biosystems). The sequencing analysis software v5.2, patch2 (Applied Biosystems) was used to aid the interpretation of the sequence electropherograms. The cases were classified as positive or negative for *IDH* mutation based on the results of sequencing.

RESULTS

The clinical, radiographic, pathological and genetic features are summarized in Tables 1 and 2.

Mutations in *IDH1* and *IDH2* genes

All GC were sequenced for codons 132 of *IDH1* and 172 of *IDH2*. Only mutations at codon 132 of *IDH1* were demonstrated. They all consisted of CGT→CAT transition, changing a single amino acid from arginine to histidine (R132H). This mutation affected five tumors in adult patients (42%) and none in the pediatric group. Immunocytochemistry for R132H mutation was carried out on all tumors. It revealed positive cytoplasmic staining of tumor cells (Fig. 1B,E,H) only in the five cases identified as mutated by sequencing.

Chromosomes 1 and 19 status in gliomatosis cerebri

The *1p/19q* status was analyzed by FISH in all GC. In one case, analysis by microsatellites was performed because of failure of hybridization by FISH.

In GC mutated for *IDH1*, co-deletion of *1p/19q* was found in two cases (Fig. 1J,K); polysomy for chromosome 1 and chromosome 19 were observed in one case each, respectively.

In GC without *IDH1* mutation, co-deletion of *1p/19q* was not observed in any of the cases. The alterations comprised of polysomy for both chromosome 1 and 19 in one case, polysomy for only chromosome 19 in two other cases and 1q deletion in the last one. The remaining six cases showed no alterations in chromosomes 1 and 19.

Clinical features related to genetic alterations

IDH1 mutated GC included five adults. The age at diagnosis varied between 23 and 75 years (mean: 48 years, median: 51 years). The common mode of presentation was generalized tonic-clonic seizures. The overall survival (OS) ranged from 13–90 months (mean: 47.5 months, median: 43.5 months). At last contact, one patient had died of disease and three patients were still alive. One patient died post-surgery.

Gliomatosis cerebri without *IDH1* mutation comprised of three children and seven adults. The age at diagnosis ranged 3–74 years (mean: 42.1 years, median: 48 years). Hemiparesis was the common presenting feature. The OS in adults was 4–57 months (mean: 17 months, median: 10.5 months). The OS in pediatric group was 5–18 months (mean: 11.3 months, median: 11 months). At last contact, four patients had died, three of disease and one from an unrelated cause. Six patients were still alive.

Radiological features related to genetic alterations

IDH1 mutated GC included four type 1 and one type 2 tumors (five adults) (Fig. 2). Among *IDH1* mutated GC, there were no radiological differences between tumors with and without concomitant *1p/19q* deletion. GC without *IDH1* mutation comprised of five type 1 (three children and two adults) and five type 2 (five adults) tumors.

Histological features related to genetic alterations

Among the five cases of GC with *IDH1* mutation, three demonstrated an astrocytic aspect and two had oligodendroglial morphology (Fig. 1A,D,G). None of these lesions showed microvascular proliferation or necrosis in the initial biopsy or resection. The Ki-67 labelling indices ranged 5%–10% (mean: 7.4%, median: 7%) (Fig. 1C). Immunohistochemistry for p53 was negative in two tumors and positive in three (Fig. 1F). Alpha-internexin was positive in one of the two tumors with oligodendroglial aspect (Fig. 1I) and in none of the three with an astrocytic appearance. Deletion of *1p/19q* was observed in two GC with oligodendroglial phenotype. Polysomy for chromosome 19 and for chromosome 1 was seen in one case each with astrocytic aspect.

All 10 cases of GC without *IDH1* mutation demonstrated an astrocytic phenotype. In addition, microvascular proliferation was observed in three cases at first biopsy or resection. Two of these also showed concomitant necrosis,

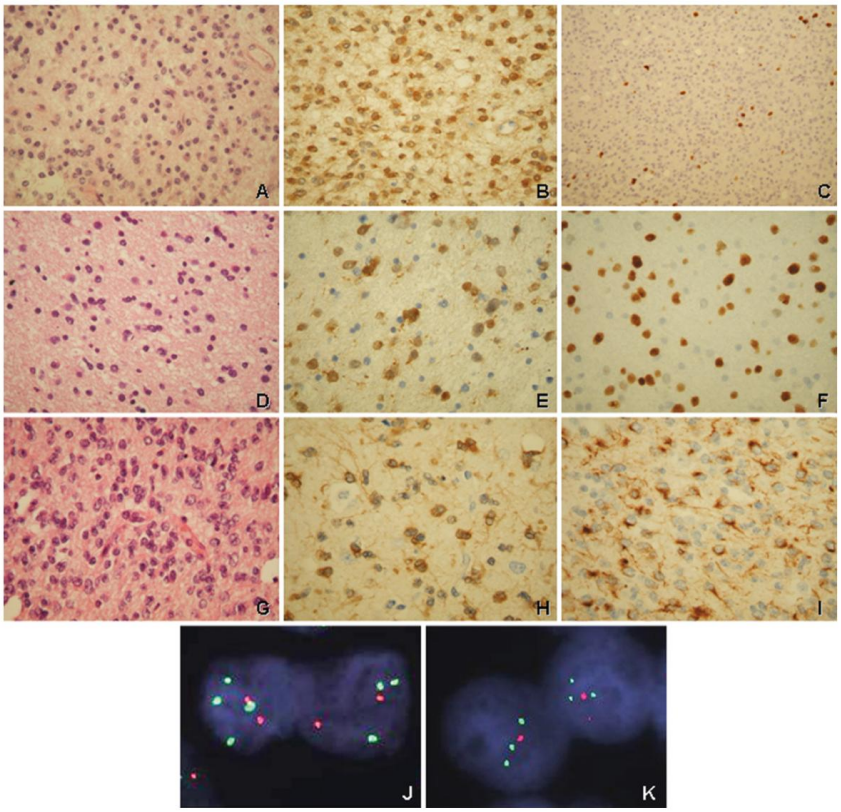

Fig. 1 Histopathological and fluorescence in situ hybridization (FISH) features of primary gliomatosis cerebri. (A–C: Case 10, D-F: Case 7, G-K: Case 9) A, D and G: HE staining. B, E and H: Positivity of tumoral cells with an antibody recognizing R132H, one of the mutant *IDH1*. C: Immunostaining with proliferation marker Ki-67. F: Positivity of tumoral cells with antibody directed against p53. I: Positivity of tumoral cells with antibody directed against alpha internexin. J and K: FISH demonstrating *1p/19q* loss (J: loss of 1p36 (red) relative to 1q25 (green); K: loss of 19q13 (red) relative to 19p13 (green).

while for the third case necrosis was apparent in the second resection. The Ki-67 labelling indices ranged 1%–20% (mean: 10%, median: 9%). Immunohistochemistry for p53 was negative in four tumors and positive in six. Alpha-internexin was negative in all nine cases tested.

Polysomy for chromosome 1 and chromosome 19 was observed in three cases and deletion of 1q in one case.

DISCUSSION

Somatic mutations in isocitrate dehydrogenase (*IDH*), a metabolic enzyme involved in the Krebs cycle have recently been reported in gliomas.[8,9,13,14] Isocitrate dehydrogenase includes three isoforms: *IDH1, IDH2* and *IDH3*. *IDH1* is cytosolic, whereas *IDH2* and *IDH3* are mitochondrial.

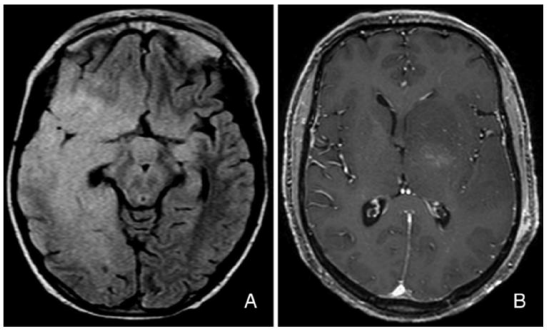

Fig. 2 MRI of primary gliomatosis cerebri. A. Type 1 – Axial fluid attenuated inversion recovery (FLAIR) sequence showing a diffusely infiltrative right hemispheric lesion (Case 2). B. Type 2 – Axial T1-weighted sequence showing a diffusely infiltrative left hemispheric lesion with focal mass in the left capsulo-lenticular region (Case 14).

IDH2 encodes the only human protein homologous to *IDH1*.[8] *IDH1* and *IDH2* use nicotinamide adenine dinucleotide phosphate ($NADP^+$) as an electron acceptor, while *IDH3* is nicotinamide adenine dinucleotide (NAD^+) dependent.[20] *IDH1* was the first isoform demonstrated to be mutated in gliomas,[7] followed by *IDH2*.[8] Since then, high rates of *IDH1* mutations have been reported in various subtypes of diffuse glioma, whereas mutations in *IDH2* are less frequent.[8,9,13,14] These mutations are considered to be early events in gliomagenesis, taking place even before the occurrence of *TP53* mutations or *1p/19q* loss.[13] Mutations of *IDH* have been associated with a methylator phenotype in glioblastoma multiforme[21] and leads to both loss and gain of enzymatic function.[22] The loss of function impairs the ability of the enzyme to convert isocitrate to α-ketoglutarate, leading to increased levels of hypoxia inducible factor-1alpha (*HIF-1α*), an important gene in activation of tumorigenesis.[22,23] The gain of function results in the ability to catalyze the reduction of α-ketoglutarate to R(−)-2-hydroxyglutarate (2HG), thereby contributing to gliomagenesis by an as yet unsolved mechanism.[22,24] Interestingly, inborn errors of 2HG metabolism are associated with increased occurrence of brain tumors.[25]

The term "gliomatosis cerebri" introduced by Nevin (1938) is currently widely accepted for glioma with exceptionally extensive infiltration of the CNS.[1,26] However, the same cannot be said for its histogenesis as reflected by the inclusion of GC under different categories in previous editions of the WHO classification of CNS tumors.[27–29] Only in the 2007 edition, GC has been categorized under "astrocytic tumors", acknowledging its glial origin.[1] Until now, genetic data have not contributed much toward resolving this issue. GC share with diffuse astrocytomas genetic abnormalities like *TP53* mutations, although it occurs with lower frequency.[1,30–34] When chromosomal alterations are considered, only deletion on chromosome 6 appears to be common to both GC and astrocytomas.[1,35] Recently, *IDH1* mutations were reported in 42% of type 2 adult GC.[15] This is in agreement with our data, where *IDH1* mutations were observed in 42% of adult primary GC, comprising of type 1 and type 2 tumors. In both series, the only *IDH1* mutation detected was the R132H, which corresponds to the most frequently observed *IDH* mutation in gliomas.[14] In some *IDH1* mutated GC, we observed additional *1p/19q* losses and expression of alpha-internexin, a proneural gene encoding a neurofilament protein, reported to be a surrogate marker of *1p/19q* co-deletion in gliomas.[36] These findings link GC and diffuse gliomas through an early genetic event in glioma tumorigenesis and contribute toward a better understanding of histogenesis of GC.

To our knowledge, the status of *IDH1/2* has not been previously reported in pediatric GC and we did not identify mutations in this age group. This is in accordance with the rarity of *IDH1/2* mutations in this population. Indeed, *IDH* mutations were reported in only about 8% of pediatric gliomas,[8–12,14,37–39] whereas in adults, 64.6% and 45.4% of low- and high-grade gliomas appear mutated.[7–9,13,14,16,40–43] Pediatric and adult gliomas also differ with respect to other genetic alterations like mutations in *TP53,* amplifications of epidermal growth factor receptor (EGFR) and platelet-derived growth factor receptor A (*PDGFRA*).[1,11,44] Our results suggest that GC in adult and pediatric age groups are probably distinct entities. However, additional studies would be required to strengthen these data.

Interestingly, clinico-histological features appeared different when comparing *IDH1*-mutated to *IDH1*-non-mutated GC. Among them, the initial symptoms were mostly epilepsy in *IDH1*-mutated GC (3/5 patients) and neurological deficits (8/10 patients) in non-mutated ones. Necrosis and microvascular proliferation were more

frequent in GC lacking *IDH1* mutations, as previously published.[15,45] Overall survival in adults also differed, with a median of 43.5 months in *IDH1* mutated GC versus 10.5 in non-mutated tumors. Most of these features are linked to prognosis, and *IDH1*-mutated GC appeared to be associated with signs of better prognosis and a trend toward longer overall survival, as for classical gliomas.

Gliomatosis cerebri is a tumor for which pathology is only used to confirm the glial nature of the lesion. Its diagnosis and subdivision into types 1 and 2, are primarily based on radiological criteria.[16] We observed R132H in four cases of GC type 1 and in one type 2. This may appear contradictory with the previous report, where only type 2 GC were identified as mutated.[15] Meanwhile, one may ask if this discrepancy could partly be explained by the fact that for some GC, the different subtypes may correspond to evolutionary stages of the same disease, since radiological progression from type 1 to type 2 GC has been observed, albeit infrequently.[16]

In conclusion, our results contribute toward establishing a genetic link between diffuse gliomas and GC through the identification of *IDH1* mutations in adults and finding subsequent *1p/19q* loss in GC with oligodendroglial differentiation. It also highlights the interest of searching for these genetic anomalies in this tumor type, as patients with *IDH1* mutated GC tend to have longer overall survival.

ACKNOWLEDGMENTS

We thank Professor F. Scaravilli and Dr M. Lamba Saini for their critical review of the manuscript. The project was supported by Fonds Maisin, Université catholique de Louvain and Credit aux Chercheurs from FNRS, Belgium. Dr Deepti AN was supported by a fellowship from le Centre du Cancer, Cliniques Universitaires Saint-Luc, Université catholique de Louvain, Brussels, Belgium.

REFERENCES

1. Fuller GN, Kros JM. *Gliomatosis cerebri*. In: Louis DN, Ohgaki H, Wiestler OD, Cavenee WK, eds. *WHO Classification of Tumours of the Central Nervous System*. Lyon: IARC, 2007; 50–52.
2. Peretti-Viton P, Brunel H, Chinot O *et al*. Histological and MR correlations in Gliomatosis cerebri. *J Neurooncol* 2002; **59**: 249–259.
3. Tancredi A, Mangiola A, Guiducci A, Peciarolo A, Ottaviano P. Oligodendrocytic gliomatosis cerebri. *Acta Neurochir (Wien)* 2000; **142**: 469–472.
4. Jennings MT, Frenchman M, Shehab T *et al*. Gliomatosis cerebri presenting as intractable epilepsy during early childhood. *J Child Neurol* 1995; **10**: 37–45.
5. Landi A, Piccirilli M, Mancarella C, Giangaspero F, Salvati M. Gliomatosis cerebri in young patients' report of three cases and review of the literature. *Childs Nerv Syst* 2011; **24**: 19–25.
6. Armstrong GT, Phillips PC, Rorke-Adams LB, Judkins AR, Localio AR, Fisher MJ. Gliomatosis cerebri: 20 years of experience at the Children's Hospital of Philadelphia. *Cancer* 2006; **107**: 1597–1606.
7. Parsons DW, Jones S, Zhang X *et al*. An integrated genomic analysis of human glioblastoma multiforme. *Science* 2008; **321**: 1807–1812.
8. Yan H, Parsons DW, Jin G *et al*. IDH1 and IDH2 mutations in gliomas. *N Engl J Med* 2009; **360**: 765–773.
9. Balss J, Meyer J, Mueller W, Korshunov A, Hartmann C, von Deimling A. Analysis of the IDH1 codon 132 mutation in brain tumors. *Acta Neuropathol* 2008; **116**: 597–602.
10. De Carli E, Wang X, Puget S. IDH1 and IDH2 mutations in gliomas. *N Engl J Med* 2009; **360**: 2248; author reply 2249.
11. Paugh BS, Qu C, Jones C *et al*. Integrated molecular genetic profiling of paediatric high-grade gliomas reveals key differences with the adult disease. *J Clin Oncol* 2010; **28**: 3061–3068.
12. Antonelli M, Buttarelli FR, Arcella A *et al*. Prognostic significance of histological grading, p53 status, YKL-40 expression, and IDH1 mutations in paediatric high-grade gliomas. *J Neurooncol* 2010; **99**: 209–215.
13. Watanabe T, Nobusawa S, Kleihues P, Ohgaki H. IDH1 mutations are early events in the development of astrocytomas and oligodendrogliomas. *Am J Pathol* 2009; **174**: 1149–1153.
14. Hartmann C, Meyer J, Balss J *et al*. Type and frequency of IDH1 and IDH2 mutations are related to astrocytic and oligodendroglial differentiation and age: a study of 1,010 diffuse gliomas. *Acta Neuropathol* 2009; **118**: 469–474.
15. Seiz M, Tuettenberg J, Meyer J *et al*. Detection of IDH1 mutations in gliomatosis cerebri, but only in tumors with additional solid component: evidence for molecular subtypes. *Acta Neuropathol* 2010; **120**: 261–267.
16. Desclée P, Rommel D, Hernalsteen D, Godfraind C, de Coene B, Cosnard G. Gliomatosis cerebri, imaging findings of 12 cases. *J Neuroradiol* 2010; **37**: 148–158.
17. Perry A, Aldape KD, George DH, Burger PC. Small cell astrocytoma: an aggressive variant that is clinicopathologically and genetically distinct from anaplastic oligodendroglioma. *Cancer* 2004; **101**: 2318–2326.
18. Godfraind C, Rousseau E, Ruchoux MM, Scaravilli F, Vikkula M. Tumour necrosis and microvascular proliferation are associated with 9p deletion and CDKN2A

alterations in 1p/19q-deleted oligodendrogliomas. *Neuropathol Appl Neurobiol* 2003; **29**: 462–471.
19. Horbinski C, Kofler J, Kelly LM, Murdoch GH, Nikiforova MN. Diagnostic use of IDH1/2 mutation analysis in routine clinical testing of formalin-fixed, paraffin-embedded glioma tissues. *J Neuropathol Exp Neurol* 2009; **68**: 1319–1325.
20. Frezza C, Tennant DA, Gottlieb E. IDH1 mutations in gliomas: when an enzyme loses its grip. *Cancer Cell* 2010; **17**: 7–9.
21. Noushmehr H, Weisenberger DJ, Diefes K *et al.* Cancer Genome Atlas Research Network. Identification of a CpG island methylator phenotype that defines a distinct subgroup of glioma. *Cancer Cell* 2010; **17**: 510–522.
22. Fu Y, Huang R, Du J, Yang R, An N, Liang A. Glioma-derived mutations in IDH: from mechanism to potential therapy. *Biochem Biophys Res Commun* 2010; **397**: 127–130.
23. Zhao S, Lin Y, Xu W *et al.* Glioma-derived mutations in IDH1 dominantly inhibit IDH1 catalytic activity and induce HIF-1alpha. *Science* 2009; **324**: 261–265.
24. Dang L, White DW, Gross S *et al.* Cancer-associated IDH1 mutations produce 2-hydroxyglutarate. *Nature* 2009; **462**: 739–744.
25. Aghili M, Zahedi F, Rafiee E. Hydroxyglutaric aciduria and malignant brain tumor: a case report and literature review. *J Neurooncol* 2009; **91**: 233–236.
26. Nevin S. Gliomatosis cerebri. *Brain* 1938; **61**: 170–191.
27. Zülch KJ. *Histological Typing of Tumours of the Central Nervous System*. Geneva, Switzerland: World Health Organization, 1979.
28. Kleihues P, Burger PC, Scheithauer BW. The new WHO classification of brain tumours. *Brain Pathology* 1993; **3**: 255–268.
29. Lantos PL, Bruner JM. *Gliomatosis cerebri*. In: Kleihues P, Cavenee WK, eds. *Pathology and Genetics of Tumours of the Nervous System*. Lyon: IARC Press, 2000; 92–93.
30. Herrlinger U, Felsberg J, Küker W *et al.* Gliomatosis cerebri: molecular pathology and clinical course. *Ann Neurol* 2002; **52**: 390–399.
31. Mawrin C, Kirches E, Schneider-Stock R *et al.* Analysis of TP53 and PTEN in gliomatosis cerebri. *Acta Neuropathol* 2003; **105**: 529–536.
32. Kros JM, Zheng P, Dinjens WN, Alers JC. Genetic aberrations in gliomatosis cerebri support monoclonal tumorigenesis. *J Neuropathol Exp Neurol* 2002; **61**: 806–814.
33. Mawrin C. Molecular genetic alterations in gliomatosis cerebri: what can we learn about the origin and course of the disease? *Acta Neuropathol* 2005; **110**: 527–536.
34. Romeike BF, Mawrin C. Gliomatosis cerebri: growing evidence for diffuse gliomas with wide invasion. *Expert Rev Neurother* 2008; **8**: 587–597.
35. Min HS, Kim B, Park SH. Array-based comparative genomic hybridization and immunohistochemical studies in gliomatosis cerebri. *J Neurooncol* 2008; **90**: 259–266.
36. Ducray F, Crinière E, Idbaih A *et al.* alpha-Internexin expression identifies 1p19q codeleted gliomas. *Neurology* 2009; **72**: 156–161.
37. Dougherty MJ, Santi M, Brose MS *et al.* Activating mutations in BRAF characterize a spectrum of paediatric low-grade gliomas. *Neuro Oncol* 2010; **12**: 621–630.
38. Reitman Z, Yan H. IDH1 and IDH2 mutations in gliomas. *N Engl J Med* 2009; **360**: 2248; author reply 2249.
39. Pollack IF, Hamilton RL, Sobol RW *et al.* IDH1 mutations are common in malignant gliomas arising in adolescents: a report from the Children's Oncology Group. *Childs Nerv Syst* 2011; **27**: 87–94.
40. Taillibert S, Chodkiewicz C, Laigle-Donadey F, Napolitano M, Cartalat-Carel S, Sanson M. Gliomatosis cerebri: a review of 296 cases from the ANOCEF database and the literature. *J Neurooncol* 2006; **76**: 201–205.
41. Korshunov A, Meyer J, Capper D *et al.* Combined molecular analysis of BRAF and IDH1 distinguishes pilocytic astrocytoma from diffuse astrocytoma. *Acta Neuropathol* 2009; **118**: 401–405.
42. Gravendeel LA, Kloosterhof NK, Bralten LB *et al.* Segregation of non-p.R132H mutations in IDH1 in distinct molecular subtypes of glioma. *Hum Mutat* 2010; **31**: E1186–E1199.
43. Ichimura K, Pearson DM, Kocialkowski S *et al.* IDH1 mutations are present in the majority of common adult gliomas but rare in primary glioblastomas. *Neuro Oncol* 2009; **11**: 341–347.
44. Nakamura M, Shimada K, Ishida E *et al.* Molecular pathogenesis of paediatric astrocytic tumors. *Neuro Oncol* 2007; **9**: 113–123.
45. Nobusawa S, Watanabe T, Kleihues P, Ohgaki H. IDH1 mutations as molecular signature and predictive factor of secondary glioblastomas. *Clin Cancer Res* 2009; **15**: 6002–6007.

DISCUSSION

Gliomatosis cerebri (GC) is a rare glioma subtype which shares some genetic features with diffuse gliomas. The identification of *IDH1* mutations in GC has strengthened this histogenetic link. As described in the introduction, rapid strides have been made in unraveling the genetic aspects of gliomas following the identification of *IDH* mutations. However, the same cannot be said of GC in view of their rarity, difficulty in obtaining fresh-frozen samples and extensive admixture of non-tumor cells. To facilitate progress in understanding GC tumor biology, the first step would be to create a consortium to gather GC samples which could then be subjected to systematic genetic analyses including exome, transcriptome and methylome interrogation. Besides, such approach could also lead to identification of novel therapeutic targets.

I. Future perspectives

I.1. Genetic profile of type 1 and type 2 GC

There is some discrepancy between studies with regard to *IDH1* mutations in GC subtypes. One study found mutations only in type 2 (mass forming subtype) {Seiz et al, 2010}; while others, including the present study identified mutations in both subtypes {Kwon et al, 2012}. The reason for these differences is not clear.

Performing exome sequencing on type 1 and type 2 tumors would shed some light on genetic differences between them. Also, comparison of diffusely infiltrating regions from both subtypes would indicate genetic similarities or differences between them. In addition, analysis of the mass forming focus of type 2 could help better understand the evolution of this phenotype. Rarely, type 1 GC can progress to type 2 during follow-up {Desclee et al, 2010}. Analysis of different components in such cases could help identify the genetic alterations that drive tumor progression.

I.2. Transcriptomic profiles of type 1 and type 2 GC

Diffuse infiltration is a feature of all gliomas driven by adhesion molecules and proteolytic enzymes produced by tumor cells {Romeike et al, 2008}. In GC, the degree of brain invasion is far more than in other gliomas. Some GC express CD44, a receptor involved in cell adhesion and migration {Mawrin et al, 2005}. However, the reason for their invasive behavior is not known.

Comparison of global transcriptomic profiles of GC, as well as diffuse gliomas by RNA sequencing may help better understand their invasive behavior.

B.UVEAL MELANOMAS

INTRODUCTION

I. Melanomas

I.1. Uveal melanomas

I.1.1. Background

I.1.1.1. Historical aspects of melanomas

Melanomas are malignant tumors arising from melanocytes, the pigment containing cells in the human body. The antiquity of melanomas is attested by their discovery in the mummies of Incas of Peru considered to be nearly 2400 years old. The first mention of melanoma can be attributed to Hippocrates. Laennec referred to it as "la mélanose," and the term 'melanoma' was first coined by Robert Carswell in 1838 {Urteaga et al, 1966; Sudhakar 2009}.

I.1.1.2. Anatomy of the human eye

The human eye is a complex anatomical structure and an optical instrument. The eyeball is composed of three layers and the contents enclosed by them. They are: fibrous, vascular and pigmented and nervous layers. The fibrous layer is composed of cornea and sclera. The uveal tract or the vascular layer consists of the choroid, ciliary body and iris. It also contains melanocytes. The neural layer is formed by the retina (**Figure 1**) {Williams et al, 1980; Tandon 2011}.

This anatomical organization gives rise to a diverse variety of benign and malignant tumors, ranging from epithelial, mesenchymal to melanocytic in origin. They can be both primary and secondary, with the former being more frequent.

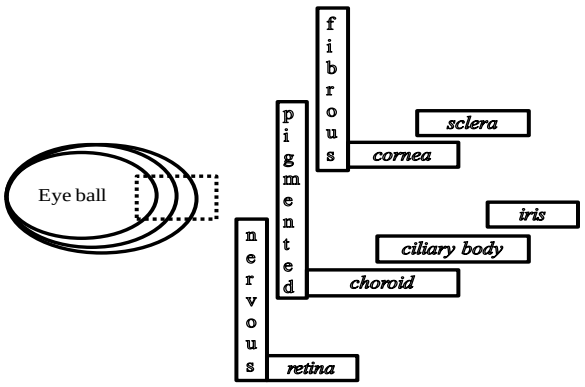

Figure 1. Schematic representation of layers of the eyeball

I.1.2. Epidemiology

In the human body, melanomas can originate from various melanocyte containing sites such as, epidermis of skin, eye, mucosal surfaces and leptomeninges. About 95% of all melanomas are cutaneous in origin, with eye and mucosae accounting for 3.1% and 1.2%, respectively {Bishop et al, 2013}. Ocular melanoma is the generic term for primary melanomas arising in the eye. They are the most common, primary, intra-ocular malignant tumors in adults. They can arise from: uveal tract (choroid, ciliary body and iris), conjunctiva and orbital tissue. About 84% of them are uveal in origin, followed by conjunctiva accounting for 7% and the remaining occurring in unspecified or in overlapping locations. 72% of uveal melanomas occur predominantly in choroid and 12% in ciliary body/iris {Bishop et al, 2013}.

The reported incidence of uveal melanomas is 4.9-5.1 per million; whereas for conjunctival it is 0.4 per million {McLaughlin et al, 2005} {Mallone et al,

2012}. This is in contrast to cutaneous melanomas with an incidence of 171.6 per million {Bishop et al, 2013}.

In Europe, there is geographical variation in incidence of uveal melanomas, ranging from 3.1 per million in South to 5.8 per million in North {Mallone et al, 2012}.

I.1.3. Risk/Predisposing factors

There are relatively few risk factors identified in uveal melanomas and in contrast to cutaneous melanomas, there is no equivocal evidence for ultraviolet exposure as a risk factor in uveal melanomas {Singh et al, 2004}, despite conflicting reports {Gallagher et al, 1985; Seddon et al, 1990; Vajdic et al, 2002}.

The recognized risk factors include:

I.1.3.1.Ocular (oculodermal) melanocytosis

This is a congenital pigmentary abnormality characterized by excess melanocytes in uvea and skin. As every 1 in 400 patients with this condition develop uveal melanoma, {Singh et al, 1998; Shields et al, 2013} it requires regular monitoring to aid early tumor detection.

I.1.3.2. Nevi

Nevi in choroid and iris, both typical and atypical are risk factors {Hammer et al, 1996; Vajdic et al, 2001; Richtig et al, 2004}. It has been estimated that one out of every 8845 nevi transform into melanoma {Singh et al, 2005}.

I.1.3.3. Host factors

Eye color is one of the strongest predictors of risk for development of uveal melanoma. Those with lighter irides like blue, green or grey have a 2-2.5 times

higher risk of developing the tumor, in comparison with brown iris {Gallagher et al, 1985; Holly et al, 1990; Vajdic et al, 2001; Weis et al, 2006}. Similarly, the relation between skin pigmentation and occurrence of uveal melanomas is also inversely related {Seddon et al, 1990; Weis et al, 2006}.

I.1.4. Clinical features

Uveal melanomas occur predominantly in adults between 50-80 years of age with a peak at 70 years and male predominance {McLaughlin et al, 2005}. Only 1% occurs in patients < 20 years {Shields et al, 2012}.

The tumor epicenter can be located in iris (3.5%), ciliary body (6.1%) or choroid (90.3%) {Shields et al, 2009}. As it is difficult to determine whether the melanoma originates in the ciliary body or choroid in practice, {Kujala et al, 2013} they are referred to as posterior (choroid and ciliary body) or anterior (iris).

Tumor size comprising of basal diameter and thickness is one of the most important clinical feature, assessed based on their maximum dimensions. Choroidal melanomas are classified as: small (<3 mm thickness and <10 mm largest basal diameter); medium (3–8 mm in thickness and <15 mm largest basal diameter); and large (8 mm in thickness and >15 mm largest basal diameter), respectively {Diener-West et al, 1992}. Medium and large-sized tumors are usually associated with retinal detachment {Kivela et al, 2001}.

Extraocular extension is one of the methods of local spread and is observed in 3% to 14.6% of tumors {Coupland et al, 2008; Bellmann et al, 2010; Kujala et al, 2013}.

Distant spread is by hematogenous dissemination, with liver being the predominant site of metastasis, being involved in 90% of patients. Other

common sites include: lung (29%), bone (17%), skin and subcutaneous tissue (12%) {Diener-West et al, 2005}.

The staging based on the tumor, node and metastasis, TNM system (seventh edition) is same for choroid and ciliary body melanomas and separate for iris melanomas. It takes into consideration tumor size, involvement of ciliary body and extraocular extension.

I.1.5. Histopathology

The morphological tumor types are based on modified Callender's classification, which recognizes spindle, epithelioid and mixed-cell types, the latter being predominantly spindle with few or small number of epithelioid cells {Callender 1931; McLean et al, 1983}. However, the proportion of epithelioid component required to reclassify spindle cell melanoma as mixed has not been defined.

Cellular proliferation in uveal melanomas has been estimated using methods such as counting of mitoses and use of proliferation markers (Ki-67) {Pe'er et al, 2001}. The mitotic activity is lower in irradiated tumors compared to untreated ones {Albert et al, 1998}.

Various morphological patterns of uveal melanoma vasculature and extravascular matrix arrangement have been described, with loops and network pattern being the most relevant one {Folberg et al, 1992; Folberg et al, 1993}. The latter is also correlated with high microvessel density {Makitie et al, 1999}.

I.1.6. Treatment modalities

The treatment of uveal melanomas can be either conservative or radical. The former attempts to conserve the eye and useful vision and includes various

modalities such as, transpupillary thermotherapy and different forms of radiotherapy (brachytherapy, proton beam). The radical treatment involves enucleation. Brachytherapy is the most common method of treating uveal melanomas, with primary enucleation being reserved for cases where other methods can cause increased morbidity. Transpupillary thermotherapy is reserved for small choroidal melanomas or as an adjuvant to brachytherapy {Damato 2010; Baurain et al, 2013}.

I.1.7. Prognostic factors

The adverse clinical prognostic factors in uveal melanomas are: age at diagnosis of more than 60 years; male gender; large tumor size; involvement of ciliary body; higher tumor stage; presence of retinal detachment and extraocular extension {Kivela et al, 2001; Shields et al, 2009; Shields et al, 2012}. The melanoma-related mortality increases with increasing stage. The survival at 5-years for stages I, IIA, IIB, IIIA, IIIB and IIIC are 96%, 89%, 81%, 66%, 45% and 26%, respectively {Kujala et al, 2013}.

The adverse histopathologic factors include: epithelioid cell type, increased mitotic activity, tumor infiltrating lymphocytes and tumor vascular networks {de la Cruz et al, 1990; Damato et al, 2010}.

I.1.8. Survival

The 5-year overall survival rate is 68.9% in Europe, with some geographical differences between Northern Europe (72.6%) and Southern Europe (63.7%) {Mallone et al, 2012}.

Metastasis is the single leading cause of mortality in uveal melanomas with 2-, 5-, and 10-year metastasis rates of 10%, 25% and 34%, respectively. The

median time from diagnosis of metastasis to death is less than 6 months {Diener-West et al, 2005}.

I.1.9. Genetic and epigenetic alterations in choroidal and ciliochoroidal melanomas

I.1.9.1. Background

The central role of genome in cancer development first emerged more than a century ago through demonstration of bizarre chromosomal aberrations in cancer cells by David von Hansemann and Theodor Boveri {Stratton et al, 2009}. It took another 70 years for this concept to be proven and to take a genomic approach to characterize cancer by launching the human genome project, the completion of which led to the development of the field of 'cancer genomics' {Garraway et al, 2013}. This went hand-in-hand with the emergence of high-throughput technologies that ushered in the 'omics' era providing new insights into cancer biology. This combination of genomic, transcriptomic and epigenomic data provides a multidimensional approach to unravel the molecular portrait of cancer {Cho 2010}. Application of these approaches has contributed to the emerging genetic landscape of uveal melanomas.

I.1.9.2. Copy number alterations

Chromosomal instability and its direct consequence, aneuploidy is a feature of cancer {Holland et al, 2012}. The chromosomal changes can be both numeric, involving gain or loss of whole chromosomes and structural, resulting in amplification, deletions or translocations {McGranahan et al, 2012}.

Most uveal melanomas exhibit low levels of aneuploidy compared to most other solid tumors {Harbour 2012}. Aneuploidy was observed in about 86/244 (35%) uveal melanomas in three independent studies {Meecham et al, 1986;

Coleman et al, 1995; Karlsson et al, 1995} which is lower compared to those of lung, bladder and ovarian (53-64%){Zack et al, 2013}.

Hence, the recurring chromosomal abnormalities reported in uveal melanomas are considered non-random and specific to tumor progression {Harbour 2012}. These aberrations frequently involve chromosomes 1, 3, 6 and 8; comprising of loss of 1p, 3, 6q and 8p and gain of 1q, 6p and 8q (**Table 1**). Other anomalies like loss of 9p and 16q are less commonly observed.

Chromosomal alteration*	N (%)
1p loss	296 (28%)
3 loss	564 (53%)
6p gain	436 (41%)
6q loss	267 (25%)
8p loss	219 (21%)
8q gain	575 (54%)

Table 1. Frequency of most common copy number alterations in uveal melanomas

** Data from a total of 1065 uveal melanomas from references: {Hoglund et al, 2004; Ehlers et al, 2008; Damato et al, 2010;*

Chromosome 1

Frequency

Loss of 1p occurs in about 28% (296/1065) of all uveal melanomas. It usually occurs in association with monosomy 3 (M3) {Hausler et al, 2005}.

Based on loss of heterozygosity (LOH) studies, the smallest common deleted region is considered to be about 55Mb extending from 1p31 to 1p35 {Hausler et al, 2005}. No mutations have been identified in this region, but there are

potential candidate genes like Notch pathway members *HES2* and *HES5*, and *TP73* {Kilic et al, 2008; Harbour 2012}.

Clinical relevance

Its presence has been correlated with other prognostic factors such as, tumor size, stage, ciliary body involvement and mitotic activity {Hausler et al, 2005; Damato et al, 2010}.

It is associated with shorter disease-free survival {Hausler et al, 2005; Kilic et al, 2005; Damato et al, 2010; Ewens et al, 2013}, but its impact may be due to its correlation with other prognostic factors{Ewens et al, 2013}.

Chromosome 3

Frequency

Monosomy 3 (M3) first identified in uveal melanomas more than 20 years ago by White and colleagues {Horsman et al, 1990} is the most extensively studied and prognostically relevant alteration {Ehlers et al, 2008; Damato et al, 2010; Ewens et al, 2013}. The loss can be complete or partial, the former reported in 53% (564/1065) of tumors. Rarely, it can be due to isodisomy (functional monosomy) {White et al, 1998}. It most commonly occurs in association with 8q gain {Sisley et al, 1997; Damato et al, 2010} and isochromosome 8q {Aalto et al, 2001; Ehlers et al, 2008}.

It has been extensively analyzed with the expectation that it may harbor tumor suppressor genes that may drive tumor progression. Several groups have attempted to characterize the minimally deleted region(s) and implicated loci like 3p13 {Blasi et al, 1999}, 3p25.3-24.3 and 3p25.1-3p25.2; {Parrella et al, 2003} and 3q24–q26 {Tschentscher et al, 2001}with putative candidate genes like *ROBO1*, *XPC*, *WNT7A* and *FBLN2*, but no mutations were identified to establish pathogenic relevance. This changed with the recent identification of

inactivating mutations in *BAP1*, located at 3p21.1 {Harbour et al, 2010} which is discussed in detail later.

Clinical relevance

M3 is associated with other variables such as, tumor size, extraocular extension, epithelioid morphology and mitotic activity {Damato et al, 2010}. The presence of M3 is associated with significantly higher melanoma-specific mortality {Damato et al, 2010; Ewens et al, 2013} due to its presence in predominantly metastasizing tumors. It is only the complete loss that facilitates an aggressive tumor behavior; whereas, reports on relevance of partial loss are variable ranging from good to intermediate clinical outcome {Damato et al, 2010; Abdel-Rahman et al, 2011}.

Chromosome 6

Frequency

The common alterations include 6p gain and 6q loss, reported in 41% (436/1065) and 25% (267/1065), respectively with the former receiving more attention. Occurrence of both abnormalities leads to isochromosome 6p, often associated with M3 {Aalto et al, 2001}; on the other hand, 6p gain alone and M3 are mutually exclusive {Ehlers et al, 2008}.

The minimal overlapping regions include 6p22-pter and 6q14-q23 {Aalto et al, 2001}, but no pathogenic mutations have been identified in them.

Clinical relevance

6p gain has been correlated with lack of ciliary body involvement {Bonaldi et al, 2008; Damato et al, 2010}.

Also, 6p gain is associated with non-metastasizing melanomas and with longer survival {Damato et al, 2010}. 6q loss is supposed to be more frequent in

metastasizing melanomas and with shorter survival {Aalto et al, 2001; Ewens et al, 2013}.

Chromosome 8

Frequency

The common alterations include 8q gain (54%; 575/1065) and 8p loss (21%; 219/1065), the latter commonly being part of isochromosome 8q {Harbour 2012}. About 45% of uveal melanomas have co-occurrence of M3 and 8q gain {Damato et al, 2010} and isochromosome 8q occurs almost exclusively in those with M3 {Ehlers et al, 2008}. The former have a positive correlation with 1p loss and negative association with 6p gain {Damato et al, 2010}.

The minimal deleted and amplified regions are 8p12-pter and 8q24.1-pter, respectively {Speicher et al, 1994; Aalto et al, 2001}. The former harbors a putative tumor suppressor gene, *LZTS1* {Onken et al, 2008} and the latter region contains potential oncogenes such as, *MYC* {Speicher et al, 1994}, *ASAP1* (*DDEF1*) {Ehlers et al, 2005} and *NBN* {Ehlers et al, 2005}. Specific amplification of *MYC* is reported in these tumors {Parrella et al, 2001} and *NBN* is its transcriptional target {Ehlers et al, 2005}. *ASAP1* plays a role in actin skeleton remodeling and cell motility; its expression correlates with gain of 8q and it is over-expressed in metastasizing melanomas {Ehlers et al, 2005}.

Clinical relevance

8q gain is associated with other clinical variables such as, tumor size, extraocular extension and histological variables like epithelioid morphology and mitotic activity {Damato et al, 2010}.

Both 8q gain and 8p loss are individually associated with metastasis-free survival {Damato et al, 2010; Ewens et al, 2013}. In addition, increasing additional copies of 8q are associated with worse prognosis; those with one or

two extra copies having relatively better survival than those with three or more extra copies {Sisley et al, 1997; van den Bosch et al, 2012}.
Co-occurrence of M3/8q gain has higher 10-year melanoma-specific mortality when compared to either M3 or 8q gain alone {Damato et al, 2010; Cassoux et al, 2013}.

Other chromosomal anomalies

Based on the meta-analysis of the cases (n=244) in Mitelman's database, other anomalies present in at least 20% of uveal melanomas include gain of 7 and loss of 9p, 10, 11q and 16q {Hoglund et al, 2004; Trolet et al, 2009}.

Sequence of chromosomal alterations in tumor progression

Based on the combination of chromosomal alterations, two pathways of uveal melanoma progression have been suggested. One is initiated by loss of chromosome 3 with associated gain of 8q and loss of 8p. They show 1p loss as a later event. The alternate sequence is initiated by gain of 6p, followed by 6q loss and other alterations such as, 16 loss {Hoglund et al, 2004; Trolet et al, 2009}. They also differ with respect to clinical outcome. The outcome is poor in the former and better with the latter {Trolet et al, 2009}.

I.1.9.3. Mutations

Genome instability is a characteristic feature of cancer cell genome {Hanahan et al, 2011}, the sources of which are mutations and chromosomal instability. Tumor cells accumulate mutations which facilitates their growth and progression through breakdown of mechanisms that monitor genomic integrity and/or increased sensitivity to mutagenic agents {Hanahan et al, 2011}.

Recently, recurrent mutations in five genes have been identified in uveal melanomas through application of whole-genome sequencing and are considered to drive tumorigenesis and progression (**Figure 2**).

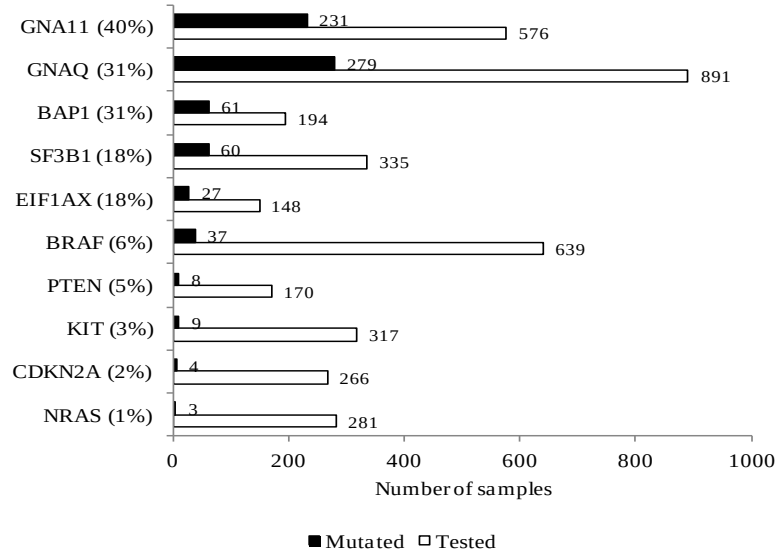

Figure 2. Frequent mutations in uveal melanomas
Source: http://cancer.sanger.ac.uk/cancergenome/projects/cosmic

GNAQ (9q21) and GNA11 (19p13)

Oncogenic mutations in RAS-RAF-MAPK pathway are widely prevalent in cancers {Hill et al, 2013}. Members of this pathway, *BRAF*, *NRAS* and *KIT* are

frequently mutated in cutaneous melanomas, but not in uveal melanomas. Discovery of mutations in *GNAQ/GNA11* as early events in uveal melanomas re-emphasized its importance in melanomagenesis {Onken et al, 2008; Van Raamsdonk et al, 2009}.

Frequency and mutational profile

GNAQ is mutated in 31% (279/891) and *GNA11* in 40% (231/576) of uveal melanomas {http://cancer.sanger.ac.uk/cancergenome/projects/cosmic }. They are somatic, gain-of-function mutations occurring in either of these genes; with concomitant mutations being very rare. In both these genes mutations occur exclusively at either codon 183 (exon 4) or codon 209 (exon 5); though very rarely both codons may be involved {Van Raamsdonk et al, 2009; Van Raamsdonk et al, 2010}. The glutamine at position 209 (Q209) is usually mutated to either leucine or proline.

Function

GNAQ [guanine nucleotide binding protein, q polypeptide] and *GNA11* [guanine nucleotide binding protein (G protein), alpha 11 (Gq class)] encode GTPases of G protein family. They act as signal transducers that connect receptors to intracellular signaling pathways such as, MAPK and PIK3/AKT {Neves et al, 2002; Hubbard et al, 2006; Patel et al, 2011; Bello et al, 2013; Sanchez-Fernandez et al, 2014}. In the MAPK pathway, they activate ERK1/2, JNK and p38 MAPK modules that control key cellular functions like proliferation, differentiation, migration and apoptosis {Turjanski et al, 2007}.

Oncogenic effects of mutant protein

This has been demonstrated in both *in vitro* and *in vivo* models. Human melanocytes transfected with mutant $GNAQ^{Q209L}$ show anchorage-independent growth and enlarged nuclei with irregular contours. Nude mice injected with

mutant melanocytes develop heavily pigmented tumors at injection sites {Van Raamsdonk et al, 2009}.

Oncogenic mechanism of mutant protein

GNAQ/GNA11 are active when bound to GTP and inactive when bound to GDP. This conversion is regulated by their GTPase domain. Mutations affecting codons 209 or 183 lead to complete or partial loss of this GTPase activity, respectively. As a consequence, the protein becomes locked in the active GTP bound state resulting in constitutive activation of downstream pathways {Chen et al, 2013}. This results in tumor development as MAPK activation stimulates melanocyte proliferation and decreases apoptosis {Van Raamsdonk et al, 2009; Chen et al, 2013}.

Clinical relevance

There is no correlation between mutation status and adverse clinicopathologic factors, chromosomal anomalies and survival {Bauer et al, 2009}.

Therapeutic relevance

The main strategy involves inhibition of the downstream, effector MAPK and PIK3/AKT pathways. This approach has been shown to reduce tumor growth in both *in vitro* and *in vivo* studies {Chen et al, 2013; Musi et al, 2014}. A recently concluded trial using selumetinib, a MEK inhibitor has shown promising results in metastatic uveal melanoma {2013}. Additional clinical trials targeting MAPK pathway are underway {Harbour et al, 2014}. Direct targeting of GNAQ/11 is as yet not possible due to lack of specific inhibitors {Harbour et al, 2014}.

BAP1 (3p21.31-p21.2)

Mutations in *BAP1* [BRCA1 associated protein-1 (ubiquitin carboxy-terminal hydrolase)] were first identified by Harbour and colleagues as occurring predominantly in metastasizing uveal melanomas with M3 {Harbour et al, 2010}. They are inactivating mutations which occur late in uveal melanoma progression coinciding with onset of metastatic behavior. Consistent with its presumed role as a tumor suppressor, it undergoes mutational inactivation in one copy and loss of other copy through M3 {Harbour et al, 2010}. In most sporadic melanomas, *BAP1* mutations are mostly somatic, with only about 3-4% demonstrating germline mutations {Njauw et al, 2012; Aoude et al, 2013}. However, germline mutations predispose to melanomas and other cancers in the familial setting (discussed below).

Frequency and mutational profile

BAP1 mutations are present in about 31.4% (61/194) of uveal melanomas. They are distributed throughout all exons and include both substitutions (~35%) and insertions/deletions (~47%) {http://cancer.sanger.ac.uk/cancergenome/projects/cosmic}. The out-of-frame deletions and nonsense mutations are truncating mutations leading to premature protein termination; whereas missense mutations are non-truncating, but probably lead to protein instability {Harbour et al, 2010}.

Function

BAP1 encodes a nuclear-localized deubiquitinating enzyme which regulates transcription and normal cell cycle, but prevents uncontrolled cell growth {Machida et al, 2009; Eletr et al, 2011} and functions as a tumor suppressor {Ventii et al, 2008} {White et al, 2012}.

BAP1 loss and metastatic behaviour

The precise role of *BAP1* loss in promoting metastasis remains unknown. In xenograft mouse models, *BAP1* depletion did not result in any of the expected behavior like increased proliferation, migration, invasion or tumorigenicity. Instead, it resulted in acquisition of a stem-like phenotype by uveal melanoma cells with increased capacity for self-replication and enhanced ability to grow in stem cell conditions {Matatall et al, 2013}. However, the link between these alterations and tumor dissemination remains to be elucidated.

Clinical relevance

The presence of *BAP1* mutation correlates with M3 and the gene expression profile characteristic of metastasizing tumors {Harbour et al, 2010}.

Therapeutic relevance

Considering its role in tumor progression, targeting mutant BAP1 or counteracting its phenotypic effect may be of therapeutic value. *In vitro* studies have demonstrated that in BAP1 deficient uveal melanoma cells histone deacetylase (HDAC) inhibitors can bring about reversal of stem-like phenotype to more differentiated cells {Matatall et al, 2013}. HDACs are being included in some uveal melanoma clinical trials {Harbour et al, 2014}.

SF3B1 (2q33.1)

Somatic mutations in splicing factor 3b, subunit 1, 155kDa (*SF3B1*) have been recently reported to occur predominantly in uveal melanomas lacking M3. They are mainly point mutations mostly affecting arginine at codon 625 {Furney et al, 2013; Harbour et al, 2013; Martin et al, 2013}. *BAP1* and *SF3B1* mutations are considered to be mutually exclusive.

Frequency and mutational profile

The prevalence of *SF3B1* mutations in uveal melanoma is about 18% (60/335). Mutational profiles comprise: missense mutations 58 (96.7%) and in frame deletions 2 (3.3%). Amongst the missense mutations, 52 (90%) involve arginine at codon 625 {http://cancer.sanger.ac.uk/cancergenome/projects/cosmic}.

Function

SF3B1 encodes a component of the spliceosome which is the intracellular machinery for splicing {Furney et al, 2013}.

Splicing converts precursor mRNA (pre-mRNA) to mRNA by removing the noncoding sequences (introns) and ligating together the coding sequences (exons). Alternative splicing refers to generation of variable forms of mRNA from the same pre-mRNA by splicing different exons. This phenomenon leads to different protein isoforms {Will et al, 2011}.

Mutant protein

Mutant SF3B1 leads to alternative splicing of genes such as, *ABCC5*, associated with multidrug resistance. However, their implication for uveal melanoma pathogenesis is presently not known {Furney et al, 2013}.

Clinical relevance

Mutant tumors are significantly associated with favourable prognostic factors such as, young age, lack of epithelioid cells, absence of M3 {Harbour et al, 2013} and better clinical outcome {Martin et al, 2013}.

EIF1AX (Xp22)

Eukaryotic translation initiation factor 1A, X-linked (*EIF1AX*) is the most recent gene reported to be recurrently mutated in uveal melanomas {Martin et al, 2013}.

Frequency and mutational profile

These mutations are present in 18% (27/148) of uveal melanomas {Martin et al, 2013; Dono et al, 2014}. They are predominantly missense, resulting in amino acid substitutions involving exons 1 and 2. *EIF1AX* and *SF3B1* mutations tend to occur in a mutually exclusive fashion {Martin et al, 2013}.

Function

EIF1AX encodes eukaryotic translation initiation factor 1A (eIF1A), which stimulates the transfer of methionyl initiator tRNA (Met-tRNAi) to the small (40S) ribosomal subunit {Martin et al, 2013}.

Mutant protein

Mutant EIF1AX is supposed to diminish the rate of translation; though its implication for melanoma pathogenesis is not known.

Clinical relevance

They occur mainly in tumors lacking M3 and have better clinical outcome.

Others

Somatic mutations in other genes, especially those involved in cutaneous melanomas are infrequent: *BRAF* 6% (37/639), *PTEN* 5% (8/170), *KIT* 3% (9/317), *CDKN2A* 2% (4/266) and *NRAS* 1% (3/281) {http://cancer.sanger.ac.uk/cancergenome/projects/cosmic }. Recently, mutations have also been reported in erythrocyte membrane protein band 4.1-like 3 (*EPB41L3*) in 1.8% (2/111) of uveal melanomas {Martin et al, 2013}.

The correlation between the above described genetic alterations has been schematized in **figure 3**.

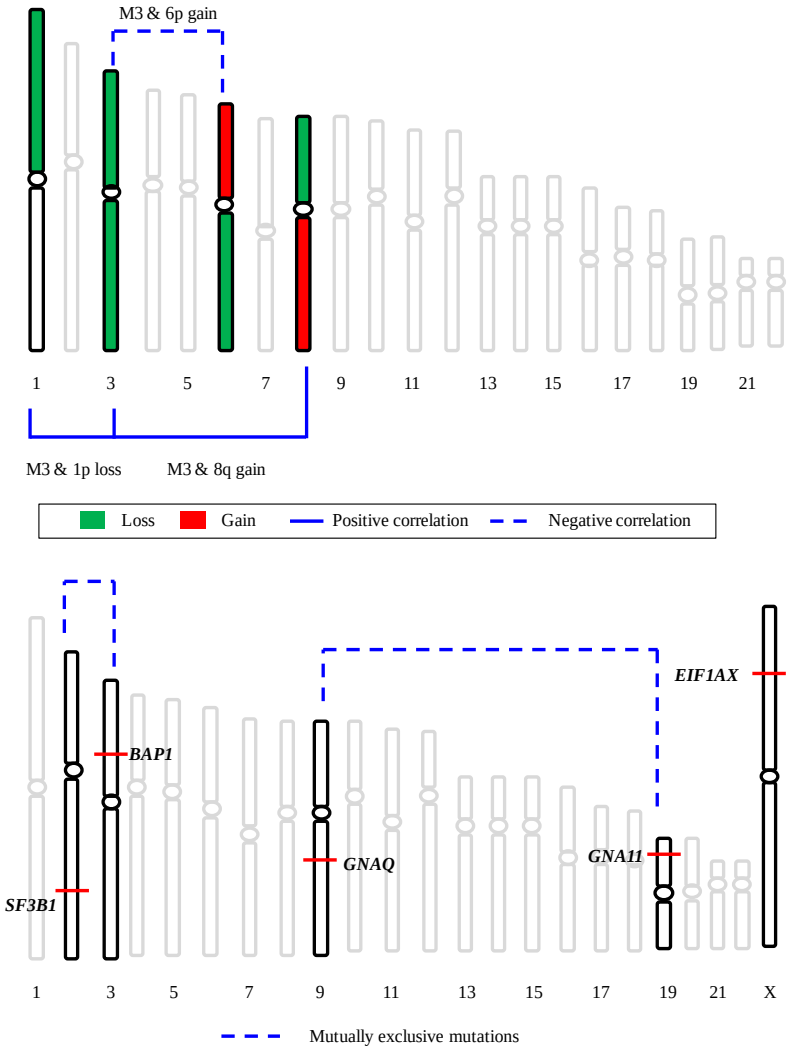

Figure 3. Correlations between copy number alterations and mutations in uveal melanomas

I.1.9.4. Transcriptomic profiles

The uveal melanoma transcriptome analyses have been carried out with two main objectives:

- to identify molecular subsets of the tumor based on their behavior (metastasizing vs. non-metastasizing)
- to better understand uveal melanomagenesis by comparing gene expression profiles of uveal melanocyte with that of uveal melanomas

Transcriptome-based tumor subgroups

The gene expression studies have identified two molecular subgroups of uveal melanomas {Onken et al, 2004; Singh et al, 2007; Petrausch et al, 2008; van Gils et al, 2008} {Onken et al, 2010; Laurent et al, 2011; Gangemi et al, 2012; Zhang et al, 2014} referred as 'class 1' and 'class 2'. The former are either non-metastasizing or metastasize late and the latter show early metastasis. In addition, Tschentscher, et al, have also compared the expression profiles of M3 tumors to that of disomy 3 {Tschentscher et al, 2003}.

The class 2 over-expressed (or class 1 under-expressed) genes are associated with cell migration and invasion such as, gap junction, adherens junction, ECM and angiogenesis {Onken et al, 2010; Zhang et al, 2014}; immune response and immune modulation {Singh et al, 2007} and cell signaling {Petrausch et al, 2008; Laurent et al, 2011}. This is to be expected as these genes are supposed to facilitate tumor cell motility and invasiveness. The class 2 under-expressed (or class 1 over-expressed) genes are related to: apoptosis {Singh et al, 2007; Zhang et al, 2014}; melanocyte development and differentiation {Onken et al, 2004; Zhang et al, 2014} and tumor suppressor genes {van Gils et al, 2008; Onken et al, 2010}. All this RNA work has led to the development of a

prognostic test, 'decisionDx-UM gene expression profile test' based on the expression of 15 genes {Harbour et al, 2013}. It can be performed using different types of tumor material (formalin fixed, fine-needle aspiration biopsy) and has been prospectively validated in a multi-centre study {Harbour et al, 2013}. Based on expression patterns, uveal melanomas are classified into class 1A, 1B and 2 with 5-year metastatic risk of 2%, 21% and 72%, respectively {Field et al, 2014}.

Comparison of expression profiles identified in different studies

Comparison of the top-discriminator genes reported in different studies demonstrates only a small degree of overlap. The reason for this is not clear. It may be due to differences in: sampling; RNA extraction protocols; type of microarray (Affymetrix, custom-made) used for hybridization and methodology applied to select significant genes {Petrausch et al, 2008}. Despite this, when these signatures are tested on independent cohorts, they accurately identify class 1 and class 2 sub-groups {Petrausch et al, 2008; van Gils et al, 2008}. **Table 2** indicates the overlapping genes between different studies and their functions.

Over-expressed in Class 2 tumors (metastasizing)										
Gene	**Chromosome**	**Study**								**Gene function**
		Singh	Tschentscher	Onken 2004	Onken 2010	Petrausch	Van Gils	Zhang	Laurent	
HTR2B	2q36		+		+		+			serotonin receptor; signals through GTPase, GNAQ
KIT	4q12	+		+						oncogene;,melanogenesis
PTGER4	5p13						+	+		prostaglandin receptor; immune modulation
RAB2A	8q12	+						+		GTPase;vesicular trafficking
KIAA1750	8q22		+	+						regulation of cell prolifertaion
PTP4A3	8q24					+			+	protein tyrosine phosphatase;cell signaling
PTPLA	10p14			+		+				protein tyrosine phosphatase;cell signaling
CDH1	16q22	+			+					cell adhesion
RAB31	18p11				+		+			G-protein;vesicle targeting
Under-expressed in Class 2 tumors (metastasizing)										
LPIN1	2p25		+	+						lipid metabolism
ROBO1	3p12		+		+					angiogenesis, neural crest migration
EIF1B	3p22			+	+			+		regulation of translation
LMCD1	3p26				+	+	+			regulates migration and differentiation
CHL1	3p26		+					+		neural cell adhesion molecule; possible signal transduction
PIK3R4	3q22			+		+				phosphoinositide biosynthesis
FXR1	3q28			+	+					fragile-X mental retardation; possible tumor suppressor
SPP1	4q22		+	+						bone mineralization;ECM receptor interaction
MTUS1	8p22				+	+	+			tumor suppressor
FZD6	8q22		+	+						negative regulator of Wnt/beta-catenin signaling
ENPP2	8q24	+		+			+			cell proliferation,motility
PHLDA1	12q15		+	+			+			anti-apoptotic
TIMP3	22q12	+	+							inhibitor of MMP and ECM

Table 2. Comparison of common genes between uveal melanoma signatures from different studies

(*From: {Tschentscher et al, 2003; Onken et al, 2004; Singh et al, 2007} {Petrausch et al, 2008; van Gils et al, 2008; Onken et al, 2010; Laurent et al, 2011; Zhang et al, 2014}*)

Transcriptomic profile of uveal melanoma versus uveal melanocyte

There are three studies that have made this comparison {Zuidervaart et al, 2003; An et al, 2011; Landreville et al, 2011; Bergeron et al, 2012}. The most under-expressed genes in uveal melanoma compared to uveal melanocyte were associated with biological processes such as, melanocyte differentiation (*DCT*, *RAB27A*, *MITF*, *TRPM1*, *TYR*), development and energy metabolism (*SLC16A6*, *ATP6V1A*, *GBA*) {Landreville et al, 2011; Bergeron et al, 2012}. The over-expressed genes in uveal melanomas were associated with cell division and proliferation (*ANLN*, *CKAP5*, *GLUL*, *TOP2A*, *LAMR1*, *ET2*) and cell adhesion (*ITGA6*) {Zuidervaart et al, 2003; Landreville et al, 2011}.

In addition, their comparison by RNA sequencing indicated a global alteration in uveal melanoma transcriptome with apparent disturbances in pathways such as, mitogen-activated protein kinase (MAPK) signaling, cell adhesion and melanogenesis {An et al, 2011}.

I.1.9.5. MicroRNA

Micro-RNAs (miRNA) are small, non-coding RNAs that regulate gene expression in many cellular processes, including cancer. They reduce translation and stability of messenger RNA (mRNA) {Farazi et al, 2013}. In cancer, they can either be oncogenic or tumor suppressors (oncomirs). miRNA expression profiling in cancers has led to the identification of signatures with diagnostic, prognostic and therapeutic relevance {Calin et al, 2006}.

miRNA expression in uveal melanomas

There are few studies that have assessed the miRNA expression profiles in these tumors {Worley et al, 2008; Radhakrishnan et al, 2009; Stark et al, 2010; Yang et al, 2011; Larsen et al, 2013} {Li et al, 2014}. Two of them identified miRNAs differentially expressed in metastasizing tumors compared to those without metastasis {Worley et al, 2008; Radhakrishnan et al, 2009}. The miRNAs over-expressed in metastasizing melanomas target tumor suppressor genes: *CDKN1A* for miR-586; *TP53* for miR-556; *BRCA2* for miR-181*; *RB1* for let-7b; as well as metastasis suppressor genes: *LZTS1* for miR-495; *DLC1* for let-7b and miR-495 {Worley et al, 2008; Radhakrishnan et al, 2009}. These miRNA have also been implicated in cell dedifferentiation and ovarian cancer {Worley et al, 2008}. Even though they were not located on chromosomes with frequent abnormalities (1p, 3, 6, 8), their altered expression correlated with presence of M3 {Worley et al, 2008}. However, there was no correlation with clinical outcome {Larsen et al, 2013}.

Yang, et al, identified the miRNA profile of uveal melanomas in comparison with normal choroid {Yang et al, 2011}. As expected, the melanoma over-expressed miRNAs are also considered oncogenic in other cancers such as, non-Hodgkin's lymphoma {He et al, 2005}, gastric and pancreatic cancers

{Xiao et al, 2009} {Dillhoff et al, 2008}. On the other hand, the under-expressed ones block cell proliferation and are pro-apoptotic {Akao et al, 2006; Li et al, 2014}. Other miRNAs (miR-182, -124a and -34b/c) have also been shown to play a role in regulation of uveal melanoma progression {Dong et al, 2012; Yan et al, 2012; Chen et al, 2013}.

Besides the tumors, alterations in miRNAs have also been demonstrated in peripheral circulation of uveal melanoma patients. The levels of some of them (miR-20a, -125b, -146a, -155 and 223) increase with the development of metastasis {Achberger et al, 2014}. Concomitantly, their expression was also increased in circulating T-cells and NK-cells {Achberger et al, 2014}. This is probably due to the role of these miRNAs in immune regulation {Tsitsiou et al, 2009}.

I.1.9.6. Methylation

Epigenetics refers to the mechanism that regulates gene expression without altering the DNA sequence. DNA methylation is an epigenetic regulatory mechanism implicated in various biological processes, including cancer. Hypermethylation of CpG-rich regions (CpG islands) localized at 5' end (near promoters) leads to gene silencing and is a common mechanism in tumor suppressor genes (TSG) {Esteller 2007; Pinto et al, 2014}.

Methylation studies in uveal melanomas have been performed mostly on single genes {Merbs et al, 1999; van der Velden et al, 2001; Edmunds et al, 2002; Lamperska et al, 2002; Maat et al, 2007; Maat et al, 2008; Calipel et al, 2011}or on few selected genes {Zeschnigk et al, 2003; Merhavi et al, 2007; Moulin et al, 2008}. Based on data from literature, about 33.5% (117/349) of tumors show hypermethylation for at least one tested gene. Common TSG in cancer with emphasis on chromosome 3 such as, *CDKN2A*, *RASSF1A*, *VHL*, *FHIT* and *CTNNB1* have been assessed, with the first two genes being tested in most studies. The relation between methylation and M3 is not reported in most of these studies except one, which did not find an association between *CDKN2A* methylation and M3 {Zeschnigk et al, 2003}.

CDKN2A and *RASSF1A* are hypermethylated in 11.6% (29/249) and 57.7% (71/123) of uveal melanomas, respectively. Even though the latter appears to be frequently involved, there is variability between studies. In addition, the hypermethylator phenotype of these two genes is associated with tumor progression {van der Velden et al, 2001; Maat et al, 2007}. There are as yet, no studies analyzing the global methylation profiles (methylome) of these tumors.

I.1.9.7. Genetic predisposition to uveal melanomas

Uveal melanomas are usually sporadic, but can be rarely familial occurring in multiple family members {Canning et al, 1988}. In addition, they also occur in families with strong history of other cancers {Abdel-Rahman et al, 2010}. This indicates that a subset of uveal melanomas could be part of a hereditary cancer predisposition syndrome.

BAP1 hereditary cancer predisposition syndrome

Germline mutations in *BAP1* have been identified in a small number of families with cancers {Abdel-Rahman et al, 2011; Testa et al, 2011; Wiesner et al, 2011; Carbone et al, 2012; Pilarski et al, 2014}.

The clinical phenotype of this syndrome includes uveal melanoma, mesothelioma, cutaneous melanoma, renal cell carcinoma, and melanocytic *BAP1*-mutated atypical intradermal tumors (MBAITs). The spectrum of associated neoplasms is still being characterized and may include other cancers as well {Pilarski et al, 2014}. It is autosomal dominant with incomplete penetrance for any cancer type {Harbour et al, 2014}.

A germline *BAP1* mutation should be suspected when a patient is diagnosed with uveal melanoma at an early age (younger than 30 years) or when one of more of the following is present in the patient or a first-degree relative: (1) multiple atypical cutaneous nevi, (2) cutaneous melanoma, (3) mesothelioma, (4) renal cell carcinoma, or (5) two or more primary cancers of any type. High-risk patients and family members should be offered *BAP1* sequencing of DNA from a blood sample {Harbour et al, 2014}.

The proposed guidelines for follow-up of mutation carriers are: annual or bi-annual ophthalmological and dermatological examinations, beginning at 11 years and 22 years of age, respectively; pulmonary and renal evaluation by

imaging and American cancer society screening guidelines {Battaglia 2014; Pilarski et al, 2014}.

Other predisposing genes

Germline mutations in *GNAQ/GNA11* have not been demonstrated in familial melanoma pedigrees with uveal melanomas {Hawkes et al, 2013}. Likewise, germline mutations are also extremely rare in *CDKN2A* and *CDK4* genes, unlike their cutaneous counterparts {Goldstein et al, 2006; Buecher et al, 2010}.

I.1.10. Iris melanomas

There are few studies which have analyzed the chromosomal aberrations in iris melanomas {White et al, 1995; Sisley et al, 1998; Mensink et al, 2011; Shields et al, 2011}. Chromosome 3 alterations in the form of partial (16/37, 43.2%) or complete monosomy (5/37, 13.5%) are present {Mensink et al, 2011; Shields et al, 2011}. Loss of 9p21, the region of *CDKN2A* has also been reported (7/20, 35%) {Mensink et al, 2011}. In view of the small sample size of these studies, it is difficult to compare them with the recurrent anomalies present in choroidal and ciliochoroidal melanomas.

Mutations in *GNAQ* are reported in 22% (2/9) {Onken et al, 2008} and *BRAF* in 47% (9/19) {Henriquez et al, 2007} of these tumors. The latter was observed mainly in recurrent tumors {Henriquez et al, 2007}. No information is available for mutations in *GNA11*, *BAP1*, *SF3B1* and *EIF1AX*.

There is only one study which has analyzed the transcriptomic profiles of iris melanomas {Harbour et al, 2013}. They were categorized as class 1 (low metastatic risk) and class 2 (high metastatic risk) based on the previously described DecisionDx test. They belonged to class 1 in 14 cases (67%) and

class 2 in 7 cases (33%) with none of the tumors developing metastasis during a follow-up period of 24 months {Harbour et al, 2013}.

I.1.11. Genetic features of metastasis of uveal melanoma

I.1.11.1. Copy number alterations

The reported recurrent anomalies are similar to primary tumors. In a single large series, the observed changes in hepatic metastases were: 1p loss (31/66, 47%), partial or complete monosomy 3 (48/66, 73%), 6p gain (21/66, 32%), 6q loss (42/66, 64%), 8p loss (30/66, 45%), 8q gain (59/66, 89%) and 16q loss (21/66, 32%). Gain of 1q (23/66, 35%) was an additional new aberration.

I.1.11.2. Mutations

Mutations in *GNAQ* and *GNA11* are present in 27% (17/64) and 56% (36/64) of metastases (from references {Van Raamsdonk et al, 2010; Abdel-Rahman et al, 2012; Griewank et al, 2014}). *SF3B1* mutations are infrequent 4% (1/26) {Griewank et al, 2014} which is to be expected since they are associated with tumors lacking M3. There is no information about *BAP1* mutations, but loss of BAP1 protein expression has been demonstrated (81%, 13/16) {Griewank et al, 2014}.

I.1.11.3. Methylation

MGMT is a DNA-repair protein epigenetically silenced in brain tumor, glioblastoma. It is infrequently methylated in hepatic metastasis of uveal melanomas {Voelter et al, 2008}.

I.2. Other melanomas

I.2.1. Genetic features of primary conjunctival melanomas

These tumors are part of ocular melanomas, but they do not share genetic features with their uveal counterparts. In fact, they are considered to be more similar to cutaneous melanomas {Griewank et al, 2013}.

I.2.1.1. Copy number alterations

The chromosomal aberrations in conjunctival melanomas are not as well characterized as in uveal melanomas. The largest cohort (n = 31) tested to date showed recurrent losses of: 1p, 3q, 6q, 8p, 9p, 10, 11q, 12q, 13, 15p, and 16q and recurrent gains of 1q, 3p, 6p, 7, 8q, 11q, 12p, 14p, and 17q {Griewank et al, 2013}. Amplification of *CDKN1A* and *RUNX2* loci (both 6p21.2) have also been demonstrated in 52.4% (11/21) and 76.2% (16/21) of tumors, respectively {Lake et al, 2011}.

I.2.1.2. Mutations

The mutational spectrum of conjunctival melanomas is yet to be characterized. Most studies have assessed for *BRAF* mutations, which occur in about 28% (47/168) of conjunctival melanomas {Griewank et al, 2013; Jin et al, 2013; Kenawy et al, 2013}. More than 90% of *BRAF* mutations occur at codon 600 with valine (V) being substituted for by glutamic acid (E) referred as V600E {Lake et al, 2011; Griewank et al, 2013}. Mutations in *NRAS* and *KIT* occur in about 14% (14/97) {Griewank et al, 2013; Kenawy et al, 2013} and 4% (3/75) of tumors, respectively {Torres-Cabala et al, 2009; Wallander et al, 2011; Griewank et al, 2013; Jin et al, 2013}. *BRAF* and *NRAS* mutations occur in a mutually exclusive manner and show no correlation with clinical outcome {Griewank et al, 2013}. Recently, mutations in *TERT* promoter have also been

identified in 32% (12/32) of conjunctival melanomas {Griewank et al, 2013}. They lack mutations in *GNAQ/GNA11* {Dratviman-Storobinsky et al, 2010} {http://cancer.sanger.ac.uk/cancergenome/projects/cosmic } (**Figure 4**).

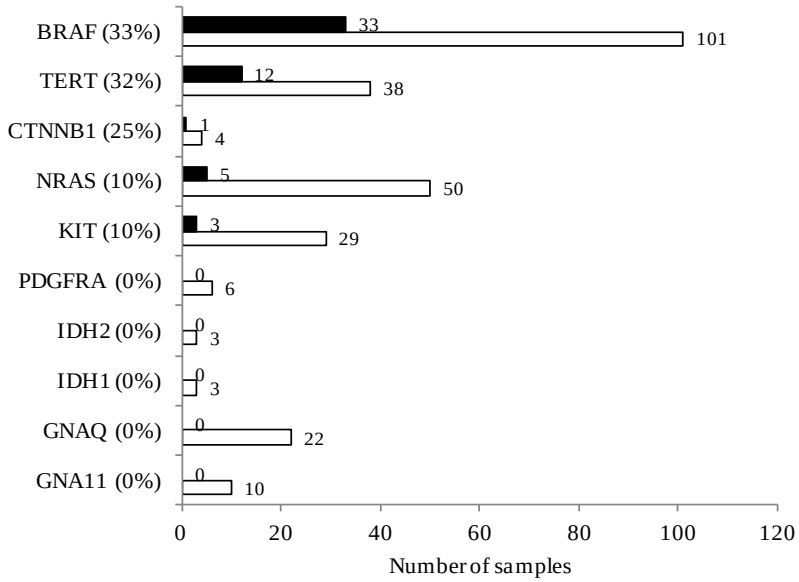

Figure 4. Frequent mutations in conjunctival melanomas
Source: http://cancer.sanger.ac.uk/cancergenome/projects/cosmic

I.2.2. Genetic features of cutaneous melanoma

I.2.2.1. Copy number alterations

The common copy number alterations include: gains on chromosomes 1q, 6p, 7, 8q, 17q and 20q and losses on chromosomes 6q, 9p, 10 and 21q {Curtin et al, 2005; Krauthammer et al, 2012}.

I.2.2.2. Mutations

Both germline and somatic mutations have been implicated in the etiology of cutaneous melanomas. Three high-risk melanoma susceptibility genes have been identified: *CDKN2A* (30-40%), *CDK4* (2-3%) and *BAP1*, with the last being present in cutaneous melanomas in conjunction with uveal melanomas {Goldstein et al, 2006; Hill et al, 2013}.

Somatic mutations are most frequently observed in: *BRAF* (45%, 6620/15235) and *NRAS* (17%, 1240/7173) genes which are part of the RAF-MEK-MAPK pathway {http://cancer.sanger.ac.uk/cancergenome/projects/cosmic; Davies et al, 2002; Hill et al, 2013}. Other mutated genes are: *CDKN2A* (23%, 406/1753), *TERT* (22%, 188/871) and *KIT* (10%, 305/3554) {http://cancer.sanger.ac.uk/cancergenome/projects/cosmic ; Curtin et al, 2006} (**Figure 5**).

Recently, whole-exome studies including more than 100 samples have identified novel highly mutated genes: *PPP6C*, *RAC1*, *SNX31*, *TACC1*, and *STK19* {Hodis et al, 2012; Krauthammer et al, 2012} in addition to the previously known genes. Another significant finding was recurrent mutations of *NF1* in *BRAF* and *NRAS* wild-type samples {Hodis et al, 2012; Krauthammer et al, 2012}. In addition, *RAC1* mutations frequently occurred in sun-exposed melanomas with UV-signature {Krauthammer et al, 2012}.

Mutations in *GNAQ* (0.8%, 7/862) and *GNA11* (0.2%, 2/773) are almost non-existent {http://cancer.sanger.ac.uk/cancergenome/projects/cosmic}.

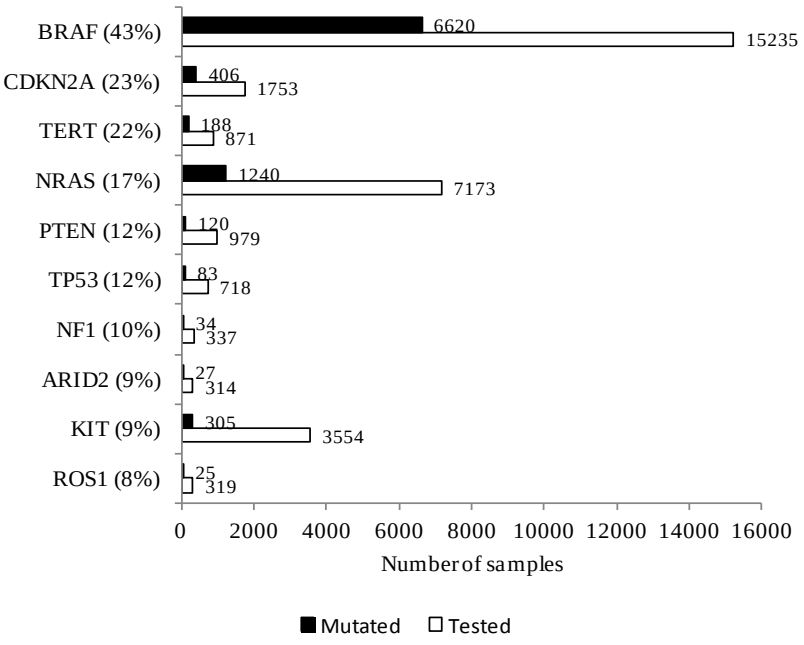

Figure 5. Frequent mutations in cutaneous melanomas
Source: http://cancer.sanger.ac.uk/cancergenome/projects/cosmic

I.2.3. Comparison of genetic features between uveal and other melanomas

The main differences between uveal melanomas and other melanomas have been summarized in **Figures 6&7 and Table 3**. Uveal melanomas are about 30 times less common than cutaneous melanomas, with a 5-year survival rate lower than their cutaneous counterparts. Also, in uveal melanomas liver is the favoured site of metastases when compared to lymph nodes, skin and subcutis favoured by cutaneous ones. The mutations which drive melanomagensis are *GNAQ/GNA11* in uveal tumors and *BRAF*, *CDKN2A* and *NRAS* in cutaneous ones.

On the other hand, there is not much data available for conjunctival melanomas, which are much rarer than uveal melanomas. Analysis of small cohorts of these tumors has indicated presence of *BRAF*, *NRAS* and *TERT* mutations in these tumors. Hence, they appear to be genetically similar to cutaneous melanomas.

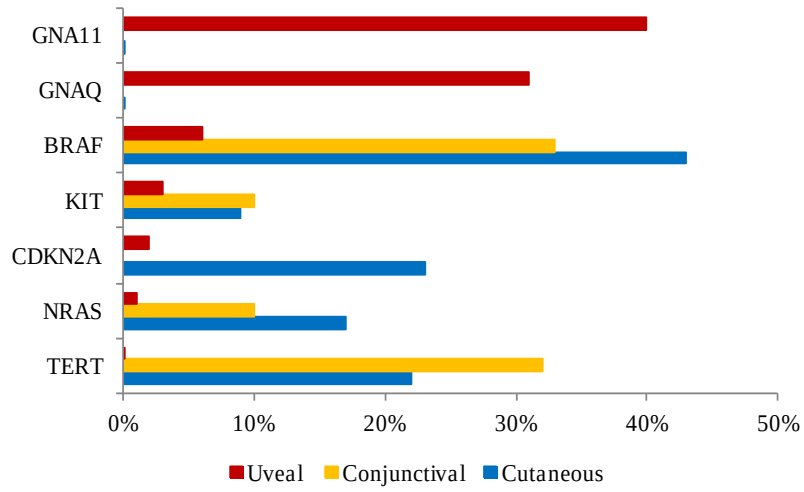

Figure 6. Comparison of frequent mutations in different melanoma subtypes
Source: http://cancer.sanger.ac.uk/cancergenome/projects/cosmic

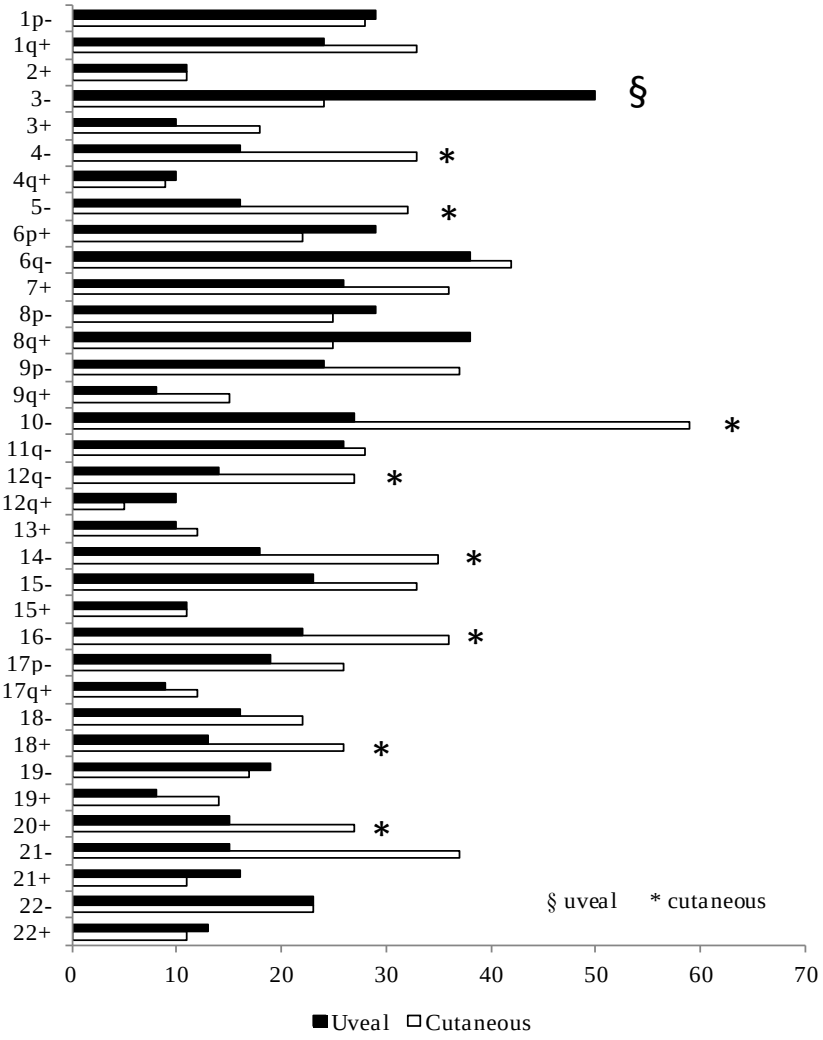

Figure 7. Copy number number alterations in uveal vs. cutaneous melanoma (f*rom: Hoglund et al, 2004)*
The indicated significantly different alterations are based on p-value <0.01

Parameter	**Uveal**	**Conjunctival**	**Cutaneous**	References
Incidence (cases per million) Trend	5.6 Stable	0.4 NA	171.6 Increasing	{Bishop et al, 2013} {McLaughlin et al, 2005}
Median age	59	62	59	{Shields et al, 2000; Shields et al, 2009; Bishop et al, 2013}
Male:female ratio	1.1	0.99	1.3	{McLaughlin et al, 2005}
5-year survival rate	68.9%* 81.6%**	93%	89%	{Mallone et al, 2012} {Singh et al, 2011} {Shields et al, 2000} {Bishop et al, 2013}
Modes of dissemination	Hematogenous	Lymphatic Hematogenous	Lymphatic Hematogenous	
Sites of dissemination	**Liver (89%)** Lung (29%) Bone (17%) Skin & subcutis (12%)	**Lymph nodes (66%)** Brain (15%) Liver (11%) Lung (8%)	Skin (13–38%) Lymph nodes (5–34%) Subcutis (32%) Lung (18–36%) Liver (14–20%) CNS (2–20%) Bone (4–17%)	{Diener-West et al, 2005} {Shields et al, 2000} {Leiter et al, 2004}
Genetic features <u>*Mutations*</u> <u>*Copy number alterations*</u>	 ***GNAQ/GNA11*** *BAP1* *SF3B1* *EIF1AX* 1p-, **3-**, 8p-6p+, 8q+	 *BRAF* *NRAS* *TERT* 9p-, 6p+,7p+,8q+, 11q+	 ***BRAF*** *NRAS* ***CDKN2A*** 4-,5-,**10-**,12q-,14-,16-	 {http://cancer.sanger.ac.uk/cancergenome/projects/cosmic } {Hoglund et al, 2004} {Griewank et al, 2013}

Table 3. Comparison of distinctive aspects of melanoma subtypes

** Europe * * USA ;* ***in bold****: distinctive feature*

II. Immune and cancer

II.1. Immune microenvironment in cancer

II.1.1. Historical aspect

The link between immune system and cancer dates back to a century when the concept that immune system contributes to cancer control was first proposed by Paul Ehrlich in 1909 {Riether et al, 2013}. This was followed fifty years later by the 'immunological surveillance' theory of Thomas and Burnet {Burnet 1970; Thomas 1982} which proposed that immune system recognized and destroyed cancer cells in early stages of tumor development. Following subsequent challenges, the concept of cancer immunosurveillance was validated and expanded {Shankaran et al, 2001; Dunn et al, 2004}. These further studies led to the emergence of the concept of 'cancer immunoediting' to describe the interaction of the tumor with the host immune system encompassing three phases: elimination, equilibrium and escape {Shankaran et al, 2001}. Elimination phase promotes complete removal of malignant cells and is the classical concept of cancer immunosurveillance; equilibrium phase is the period of immune-mediated latency and escape refers to outgrowth of tumors that have overwhelmed the immune system {Dunn et al, 2004}.

II.1.2. Tumor microenvironment

II.1.2.1. Concept

Over the last decade, the focus of cancer research has expanded to incorporate the 'tumor microenvironment' (TME) constructed by cancer cells during the multistep process of tumorigenesis {Hanahan et al, 2012}. They enlist the help

of normal host cells and establish collaborative interactions with the stroma {Hanahan et al, 2012} to take advantage of the host for energy and nutrients.

II.1.2.2. Components

The components of TME can be broadly divided into vasculature and stromal cells. The former includes blood vessels and lymphatics. The stromal cells can be divided into three major types with a spectrum of subpopulations within each subtype {Hanahan et al, 2012}:

- Infiltrating immune cells: lymphocytes, macrophages, monocytes, neutrophils, mast cells
- Angiogenic vascular cells: endothelial cells, pericytes
- Cancer associated fibroblastic cells: fibroblasts, myofibroblasts, mesenchymal stem cells

The rest of the section will focus on the immune cell component of the microenvironment.

II.1.3. Role of immune microenvironment

Virtually every neoplastic lesion contains immune cell infiltrate ranging in densities from subtle to dense. Much progress has been made in assessing these immune cells since their observation under the microscope. These advances can be attributed to progress in availability of markers to subtype various immune cells, application of microarray technologies to dissect the immune landscape and analysis of large cohorts of tumors.

II.1.3.1. Infiltrating immune cells

Inflammatory cells are assimilated into the neoplastic process through chronic infection and inflammation. There are many examples such as, inflammatory bowel disease predisposing to colon carcinogenesis, hepatitis C for liver cancer

and Heliocobacter pylori infection being the commonest cause of gastric cancer {Coussens et al, 2002}. However, the subtle infiltrates observed in most cancers do not qualify as inflammation, but play a role in cancer progression. Hence, the term 'infiltrating immune cells' (IICs) is applied to them {Hanahan et al, 2012}.

They include cells of both innate and adaptive immune systems. The former includes tumor-associated macrophages (TAMs), dendritic cells; myeloid-derived suppressor cells (MDSCs), granulocytes, TIE2-expressing monocytes and natural-killer cells. The latter cells are B- and T-lymphocytes (**Figure 8**).

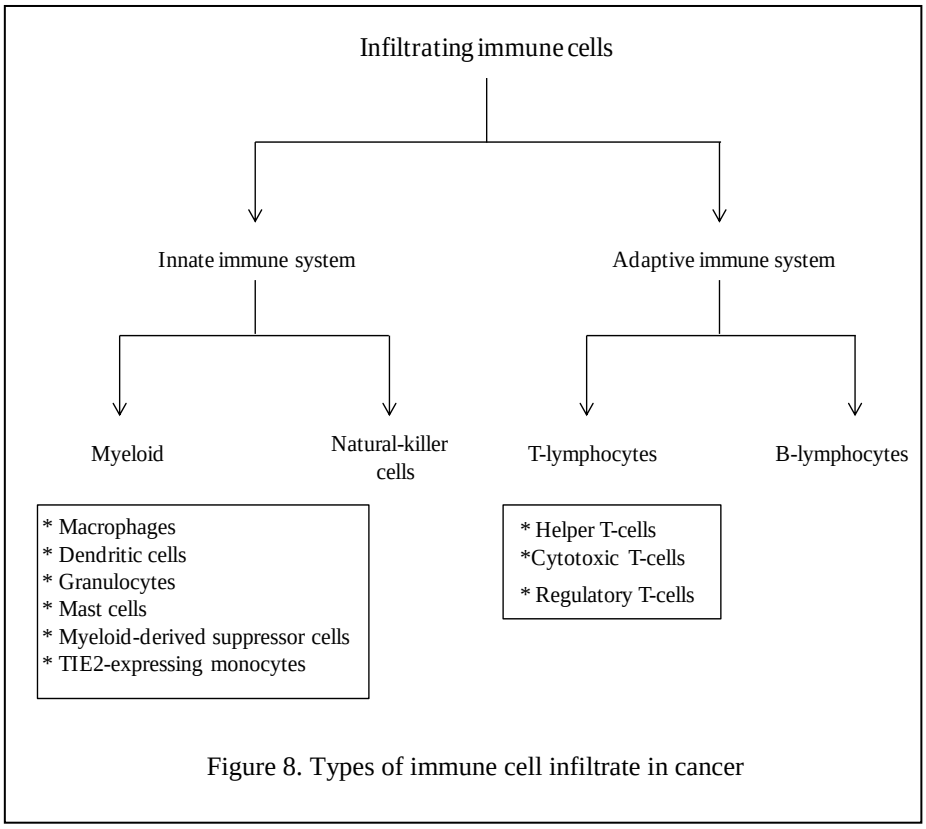

Figure 8. Types of immune cell infiltrate in cancer

II.1.3.2. Pro-tumorigenic and anti-tumorigenic effects of infiltrating immune cells

From the concept of cancer immunoediting it is clear that the immune system has the capacity to either block tumor development or to promote tumor progression. As to which side the immune system is polarized towards depends on the balance between the protumor and antitumor influence of both innate and adaptive immunity {Ostrand-Rosenberg 2008}.

Both these aspects of the tumor immune microenvironment will be discussed in the following sections.

II.1.3.3. Hallmarks of cancer

The hallmarks of cancer are biological capabilities when acquired by normal cells enables them to become tumorigenic and ultimately, malignant. They provide a logical framework for understanding the diversity and complexity of cancer biology {Hanahan et al, 2000} {Hanahan et al, 2011}. The immune component is an active participant in supporting the cancer cells in acquiring these hallmark capabilities.

The original core hallmarks were:

- Sustaining proliferative signaling
- Evading growth suppressors
- Resisting cell death
- Enabling replicative immortality
- Inducing angiogenesis
- Activating invasion and metastasis

Following a recent update, in keeping with the accumulation of scientific evidence over the decade, two enabling characteristics and two emerging hallmarks have been included (**Figure 9**). The former facilitate the acquisition

of other hallmarks; whereas, the latter are functionally important for development of cancer {Hanahan et al, 2011}.

Enabling characteristics:

- Genome instability and mutation
- Tumor-promoting inflammation

Emerging hallmarks:

- Reprogramming energy metabolism
- Evading immune destruction

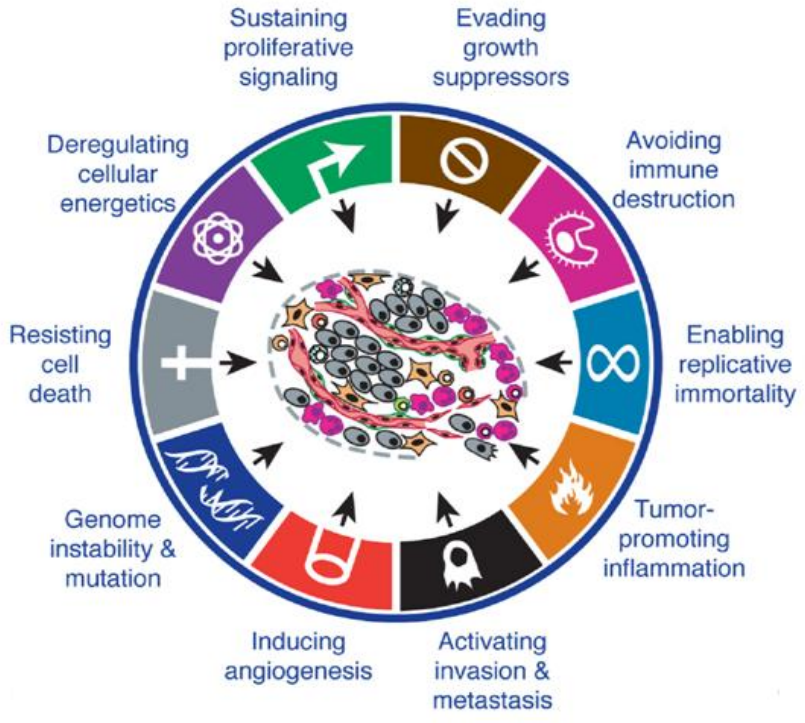

Figure 9. Hallmarks of cancer

From: Hanahan D & Weinberg RA. Cell. 2011;144: 646-74

II.1.3.4. Pro-tumorigenic effects of immune cells from the perspective of cancer hallmarks

Sustaining proliferative signaling

The immune cells in the milieu can drive increased proliferation, promoting tumor growth {Grivennikov et al, 2010}. IICs supply mitogenic signals to tumor cells both directly and indirectly. The former is by production of factors such as chemokines and cytokines; transforming growth factor- beta (TGF-β), tumor necrosis factor-alpha (TNF-α) and fibroblast growth factors (FGFs), which in turn mediate activation of transcription factors, NF-κB, STAT3, HIFs and AP-1 that stimulate cell proliferation and survival {Grivennikov et al, 2010; Wu et al, 2014}. For instance, in colon cancer interleukin-6 (IL-6) produced by immune cells activates *STAT3* which controls cell proliferation and survival by regulating the expression of *MYC*, *MCL1*, *CCND1* and *BCL2* {Becker et al, 2004}.

Another mechanism is through production of diverse proteolytic enzymes that degrade the extracellular matrix (ECM) to release mitogenic mediators {Grivennikov et al, 2010; Lu et al, 2011; Hanahan et al, 2012}. Deregulated ECM dynamics can activate growth factor signaling pathways such as Wnt, FGF, integrin that can promote cell proliferation and survival {Lu et al, 2011}. For example, tumor infiltrating macrophages and neutrophils secrete proteases which promote proliferation of breast cancer cells {Glondu et al, 2002; Mohamed et al, 2006}.

Evading growth suppressors

Maintenance of tissue architecture, organization and polarity is achieved by the crosstalk between the cell and it's surrounding ECM. Disruption of these interactions can lead to loss of this inhibitory effect. If normal tissue

architecture and polarity is a ‘tumor suppressor’, then proteases which degrade ECM can be considered as ‘oncogenic’{Nelson et al, 2006}. Immune cells through their secretion of proteolytic enzymes can lead to destruction of tissue organization and thereby to loss of its regulatory effect {Mohamed et al, 2006; Lu et al, 2011}.

Evidence from *in vivo* and *in vitro* models has shown that genetic ablation of proteases can attenuate cancer development {Mohamed et al, 2006}; whereas, the presence of matrix-metalloproteinases (MMPs) can alter cellular morphology and lead to impairment of cell-cell interactions {Nelson et al, 2006}.

Resisting cell death

A primary response to inflammation is increased survival of the target cell through blockade of apoptosis by immune mediators {Chen et al, 2010}. This analogy can also be extended to immune cells in the microenvironment which aid the cancer cells to evade death through activation of anti-apoptotic mechanisms. For example, in cancers of liver and colon, the infiltrating macrophages produce IL-6 which leads to induction of anti-apoptotic molecules like Bcl2l1 and Bcl-2 {Atreya et al, 2005; Liu et al, 2010}.

Enabling replicative immortality

Telomeres protect the ends of chromosomes and are involved in capacity for unlimited cell proliferation. Prevention of teleomere loss can lead to immortalization of a cell. However, presently, there is no evidence for the role of immune infiltrate in telomere stabilization {Hanahan et al, 2012}.

Inducing angiogenesis

Angiogenesis is the outgrowth of new vessels from pre-existing vessels {Naumov et al, 2006}. Tumor growth beyond the critical size of about 1-2mm^3 requires the formation of neovessels. This change in phenotype from non-angiogenic to angiogenic is termed as the 'angiogenic switch' {Naumov et al, 2006}. The angiogenic switch is driven by hypoxia leading to expression of HIF-1α tilting the balance in favour of a pro-angiogenic state. The latter is accomplished through combined efforts of tumor cells, as well as those of the microenvironment. Together, they contribute various soluble factors such as vascular endothelial growth factor (VEGF), platelet-derived growth factor (PDGF), angiopoietins; growth factors such as, fibroblast growth factor (FGF), epidermal growth factor (EGF), insulin-like growth factor (IGF); cytokines and chemokines including integrins, IL-1, IL-6; proteolytic enzymes which degrade the ECM such as, MMPs all of which contribute to vascular proliferation, motility and tissue remodeling culminating in formation of new vessels {Weis et al, 2011; Mittal et al, 2014}.

The pro-angiogenic role of immune cells has been investigated in experimental models. Depletion of macrophages and neutrophils in animal models decreased angiogenesis and delayed angiogenic switch; while their restoration reversed the effects {Lin et al, 2006; Nozawa et al, 2006; Zhang et al, 2010}.

Activating invasion and metastasis

The development of metastasis involves several steps comprising of: epithelial-to-mesenchymal transition (EMT) and local invasion; intravasation into vasculature; transit through circulation; extravasation and seeding, followed by survival and growth at metastatic site {Smith et al, 2013}. The immune cells in

the TME facilitate establishment of metastases by aiding the tumor cells in each of these stages.

EMT is the initial process wherein the tumor cells develop mesenchymal characteristics and acquire the invasive, migratory phenotype. Macrophages, lymphocytes, neutrophils secreted soluble factors such as, interleukins, IL-6, IL-8; TNF-α, and TGF-β can initiate EMT. In addition, the tumor cells undergoing EMT release cytokines like IL-6, IL-8 which act in a paracrine fashion on adjoining tumor cells to facilitate their transition {Palena et al, 2012; Smith et al, 2013}.

Migration of tumor cells requires ECM remodeling by proteolytic enzymes which are secreted by macrophages, lymphocytes, mast cells and neutrophils {Mohamed et al, 2006; Hua et al, 2011; Smith et al, 2013}.

Once they enter the circulation, the tumor cells need to survive the turbulence, as well as the exposure to natural-killer (NK) cells for successful establishment of metastasis. The circulating tumor cells cover themselves with platelet aggregates through activation of coagulation cascade. Platelets improve their chances of survival by providing a physical barrier against shear forces and also by suppressing NK cell cytotoxic activity {Sharma et al, 2014}.

Even before the circulating tumor cells reach the site/s of metastasis, the primary tumor secretes certain growth factors to create premetastatic and metastatic niche. They constitute favorable local environment for the arriving tumor cells to survive and proliferate. At these niches, myeloid-derived suppressor cells and TAMs secrete soluble factors, chemokines and MMPs to aid tumor cell engraftment {Psaila et al, 2009; Smith et al, 2013}.

Genome instability and mutation

An unstable genome is a hallmark of cancer resulting from increased DNA damage or defective repair mechanisms {Hanahan et al, 2011}. Reactive oxygen species and nitrogen intermediates generated by inflammatory cells can induce DNA damage {Colotta et al, 2009}. They contribute to genomic instability through different mechanisms such as, downregulation of mismatch repair (MMR) proteins which correct base mispairing, defective mitotic checkpoints through inactivation of retinoblastoma protein and directly by inducing double-strand breaks {Colotta et al, 2009}. Colitis associated cancers show decreased MMR protein and activated neutrophils in colitis have been demonstrated to increase replication errors in colonic cells {Campregher et al, 2008}.

Reprogramming energy metabolism

Tumor cell metabolism is adapted to provide abundant ATP to maintain energy status and increased synthesis of biomolecules to sustain cell proliferation and survival. They use alternative metabolic pathways than normal cells. The best characterized metabolic phenotype in cancer cells is Warburg effect which refers to use of glycolysis to produce energy under normoxic conditions {Cairns et al, 2011; Phan et al, 2014}.

The metabolic phenotype of tumor cells is shaped by genetic alterations, as well the microenvironment. There are as yet, no genetic studies demonstrating alteration of tumor metabolism by immune cells. However, in view of the influence of macrophages on metabolism in obesity and other metabolic pathologies, one would expect an association in cancer cell metabolism as well {Biswas et al, 2012; Hanahan et al, 2012}.

Evading immune destruction

The tumor cells have developed multiple mechanisms to escape detection and killing by immune system. The main mechanisms by which they accomplish this include:

- *Reduced immunogenicity*

Through altered expression of cell surface molecules like MHC class I and II utilized by immune cells to recognize cancer cells

- *Resistance to immune-mediated killing by cytotoxic T-cells*

By downregulation or mutation of death receptors such as, Fas and TRAIL

- *Direct suppression of effector T-cells*

Expression of indoleamine 2,3-dioxygenase (IDO) which inhibits T-cell proliferation

- *Creating an immune suppressive microenvironment*

Through alteration of the balance between innate and adaptive immune cells and cytokine signaling network {Lakshmi Narendra et al, 2013; Burkholder et al, 2014; Mittal et al, 2014}.

Amongst these, the tumor-induced changes in immune cell populations in TME are considered the most important mechanism of immune evasion {Burkholder et al, 2014}. The immune cells that contribute to tumor progression by immunosuppression are: TAMs, regulatory T-cells (Tregs), MDSCs, Th2 CD4+ T-cells and neutrophils. In addition, the cytokine milieu containing TGF-β, chemokines and cytokines (IL-4, IL-6, IL-10, IL-13) also contribute towards evasion of immunosurveillance {Stewart et al, 2011; Burkholder et al, 2014}.

Another way of looking at these hallmarks is their application to uveal melanomas per se. This has been done in **Table 4**, where the hallmarks have been adapted to uveal melanomas and the experimental evidence has been indicated.

Hallmark	Mechanism	Applied to uveal melanoma	References
Sustaining proliferative signaling	Activation of key signaling pathways	GNAQ/GNA11 mutations: Constitutive activation of MAPK pathway and melanocyte proliferation PI3K/Akt pathway activation: melanocyte proliferation and survival	{Saraiva et al, 2005; Van Raamsdonk et al, 2009; Babchia et al, 2010; Van Raamsdonk et al, 2010}
Evading growth suppressors	Loss or inhibition of *RB1* and *TP53* tumor suppressor pathways	RB1 inactivation through hyperphosphorylation Inhibition of TP53 protein through *MDM2* overexpression	{Brantley et al, 2000} {Brantley et al, 2000} {Coupland et al, 2000}
Resisting cell death	Anti-apoptotic and pro-apoptotic signals	Overexpression of anti-apoptotic molecules: Bcl2 PI3K/Akt pathway activation: decreased apoptosis	{Brantley et al, 2000} {Babchia et al, 2010}
Enabling replicative immortality	Prevention of telomere loss	Increased telomerase activity	{Heine et al, 2000}
Inducing angiogenesis	Pro-angiogenic signals	VEGF and its receptor (VEGFR2) are expressed by uveal melanoma cells	{Li et al, 2014} {Ijland et al, 1999; Logan et al, 2013}

Table 4. Hallmarks of cancer adapted to uveal melanoma

Hallmark	Mechanism	Applied to uveal melanoma	References
Activating invasion and metastasis	Adhesion molecules, extracellular matrix degradation, epithelial-mesenchymal transition	Increased expression of cell adhesion molecules (ALCAM, MCAM): increase tumor cell motility and metastasis in uveal melanomas HGF associated activation of PIK3/Akt: increased uveal melanoma cell migration Overexpression of matrix metalloproteinases (MMP-1,-9,-19) by uveal melanoma cells Aberrant activation of Hedgehog pathway: increased migration and EMT in uveal melanoma cells	{Jannie et al, 2012} {Beutel et al, 2009} {Lai et al, 2008; Ye et al, 2008} {Duan et al, 2014}
Reprogramming energy metabolism	Tumor hypoxia leads to increased glycolysis Upregulation of glucose transporters (GLUT) to import glucose into the cell for glycolysis	Upregulation of HIF-1α increases glycolysis: uveal melanoma cells overexpress HIF-1α	{Mouriaux et al, 2014}
Evading immune destruction	Impairment of T-cell function	As described in detail in section on immune microenvironment in uveal melanoma	
Genome instability and mutation	Mutations, copy number alterations, epigenetic modifications	As described in detail in section on genetics	
Tumor-promoting inflammation	Immune cell infiltration	As described in detail in section on immune microenvironment in uveal melanoma	

Table 4. Hallmarks of cancer adapted to uveal melanoma (continued)

II.1.3.5. Anti-tumorigenic effects of immune cells

The evidence for tumor destruction by immune cells has mainly come from mouse models. Immunodeficient mice develop more spontaneous and carcinogen induced tumors than immunocompetent ones {Dunn et al, 2006}. In addition, accumulation of data from studies on large cohorts of human cancers have indicated that presence of high numbers of T- lymphocytes is an indicator of good prognosis in different cancer types such as, cutaneous melanoma; cancers of lung, breast, ovary, esophagus and colorectal (discussed in detail further below). The principal cells involved in anti-tumor immunity are CD4+ helper (Th1) and CD8+ effector cells, respectively. They promote tumor destruction and long-term immune memory against recurrence {Yu et al, 2006; Ostrand-Rosenberg 2008}. In addition, cells such as macrophages and neutrophils can have both pro- and anti-tumorigenic roles depending on their phenotype. There are two phenotypes of macrophages: M1 and M2. M1 is important for defense against infections and can be tumoricidal. M2 is involved in angiogenesis, tissue remodeling and anti-inflammatory processes. Tumor-associated macrophages are considered to be of M2 type. Likewise, there are N1 (anti-tumor) and N2 (pro-tumor) neutrophils.

The main pro- and anti-tumorigenic actions of individual cell types have been summarized in **Table 5**.

Cell type	Pro-tumorigenic actions	Anti-tumorigenic actions
Macrophages M1: Pro-inflammatory M2: Pro-angiogenic, anti-inflammatory	Immunosuppression; ECM remodeling; angiogenesis; proliferation	Antigen presentation T-cell activation
Dendritic cells (DCs)	T-cell anergy; promote Treg expansion (immature DCs)	Antigen presentation and priming of T-cells (mature DCs)
Neutrophils	ECM remodeling; angiogenesis; proliferation	Direct cytolysis
MDSCs (Immature myeloid cells)	Immunosuppression Treg recruitment angiogenesis	
Mast cells	Angiogenesis Recruitment of MDSCs	Enhancement of NK-cell activity
TIE2-expressing monocytes	Angiogenesis; tissue remodeling	
Natural-killer cells		Direct cytotoxicity
Cytotoxic (CD8) T-cells		Direct cytotoxicity
Helper (CD4) T-cells		Help CD8 cells in tumor cell lysis
Regulatory T-cells (Tregs)	Immunosuppression	

Table 5. Pro- and anti-tumorigenic actions of immune cell subtypes

II.1.3.6. Molecular mechanisms linking immune cells and cancer

The important players linking immune infiltrate and cancer include: tumor-associated antigens; chemokines and cytokines; transcription factors (TF) *NF-κB*, *STAT1*/*STAT3* and hypoxia-inducible factor (*HIF*); lipid mediators; reactive oxygen species and nitric oxide intermediates {Porta et al, 2009; Wu et al, 2014}. The most important ones are described below.

Tumor-associated antigens

Tumor-associated antigens (TAA) are fundamental triggers of T-cell response against tumors {Spurrell et al, 2014}. The main sources of TAAs are:

- *Cancer-germline genes*

Their expression is normally restricted to spermatocytes and trophoblastic cells which do not carry HLA molecules. Hence, their expression elsewhere in the body triggers T-cell activation. They are expressed in different tumor types and are important sources of tumor-specific antigens {Coulie et al, 2014}. Examples include, *MAGE*, *BAGE* and *GAGE* {Traversari et al, 1992; Boel et al, 1995; Van den Eynde et al, 1995}.

- *Genes coding for differentiation antigens*

They are expressed by both tumor cells and their normal tissue of origin. In uveal melanomas, important antigens of this group include: melanocyte differentiation proteins such as gp100, melanA or tyrosinase {Spurrell et al, 2014}.

- *Genes that are over-expressed in tumor cells vs. normal cells*

Increased expression triggers T-cell response; whereas expression in normal tissue does not. The best example is HER2-neu {Fisk et al, 1995 250}.

- *Genes that are mutated in the tumor*

Mutations and splicing aberrations can generate a protein that is foreign to the immune system. Mutations contribute to nearly 50% of tumor-specific antigens eliciting spontaneous T-cell responses, with the latter dependent on the mutation load of the tumor {Coulie et al, 2014}. In addition, chromosomal translocations can result in fusion protein which may be recognized as non-self by the host immune system. BCR-ABL in CML is one such example {Chen et al, 1992}.

In uveal melanomas, there is little information regarding tumor-associated antigens, unlike their cutaneous counterparts. They are reported to have high expression of melanocyte differentiation proteins; but only low levels of cancer-testis antigens (MAGE and NY-ESO-1) {Mulcahy et al, 1996; Errington et al, 2012}.

Cytokines

Cytokines are immune modulator molecules that can play dual pro- and anti-tumorigenic actions. Tumor necrosis factor-alpha (TNFα) was initially considered to be useful in cancer treatment, but accumulating evidence has indicated that it has tumor promoting effects as well. Studies in animal models have shown that TNFα produced by malignant cells promote growth and spread of tumors of skin, ovary and bowel {Balkwill 2009}. The same goes for interleukin-1 (IL-1). On the other hand, interleukins-6,-7 and -17 are pro-tumorigenic and immunosuppressive {Porta et al, 2009}.

Chemokines

Chemokines are small cytokines with chemoattractant properties. Along with their receptors, they play important roles in recruiting immune cells into the TME. In addition, they also facilitate tumor proliferation and organ-specific

metastasis {Porta et al, 2009; Zlotnik et al, 2011; Viola et al, 2012}. They can contribute to tumor control, as well as tumor progression. As to which action is favoured depends on the type of chemokines produced.

Pro-tumorigenic role

They contribute to tumor progression through multiple mechanisms: recruitment of immune suppressive cells, aiding angiogenesis and orchestrating the trafficking of tumor cells to distant organs. CCL2, CCL5 and CCL7 play important roles in TAM recruitment {Mantovani et al, 2010}; CCR2 and CXCR2 have been implicated in MDSC tumor dynamics {Sawanobori et al, 2008}. Production of CCL22 and CCL28 by ovarian carcinoma cells attracts Tregs into the microenvironment {Curiel et al, 2004; Facciabene et al, 2011}. The CXC chemokines, CXCL1, CXCL3, CXCL6, CXCL8 promote migration and proliferation of endothelial cells {Mukaida et al, 2012}. The CXCL12-CCR4 is the combination implicated in metastasis of cancers of breast {Sun et al, 2014}, ovary {Jiang et al, 2006; Kajiyama et al, 2008}, colon {Kim et al, 2006}, prostate {Qin et al, 2014} and melanoma {Franco et al, 2010; Franco et al, 2010}. Another important ligand-receptor combination, CCL21-CCR7 is responsible for lymph node metastasis of cancers {Sperveslage et al, 2012; Jung et al, 2014}.

Anti-tumorigenic role

Some of the cytokines secreted could recruit immune cells that mediate antitumor immunity such as, cytotoxic and helper T-cells and NK cells. CCR5 is the receptor for RANTES (CCL3, CCL4, CCL5). It boosts anti-tumor immune responses through CD8+ T-cell activation and efficient antigen presentation {Gonzalez-Martin et al, 2011}. In addition, chemokines CXCL9 and CXCL10 acting at CXCR3 also recruit lymphocytes. Fractalkine (CX3CL1) positively influences NK cells and CD8+ T-cells into the

microenvironment {Hyakudomi et al, 2008; Mantovani et al, 2010}. The CXC chemokines, CXCL9 and CXCL10 also inhibit angiogenesis by blocking the CXCR3 receptor on endothelial cells {Viola et al, 2012}.

Transcription factors

NF-κB is activated in both immune cells and tumor cells leading to expression of cytokines, adhesion molecules and angiogenic factors. Cytokines can in turn, activate *NF-κB*. Likewise, *STAT3* constitutively activated in tumor and immune cells is a convergent point for oncogenic signaling pathways. *HIF-1α* activated by a combination of hypoxia, inflammatory mediators (TNFα, IL-1) and growth factors (EGF) is another important player that links inflammation and cancer {Colotta et al, 2009; Porta et al, 2009; Wu et al, 2014}.

II.1.3.7. MHC class I and II molecules

The major histocompatibility complex (MHC), class I and II molecules bind intracellular peptides and present them at the cell surface to CD8+ and CD4+ T-cells, respectively {Neefjes et al, 2011}. They function in conjunction with other molecules such as, β2 microglobulin, TAP1/2 which are part of the antigen-processing machinery {Neefjes et al, 2011}. MHC class I molecules are classical (HLA-A,-B,-C) and non-classical (HLA-E,-F,-G). The latter are involved in inducing immune tolerance to regulate the harmful effects of inflammatory response {Kochan et al, 2013}.

Altered HLA expression is one of the strategies used by tumors to escape immune surveillance. On the other hand, tumor cells can express neoantigens generated as a result of genomic instability which can elicit an immune response {Chamuleau et al, 2006}.

MHC class I expression in cancer

Reduced expression or complete loss of classical HLA class I molecules, HLA-A, -B and -C has been reported in a variety of solid tumors {Vitale et al, 1998; Kageshita et al, 1999; Atkins et al, 2004; Ramnath et al, 2006; Han et al, 2008}. The reasons for this impaired expression are both genetic and epigenetic {Bukur et al, 2012}.

The association of HLA expression by tumor cells with clinical outcome is variable. Decreased expression can correlate with poor (cutaneous melanoma, ovary) {Kageshita et al, 1999} {Han et al, 2008} or improved survival (lung cancer) {Ramnath et al, 2006}. In addition, it has been correlated with other adverse prognostic factors such as, stage {Kageshita et al, 1999} and grade {Vitale et al, 1998}.

On the other hand, aberrant expression of non-classical molecules has been observed in different cancer types. Their expression by tumor cells leads to inhibition of cytotoxic T-cells and NK-cells and expansion of MDSCs {Kochan et al, 2013}.

MHC class II expression in cancer

Expression of class II molecules has been demonstrated in different tumor types such as, carcinomas of breast, ovary, thyroid and cutaneous melanomas, usually in association with presence of increased numbers of lymphocytes {Rees et al, 1999; Barbieri et al, 2011}. In addition, their low expression has been correlated with poor clinical outcome in cutaneous melanoma {Anichini et al, 2006}, non-Hodgkin lymphoma {Rimsza et al, 2004}; colorectal {Matsushita et al, 2006}, hepatocellular and gastric carcinomas {Chamuleau et al, 2006}.

II.1.3.8. Comparison of immune microenvironment of primary tumors and their corresponding metastases

There are few studies which have compared the immune environment in primary tumors and their corresponding metastases {Cimino-Mathews et al, 2013; Halama et al, 2013; Remark et al, 2013}. In colorectal cancers, the primary and their corresponding liver metastases were categorized as immune-high and -low based on immune infiltrate. Some pairs were discordant with respect to the degree of immune infiltrate {Halama et al, 2013}. In another study where primary colorectal cancers and their corresponding lung metastases were analyzed, the former had a significantly higher CD8+ T-cell density; however, they had a positive correlation. Also, pair-wise analysis of primary renal cell carcinoma and their lung metastases showed similar densities of CD8+ T-cells {Remark et al, 2013}. In breast cancer, the metastatic tumors had lower infiltrating lymphocytes than their primary counterpart. In addition, their impact on survival was also different. High CD8+ T-cells to Tregs ratio was associated with good clinical outcome in the primary and poor outcome in metastases {Cimino-Mathews et al, 2013}. Moreover, the site of metastasis may also make a difference; brain metastasis of breast cancer show sparse lymphocytes when compared to liver, lung and bone metastases {Cimino-Mathews et al, 2013}. Analysis of larger cohorts would probably give a better perspective on these results.

II.1.4. Clinical relevance of immune cell infiltrate

II.1.4.1. Prognostic role

A prognostic marker predicts individual outcome such as, overall survival and disease-free survival independent of therapy {Galon et al, 2013}. The prognostic role of different immune cell types is well reported in literature. The impact on outcome varies depending on the individual cell type, as well as tumor type. In addition, there is also some variation between studies. One common theme amongst various cancers and cell types is that in majority of cancers, presence of CD8+ T-cells is a marker of good clinical outcome with rare exceptions such as, renal cell carcinoma and uveal melanomas {de la Cruz et al, 1990; Nakano et al, 2001}.

The prognostic impact of cells of innate and adaptive immune systems in different cancers has been indicated in **tables 6 and 7**, respectively. This data has been collated through pubmed search by inclusion of studies that have assessed the clinical outcome through survival analysis (Kaplan-Meier or Cox univariate; $p \leq 0.05$). In addition, it has been limited to impact of intra-tumoral infiltrate in primary, untreated cancers. They have been dichotomized as immune-privileged and non-immune privileged since eye belongs to the former category (discussed below).

II.1.4.2. Predictive role

A predictive marker is a clinical or biologic characteristic that provides information on the likely benefit from treatment (either in terms of tumor shrinkage or survival) {Italiano 2011}. Immune infiltrate can be a predictive marker in some malignancies, though no generalizations can be made. Again, presence of CD8+ T-cells is most often a marker of better response to therapy {Galon et al, 2013}.

Presence of higher number of T lymphocytes is a predictor of better response to chemoradiotherapy in head and neck cancers {Balermpas et al, 2014}. Likewise, CD4+, CD8+ T-cells are predictors of complete response to chemotherapy in breast cancer {Oda et al, 2012; Seo et al, 2013}. Surprisingly, breast cancers with higher numbers of Foxp3+ Tregs also respond better to chemotherapy {Oda et al, 2012}. This may be because the anti-tumor effect of chemotherapy is partially mediated by Treg suppression {Oda et al, 2012}. On the other hand, increased Treg to CD8+ ratio was predictor of poor response to chemotherapy in lung cancer {Liu et al, 2012}. Transcriptomic studies in cutaneous melanomas prior to and after immunotherapy also indicate that those with active immune microenvironment and expression of interferon-gamma (IFNG) stimulated genes respond better {Weiss et al, 2011; Ji et al, 2012}.

II.1.4.3. Therapeutic strategies to harness the immune system

The immune-based therapies for cancer are aimed at augmenting the antitumor immunity and overcoming the tumor-induced immune suppression.

Strategies to increase tumor immune surveillance

These include: adoptive cell transfer and cancer vaccines {Topalian et al, 2011; Zigler et al, 2013}.

Adoptive cell transfer is harvesting a cancer patient's own T-lymphocytes; identifying and expanding T-cells with anti-tumour activity *in vitro* and re-infusing them back into the patient {Topalian et al, 2011; Gajewski 2012}. Cutaneous melanoma is a model for this type of therapy {Dudley et al, 2008; Rosenberg et al, 2008; Straetemans et al, 2012}.

Cancer vaccines are designed against tumor associated antigens. Their therapeutic objective is to induce tumor-antigen specific CD8+ T-cells

{Gajewski 2012}. Randomized trials have demonstrated the beneficial effect of vaccines in metastatic prostate cancer and advanced melanoma {Kantoff et al, 2010; Schwartzentruber et al, 2011}.

Strategies to target pro-tumorigenic effects of immune microenvironment

These strategies include:

- *Inhibition of trafficking of immune cells into microenvironment*

This can be achieved through inhibition of chemokines or other soluble factors which recruit cells. For example, CCL2 recruits macrophages; use of antibodies against CCL2 or its receptor CCR2 could be beneficial {Tang et al, 2013}.

- *Depletion of immune cells using cytotoxic agents or monoclonal antibodies*

Trabectedin is an agent that targets macrophages and has been beneficial in sarcomas and ovarian cancer {Grosso et al, 2007}. Likewise, the FDA approved anti-CD25 mAb (daclizumab) can deplete Tregs {Nishikawa et al, 2010}.

- *Modification of immune cell phenotype*

This is aimed at converting the phenotype of the immune cell from pro- to anti-tumorigenic. Macrophages can be polarized from M2 to M1 using immunostimulants like CpG-ODN, {Allavena et al, 2012}. This approach is being used in several cancers {Krieg 2006}. Likewise, immature phenotype of MDSC can be stimulated to differentiate using agents such as, all-trans retinoic acid (ATRA) {Diaz-Montero et al, 2014}.

- *Targeting immune suppression*

Immune checkpoints are T-cell inhibitory signals such as, cytotoxic T-lymphocyte-associated protein 4 (CTLA4) and programmed cell death 1 (PD-1) which prevent uncontrolled immune reaction. Antibodies which block them

enable prolonged T-cell signaling {Vanneman et al, 2012; Zigler et al, 2013}. The well-known one, anti-CTLA4 (ipilimumab) causes tumor regression and has been approved for treatment in metastatic melanomas {Hodi et al, 2010; Luke et al, 2013}. In addition, it also attenuates Treg function since they also express CTLA4 {Nishikawa et al, 2010}.

Table 6. Prognostic impact of cells of innate immune system in various cancers

Cancer type	Tumor associated macrophages	Dendritic cells (DC)	Plasma cytoid DC	MDSC*	Neutrophils	NK cells	Mast cells
Non-immune privileged sites							
Lung	**Good** {Welsh et al, 2005; Dai et al, 2010} **None** {Carus et al, 2013}	**Good** {Dieu-Nosjean et al, 2008; Dai et al, 2010; Germain et al, 2014; Goc et al, 2014}		**Poor** {Huang et al, 2013}	**None** {Carus et al, 2013}	**Good** {Takanami et al, 2001; Villegas et al, 2002}	**Good** {Welsh et al, 2005}
Breast	**Poor** {DeNardo et al, 2011; Eiro et al, 2012; Tymoszuk et al, 2014}	**Good** {Iwamoto et al, 2003; Gulubova et al, 2012} **None** {Treilleux et al, 2004; Park et al, 2012}	**Poor** {Treilleux et al, 2004}			**Good** {Ascierto et al, 2013}	
Cutaneous melanoma	**None** {Hillen et al, 2008; Storr et al, 2012} **Poor** {Jensen et al, 2009}	**None** {Ladanyi et al, 2007; Jensen et al, 2012}	**Poor** {Jensen et al, 2012}		**Poor** {Jensen et al, 2012}		**Poor** {Ribatti et al, 2003} **None** {Schadendorf et al, 1995}
Head and neck	**Poor** {Lin et al, 2011; Fujii et al, 2012; Costa et al, 2013; He et al, 2014; Wang et al, 2014}	**Good** {Reichert et al, 2001}	**Poor** {O'Donnell et al, 2007}		**Poor** {Trellakis et al, 2011}		
Thyroid	**Good** {Cunha et al, 2012} **Poor** {Ryder et al, 2008}	**None** {Hilly et al, 2013}					
Esophagus	**Poor** {Dutta et al, 2012; Shigeoka et al, 2013} **Good** {Zhang et al, 2014}	**Good** {Ishigami et al, 2003; Lu et al, 2013}				**Good** {Hsia et al, 2005; Lv et al, 2011}	**None** {Tinge et al, 2010}

Gastric	**Poor** {Ishigami et al, 2003} **Good** {Ohno et al, 2003; Wang et al, 2011}	**Good** {Ananiev et al, 2011; Kashimura et al, 2012}		**Poor** {Dong et al, 2013}		**Good** {Ishigami et al, 2000}	
Colorectal	**Good** {Nagtegaal et al, 2001; Lackner et al, 2004} **Poor** {Herrera et al, 2013}	**Poor** {Sandel et al, 2005}			**Poor** {Khanhdo et al, 2011; Edin et al, 2012}		**Good** {Nielsen et al 1999}
Liver	**Poor** {Ding et al, 2009; Fan et al, 2014; Zhu et al, 2014} **Good** {Li et al, 2009} **None** {Zhu et al, 2008; Kong et al, 2013; Avadanei et al, 2014}	**Good** {Ido et al, 1994; Cai et al, 2006}			**None** {Kuang et al, 2011} **Poor** {Li et al, 2011}	**Good** {Chew et al, 2012; Wu et al, 2013}	
Gall bladder & biliary tract	**Poor** {Hasita et al, 2010}	**Good** {Nakakubo et al, 2003}				**None** {Nakakubo et al, 2003}	
Pancreas	**Poor** {Kurahara et al, 2011; Kurahara et al, 2012; Ino et al, 2013}				**Poor** {Ino et al, 2013}		
Renal	**Poor** {Xu et al, 2014}				**Poor** {Jensen et al, 2009}		**Poor** {Nonomura et al, 2007}
Prostate	**Poor** {Lanciotti et al, 2014} **Good** {Shimura et al, 2000}	**Good** {Liu et al, 2013}					
Urinary bladder	**None** {Ayari et al, 2013; Sjodahl et al, 2014} **Poor** {Hanada et al, 2000; Ajili et al, 2013}	**Poor** {Ayari et al, 2013}					
Cervical	**Good** {de Vos van Steenwijk et al, 2013} **None** {Carus et al, 2013}				**None** {Carus et al, 2013}		
Uterine	**None** {Jiang et al, 2012}						

Immune privileged sites							
Cancer type	**Tumor associated macrophages**	**Dendritic cells (DC)**	**Plasma cytoid DC**	**MD SC***	**Neutr ophils**	**NK cells**	**Mast cells**
Ovary	**None** {Milne et al, 2009; Mhawech-Fauceglia et al, 2013; Zhang et al, 2014} **Poor** {He et al, 2013; Lan et al, 2013}						
Brain	**Poor** {Prosniak et al, 2013}						
Uveal melanoma	**Poor**{Makitie et al, 2001; Maat et al, 2008; Bronkhorst et al, 2011} **None**{Anastas siou et al, 2001}						

*MDSC: Myeloid-derived suppressor cell

Table 7. Prognostic impact of cells of adaptive immune system in various cancers

Cancer type	CD3 T-cells	CD4 T-cells	CD8 T-cells	Memory T-cells	Regulatory T-cells	B-cells
Non-immune privileged sites						
Lung	**Good** {Johnson et al, 2000}	**Good** {Donnem et al, 2010}	**Good** {Al-Shibli et al, 2008; Kawai et al, 2008; Donnem et al, 2010; Goc et al, 2014}	**Good** {Goc et al, 2014}		**Good** {Al-Shibli et al, 2008; Germain et al, 2014}
Breast	**None** {Eiro et al, 2012}	**Poor** {DeNardo et al, 2011; Ma et al, 2012} **Good** {Gu-Trantien et al, 2013} **None** {Matkowski et al, 2009}	**Good** {DeNardo et al, 2011; Mahmoud et al, 2011; Liu et al, 2012; West et al, 2013} **None** {Matkowski et al, 2009; Liu et al, 2011; Ma et al, 2012; Park et al, 2012; Sun et al, 2014; Yu et al, 2014}		**Poor** {Liu et al, 2011; Mahmoud et al, 2011; Yan et al, 2011; Ma et al, 2012; Demir et al, 2013; Takenaka et al, 2013; Maeda et al, 2014} **Good** {West et al, 2013} **None** {Sun et al, 2014}	**Good** {Schmidt et al, 2008} **None** {Eiro et al, 2012}
Cutaneous melanoma	**Good** {Burton et al, 2011; Grotz et al, 2013; Thomas et al, 2013} **Poor** {Hillen et al, 2008}	**Good** {van Houdt et al, 2008}	**Good** {Piras et al, 2005; van Houdt et al, 2008} **None** {Hillen et al, 2008; Jensen et al, 2012}		**None** {Hillen et al, 2008; Ladanyi et al, 2010} **Poor** {Miracco et al, 2007}	**Good** {Ladanyi et al, 2011} **Poor** {Martinez-Rodriguez et al, 2014} **None** {Hillen et al, 2008}

Head and neck	**Good** {Hsu et al, 1989; Wansom et al, 2012; Jung et al, 2013}	**Good** {Badoual et al, 2006} **None** {Nordfors et al, 2013}	**Good** {Distel et al, 2009; Watanabe et al, 2010; Nasman et al, 2012; Jung et al, 2013; Nordfors et al, 2013;{Cunha et al, 2012} **None**{Hasmim et al, 2013}		**Good** {Badoual et al, 2006; Zhang et al, 2010; Wansom et al, 2012; Bron et al, 2013} **Poor** {Weller et al, 2014} **None** {Pretscher et al, 2009}	**Good** {Distel et al, 2009}
Esophagus	**Good** {Hosch et al, 1997; Rauser et al, 2010; Chen et al, 2011} **None** {Zingg et al, 2010}	**Good** {Cho et al, 2003; Yoshioka et al, 2008; Tsuchikawa et al, 2011} **None** {Zingg et al, 2010}	**Good** {Schumacher et al, 2001; Cho et al, 2003; Yoshioka et al, 2008; Lv et al, 2011; Tsuchikawa et al, 2011; Zhang et al, 2011} **None** {Zingg et al, 2010}	**Good** {Rauser et al, 2010; Enomoto et al, 2012}	**Good** {Yoshioka et al, 2008} **Poor** {Kono et al, 2006} **None** {Zingg et al, 2010}	
Gastric	**None** {Kim et al, 2011} **Good** {Chiaravalli et al, 2006}	**Good** {Kim et al, 2014} **None** {Shen et al, 2010}	**Good** {Ohno et al, 2003; Chiaravalli et al, 2006; Dong et al, 2013; Kim et al, 2014} **None** {Shen et al, 2010; Kim et al, 2011}	**Good** {Wakatsuki et al, 2013}	**Poor** {Kono et al, 2006; Perrone et al, 2008; Shen et al, 2010; Du et al, 2011; Ishigami et al, 2012; Kashimura et al, 2012; Zhou et al, 2013; Hou et al, 2014; Ma et al, 2014} **Good** {Wang et al, 2011; Kim et al, 2014} **None** {Kim et al, 2011}	**Good** {Dong et al, 2013}

Colorectal	**Good** {Guidoboni et al, 2001; Nagtegaal et al, 2001; Sinicrope et al, 2009; Deschoolmeester et al, 2010; Peng et al, 2010; Peng et al, 2010; Simpson et al, 2010; Dahlin et al, 2011}	**Good** {Nagtegaal et al, 2001}	**Good** {Guidoboni et al, 2001; Nagtegaal et al, 2001; Chiba et al, 2004; Prall et al, 2004; Zlobec et al, 2007; Pages et al, 2009; Salama et al, 2009; Deschoolmeester et al, 2010; Chew et al, 2011; Yoon et al, 2012; Lee et al, 2013; Ling et al, 2014}	**Good** {Pages et al, 2009; Peng et al, 2010; Peng et al, 2010; Chew et al, 2011; Lee et al, 2013} {Salama et al, 2009}	**Good** {Salama et al, 2009; Chew et al, 2011; Xu et al, 2013} **None** {Sinicrope et al, 2009; Salama et al, 2012}	
Liver	**None** {Gao et al, 2007; Chen et al, 2012; Lin et al, 2013} **Good** {Cai et al, 2006; Cariani et al, 2012}	**None** {Gao et al, 2007; Cariani et al, 2012; Chen et al, 2012; Lin et al, 2013; Huang et al, 2014} **Good** {Cai et al, 2006; Fu et al, 2013}	**Good** {Cai et al, 2006; Gao et al, 2007; Gao et al, 2009; Li et al, 2011; Cariani et al, 2012; Chew et al, 2012} **None** {Chen et al, 2012; Huang et al, 2012; Lin et al, 2013; Huang et al, 2014}	**Good** {Cai et al, 2006; Li et al, 2009; Gao et al, 2012}	**Poor** {Fu et al, 2007; Gao et al, 2007; Kobayashi et al, 2007; Sasaki et al, 2008; Gao et al, 2009; Zhou et al, 2009; Lin et al, 2010; Shen et al, 2011; Chen et al, 2012; Huang et al, 2012; Wang et al, 2012; Lin et al, 2013; Huang et al, 2014}	
Gall bladder & biliary tract	**Good** {Goeppert et al, 2013}	**Good** {Nakakubo et al, 2003} {Goeppert et al, 2013}	**Good** {Nakakubo et al, 2003; Oshikiri et al, 2003; Goeppert et al, 2013}		**Poor** {Zhang et al, 2013}	
Pancreas		**Good** {Fukunaga et al, 2004; Ino et al, 2013}	**Good** {Fukunaga et al, 2004; Ino et al, 2013}		**Poor** {Hiraoka et al, 2006; Ino et al, 2013}	

Renal		**Poor** {Bromwich et al, 2003; Hotta et al, 2011} **None** {Lamb et al, 2008}	**Poor** {Nakano et al, 2001} **None** {Bromwich et al, 2003; Lamb et al, 2008; Hotta et al, 2011}	**Poor** {Hotta et al, 2011}	**Poor** {Siddiqui et al, 2007; Kang et al, 2013} **None** {Zhan et al, 2012}	
Prostate		**Poor** {McArdle et al, 2004}	**None** {McArdle et al, 2004}		**Poor** {Flammiger et al, 2013}	**None** {Flammiger et al, 2012}
Urinary bladder	**Good** {Winerdal et al, 2011; Otto et al, 2012; Sjodahl et al, 2014}	**None** {Hilmy et al, 2006}	**None** {Hilmy et al, 2006; Sjodahl et al, 2014} **Good**{Sharma et al, 2007}		**Good** {Winerdal et al, 2011} **None** {Sjodahl et al, 2014}	
Cervical	**Good** {Nedergaard et al, 2007} {Bethwaite et al, 1996}	**None** {Shah et al, 2011} **Good** {Nedergaard et al, 2007}	**None** {Shah et al, 2011} **Good** {Nedergaard et al, 2007}		**Poor** {Jordanova et al, 2008; Shah et al, 2011}	
Uterine			**Good** {Kondratiev et al, 2004; de Jong et al, 2009; de Jong et al, 2012}	**Good** {de Jong et al, 2009}	**Poor** {Yamagami et al, 2011} **None** {Giatromanolaki et al, 2008}	
Cancer type	**CD3 T-cells**	**CD4 T-cells**	**CD8 T-cells**	**Memory T-cells**	**Regulatory T-cells**	**B-cells**
Immune privileged sites						
Ovary	**Good** {Raspollini et al, 2005; Han et al, 2008; Tomsova et al, 2008; Milne et al, 2009; Stumpf et al, 2009; Al-Attar et al, 2010} **None** {Sato et al, 2005;	**None** {Sato et al, 2005; Dogan et al, 2009; Milne et al, 2009; Mhawech-Fauceglia et al, 2013} **Good** {Le Page et al, 2012}	**Good** {Matsushita et al, 2003; Sato et al, 2005; Hamanishi et al, 2007; Callahan et al, 2008; Han et al, 2008; Adams et al, 2009; Clarke et al, 2009; Leffers et al, 2009; Liu et al, 2009; Milne et al, 2009;	**Good** {Leffers et al, 2009}	**Good** {Leffers et al, 2009; Milne et al, 2009; Le Page et al, 2012; Nielsen et al, 2012; Mhawech-Fauceglia et al, 2013} **Poor** {Adams et al, 2009} **None** {Sato et al, 2005}	**Good** {Milne et al, 2009} **Poor** {Yang et al, 2013}

	Adams et al, 2009; Clarke et al, 2009; Dogan et al, 2009; Le Page et al, 2012; Mhawech-Fauceglia et al, 2013}		Stumpf et al, 2009; Vermeij et al, 2011; Nielsen et al, 2012; Bachmayr-Heyda et al, 2013; Webb et al, 2014} None{Dogan et al, 2009; Le Page et al, 2012; Mhawech-Fauceglia et al, 2013}			
Glioma	**Good** {Kmiecik et al, 2013}	**Good** {Donson et al, 2012} **None** {Kmiecik et al, 2013}	**Good** {Donson et al, 2012; Kim et al, 2012; Kmiecik et al, 2013}		**Poor** {Jacobs et al, 2010} **None** {Heimberger et al, 2008}	
Uveal melanoma	**Poor** {Whelchel et al, 1993; Anastassiou et al, 2001; Lagouros et al, 2009} **None** {Bronkhorst et al, 2012}	**None** {Mougiakakos et al, 2010; Bronkhorst et al, 2012}	**Poor** {Anastassiou et al, 2001} **None** {Bronkhorst et al, 2012}		**None** {Mougiakakos et al, 2010; Bronkhorst et al, 2012}	

II.1.5. Approaches to study tumor microenvironment

The immune component is but one part of a multidimensional microenvironment of solid tumors. The multitude of different components, mesenchymal, vascular, immune along with the heterogeneous tumor cells make it difficult to understand their interactions at a molecular level {Bolouri 2014}.

Most of the data about tumor-stromal interactions have come from model systems such as, genetically engineered mice, xenografts (implantation of human tumor cell lines into immune compromised mice) and cell culture assays {Walrath et al, 2010; Hanahan et al, 2012; Budhu et al, 2014}. The more recent sequencing-based high throughput technologies can provide a genome-wide molecular characterization of the tumor along with its microenvironment {Bolouri 2014}. However, this still does not provide information about individual cell types in situ {Bolouri 2014}.

Study of individual cell type and their interactions is more complicated. It requires precise identification of the cell type using specific antibody followed by isolation using laser capture microdissection or flow cytometry. High-throughput sequencing and bioassays can help with further characterization {Hanahan et al, 2012}.

In addition, use of tissue engineering has led to construction of three dimensional microengineered tumor models that facilitate a better understanding of tumor-ECM and cell-cell interactions {Infanger et al, 2013}.

II.1.6. Immune microenvironment in uveal melanomas

II.1.6.1. Components

Immune cells

Uveal melanomas show infiltration by cells of both innate and adaptive immune systems {de la Cruz et al, 1990; Makitie et al, 2001; Staibano et al, 2006; Polak et al, 2007; Bronkhorst et al, 2011; Bronkhorst et al, 2012} with T-lymphocytes and macrophages being most frequent.

Lymphocytic infiltration is present in about 15% of tumors (derived from references {Lang et al, 1977},{Durie et al, 1990},{de la Cruz et al, 1990},{Anastassiou et al, 2001; Staibano et al, 2006},{Lagouros et al, 2009}). It is composed mainly of T-cells {Lang et al, 1977; de la Cruz et al, 1990; Durie et al, 1990; Staibano et al, 2006; Bronkhorst et al, 2012}, than B-cells {Whelchel et al, 1993}. Cytotoxic CD8+ T-cells predominate, but CD4+ T-cells were also identified {Durie et al, 1990; Bronkhorst et al, 2012}. Occasional studies have also assessed for presence of regulatory T-cells with a prevalence of about 25% {Lagouros et al, 2009; Mougiakakos et al, 2010}.

Macrophages are another frequently observed cell type {Makitie et al, 2001; Maat et al, 2008; Bronkhorst et al, 2011; Herwig et al, 2013} and are considered to be mainly of M2 type {Herwig et al, 2013}.

Dendritic cells and NK cells are sparsely distributed with the former considered to be of immature phenotype {Staibano et al, 2006; Polak et al, 2007}.

MHC molecules

Uveal melanomas have been shown to express MHC I and II molecules {Blom et al, 1997; Ericsson et al, 2001; Krishnakumar et al, 2003; Krishnakumar et al, 2003; Krishnakumar et al, 2004}. Their expression shows a positive correlation

with other components of antigen processing machinery {Krishnakumar et al, 2003; Krishnakumar et al, 2004}. However, the tumors lack expression of HLA-G, a nonclassic MHC class I molecule that inhibits NK-cell activity {Hurks et al, 2001; Anastassiou et al, 2003}. Also, MHC molecule expression by tumor cells was decreased following prior radiotherapy {Jager et al, 1988}. On the other hand, the HLA genotype shows no correlation with increased risk of developing uveal melanoma {Metzelaar-Blok et al, 2005; Maat et al, 2006}.

Chemokines

Uveal melanomas have been analyzed for expression of chemokine receptors and ligands {Franco et al, 2010; Dobner et al, 2012; Lattanzio et al, 2013; van den Bosch et al, 2013}.

There has been focus on CXCR4-CXCL12 receptor and ligand axis since circulating CXCR4+ tumor cells are hypothesized to home to organs expressing CXC12 such as, hepatocytes {Dobner et al, 2012}. The tumors have been shown to express CXCR4 {Franco et al, 2010; Dobner et al, 2012}. In addition, inhibition of CXCR4 expression inhibits their invasive potential {Li et al, 2009}. On the other hand, CCR7 expression by melanoma cells was associated with metastatic potential. This is somewhat surprising, since CCR7 mediates lymphocyte migration to lymph nodes {Dobner et al, 2012; van den Bosch et al, 2013}. They also express CCL2 and CCL22 which are chemoattractant for macrophages and Tregs {Bronkhorst et al, 2012}.

In addition, in melanoma harboring eyes, cytokine levels are also elevated in aqueous humor and vitreous {Ly et al, 2010; Nagarkatti-Gude et al, 2012}.

II.1.6.2. Clinical relevance

Lymphocytic infiltrate and high MHC expression correlate with epithelioid histology {Blom et al, 1997; Bronkhorst et al, 2012}, presence of extrascleral extension {Krishnakumar et al, 2004} and M3 {Maat et al, 2008; Bronkhorst et al, 2012}.

In contrast to other cancers, increased numbers of T-lymphocytes are associated with poor clinical outcome in uveal melanomas.

There are two prognostic groups of uveal melanoma based on the density of immune infiltrate. Higher CD8+ T-cell infiltrate is associated with poor overall survival and metastasis-free survival {Anastassiou et al, 2001; Lagouros et al, 2009}. The same holds true even for intra-tumoral infiltrate of Tregs {Mougiakakos et al, 2010} and macrophages {Makitie et al, 2001; Bronkhorst et al, 2011}. Likewise, high expression of MHC class I and II molecules is also associated with decreased survival due to development of metastasis {Blom et al, 1997; Ericsson et al, 2001}.

II.1.6.3. Immune privileged status of eye

Immune privileged organs are defined as "sites where foreign tissue grafts can survive for extended periods of time, whereas similar grafts placed at conventional sites undergo acute rejection" {Streilein 2003}. It is an evolutionary adaptation to protect tissues with limited regenerative capacity from potentially damaging effects of uncontrolled inflammatory reaction {Benhar et al, 2012}. Eye, brain, pregnant uterus, ovary and testis are amongst the immune-privileged sites which benefit from it.

In the eye, immune privilege is the result of several anatomical, physiological and immune mechanisms that together orchestrate strategies to prevent or modify innate and adaptive immune reactions {Streilein 2003}. The anatomical

ones are the blood-ocular barrier and absence of lymphatics. The former is due to the specialized non-fenestrated endothelium which prevents the leukocytes from gaining entry into the eye {Shechter et al, 2013}. The cornea, sclera, uveal tract and retina are devoid of lymphatic channels {Chen 2009}.

The physiological barriers include: reduced expression of MHC class I and II antigens, expression of immune modulator molecules and aqueous humor components. Majority of ocular tissues do not express human leukocyte antigens (HLA) class Ia and II molecules, with the exception of ocular endothelium {Abi-Hanna et al, 1988}resulting in protection from cytotoxic T-cell mediated lysis. Moreover, some of them express non-classical HLA-G, which inhibits NK-cell mediated lysis {Le Discorde et al, 2003}. In addition, the ocular tissues and aqueous humor contain pro-apoptotic molecules (Fas ligand, PD-L1, IDO1) {Griffith et al, 1995; Malina et al, 1996; Francisco et al, 2010} and complement inhibitors which suppress inflammation {Sohn et al, 2000}. To add to this mix, aqueous humor contains immunosuppressive molecules such as TGFβ and MIF {Niederkorn 2009}. In addition, there is anterior chamber associated immune deviation (ACAID), a special type of immune response in the eye that leads to suppression of cell mediated immune response {Niederkorn 2009}. Uveal melanomas benefit by recapitulating some of these mechanisms as described below.

II.1.6.4. Immune escape mechanisms

Uveal melanomas have developed mechanisms akin to those contributing to immune privilege in the normal eye. This is referred as ‘immunological plagiarism’ {Niederkorn 2012}.

They employ various mechanisms to elude the innate and adaptive immune effectors {Niederkorn 2009}. The interferon-gamma secreted by tumor-

infiltrating lymphocytes (TILs) helps uveal melanoma progression through three mechanisms:

- *By up-regulating indoleamine 2,3 dioxygenase (IDO) {Chen et al, 2007} and programmed death ligand-1 (PD-L1)* {Yang et al, 2008}.

IDO inhibits proliferation and survival of T-lymphocytes and NK-cells. It does so by depleting tryptophan vital for T-cell activities. PD-L1 expressed by melanoma cells binds to its receptor PD-1 on T-cells resulting in inhibition of lymphocyte proliferation and apoptosis {Niederkorn 2009}.

- *Resistance to perforin-mediated cytolysis*

For cytolysis, CD8+ and NK-cells secrete perforin and granzyme granules. The former perforates the cell membrane for granzyme to enter the cell and activate apoptosis of target cell. In presence of IFNG, uveal melanoma cells become less susceptible to the actions of cytolytic granules {Hallermalm et al, 2008}.

- *Up-regulation of MHC class I molecules*

Increased MHC class I molecule expression by uveal melanoma cells protects them from NK-cells since the latter are programmed not to kill MHC I expressing cells {Niederkorn 2009}.

Moreover, uveal melanomas also express complement regulatory proteins which inhibit complement proteins that are part of the innate immune system {Goslings et al, 1996}. In addition, they secrete factors such as TGF-β {Esser et al, 2001} and macrophage migration inhibitory factor (MIF) {Repp et al, 2000} which are immunosuppressive.

II.1.6.5. Paradox of lymphocyte infiltration and poor outcome in cancers

In majority of solid tumors, robust intra-tumoral infiltration by CD8+ cytotoxic T-cells is associated with good clinical outcome (**Figure 10a**). However, as already indicated, renal cell carcinoma and uveal melanoma are rare exceptions (**Figure 10b**).

In uveal melanomas, CD3+ and CD8+ T-cell infiltrate was associated with poor clinical outcome in three studies {Whelchel et al, 1993; Anastassiou et al, 2001; Lagouros et al, 2009}. In one study, a similar trend was observed, even though the p-value was not significant {Bronkhorst et al, 2012}. The interferon-gamma secreted by TILs helps tumor progression {Niederkorn 2009}. This could be one of the reasons for poor outcome of tumors with more lymphocytic infiltrate.

In renal cell carcinoma, CD8+ T-cells was a marker of poor clinical outcome in one study {Nakano et al, 2001} and without significant impact in three others {Bromwich et al, 2003; Lamb et al, 2008; Hotta et al, 2011}. Also, in the study of Nakano, et al, cytotoxic T-cells was a marker of poor prognosis when considered overall. However, when only proliferating CD8+ T-cells (positive for Ki-67) were considered, they were associated with longer survival. This is supposed to be due to their stronger anti-tumor response {Nakano et al, 2001}. Additional studies are required to better understand the role of CD8+ T-cells in renal cell carcinoma.

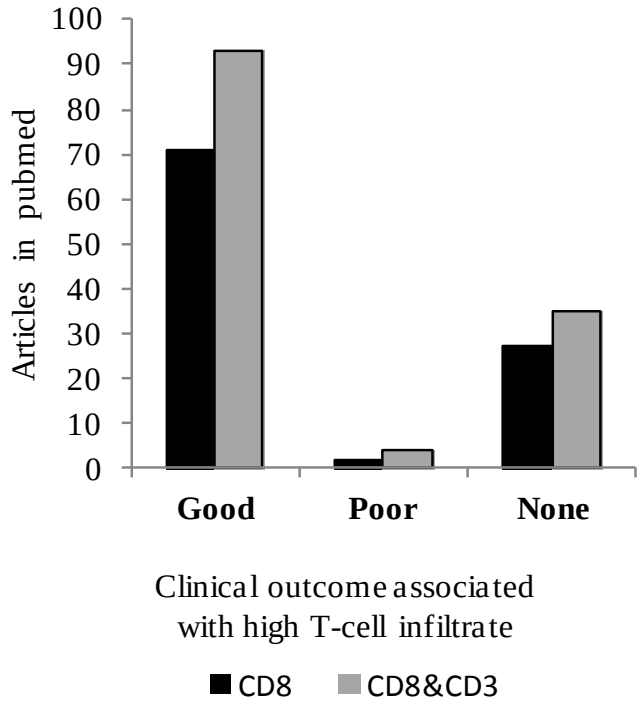

Figure 10a. Clinical impact of high T-cell infiltrate in various cancers in literature

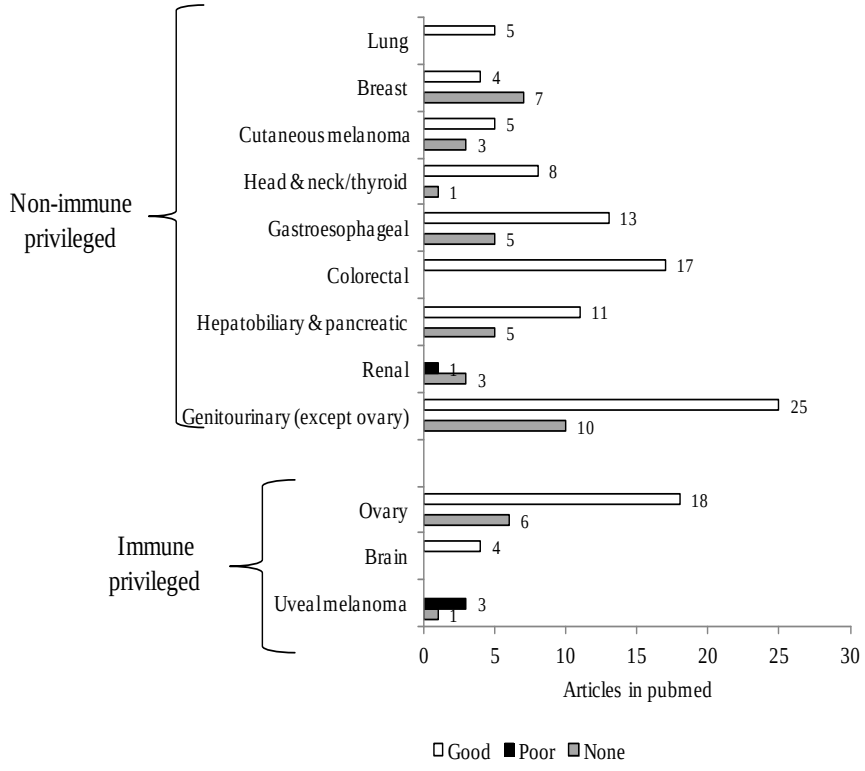

Figure 10b. Clinical impact of high T-cell infiltrate (CD8 & CD3) in main cancer types in literature

II.2. Immune and solid tumors

II.2.1. Immune gene signatures in solid tumors

In a variety of cancers, global transcriptomic analyses have led to the identification of gene signatures that bear the molecular footprint of immune activation leading to tumor dichotomization into immunologically active or quiescent phenotypes. They are characterized by: IFNG stimulated genes of STAT1-IRF1 axis with Th1 orientation; chemokine ligands which attract lymphocytes and macrophages (*CCL5*, *CXCL9*, *CXCL10*) and cytotoxic effectors (*PRF1*, *GZMB*, *GNLY*) {Pages et al, 2009; Ascierto et al, 2011; Ascierto et al, 2012; Carretero et al, 2012; Mann et al, 2013}. The IFNG signaling/STAT1-IRF1 axis is the common denominator between different cancer types {Jonsson et al, 2010; Mlecnik et al, 2011; Ascierto et al, 2012; Vauleon et al, 2012; Galon et al, 2013}. The presence of this signature is also associated with good clinical outcome {Pages et al, 2009; Ascierto et al, 2012}. So far, in uveal melanomas, there have been no studies comparing the transcriptomic profiles of tumors with high and low densities of immune cells. The present work is the first study to describe an IFNG induced gene signature in uveal melanomas.

II.2.2. Correlation between immune infiltrate and genetic features in solid tumors

It is interesting to understand the association between the genetic aspects of cancer cell *per se* and immune infiltrate which is part of the microenvironment, as both are considered as biomarkers in their own right.

This association has been studied in different cancer types such as, colorectum, breast; glioblastoma; cutaneous and uveal melanomas {Ogino et al, 2009;

Jonsson et al, 2010; Bronkhorst et al, 2012; Curtis et al, 2012; Rutledge et al, 2013}. In colorectal carcinoma, there was correlation between lymphocytic infiltration and microsatellite instability {Ogino et al, 2009}. In cutaneous melanoma, breast cancer and glioblastoma, the immune phenotype was correlated with distinct copy number alterations and mutations {Jonsson et al, 2010; Curtis et al, 2012; Rutledge et al, 2013}. In uveal melanomas, lymphocytic infiltrate was correlated with presence of M3, but not with *GNAQ/GNA11* mutations {Bronkhorst et al, 2012}.

There are paucity of studies which have assessed the relative prognostic impact of molecular features and immune infiltrate. In colorectal cancer, both lymphocytic infiltration and microsatellite instability are good prognostic factors. However, high lymphocytic infiltrate was of good prognosis irrespective of other genetic features {Ogino et al, 2009}. In uveal melanomas, at this point of time there is no data in literature on comparison of prognostic impact of genetic alterations and immune infiltrate. The present work is the first to assess the relative prognostic relevance of copy number alterations and immune infiltrate.

II.2.3. Immune cells and cancer stem cells cross-talk

Cancer stem cells (CSCs), also designated as tumor initiating cells (TICs) can be defined as rare subpopulation of tumor cells endowed with the properties of self-renewal, differentiation, multipotency and tumor initiation {Maccalli et al, 2014}. Immune cells and CSCs appear to benefit from each other's presence. Immune cells in TME can promote tumor progression through their cross-talk with CSC {Park et al, 2014}. TAMs interact with CSCs in cancers of breast, colon and gliomas {Ye et al, 2012; Fan et al, 2014; Park et al, 2014}. In hepatocellular carcinoma, they promote acquisition of CSC-like properties by

tumor cells {Fan et al, 2014}. Likewise, they also promote the invasive potential of glioma stem-like cells through secretion of TGF-β {Ye et al, 2012}. In addition, immune cells can also help CSCs become chemoresistant {Lee et al, 2012}.

On the other hand, CSCs can help tumor cells evade immune surveillance through secretion of TGF-β, IL-10; recruitment of Tregs and inhibition of T-cell proliferation {Di Tomaso et al, 2010; Schatton et al, 2010; Maccalli et al, 2014}.

II.2.4. Tumor dormancy and immune microenvironment

Dormancy is a survival strategy used by cancer cells, wherein they remain occult for a prolonged period of time {Paez et al, 2012}. The dormancy can be: cellular (G0-G1 arrest), angiogenic (poor vascularisation) and immune (CD8+ T-cells, IFN-γ) {Paez et al, 2012}. The proposed reasons for occurrence of tumor dormancy include {Sosa et al, 2013}:

- Hostile target organ microenvironment
- Stressful microenvironment of primary tumors leads to the emergence of clones of dormant cells
- Cells disseminating from early stage primary lesions which are not fit to initiate metastatic growth

The immune cells and the cytokines in the microenvironment play an important role in inducing tumor dormancy. It has been demonstrated in *in vivo* models that tumor-specific Th1 response induces permanent senescence in cancer cells in presence of cytokines, IFN-γ and TNF. Moreover, in murine uveal melanoma models, CD8+ T-cell depletion hastened the development of visceral metastases {Eyles et al, 2010}.

There is also some evidence that cancer stem cells may also contribute towards tumor dormancy. When disseminated tumor cells become dormant in the foreign environment of target organs, CSCs prolong their survival with their increased anti-apoptotic and DNA-repair capabilities {Patel et al, 2012}.
In melanomas clinical dormancy is well known, with ~50% of uveal and ~5% of cutaneous ones being free of overt metastases for nearly a decade {Ossowski et al, 2010}. The reason for longer dormancy in uveal tumors is not known, but in one autopsy study it has been attributed to inability of the disseminated cells to grow in target organs {Borthwick et al, 2011}. It may also have something to do with their origin in a unique immune milieu which might render them less adaptable or may be due to early dissemination {Ossowski et al, 2010}. There is as yet no information regarding the genetic/epigenetic mechanisms responsible for or the role of stem cells in uveal melanoma dormancy.

RESULTS

Synopsis of publication II

(Manuscript in preparation)

Uveal melanoma prognosis is better assessed by a three-tier classification based on four copy number alterations and high immune infiltration is associated with high risk-group

Narasimhaiah D, Munda M, Remark R, Legrand C, Damotte D, De Potter P, Coulie PG, Vikkula M, Godfraind C

When this project was started, UM were predominantly stratified into two prognostic groups.

The objective of this work was to better define prognostic groups for disease-free survival using clinical, histological, genetic and immune markers. We demonstrated that stratifying UM into three risk-groups leads to better prognostication than conventional two groups independently through three multivariate Cox models (CNA, immune-CNA and combined). Of these, copy number alteration (CNA) model based on M3, 8q gain, *LZTS1* deletion and *NBL1* deletion emerged as the one suitable for clinical use. Another, combining immune and CNA, demonstrated that UM with high degree of immune infiltrate (immune-high) stratified more frequently to high risk-group (73.7%), than to intermediate (21%) and low (5.3%). This suggested a possible reason for the paradoxical association between immune infiltration and poor clinical outcome in UM. Furthermore, the prognostic impact of high immune infiltrate varied between risk-groups, with no survival effect in high risk-group, but with a poorer outcome in intermediate risk-group. This indicated that impact of immune on outcome is dependent on associated chromosomal alteration.

New information from this work:

- CNA three-tier model based on four markers better stratifies UM
- Demonstration that prognostic impact of high immune infiltrate is dependent on associated CNA
- Large proportion of immune-high UM show high-risk CNA

The author carried out the vast majority of experiments and analyses in this study.

Uveal melanoma prognosis is better assessed by a three-tier classification based on four copy number alterations and high immune infiltration is associated with high risk-group

Narasimhaiah D[1,], Munda M[2], Remark R[3], Legrand C[2], Damotte D[3], De Potter P[4], Coulie PG[5], Vikkula M[1], Godfraind C[1,6]

[1]Laboratory of Human Molecular Genetics, de Duve Institute, [2]Institute of Statistics, Biostatistics and Actuarial Sciences, [4]Department of Ophthalmology, [5]de Duve Institute, Université catholique de Louvain, Belgium.
[3] INSERM U1138, Team <Cancer, Immune control, and Escape>, Centre de Recherche des Cordeliers, 15 rue de l'Ecole de Médecine, 75006 Paris, France
[6]Département d'Anatomie et Cytologie Pathologiques DACP, Pôle de Biologie, Institut de Biologie et de Pathologie, CHU A Michallon, CS 10217, Grenoble 38043, France.

Running title: Risk-groups in uveal melanoma

Key words: melanoma, uveal, immune, copy number alteration, Cox model

Corresponding author:

Catherine Godfraind MD, PhD
Professor,
Département d'Anatomie et Cytologie Pathologiques DACP,
Pôle de Biologie, Institut de Biologie et de Pathologie
CHU A Michallon, CS 10217,
38043 Grenoble cedex 09
tel: 04 76 76 73 77- 06 63 71 48 42
fax: 04 76 76 59 49
email: cgodfraind@chu-grenoble.fr

Conflict of interest: None

Abstract

Purpose

In uveal melanomas (UM), metastatic disease is a major cause of mortality. Lack of improvement in survival over decades indicates need for better identification of the likely clinical prognosis of every patient, a fundamental step to permit further personalized therapy. Therefore, multivariate Cox models were constructed, compared and validated. It concurrently allowed for better understanding of the relationship between various biomarkers.

Experimental design

Copy number alterations (CNA), clinical, histological and immune infiltration characteristics of 89 primary, untreated large UM, most with retinal detachment were established and analyzed using survival statistics.

Results

Five multivariate Cox models were constructed to assess disease-free survival (DFS). ROC curves indicated three performed better. They independently delineated the presence of three prognostic groups (all, $p < 0.001$). Amongst the models, CNA based on 3-, 8q+, *LZTS1* deletion and *NBL1* deletion emerged as the strongest one. Another, combining immune and CNA, demonstrated UM with high degree of immune infiltrate stratified more frequently to high risk-group (73.7%), than to intermediate (21%) and low (5.3%). It also revealed that in the high risk-group, the degree of immune infiltrate, whether high or low did not influence DFS.

Conclusions

CNA with three risk-groups emerges as the strongest biomarker to stratify patients with retinal detached UM. It separates patients with 90% probability of DFS at 10 years from the ones with 90% probability of metastasis at three years. Besides, the neutral effect of immune response in high-risk group suggests that in the latter, UM prognosis is CNA dependent.

Translational relevance

This is the first study describing a prognostic model allowing to distinguish amongst patients affected by UM with retinal detachment, those with 90% DFS at 10 years from the ones with 90% probability of metastases at three years. It is a three-tier model constructed from four genetic anomalies: 3-, 8q+, *LZTS1* and *NBL1* deletions. It is cost-effective and clinically suitable in view of its applicability to fine needle aspiration samples and conceivably to circulating tumor DNA. Moreover, this study is the first to compare various biomarkers in UM, establishing CNA as the best one; even superior to immune infiltration. In addition, it demonstrates the neutral effect of the latter in CNA-high-risk group UM. This stratification will facilitate the development of innovative therapeutic strategies for UM treatment.

Introduction

Cancer treatment involves not only dealing effectively with primary tumors, but also preventing progression to metastatic disease {Ferrarelli 2014}. In uveal melanomas (UM), there has been no improvement in five-year survival rates for over three decades {Singh et al, 2011}. Metastatic disease remains a major cause of mortality. Better stratification of patients into risk-groups, using biomarkers ranging from clinicopathologic to molecular is therefore another objective of cancer translational research. It has helped increase survival in various solid tumors {Harbeck et al, 2014; Voskoboynik et al, 2014}.

Clinical, histologic and molecular prognostic factors have been identified in UM, with 3- (monosomy 3, M3) being the most accepted one {Diener-West et al, 2005; Damato et al, 2010; Onken et al, 2010}. It divides UM into two metastatic risk-groups according to the presence or absence of this anomaly. Gene expression profile studies correlate this partition, {Singh et al, 2007; Petrausch et al, 2008; Onken et al, 2010} as does the degree of immune cell infiltrate {de la Cruz et al, 1990; Makitie et al, 2001}(*Narasimhaiah D, et al.* Manuscript in preparation). Meanwhile, this partition is imperfect, leaving some tumors in transition from one class to the other {Harbour et al, 2014}, indicating a need for better risk-stratification of UM.

In oncology, various modeling strategies are applied, with Cox proportional hazards being the most common one {Chen et al, 2012}. The relative performances of the constructed model are then assessed using methods such as, discrimination and validation. Time-dependent receiver operating characteristic (ROC) curves is one of the methods to assess how well a model

discriminates patients who experience the event of interest from those who do not {Heagerty et al, 2005; Steyerberg et al, 2010}. Validation measures if the model works satisfactorily for patient cohort other than the one used to develop the model. It can either be internal, based on the same series, applying methods like bootstrapping and cross-validation {Mallett et al, 2010} or external, using an independent series from another hospital and is therefore more stringent. Finally, for routine clinical application, the model can be converted into a user-friendly graphical version called nomogram {Iasonos et al, 2008}.

Such modeling strategies were achieved in a series of 89 primary, untreated, large choroidal and ciliochoroidal melanomas, most with retinal detachment. Copy number alterations (CNA) and immune markers, alongside clinical and histological features were used to create risk-stratification models, evaluate their predictive accuracies through ROC curves and validate them. Clinical, histological, CNA and immune indicators were identified and used to define three distinct risk-groups, with a possible fourth one. The CNA model based on four distinct molecular anomalies appears to be the best and clinically feasible prognostic marker. In addition, the relationship between immune infiltration and CNA has been delineated, demonstrating immune infiltration to be neutral in the high-risk group UM.

Materials and Methods

Study series

The series included 89 choroidal and ciliochoroidal melanomas from patients enucleated in Ophthalmology department at Saint-Luc Hospital, Brussels, Belgium between 1997 and 2010. They were previously untreated. Clinicoradiological data and follow-up information were obtained from hospital or General Practitioner records for a total of 89 tumors. Tumor thickness and diameter were measured by Echo-B scan. Haematoxylin and eosin (H&E) stained sections were assessed for tumor cell morphology, mitotic activity, extrascleral extension and histological typing to classify them according to modified Callender's classification {Font et al, 2006}). TNM staging was performed according to 7th edition of American Joint Committee on Cancer guidelines {Sobin et al, 2010}. Screening for hepatic and pulmonary metastases was done by abdominal ultrasound and chest radiography pre/peri operatively and reviewed every six months. The study was carried out according to our institutional ethics committee guidelines.

Immunohistochemistry

FFPE-sections from all tumors were tested for immune infiltrate using immunohistochemistry (IHC) with antibodies directed against CD3, CD4, CD8, CD163 and HLA-DRA (*Narasimhaiah D, et al*. Manuscript in preparation).

Immune infiltrate scoring system

The HLA-DRA and CD3-immunopositive cells were scored using a semi-quantitative scoring system with their sum resulting in 'immune score'. It was

used to differentiate immune-high tumors (immune score ≥ 14) from immune-low ones (immune score < 14) (*Narasimhaiah D, et al*. Manuscript in preparation).

Multiplex ligation-dependent probe amplification (MLPA) and comparative genomic hybridization (CGH)

Chromosomes 1p, 3, 6 and 8 status was analyzed in the tumor series using DNA extracted from FFPE tissues and the SALSA MLPA kit P027-C1 (MRC Holland, Amsterdam, Netherlands). Data were obtained with GeneMarker v2.2 software (Softgenetics, State College, PA) after population normalization and tumor to reference ratio calculation. Ratios were corrected following assessment of MLPA and comparative genomic hybridization data in the 17/89 tumors (OncoScan™ FFPE Express 2.0 Services, Affymetrix, Santa Clara, CA). Corrected ratio of ≤ 0.88: loss and ≥ 1.24: gain was used. The detailed procedure has been provided in **Supplementary methods**.

Statistical analyses

All analyses were based on disease-free survival (DFS), defined as time from enucleation to radiological diagnosis of metastases for patients developing metastases. Patients still alive and metastases-free at the time of analysis were censored at date of last follow-up {Tosolini et al, 2011} and included only if at least 24 months post-enucleation follow-up was available.

Cox univariate and multivariate proportional hazards regression models were used to investigate the association between variables and DFS. In multivariate analyses, final models were constructed based on a stepwise variable selection procedure. Prognostic scores were computed based on these final models {Bulian et al, 2012} and patients were divided into three- or four risk-groups

using cut-off values based on tertiles and quartiles, respectively (**Table M1**). DFS was estimated by Kaplan-Meier (KM) curves and compared using log-rank test.

The predictive accuracies of Cox models were assessed by Harrell's C-indices and time-dependent receiver operating characteristic (ROC) curves {Heagerty et al, 2005}. Internal validation was performed by leave-one-out method for models with highest predictive accuracies and nomograms {Harrell 2001} were constructed.

The statistical methods have been described in detail in **Supplementary methods**. All statistical tests were two-sided and a $p \leq 0.05$ was considered significant; no multiplicity adjustment was made considering the exploratory nature of these analyses. All analyses were performed in IBM SPSS Statistics v20, v21 (IBM, Armonk, NY) and R software v2.15 using survival, risksetROC and rms packages (http://CRAN.R-project.org/package=survival) (http://CRAN.R-project.org/package=risksetROC) (http://cran.r-project.org/package=rms). The results were reviewed by a biostatistician (CL).

Supplementary methods

Multiplex ligation-dependent probe amplification (MLPA)

MLPA was performed on FFPE uveal melanomas. FFPE cortectomies from epilepsy surgeries were used as controls. The H&E slides were reviewed to ensure samples consisted of ≥ 80% tumor cells. The tumor and control tissue were micro-dissected from 10-15, 10µm FFPE sections and stored at 4°C. Following deparaffinization, tissue lysis and protein digestion were performed. For this, the tissue was incubated in 200µl of lysis buffer (10mM TRIS, 1mM EDTA pH 8.5, 0.01% Tween-20) containing 5% Chelex-100 beads (Code # 142-1253, Bio-Rad, Hercules, CA) and 2µg/µl of Proteinase K (Code # P2308, Sigma-Aldrich, St.Louis, MO), overnight at 56°C with continuous shaking. This was followed by inactivation of proteinase K at 100°C for 10 minutes and centrifugation at 13,000 rpm for 10 minutes {de Jong et al, 2004}. The supernatant containing the DNA was collected and purified with QIAquick PCR purification kit using the manufacturer recommended microcentrifuge protocol (Qiagen, Valencia, CA). The DNA concentration was assessed by NanoDrop 1000 spectrophotometer (Thermo Scientific Wilmington, DE). The SALSA MLPA kit P027-C1 uveal melanoma (MRC Holland, Amsterdam, Netherlands) was used to identify chromosomal abnormalities in 89 tumor samples. The DNA was diluted in TE (10mM Tris-HCL pH 8.2, 0.1mM EDTA). The total DNA concentration was ~200-250 ng in a volume of 5µl. In each MLPA assay, two to three non-tumor controls were incorporated. The reactions were carried out as per the manufacturer's recommendations in a C1000 thermal cycler (Bio-Rad). A mixture of 0.7µl of PCR product, 9µl of Hi-Di formamide (Applied Biosystems, Carlsbad, CA) and 0.2 µl GeneScan-500 LIZ size standard

(Applied Biosystems) was analyzed by capillary electrophoresis on an ABI-3130XL genetic analyzer (Applied Biosystems). Fragment analysis was performed using GeneMarker v2.2 software (Softgenetics, State College, PA). The peak heights and the sizes of various probes were determined. The peak intensities were normalized by population normalization. The reference sample was calculated from the median intensities of non-tumor controls with standard deviation of ≤ 0.1 for both internal control and sample probes. For each probe, a ratio was obtained by comparing the peak heights of the samples to that of the reference. Loss of DNA was defined as a ratio of ≤ 0.88 and gain as ≥ 1.24. This cut-off was calculated based on the average ratio of all probes on chromosome 3 (for loss) and on chromosome 8q (for gain) in tumors displaying mosaicism by CGH. The chromosomal aberrations were considered as absent or present based on the number and location of aberrant probes.

Statistical methods

Continuous variables are reported as mean (standard deviation) and median (range), and are also categorized; binary and categorical variables are reported as frequencies and relative frequencies. Cox proportional hazards regression model was used to investigate the association between each variable and DFS.

i. Variable selection for Cox multivariate analysis

All categorical covariates were transformed into numeric codes before they were entered into Cox model. Potential prognostic biomarkers were first investigated in univariate analyses. For each category of biomarkers (clinical features, histological features, immune infiltrate, copy number alterations), all potential prognostic factors were then studied in a multivariate Cox

proportional hazards model and a final model was constructed based on a stepwise variable selection procedure. A combined multivariate model, including variables from different categories of biomarkers, was also constructed via a stepwise variable selection procedure (starting from a model including all variables with p-value of at least 0.1 in the univariate analyses). Model minimization was performed by backward stepwise conditional LR method in SPSS, except for immune-copy number alteration model where the variable, immune score was forced into the model using enter method in SPSS. The default probability for variable entry (0.05) and removal (0.1) with 20 iterations were used.

ii. Assessment of model performance

The performance of both univariate and multivariate Cox models were quantified using Harrell's C-index, a measure of concordance. A c-index of 0.5 indicates that the model has no discriminative ability, whereas a c-index of 1 indicates that the model perfectly distinguishes between those with poor prognosis (early metastasis) from those with good prognosis (late metastasis). The models were also evaluated in a time-specific manner by constructing time-dependent ROC curves at fixed time-points (12, 24, 36, 48 and 64 months) and AUC plots up to a specified time-point (12, 24, 36, 48 and 64 months) by integrating AUC values to obtain a global concordance (C^T). The assumption of proportional hazards (PHA) was tested and retained for all categorical variables except for age and mitotic activity. For the latter, time-dependent ROC curves and AUC plots were constructed using Local Cox method {Heagerty et al, 2005}. The R code for computation of ROC curves was downloaded from http://faculty.washington.edu/heagerty/Software/SurvROC/RisksetROC.

iii. Prognostic indices

The prognostic score was based on the estimated regression coefficient of all variables in the final Cox model. The score of each variable was its estimated coefficient rounded to the first decimal point using Microsoft Excel Round function and multiplied by 10. Individual patient score was obtained by adding up the scores of unfavourable factors present. The samples were split into risk-groups based on tertiles (three groups) and quartiles (four groups). The KM plots of risk groups were compared by log-rank test.

iv. Leave-one-out cross-validation

The misclassification error associated with each of the models was estimated by leave-one-out method. In each iteration, one observation was omitted and the prognostic score of the omitted observation was predicted based on the model built on the (n-1) other observations. This was repeated for all observations, resulting in cross-validated scores. The samples were split into risk groups based on the cross-validated scores using the same cut-off as used for the original models. The prediction was considered as 'true' if the predicted and original risk-groups were the same and as 'false' if they were different. The misclassification error rate was determined based on the number of false observations.

Table M1. Prognostic score calculation and cut-off estimation for multivariate models

Model	Variable	RC[#]	Score (RC*10)	Tertile cut-off	Quartile cut-off
CNA	Monosomy 3	2.4	present = 24	< 31 31-51 > 51	< 18 18-38 39-54 > 54
			absent = 0		
	8q gain	1.4	present = 14		
			absent = 0		
	LZTS1 deletion	1.7	present = 17		
			absent = 0		
	NBL1 deletion	1.7	present = 17		
			absent = 0		
Immune-CNA	Immune score	0.5	present = 5	< 31 31-47 > 47	< 19 19-35 36-49 > 49
			absent = 0		
	Monosomy 3	2.2	present = 22		
			absent = 0		
	8q gain	1.3	present = 13		
			absent = 0		
	LZTS1 deletion	1.5	present = 15		
			absent = 0		
	NBL1 deletion	1.8	present = 18		
			absent = 0		
Combined	Immune-low/M3-	0	Immune-low/M3- = 0	< 21 21-32 > 32	< 13 13-22 23-35 > 35
	Immune-high/M3+	2.4	Immune-high/M3+ = 24		
	Immune-low/M3+	2.1	Immune-low/M3+ = 21		
	Mitotic activity	1.2	>10/40hpf = 12		
			<10/40hpf = 0		
	Extrascleral extension	1.7	present = 17		
			absent = 0		
	LZTS1 deletion	1	present = 10		
			absent = 0		

#: regression co-efficient; hpf: high power field

Results

The study included 89 primary, untreated, large uveal melanomas majority of which had retinal detachment. 86 were eligible for survival analysis. The patient follow-up ranged from 2 months to 175 months, with a median of 41 months. Among these 86 patients, 38 developed metastases and 20 had died of metastases.

1. Clinical features

1.1. Series

The clinical parameters have been summarized in **Table S1**. Briefly, the age at diagnosis varied from 35 years to 90 years with a median of 67. The male to female ratio was 1.1. The median basal diameter was 18mm and median thickness was 11.1mm with tumors mainly belonging to T3 and T4 (91%) categories. Retinal detachment status was available for 81 tumors and present in 79 of them.

1.2. Patient outcome

Univariate analysis of the clinical features demonstrated that tumor stage (II vs. III-IV, hazards ratio (HR) = 2.5; p = 0.03) and extrascleral extension (absent vs. present, HR = 3.5; p = 0.005) displayed significant adverse association with DFS (**Table 1**). In multivariate analysis, these variables were also the only significant ones (tumor stage: p = 0.03; extrascleral extension: p = 0.02; **Table 2**).

2. Histological features

2.1. Series

The epithelioid component constituted up to 25% of the tumoral population in 51 tumors (58%), and was greater in the remaining (42%). Mitotic activity was up to 10/40 high power fields (hpf) in 43 tumors (48.9%) and higher in 45 (51.1%). Necrosis was present in 11 tumors (12.4%) and absent in 78 (87.6%) (**Table S1**).

2.2 Patient outcome

In univariate analysis, epithelioid component (≤25% vs. >25%, (HR = 3.0; p = 0.001), mitoses (≤10 vs. >10/40hpf, (HR = 4.4; p < 0.001) and necrosis (absent vs. present, (HR = 3.4; p = 0.001) were the features significantly associated with DFS (**Table 1**). Only the first two variables remained significant in the multivariate analysis (epithelioid component: p = 0.04; mitoses: p = 0.008; **Table 2**).

3. Immune infiltrate

3.1. Series

The immune infiltrate comprised predominantly of tumor-associated macrophages (TAMs, HLA-DRA+CD163+) and cytotoxic T-lymphocytes (CD3+CD8+), with absence of T-helper cells (CD3+CD4+). It allowed categorization of UM into immune-high tumors (19/89, 21.3%) and immune-low tumors (70/89, 78.7%).

3.2. Patient outcome

Immune score (immune-high vs. immune-low) showed a significant association with DFS with a worse outcome for immune-high tumors (**Table 1**), as also demonstrated by the KM curves (log-rank test $p < 0.001$, **Figure.1**). At 36 months, DFS was 26.3% [95% CI: 6.7-45.9] for immune-high tumors and 72.7% [95% CI: 60.9-84.5] for immune-low tumors. In univariate analysis, the immune score was associated with HR = 4.6 ($p < 0.001$).

4. Copy number alterations

4.1. Series

CNA for the 84/89 tumors for which MLPA was analyzable have been schematized in **Figure.2a**. Briefly, 3- (M3+) was identified in 48/84 tumors (57.1%). With the exception of two, all M3+ tumors showed a combined 8q gain (8q+) restricted to *MYC* (12/46) or affecting the whole arm (34/46). The latter was sometimes part of chromosome 8 gain (8+) (9/34) or of an isochromosome 8q (i8q) (15/34). They additionally showed *LZTS1* deletion (8p21.3) as part (15/34) or not (5/34) of an i8q, and/or *NBL1* deletion (1p36.13) related (3/10) or not (7/10) to 1p loss (1p-). Three tumors were simultaneously deleted for both genes. A negative association was observed between M3+ and 6p gain (6p+), being present in only seven tumors (7/48, 14.6%).

In tumors devoid of M3 (M3-) (36/84, 42.9%), the most common co-alteration was 6p+ (20/36), being part (12/20) or not (8/20) of an i6p. The 6p+ tumors additionally showed 8q+ (4/20), deletion of *LZTS1*, associated (9/20) or not (6/20) with *NBL1* deletion. The latter deletion was also observed in 5 of the 16 cases lacking 6p+.

4.2. Patient outcome

4.2.1. Individual MLPA probes model

Individual MLPA probes were analyzed to better understand their relevance to outcome (**Table S2**). In univariate analysis, majority of probes on chromosomes 3 and 8q were significantly associated with outcome. Amongst those on chromosomes 1p, 6 and 8p, only *NRG1* (8p12) was significant. For multivariate analysis, probes on chromosomes 3 and 8q were considered *en masse* as M3 and 8q+, whereas for chromosomes 1p, 6 and 8p, individual probes were included. This resulted in a final model comprising of M3, 8q+, *LZTS1* deletion and *NBL1* deletion. Hence, for all further analysis, the latter two alterations were considered as separate variables.

4.2.2. Copy number alteration model

In univariate analysis, M3 (HR = 7; p = <0.001), i8q (HR = 5.4; p = <0.001), 8q+ (HR = 5.2; p = <0.001) and 8p- (HR = 2.6; p = 0.005) were significantly associated with DFS (**Table 1**), as also indicated by KM plots (**Figures.S1a-1e**). *LZTS1* deletion showed a trend in univariate analysis (p = 0.07); while 6p+, 1p- and *NBL1* deletion were not significant. In multivariate analysis, M3, *LZTS1* deletion, *NBL1* deletion (for all, p < 0.001) and 8q+ (p = 0.002) were significant variables constituting the copy number alteration model (CNA model) (**Table 2**).

4.2.3. Risk-groups based on copy number alteration model

4.2.3.1. Tertile-based risk-groups

Prognostic score was computed based on the regression coefficients of the CNA model. Tumors were stratified into three groups using cut-off values as

described in materials and methods. KM plots for these groups indicated distinct differences in DFS between them (log-rank test $p < 0.001$; **Figure.2b**). The high risk-group had a median DFS of 20 months [95% CI: 9.8-30.2]; whereas in the intermediate and low risk-groups the median DFS was not reached. The DFS at 36 months was 12.2% [95% CI: -0.7-25.1] for high, 75.9% [95% CI: 60.4-91.4] for intermediate and 96% [95% CI: 88.4-103.6] for low risk-groups, respectively. The overall rate of metastases was 91.9% for high, 45.1% for intermediate and 4% for low risk-groups, respectively.

The risk of metastases was related to the number and type of CNA (**Figure.2c**). High risk-group had at least three CNA with M3+ always observed, most frequently in association with 8q+/*LZTS1* deletion (17/27, 63%) and secondly with 8q+/*NBL1* deletion (7/27, 25.9%). The intermediate risk-group had two CNA, with the exception of one tumor with three: 8q+/*LZTS1* and *NBL1* co-deletion. M3+ was found in about half of these tumors (17/29, 58.6%). The frequent associations were: M3+/*NBL1* deletion (9/29, 31%); M3+/8q+ and co-deletion of *LZTS1*/*NBL1* (7/29, 24.1%). The low risk-group either had one or no CNA. M3+ was observed as a single alteration in three tumors (12%). The more frequent alterations were: *LZTS1* deletion (8/25, 32%) and *NBL1* deletion (7/25, 28%). Five tumors (20%) did not display any of the four alterations.

4.2.3.2. Quartile-based risk-groups

In order to better define the intermediate risk-group, tumors were divided into four groups using cut-off values as described in supplementary methods. KM plots indicated differences between the groups (log-rank test $p < 0.001$; **Figure.2d**). With this stratification, the high risk-group remained the same, while the intermediate risk- group split into intermediate-high and intermediate-low. In the former group, median DFS was 64 months [95% CI:

38.9-89.1]; survival at 36 months was 72.7% [95% CI: 46.4-99.0]; overall rate of metastases was 68.8% and the most frequent alteration was M3+/*NBL1* deletion (9/11, 81.8%). In the intermediate-low group, median DFS was not reached; survival at 36 months was 81.7% [95% CI: 64.1-97.9]; overall rate of metastases was 23.8% and the most frequent alterations were: M3+/8q+ or co-deletion of *LZTS1*/*NBL1* (both, 7/21, 33.3%) (**Figure.2e**).The low risk- group remained the same, with the exception of three tumors with only M3+ which were included in intermediate-low group.

4.2.4. M3/8q+ model

The series was tested according to a prognostic model of UM based on status of chromosome 3 and 8q+ {Cassoux et al, 2013}. The KM plots indicated differences between the groups tested: M3+/8q+, M3+/no 8q+, M3-/8q+ and M3-/no 8q+ (log-rank test $p < 0.001$; **Figure.S1f**). For M3+/8q+ the median DFS was 25 months [95% CI: 19.6-30.4]; for both M3+/no 8q+ and M3-/8q+ it was 64 months and for M3-/no 8q+ it was not reached. The DFS at 36 months was 29% [95% CI: 13.3-44.7] for M3+/8q+, 71.4% [95% CI: 47.7-95.1] for M3+/no 8q+, 71.4% [95% CI: 37.9-104.9] for M3-/8q+ and 92.6% [95% CI: 82.8-102.4] for M3-/no 8q+. The overall rate of metastases was 77.5% for M3+/8q+, 53.7% for M3+/no 8q+, 52.4% for M3-/8q+ and 7.4% for M3-/no 8q+.

5. Copy number alterations related to immune groups

5.1. Series

The CNA with regard to immune infiltrate have been schematized in **Figure.2f**. In the immune-high group, M3+ was present in 17/19 tumors (89.5%), of which 16 (16/17, 94.1%) also demonstrated 8q+ being part of an i8q (12/16,

75%) or of 8+ (3/16, 18.8%). No other tumor showed deletion of *LZTS1* other than the ones demonstrating i8q. The other analyzed genetic anomalies were rarely observed.

In the immune-low group, M3+ was present in 31/65 tumors (47.7%) and absent in the rest (34/65, 52.3%). The M3+ tumors demonstrated 8q+ in 18/31 tumors (58.1%), sometimes being part of i8q (3/18, 16.7%) or of 8+ (6/18, 33.3%). The additional analyzed genetic anomalies were infrequent. In contrast, the immune-low/M3+ tumors devoid of chromosome 8 anomalies (13/31) demonstrated i6p (2/13, 15.4%) and *NBL1* deletion (9/13, 69.2%) linked (6/13, 46.2%) or not (3/13, 23.1%) to 1p-. The 34 immune-low/M3- tumors had similar chromosome 6 and 1 alterations: frequent i6p (12/34, 35.3%); *NBL1* deletion related (9/34, 26.5%) or not (11/34, 32.4%) to 1p- and *LZTS1* deletion related (6/18, 33.3%) or not (12/18, 66.7%) to 8p-.

5.2. Patient outcome

5.2.1. Immune-CNA model

An immune and copy number alteration model (immune-CNA) was constructed by forcing the immune variable into the CNA model. The significant variables were: M3, *LZTS1* deletion, *NBL1* deletion (p for all $\leq$ 0.001) and 8q+ (p = 0.005). In this multivariate analysis, immune infiltrate was not significant (p = 0.2) (**Table 2**).

5.2.2. Tertile-based risk-groups

Prognostic score was computed based on the regression coefficients of the immune-CNA model. Tumors were stratified into three groups using cut-off values as described in supplementary methods. The high risk-group contained 14/19 immune-high tumors (73.7%) and 13/62 immune-low tumors (21%),

respectively. In the intermediate risk-group, 4/19 immune-high tumors (21%) and 25/62 immune-low tumors (40.3%) were found. The low risk-group comprised of 1/19 immune-high tumor (5.3%) and 24/62 immune-low tumors (38.7%) (**Figures.2g/2h**). The median DFS and survival at 36 months in the risk-categories were same as described for CNA model.

In high risk-group, all tumors had at least three CNA. The most common genetic profile in this group was M3+/8q+/*LZTS1* deletion (19/27, 70.4%) corresponding to 12 immune-high tumors and 7 immune-low tumors. In the intermediate risk-group, all tumors had two CNA, with the exception of one. The most common alteration was M3+/*NBL1* deletion (9/29; 31%), corresponding to one immune-high and eight immune-low tumors. It was followed by M3+/8q+ (7/29, 24.1%) in two immune-high and five immune-low tumors, and co-deletion of *LZTS1*/*NBL1* (7/29, 24.1%) in immune-low tumors only. The low risk-group tumors either had one or none of the four CNA. The more frequent alterations were: *LZTS1* deletion (8/25, 32%) and *NBL1* deletion (7/25, 28%), both observed in immune-low tumors only. Five tumors (20%), corresponding to one immune-high and four immune-low tumors did not display any of the four alterations.

5.2.3. Quartile-based risk-groups

In order to better define the intermediate risk-group, tumors were divided into four groups using cut-off values as described in supplementary methods. With this, the high risk-group remained the same, while the intermediate risk-group split into intermediate-high and intermediate-low (**Figures.2i/2j**). The most frequent alteration in intermediate-high group was M3+/*NBL1* deletion (9/13, 69.2%), corresponding to one immune-high and eight immune-low tumors; median DFS was 41 months [95% CI: 22.7-59.4]; survival at 36 months was

69.2% [95% CI: 44.1-94.3] and overall rate of metastases was 74%. In intermediate-low, the common alterations were: co-deletion of *LZTS1* and *NBL1* (7/19, 36.8%), followed by M3+/8q+ (5/19, 26.3%), both in immune-low tumors; median DFS was not reached; survival at 36 months was 84.2% [95% CI: 67.7-100.3] and overall rate of metastases was 15.8%. The low risk-group remained the same, with the exception of three tumors with only M3+ which were included in intermediate-low group. The immune-high and immune-low tumors with similar alterations were in same prognostic groups, with one exception. Two immune-high tumors with M3+/8q+ were in intermediate-high, whereas their immune-low counterparts were in the intermediate-low group.

5.2.4. Prognosis

To examine the effect of immune infiltration, immune-high and immune-low melanomas with same CNA in each risk-category were compared. In high risk-group, there was no difference in disease-free survival between immune-high and immune-low tumors (log-rank test p = 0.75) (**Figure.S2a**). In intermediate risk-group, there was a difference in DFS between the two groups (log-rank test p = 0.04) (**Figure.S2b**).

6. Combined model

The combined model simultaneously analyzed clinicopathologic features, immune infiltration and CNA. Immune infiltrate and M3 were included as a composite variable (**Table 1**). The significant variables were: immune-high/M3+ ($p < 0.001$), immune-low/M3+ ($p = 0.001$), >10 mitoses/40hpf ($p = 0.006$), *LZTS1* deletion ($p = 0.02$) and presence of extrascleral extension ($p = 0.002$) (**Table 2**).

6.1. Tertile-based risk-groups

Prognostic score was computed based on the regression coefficients of the combined model. Three-tier stratification was performed using cut-off values as described in supplementary methods. KM plots denoted differences between the three groups (log-rank test $p < 0.001$) (**Figure.3a**). Median DFS was 18 months [95% CI: 8.8-27.2] in the high risk-group and not reached in the intermediate and low risk ones. The survival at 36 months was 23.7% [95% CI: 8.6-38.8] for high, 81.8% [95% CI: 65.7-97.9] for intermediate and 92% [95% CI: 81.4-102.6] for low risk-groups, respectively. Overall rate of metastases reached 83.1% for high, 18.2% for intermediate and 8% for low risk- groups, respectively. The variables associated with each group have been schematized in **Figure.3b**.

In the high risk-group, the most common alteration was mitoses >10/40hpf with either immune-high/M3+ or immune-low/M3+ (29/32, 90.6%). *LZTS1* deletion was present in 16/29 tumors (55.2%) with mitotic activity of >10/40hpf. Also, 15/19 (78.9%) immune-high tumors belonged to high risk-group and 13/15 (86.7%) of them had mitoses >10/40hpf.

In the intermediate risk-group, no single predominant alteration was identified. The major changes were: immune-low/M3+ alone (10/22, 45.5%), followed by immune-low/M3- with mitoses >10/40hpf and *LZTS1* deletion (6/22, 27.3%). The low risk-group included only immune-low/M3- tumors with no additional associated alteration (9/25, 36%) or with either *LZTS1* deletion (9/25, 36%) or mitoses >10/40hpf (7/25, 28%).

6.2. Quartile-based risk-groups

The four-tier stratification using cut-off values as described in supplementary methods also reached significance in this model (KM plots, log-rank test $p < 0.001$, **Figure.3c**); but in contrast to other models, only the low risk-group remained similar (**Figure.3d**). The median DFS was 12 months [95% CI: 5.4-18.6] in the high risk-group, 37 months [95% CI: 28.6-45.4] in the intermediate-high group and not reached in the intermediate-low and low risk-groups. The survival at 36 months was 5% [95% CI: -4.6-14.6] for high, 53.2% [95% CI: 29.3-77.1] for intermediate-high, 93.8% [95% CI: 81.8-105.8] for intermediate-low and 92% [95% CI: 81.4-102.6] for low risk-groups, respectively. The overall rate of metastases was 95% for high, 73.3% for intermediate-high, 29.7% for intermediate-low and 8% for low risk-groups, respectively. The most frequent alteration in high risk-group was either Immune-high/M3+ or immune-low/M3+ with mitoses >10/40hpf and *LZTS1* deletion (16/20, 80%). The common alteration in intermediate-high group was immune-low/M3+ with mitoses >10/40hpf (10/18, 55.6%) and in intermediate-low group it was immune-low/M3+ only (10/16, 62.5%).

7. Predictive accuracies and cross-validation of univariate and multivariate Cox models

In univariate analysis, the highest predictive accuracies were observed for 8q+, M3 and mitotic activity which had Harrell's C-indices of 0.699, 0.692 and 0.690, respectively. They were followed by immune score and tumor stage with C-indices of 0.653 and 0.61, respectively. Epithelioid component and i8q also had C-indices similar to immune score. While assessing the performance at 36 months, the highest area under the curve (AUC) was observed for M3 and

8q+ of 0.725 and 0.711, respectively. They were followed by immune score with AUC of 0.628 and tumor stage with AUC of 0.62.

Amongst the multivariate models, the combined model had the highest Harrell's C-index of 0.851. It was followed by immune-CNA model and CNA model with Harrell's C-indices of 0.809 and 0.797, respectively. The histology model and clinical model had Harrell's C-indices of 0.743 and 0.631, respectively. The AUC at 36 months for immune-CNA, CNA and combined models were 0.837, 0.832 and 0.805, respectively. For the histology and clinical models, it was 0.722 and 0.618, respectively (**Figure.3e**). A similar trend was also observed for integrated AUC (C^T) until 36 months (**Figure.3f**). The C-indices and AUC for all univariate and multivariate models has been provided in **Table S3**. In addition, the Harrell's C-index and the AUC at 36 months for the M3/8q+ model described by Cassoux {Cassoux et al, 2013} applied to our data (external validation) was 0.748 and 0.778, respectively.

A leave-one-out cross-validation was performed on CNA, immune-CNA and combined models which had the highest AUC. Misclassification error rates were 1.2%, 1.2% and 24.1% for three group stratification, and 24.7%, 8.6% and 44.3% for four group stratification, for CNA, immune-CNA and combined models, respectively (**Figure.3g**). The KM plots based on the model predicted prognostic scores have been indicated in **Figures.S3a-S3f**.

8. Nomogram

Nomograms were constructed for prediction of DFS based on CNA and immune-CNA models (**Figures.3h/3i**). According to the CNA model nomogram, if a tumor has M3+ (100 points), 8q+ (58 points) and *LZTS1* deletion (72 points), the total score is 230 points. This translates into DFS

probabilities at 24 and 48 months respectively of approximately 0.4 and 0.1. The median survival time is approximately 20 months.

9. High-risk cohorts and outcome

The univariate analyses were also repeated in the high-risk cohorts, M3+ tumors (n=47) and M3+/8q+ tumors (n=33). Multivariate analyses were not performed in them due to small sample size.

9.1. M3+ tumors and outcome

Forty seven tumors could be included for survival analysis. The influence of immune score was present even in the M3+ cohort. The KM curves indicated significant difference in DFS between immune-high and immune-low sub-groups (log-rank test p = 0.01) (**Figure.3j**). In univariate analysis, the high immune infiltrate group had a HR of 2.3 in comparison with immune-low group (p = 0.02). The other significant variables were: mitotic activity, necrosis, extrascleral extension, 8q+, i8q and *LZTS1* deletion (p = 0.04 - 0.001) (**Table 3, Figures.S4a-S4f**).

9.2. M3+/8q+ tumors and outcome

Thirty-three tumors could be included for analysis. In univariate analysis, the only significant variables were mitotic activity (p = 0.04) and *LZTS1* deletion (p = 0.01) (**Table 3**) and (**Figures.3k/3l**). Immune score was not significant in this cohort.

Discussion

Uveal melanomas are amongst the rare cancers for which no therapeutic advancement has been observed these last three decades {Singh et al, 2011}. Better definition of patient metastatic risk is a needed step for future development of efficient clinical trials. To this intent, a comprehensive analysis of clinical, histologic, genetic and immune parameters in 89 primary, untreated, large and retinal detached uveal melanomas was undertaken.

At diagnosis of UM, about 75% of the patients have concomitant retinal detachment. The latter is usually associated with medium- and large-sized tumors {Kivela et al, 2001}. The present series is predominantly constituted of large tumors, 97.5% of which had retinal detachment. The latter has been associated with poorer clinical outcome {Kivela et al, 2001; Laurent et al, 2011}. Consequently, this clinical feature has to be taken into account when comparing studies and conceivably, while stratifying patients.

To stratify UM, the reference biomarker is still 3- (monosomy 3, M3+) {Damato et al, 2010}; meanwhile, it appears suboptimal {Onken et al, 2012}. Thus, as others {Onken et al, 2012; Cassoux et al, 2013}, we wished to develop innovative prognostic models. With this idea, five different multivariate Cox models were built. Their performances were compared to the published models, including M3, using ROC curves {Heagerty et al, 2005}. All our models except one, performed better than only M3. Amongst them, the CNA-model based on four DNA alterations, M3, 8q+, *LZTS1* deletion and *NBL1* deletion emerged as most accurate.

Using a model based on a single biomarker only allows for two-tier stratification. When created with more than one biomarker, models permit definition of at least three risk-groups. All our models demonstrated three-tier stratification to be more accurate in predicting DFS in UM. This reinforces the recently published relevance of three risk-group models {Cassoux et al, 2013; Field et al, 2014} and advocate the use of three-tier stratification in future UM therapeutic trials.

Clinical aspects, histological criteria, degree of tumoral immune infiltration and CNA were the features tested in univariate analyses that subsequently allowed design of various multivariate models. Amongst the former, CNA, immune-CNA and combined models performed equally well. However, on cross-validation, the combined model had high misclassification error and was therefore considered not pertinent for external datasets. On the contrary, CNA and immune-CNA models were significant. Between them, CNA model appears more suitable for clinical use because of its robustness, low-cost, applicability on fine needle aspiration samples {Cassoux et al, 2013} and possibly on circulating tumor DNA.

In the three-tier CNA model we constructed, the risk of metastasis happens to be proportionate to the number of genetic anomalies observed. Three or more in high, two in intermediate and one or none in low risk-groups, respectively. This is understandable, as aneuploidy correlates with prognosis in cancer {Ehlers et al, 2008; Lassus et al, 2011; Keyes et al, 2013}.

In addition, in this CNA-model, the addition of *LZTS1* and *NBL1* status refined the prognostic significance of a previously published model that only

considered M3 and 8q+ {Cassoux et al, 2013}. Indeed M3+/8q+ was observed in both intermediate and high risk-groups of UM, but only in the latter when associated with *LZTS1* and/or *NBL1* deletions. This is comprehensible, as *LZTS1* deletion is associated with metastatic potential {Onken et al, 2008} and *NBL1* to tumor progression {Hanaoka et al, 2000; Hayashi et al, 2013}.

Meanwhile, this three-tier CNA model was not perfect, since the intermediate risk-group contained a combination of tumors with (40%) and without (60%) metastatic evolution. The use of a quartile-based model split this mixed risk-group, revealing a subgroup with 'intermediate-high' risk for metastases (n=7/11, 63%) and one with "intermediate-low" risk. In the former, all metastasizing tumors except one carried *NBL1* deletion, in addition to M3+ and absence of 8q+. This highlights the relevance of *NBL1* in stratification of UM. Moreover, presence of four statistically significant risk-groups was also pertinent in two other models. This suggests the need for future testing of quartile model on additional tumors in order to better differentiate this intermediate risk-group.

Immune infiltrate is nowadays a recognized biomarker of prognosis in cancer. With the exception of renal cancer {Nakano et al, 2001} and of uveal melanomas {de la Cruz et al, 1990; Anastassiou et al, 2001}, high degree of T-lymphocytic infiltration is associated with better clinical outcome in solid tumors {Fridman et al, 2012}. In contrast, tumor-associated macrophages (TAM) are of bad prognosis in most cancers {Zhang et al, 2012} including UM {Makitie et al, 2001}. These were confirmed in our series where, immune-low UM with demonstrated a better outcome than immune-high ones.

To compare the respective prognostic power of immune infiltrate and of DNA alterations in UM, an immune-CNA model was constructed. It showed occurrence of immune-high UM through all risk-groups; meanwhile, it was more frequent in high risk-group (73.7%), than in intermediate (21%) and low (5.3%) risk-groups. This and the results of multivariate analysis, revealed that immune infiltrate in UM was not an independent factor from the studied CNA. On the contrary, in colorectal cancer the survival benefit of lymphocytic infiltration is an independent factor {Ogino et al, 2009}.

Interestingly, there was no survival difference between immune-high and immune-low UM ($p = 0.75$) in the high risk-group of immune-CNA model. This indicates a neutral effect of the cytotoxic T-cell response in this risk-group of UM, while in the literature it is associated to a negative outcome {Anastassiou et al, 2001}. Even though our results may appear contradictory to published data, it is not the case, as in other studies, the impact of immune reaction was neither compared with other biomarkers, nor analysed depending on risk-groups.

Also, in the intermediate risk-group, the outcome of immune-high UM was worse than the one of immune-low ($p = 0.04$). The reason for this is unclear. It may be related to small sample size, but also to the plasticity of immune reaction as recently demonstrated in colon cancer {Bindea et al, 2013}. It may also indicate that in UM, the effect of immune infiltration on prognosis depends on the CNA status. If confirmed, it raises an important question from a therapeutic point of view – whether different components of a cancer need to be dissimilarly targeted in different risk-groups.

Mutations are an important source of tumor-specific antigens that elicit spontaneous T-cell responses in cancers {Coulie et al, 2014}. This may be the reason for higher degree of T-lymphocytic infiltrate in part of high-risk UM. As they demonstrate higher degree of aneuploidy, they probably have higher genomic instability and increased mutation load leading to a T-cell response. The latter however is either insufficient for UM rejection or is being overwhelmed by immune escape mechanisms involving IDO1 and PD-L1 molecules mounted by the tumor {Chen et al, 2007; Yang et al, 2008}. Therefore, they raise the consideration of boosting the T-cell response or blocking the molecules of immune escape in patients belonging to this risk-group in future therapeutic trials.

To the best of our knowledge, this is the first study to combine copy number alterations and immune for risk-stratification in cancer. This is also the first time the relative prognostic values of immune infiltrate and genetic anomalies have been compared in uveal melanomas; thereby indicating that impact of immune on outcome is copy number driven. In addition, the delineation of the link between high immune infiltrate and high-risk CNA suggests a possible reason for the paradoxical association between immune infiltration and poor clinical outcome in a large proportion of uveal melanomas.

Acknowledgements

The authors thank Dr. Bastiaan B.J.Tops for help with MLPA DNA extraction protocol and Ms. Liliana Niculescu for secretarial assistance.

Funding support

This project was supported by Fonds Maisin (Université catholique de Louvain), F.R.S.-FNRS (CDR J.0049.13) and Télévie (7.4607.10), all to CG. ND was supported by fellowship from le Centre du Cancer, Cliniques Universitaires Saint-Luc, Université catholique de Louvain, Brussels, Belgium and grants from Télévie (7.4607.10 and 7.4585.12F).

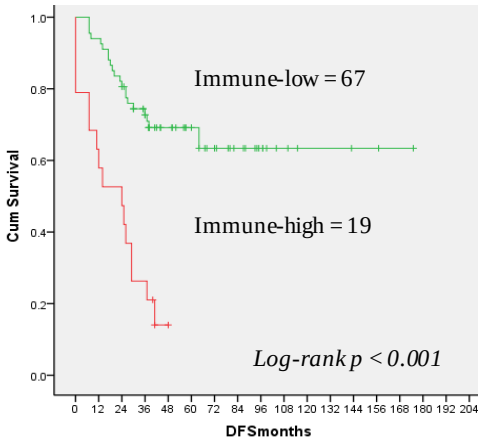

Figure 1. Kaplan-Meier plots for the duration of DFS in immune-high and immune-low uveal melanoma

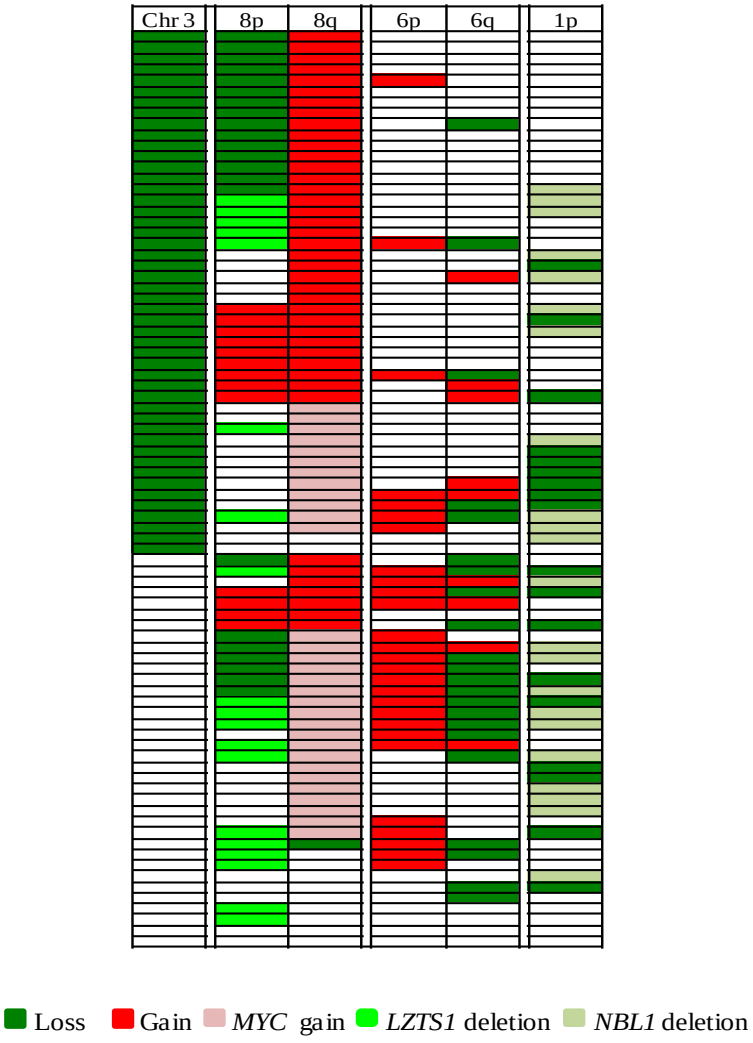

Figure 2a. Schematic representation of copy number alterations in all uveal melanomas (n = 84)

2b

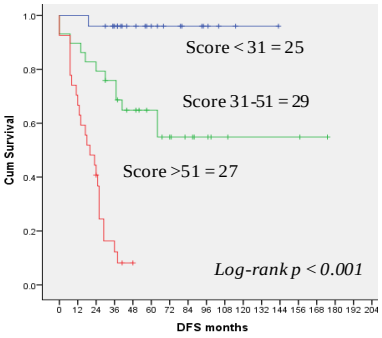

2c

Risk group	Monosomy 3	8q gain	LZTS1 deletion	NBL1 deletion	n (%)	Metastases(%)
High	■	■	■	■	2 (7.4)	2 (100)
	■	■	■		17 (63)	15 (88.2)
	■	■		■	7 (25.9)	6 (85.7)
	■		■	■	1 (3.7)	1 (100)
					27 (33.3)	24 (88.9)
Intermediate	■	■			7 (24.1)	2 (28.6)
	■			■	9 (31)	6 (66.7)
	■		■		1 (3.4)	0 (0)
			■	■	7 (24.1)	1 (14.3)
		■		■	3 (10.3)	1 (33.3)
		■	■		1 (3.4)	1 (100)
		■	■	■	1 (3.4)	1 (100)
					29 (35.8)	12 (41.4)
Low	■				3 (12)	0 (0)
		■			2 (8)	0 (0)
			■		8 (32)	0 (0)
				■	7 (28)	1 (14.3)
					5 (20)	0 (0)
					25 (30.9)	1 (4)

■ Alteration present □ Alteration absent

2d

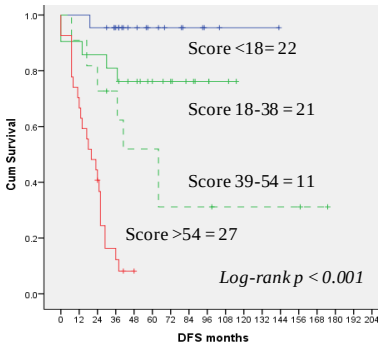

2e

Risk group	Monosomy 3	8q gain	LZTS1 deletion	NBL1 deletion	n (%)	Metastases(%)
High	■	■	■	■	2 (7.4)	2 (100)
	■	■	■		17 (63)	15 (88.2)
	■	■		■	7 (25.9)	6 (85.7)
	■		■	■	1 (3.7)	1 (100)
					27 (33.3)	24 (88.9)
Intermediate-high	■		■		1 (9.1)	0 (0)
	■			■	9 (81.8)	6 (66.7)
		■	■	■	1 (9.1)	1 (100)
					11 (13.6)	7 (63.6)
Intermediate-low	■	■			7 (33.3)	2 (28.6)
	■				3 (14.3)	0 (0)
		■	■		1 (4.8)	1 (100)
		■		■	3 (14.3)	1 (33.3)
			■	■	7 (33.3)	1 (14.3)
					21 (25.9)	5 (23.8)
Low		■			2 (9.1)	0 (0)
			■		8 (36.4)	0 (0)
				■	7 (31.8)	1 (14.3)
					5 (22.7)	0 (0)
					22 (27.2)	1 (4.5)

Figures 2b-2e. Prognostic relevance of CNA model

Kaplan-Meier plots for the duration of DFS (2b) and associated alterations (2c) for tertile-based risk-groups in CNA model
Kaplan-Meier plots for the duration of DFS (2d) and associated alterations (2e) for quartile-based risk-groups in CNA model

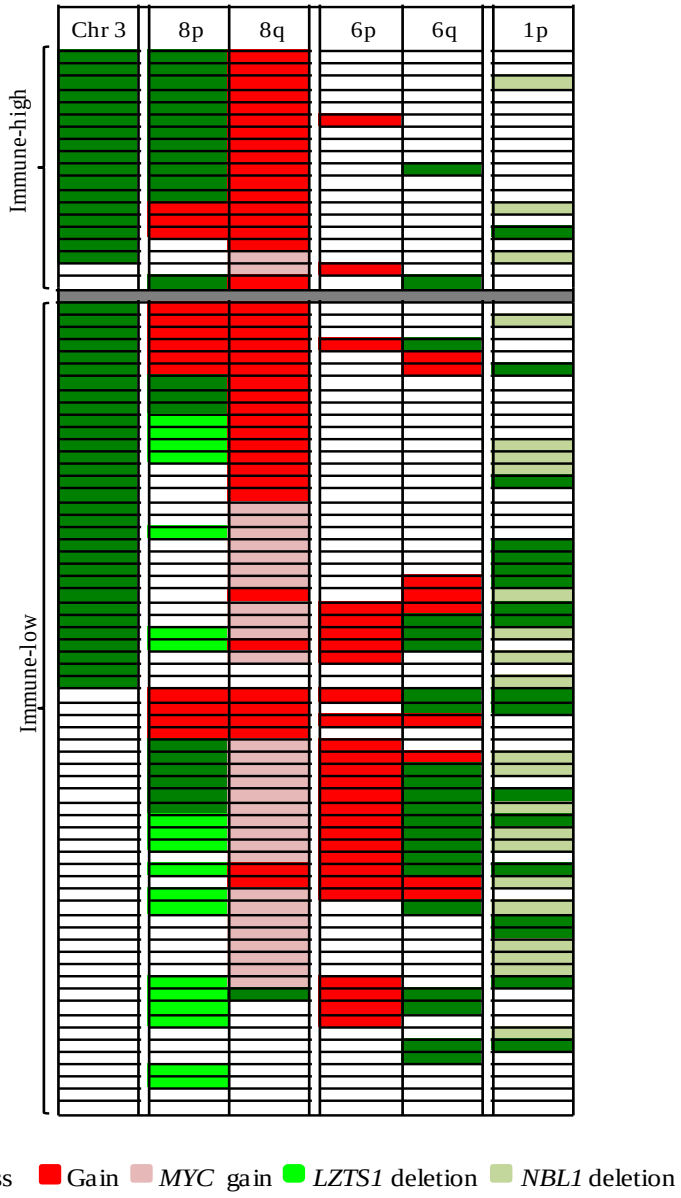

Figure 2f. Schematic representation of copy number alterations in immune-high and immune-low uveal melanomas (n = 84)

2g

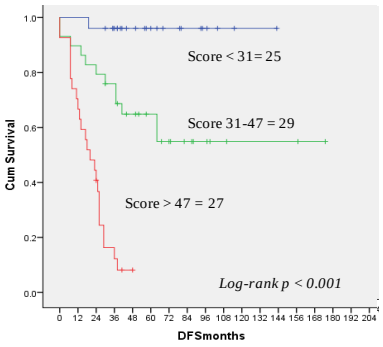

2h

Risk	Immune	Monosomy 3	8q gain	LZTS1 deletion	NBL1 deletion	n(%)	Metastases (%)
High						1 (3.7)	1 (100)
						11 (40.7)	9 (81.8)
						2 (7.4)	2 (100)
						1 (3.7)	1 (100)
						6 (22.2)	6 (100)
						5 (18.5)	4 (80)
						1 (3.7)	1 (100)
						27 (33.3)	**24 (88.9)**
Intermediate						2 (6.9)	2 (100)
						1 (3.4)	1 (100)
						1 (3.4)	1 (100)
						5 (17.2)	0 (0)
						1 (3.4)	0 (0)
						8 (27.6)	5 (62.5)
						1 (3.4)	1 (100)
						3 (10.3)	1 (33.3)
						7 (24.1)	1 (14.3)
						29 (35.8)	**12 (41.4)**
Low						1 (4)	0 (0)
						3 (12)	0 (0)
						2 (8)	0 (0)
						8 (32)	0 (0)
						7 (28)	1 (14.3)
						4 (16)	0 (0)
						25 (30.9)	**1 (4)**

alteration present ☐ alteration absent immune-high immune-low

2i

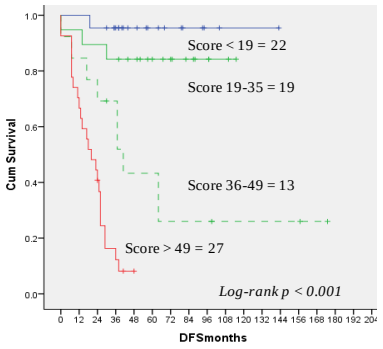

2j

Risk	Immune	Monosomy 3	8q gain	LZTS1 deletion	NBL1 deletion	n (%)	Metastases (%)
High						1(3.7)	1(100)
						11(40.7)	9(81.8)
						2 (7.4)	2 (100)
						1(3.7)	1(100)
						6 (22.2)	6 (100)
						5 (18.5)	4 (80)
						1(3.7)	1(100)
						27 (33.3)	**24 (88.9)**
Intermediate-high						2 (15.4)	2 (100)
						1(7.7)	1(100)
						8 (61.5)	5 (62.5)
						1(7.7)	0 (0)
						1(7.7)	1(100)
						13 (16)	**9 (69.2)**
Intermediate low						1(5.3)	1(100)
						5 (26.3)	0 (0)
						3 (15.8)	0 (0)
						7 (36.8)	1(14.3)
						3 (15.8)	1(33.3)
						19 (23.5)	**3 (15.8)**
Low						1(4.5)	0 (0)
						2 (9.1)	0 (0)
						8 (36.4)	0 (0)
						7 (31.8)	1(14.3)
						4 (18.2)	0 (0)
						22 (27.2)	**1 (4.5)**

Figures 2g-2j. Prognostic relevance of immune-CNA model

Kaplan-Meier plots for the duration of DFS (2g) and associated alterations (2h) for tertile-based risk-groups in immune-CNA model
Kaplan-Meier plots for the duration of DFS (2i) and associated alterations (2j) for quartile-based risk-groups in immune-CNA model

3a

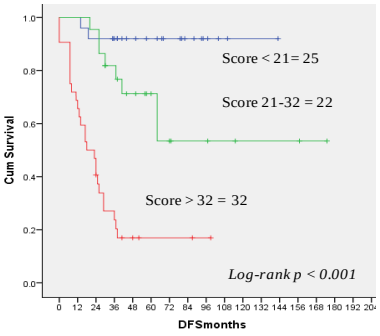

3b

Risk group	II/M3	mitoses >10/40hpf	LZTS1 deletion	extra scleral	n (%)	Metastases (%)
High					10 (31.3)	9 (90)
					2 (6.3)	2 (100)
					1 (3.1)	1 (100)
					2 (6.3)	1 (50)
					2 (6.3)	2 (100)
					4 (12.5)	4 (100)
					10 (31.3)	6 (60)
					1 (3.1)	1 (50)
					32 (40.5)	26 (81.3)
Intermediate					2 (9.1)	2 (100)
					3 (13.6)	2 (66.7)
					10 (45.5)	2 (20)
					6 (27.3)	1 (16.7)
					1 (4.5)	1 (100)
					22 (27.8)	8 (36.4)
Low					7 (28)	2 (28.6)
					9 (36)	0 (0)
					9 (36)	0 (0)
					25 (31.6)	2 (8)

alteration present alteration absent
immune-high/M3+ immune-low/M3+ immune-low/M3-

3c

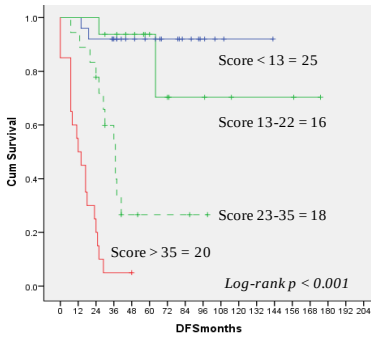

3d

Risk group	II/M3	mitoses >10/40hpf	LZTS1 deletion	extra scleral	n (%)	Metastases (%)
High					10 (50)	9 (90)
					2 (10)	2 (100)
					1 (5)	1 (100)
					4 (20)	4 (100)
					2 (10)	2 (100)
					1 (5)	1 (100)
					20 (25.3)	19 (95)
Intermediate high					2 (11.1)	1 (50)
					2 (11.1)	2 (100)
					10 (55.6)	6 (60)
					3 (16.7)	2 (66.7)
					1 (5.6)	1 (100)
					18 (22.8)	12 (66.7)
Intermediate low					10 (62.5)	2 (20)
					6 (37.5)	1 (16.7)
					16 (20.3)	3 (18.8)
Low					7 (28)	2 (28.6)
					9 (36)	0 (0)
					9 (36)	0 (0)
					25 (31.6)	2 (8)

Figures 3a-3d. Prognostic relevance of combined model

Kaplan-Meier plots for the duration of DFS (3a) and associated alterations (3b) for tertile-based risk-groups in combined model
Kaplan-Meier plots for the duration of DFS (3c) and associated alterations (3d) for quartile-based risk-groups in combined model

3e **3f**

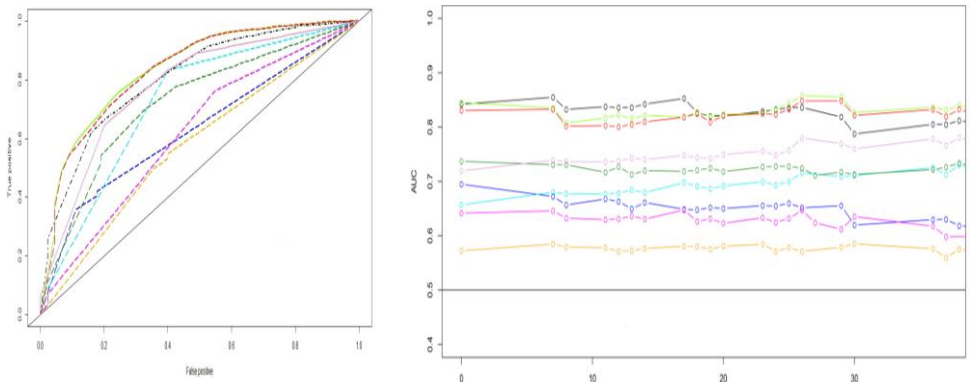

immune infiltrate, M3 *LZTS1* deletion clinical, histology, CNA, immune-CNA, combined M3/8q+ (external)

3g

Model	True	False	Misclassification error rate
CNA			
3 groups	80	1	1.2%
4 groups	61	20	24.7%
Immune-CNA			
3 groups	80	1	1.2%
4 groups	74	7	8.6%
Combined			
3 groups	60	19	24.1%
4 groups	44	35	44.3%

Figures 3e-3g. Comparison of model performances and their cross-validation

Time-dependent ROC curves (3e) at 36 months and AUC plots (3f) up to 36 months for the duration of DFS for Cox univariate and multivariate models

3g: Leave-one-out cross-validation of CNA, immune-CNA and combined

3h

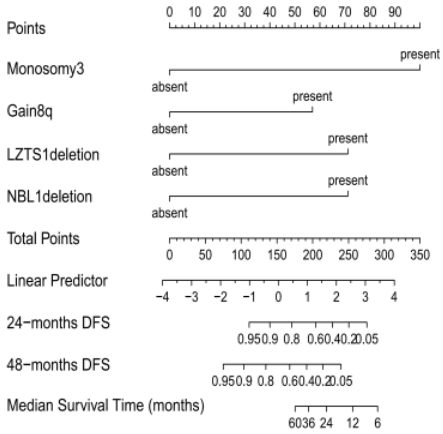

3i

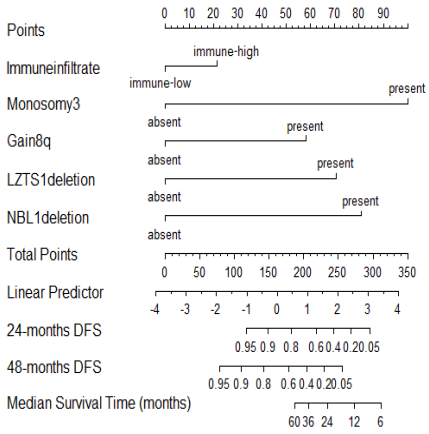

Figures 3h-3i. Nomograms for prediction of DFS based on CNA (3h) and immune-CNA (3i) models

To read the nomogram, a vertical line should be drawn from each tick marker indicating the status of a predictor to the top axis labelled 'Points'. Sum the points and find the corresponding number on the axis labelled 'Total Points'. Draw a vertical line down to the axes showing 24- and 48-months DFS to get the survival.

3j

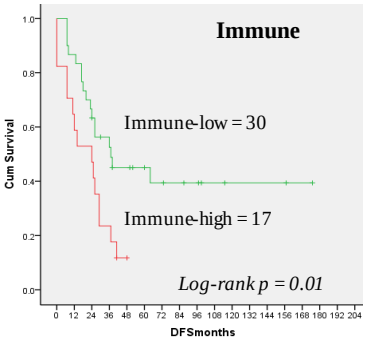

3k

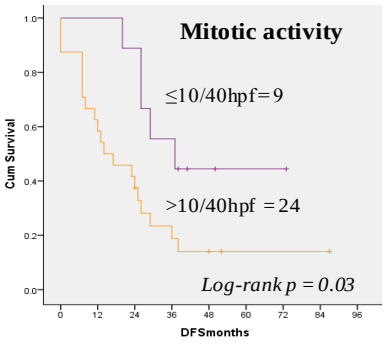

3l

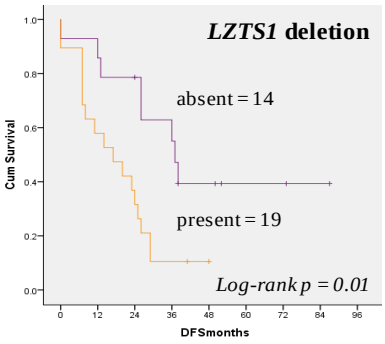

Figures 3j-3l. Clinical relevance of markers in M3+ and M3+/8q+ uveal melanomas

3j: Kaplan-Meier plots for the duration of DFS in M3+ cohort for immune-high and immune-low

Kaplan-Meier plots for the duration of DFS in M3+/8q+ cohort for mitotic activity (3k) and LZTS1 deletion (3l)

Table1. Cox univariate analyses for the duration of DFS in uveal melanomas according to clinical, histological, genetic and immune infiltrate parameters

Variable			n	HR	95% CI for HR	p-value
Clinical features	Age	≤ 60 years	31	1.0		
		> 60 years	55	1.2	0.6-2.4	0.6
	Gender	female	41	1.0		
		male	45	1.6	0.9-3.1	0.1
	Diameter	≤ 15mm	16	1.0		
		> 15mm	58	1.0	0.4-2.4	1.0
	Thickness	≤ 8mm	15	1.0		
		> 8mm	66	0.9	0.4-1.9	0.7
	Location	choroid	36	1.0		
		choroid+CB	50	1.4	0.7-2.7	0.3
	Stage	II	25	1.0		
		III & IV	50	2.5	1.1-5.9	0.03*
	Extrascleral extension	absent	79	1.0		
		present	7	3.5	1.5-8.6	0.005*
Histological features	Epithelioid component	≤ 25%	49	1.0		
		> 25%	36	3.0	1.6-5.8	0.001*
	Mitoses	≤ 10/40 hpf	41	1.0		
		> 10/40 hpf	44	4.4	2.1-9.0	< 0.001*
	Necrosis	absent	75	1.0		
		present	11	3.4	1.6-7.3	0.001*
	Pigmentation	≤ 25%	66	1.0		
		> 25%	20	1.3	0.6-2.6	0.5
Copy number alterations	Monosomy 3	absent	34	1.0		
		present	47	7.0	2.7-17.9	< 0.001*
	Isochromosome 8q	absent	65	1.0		
		present	16	5.4	2.7-10.8	< 0.001*
	8q+	absent	41	1.0		
		present	40	5.2	2.4-11.1	< 0.001*
	8p loss	absent	59	1.0		
		present	22	2.6	1.3-5.0	0.005*
	6p gain	absent	55	1.0		
		present	26	0.5	0.3-1.2	0.1
	1p loss	absent	63	1.0		
		present	18	1.2	0.6-2.5	0.6
	LZTS1 deletion	absent	43	1.0		
		present	38	1.8	1.0-3.5	0.07
	NBL1 deletion	absent	44	1.0		
		present	37	1.2	0.6-2.2	0.6
Immune	Immune infiltrate	Immune-low	67	1.0		
		Immune-high	19	4.6	2.4-9.0	< 0.001*
Immune and monosomy 3	II/M3 composite	Immune-low/M3-	32	1.0		
		Immune-low/M3+	30	6.3	2.1-18.8	0.001*
		Immune-high/M3+	17	15.3	5.0-47.2	< 0.001*

* $p \leq 0.05$ considered significant CB: ciliary body

Table2. Cox multivariate analyses for the duration of DFS in uveal melanomas according to clinical, histological, genetic and immune infiltrate parameters

Model		HR	95.0% CI for HR	p-value
Before stepwise	**Clinical**			
	Age	1.0	0.5-2.1	0.9
	Gender	1.6	0.8-3.3	0.2
	Stage	3.9	1.2-12.3	0.02*
	Location	0.6	0.2-1.6	0.3
	Extrascleral extension	2.0	0.6-6.5	0.3
Final model	Stage	2.5	1.1-5.8	0.03*
	Extrascleral extension	3.2	1.2-8.3	0.02*
Before stepwise	**Histology**			
	Epithelioid component	2.0	1.0-4.0	0.05*
	Mitotic activity	3.0	1.4-6.6	0.006*
	Pigmentation	1.3	0.6-2.7	0.5
	Necrosis	2.1	0.9-4.5	0.07
Final model	Epithelioid component	2.1	1.0-4.1	0.04*
	Mitotic activity	2.9	1.3-6.5	0.008*
	Necrosis	2.1	1.0-4.6	0.06
Before stepwise	**CNA**			
	8p loss	1.5	0.5-4.6	0.5
	Monosomy 3	14.5	3.7-55.9	< 0.001*
	8q+	4.4	1.7-11.2	0.002*
	6p gain	1.5	0.5-4.3	0.5
	LZTS1 deletion	4.3	1.4-13.6	0.01*
	1p loss	1.5	0.6-4.0	0.4
	NBL1 deletion	5.1	1.8-14.5	0.002*
Final model	Monosomy3	11.0	3.4-35.7	< 0.001*
	8q gain	3.9	1.6-9.2	0.002*
	LZTS1 deletion	5.3	2.2-12.8	< 0.001*
	NBL1 deletion	5.3	2.2-13.0	< 0.001*
Before stepwise	**Immune-CNA**			
	8p loss	1.5	0.5-4.6	0.5
	Monosomy 3	14.5	3.7-55.9	< 0.001*
	8q+	4.4	1.7-11.2	0.002*
	6p gain	1.5	0.5-4.3	0.5
	LZTS1 deletion	4.3	1.4-13.6	0.01*
	1p loss	1.5	0.6-4.0	0.4
	NBL1 deletion	5.1	1.8-14.5	0.002*
Final model [a]	Monosomy3	9.2	2.7-31.1	< 0.001*
	8q+	3.6	1.5-8.7	0.005*
	LZTS1 deletion	4.6	1.8-11.6	0.001*
	NBL1 deletion	5.8	2.3-14.8	< 0.001*
	Immune infiltrate	1.6	0.7-3.7	0.2

Table2 continued

	Model	HR	95.0% CI for HR	p-value
Before stepwise	Immune-low/M3-	Ref		
	Immune-high/M3+	10.8	1.8-63.5	0.009*
	Immune-low/M3+	11.5	2.2-60.5	0.004*
	8p loss	1.8	0.4-8.5	0.4
	8q+	1.4	0.4-4.2	0.6
	LZTS1 deletion	2.3	0.6-8.9	0.2
	6p gain	1.5	0.5-4.5	0.5
	Gender	0.6	0.2-1.5	0.3
	Stage	0.9	0.3-2.4	0.8
	Epithelioid component	1.5	0.6-3.9	0.4
	Mitotic activity	2.8	1.0-7.9	0.06
	Necrosis	2.4	0.7-8.8	0.2
	Extrascleral extension	6.2	1.4-26.8	0.01*
Final model	Immune-low/M3-	Ref		
	Immune-high/M3+	10.6	3.3-34.2	< 0.001*
	Immune-low/M3+	8.0	2.3-27.6	0.001*
	Mitotic activity	3.4	1.4-8.2	0.006*
	Extrascleral extension	5.5	1.8-16.3	0.002*
	LZTS1 deletion	2.8	1.2-6.9	0.02*

* $p \leq 0.05$ considered significant
[a] Immune forced into the model

M3+: monosomy 3 present
M3-: monosomy 3 absent
Ref: reference

Table3. Cox univariate analyses for the duration of DFS in M3+ and M3+/8q+ cohorts

		Tumors with M3+				Tumors with M3+8q+		
Variable		**HR**	**95% CI for HR**	**p-value**		**HR**	**95% CI for HR**	**p-value**
Immune infiltrate	Immune-low	1.0						
	Immune-high	2.3	1.2-4.7	0.02*		1.8	0.8-4.1	0.1
Age	≤ 60 years	1.0						
	> 60 years	0.8	0.4-1.7	0.6		0.6	0.2-1.3	0.2
Gender	female	1.0						
	male	1.8	0.9-3.7	0.1		1.4	0.6-3.5	0.4
Diameter	≤ 15mm	1.0						
	> 15mm	1.1	0.5-2.9	0.8		1.0	0.3-2.9	0.9
Thickness	≤ 8mm	1.0						
	> 8mm	0.9	0.4-2.1	0.8		0.9	0.3-2.2	0.8
Location	choroid	1.0						
	choroid+CB	1.0	0.5-2.1	1.0		0.5	0.2-1.3	0.2
Stage	II	1.0						
	III & IV	1.9	0.7-5.0	0.2		1.2	0.4-3.5	0.8
Extrascleral extension	absent	1.0						
	present	3.6	1.3-9.8	0.01*		2.7	0.9-8.2	0.08
Epithelioid component	≤ 25%	1.0						
	> 25%	2.0	1.0-4.1	0.06		1.6	0.7-3.7	0.2
Mitoses	≤ 10/40hpf	1.0						
	> 10/40hpf	3.8	1.7-8.5	0.001*		2.9	1.1-7.8	0.04*
Necrosis	absent	1.0						
	present	2.8	1.2-6.5	0.02*		2.1	0.9-5.0	0.1
Pigmentation	≤ 25%	1.0						
	> 25%	1.0	0.5-2.3	0.9		0.7	0.3-1.6	0.4
Isochromosome 8q	absent	1.0						
	present	2.6	1.2-5.3	0.01*		2.0	0.9-4.3	0.1
8q+	absent	1.0						
	present	2.4	1.0-5.7	0.04*		–	–	–
6p gain	absent	1.0						
	present	1.3	0.6-3.3	0.5		0.9	0.2-4.0	0.9
1p loss	absent	1.0						
	present	1.1	0.5-2.5	0.9		1.7	0.5-5.7	0.4
LZTS1 deletion	absent	1.0						
	present	3.4	1.6-7.1	0.001*		2.9	1.2-7.0	0.01*
NBL1 deletion	absent	1.0						
	present	1.3	0.7-2.6	0.5		1.5	0.6-3.4	0.4

* $p \leq 0.05$ considered significant CB: ciliary body

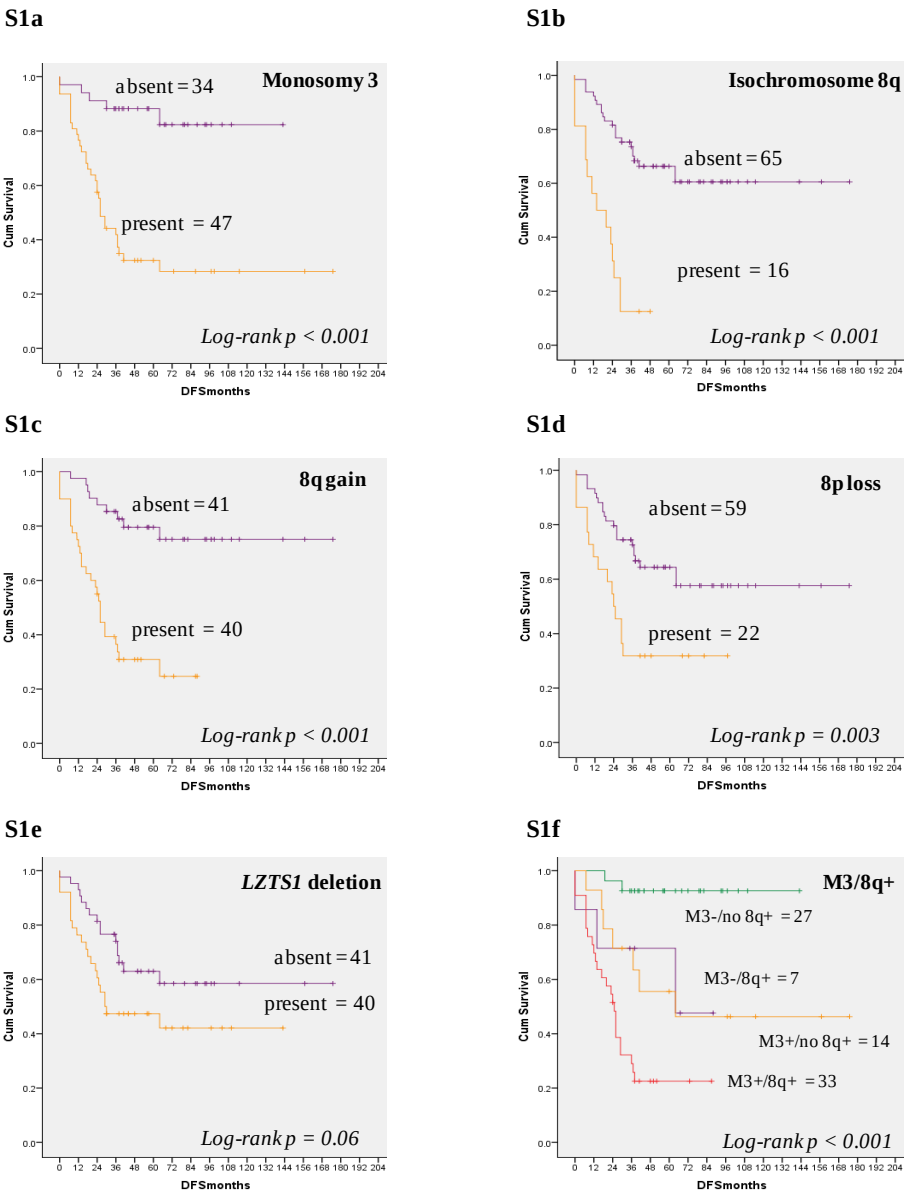

Figure S1. Kaplan-Meier plots for the duration of DFS in uveal melanomas with different chromosomal aberrations

S2a

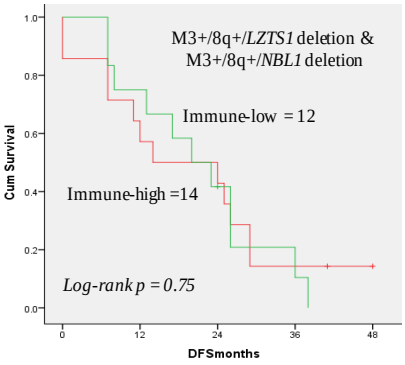

S2b

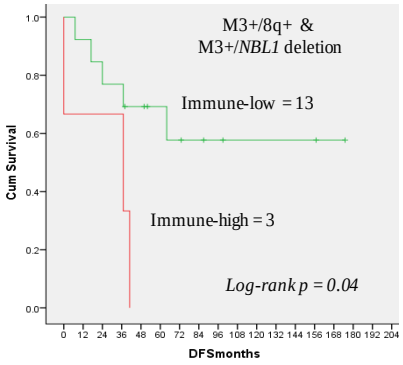

Figure S2. Kaplan-Meier plots for the duration of DFS between immune-high and immune-low tumors in high-risk (S2a) and intermediate-risk (S2b)

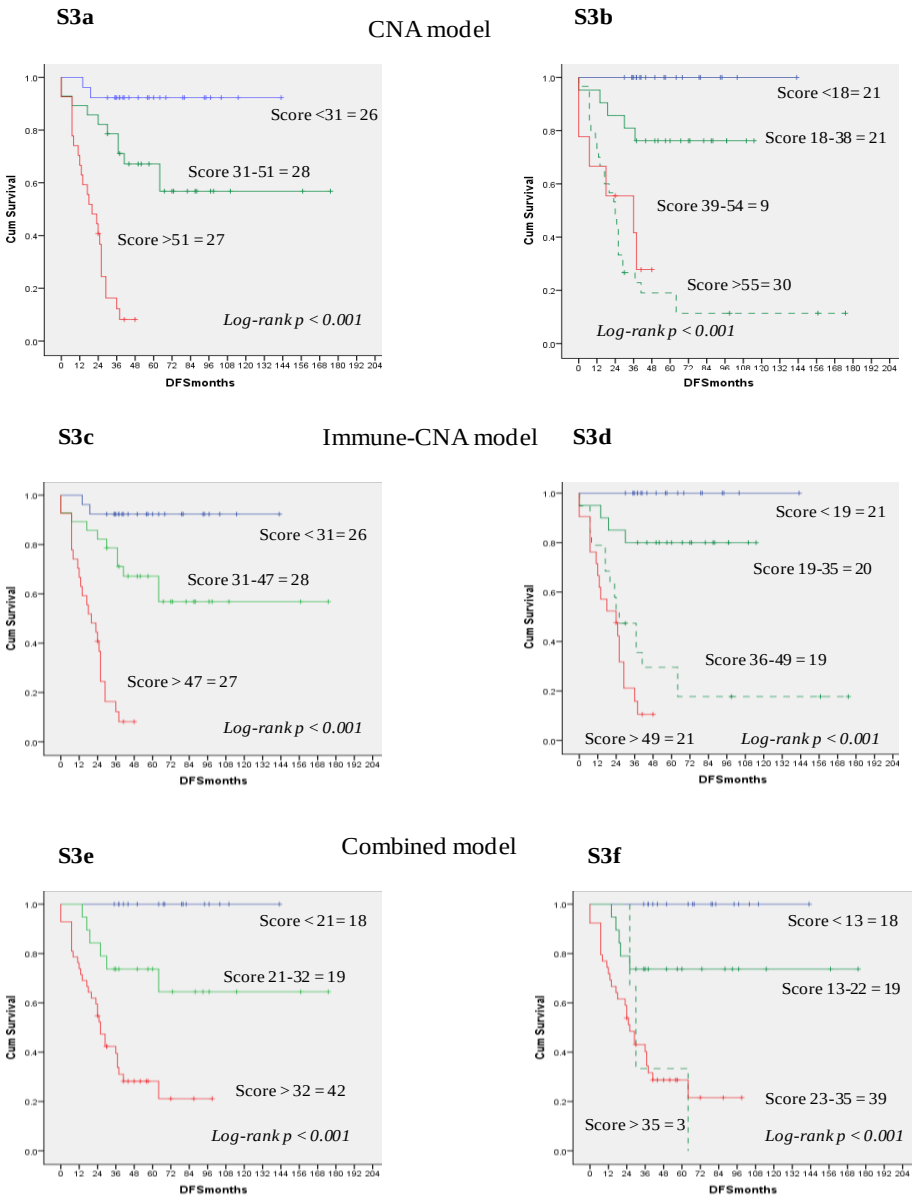

Figure S3. Prognostic groups based on cross-validated multivariate models

Kaplan-Meier plots for tertile and quartile-based risk-groups in CNA (3a & 3b), immune-CNA (3c & 3d) and combined models (3e & 3f)

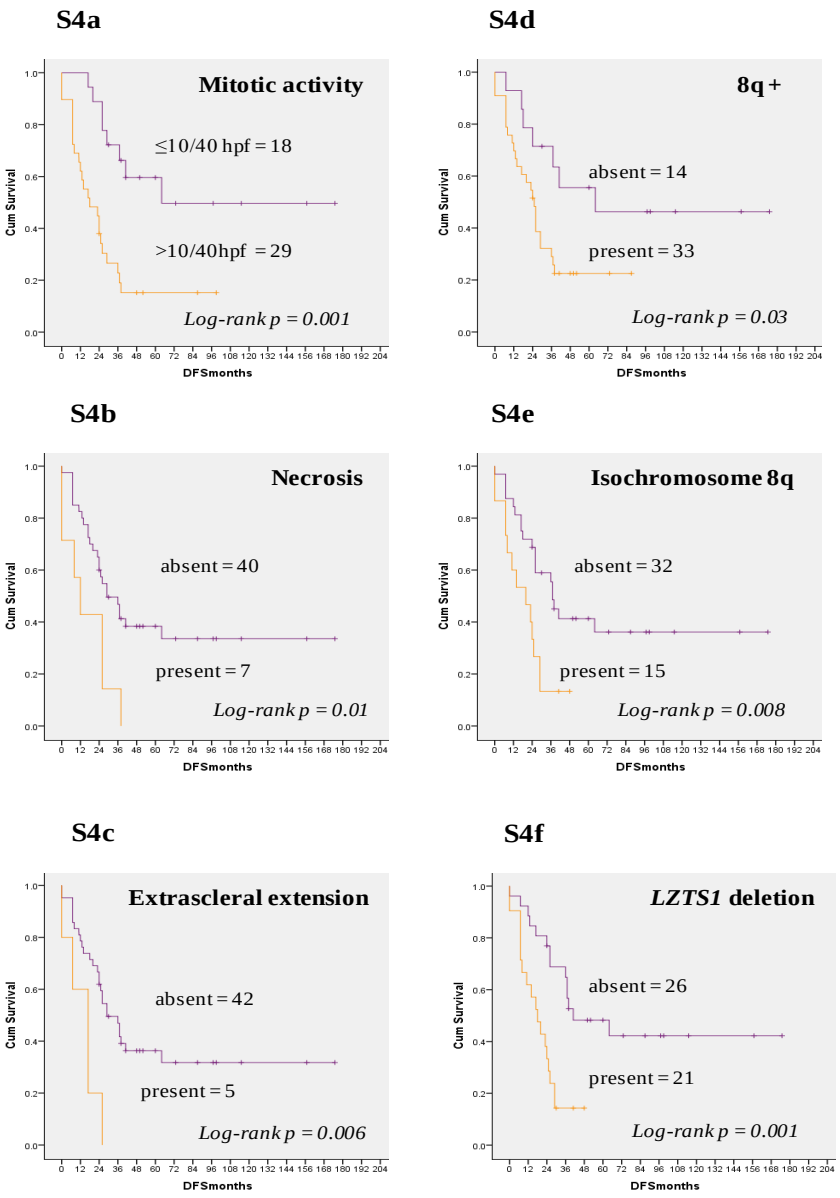

Figure S4. Kaplan-Meier plots for the duration of DFS for different variables in M3+ uveal melanomas

Table S1. Baseline details for tumor series

Variable		Valid N	Not available
Clinical			
Age at diagnosis(years)		89	0
Mean(SD)	64.7(13.5)		
Median(Range)	67(35-90)		
upto 60 years	32(36%)		
> 60 years	57(64%)		
Gender		89	0
Female	43 (48.3%)		
Male	46 (51.7%)		
Stage		78	11(12.4%)
IIA	6(7.7%)		
IIB	20(25.6%)		
IIIA	17(21.8%)		
IIIB	30(38.5%)		
IIIC	1(1.3%)		
IV	4(5.1%)		
T category		77	12(13.5%)
T1c	1(1.3%)		
T2a	5(6.5%)		
T2b	1(1.3%)		
T3a	20(25.9%)		
T3b	10(13%)		
T3c	2(2.6%)		
T4a	5(6.5%)		
T4b	31(40.3%)		
T4c	1(1.3%)		
T4d	1(1.3%)		
Basal diameter (mm)		77	12(13.5%)
Mean(SD)	17.8(3.1)		
Median(Range)	18(7-25)		
upto 15mm	16(20.8%)		
>15mm	61(79.2%)		
Thickness(mm)		84	5(5.6%)
Mean(SD)	10.5(3.1)		
Median(Range)	11.1(1.6-18)		
upto 8mm	16(19%)		
>8mm	68(81%)		
Location		89	0
Choroid	37(41.6%)		
Choroid & ciliary body	52(58.4%)		
Retinal detachment		81	8(9%)
absent	2(2.5%)		
present	79(97.5%)		
Extrascleral extension		89	0
absent	82(92.1%)		
present	7(7.9%)		

Table S1. continued

Histologic			
Variable		**Valid N**	**Not available**
Epithelioid component (%)		88	1(1.1%)
Mean(SD)	29.7(31.2)		
Median(Range)	20(0-100)		
upto 25%	51(58%)		
> 25%	37(42%)		
Mitoses (40hpf*)		88	1(1.1%)
Mean(SD)	12.7(11)		
Median(Range)	11(0-54)		
upto 10/40hpf	43(48.9%)		
>10/40hpf	45(51.1%)		
Pigment		89	0
Mean(SD)	16.2(21.6)		
Median(Range)	7.5(0-100)		
upto 25%	69(77.5%)		
>25%	20(22.5%)		
Necrosis		89	0
absent	78(87.6%)		
present	11(12.4%)		

*hpf: high power fields

Table S2. Cox univariate and multivariate analyses for the duration of DFS on MLPA genes

Chromosome /alteration	Gene	HR	95.0% CI for HR	p-value
Univariate				
1p loss	*MFN2*	1.0	0.5-1.9	0.9
	NBL1	1.2	0.6-2.2	0.6
	PTAFR	1.0	0.5-2.0	1.0
	GJB3	0.7	0.4-1.4	0.3
	MUTYH	0.8	0.4-1.6	0.5
	RPE65	1.1	0.6-2.2	0.8
	NOTCH2	1.0	0.5-2.0	0.9
3p loss	*CHL1*	2.2	1.1-4.6	0.03*
	VHL	2.7	0.8-8.8	0.1
	C3ORF10	5.6	2.0-15.8	0.001*
	PPARG	2.7	1.4-5.3	0.004*
	XPC	3.1	1.0-10.2	0.06
	MIR128	4.7	2.0-11.4	0.001*
	MLH1	3.7	1.5-9.0	0.003*
	CTNNB1	2.1	1.0-4.3	0.04*
	RBM5	2.7	1.3-5.7	0.01*
	BAP1	3.3	1.2-9.3	0.03*
	FHIT	7.1	2.2-23.3	0.001*
	ROBO1	2.3	0.8-6.5	0.1
3q gain	*PROS1*	2.6	1.2-5.8	0.02*
	CASR	2.6	1.2-5.6	0.01*
	MME	6.1	2.1-17.2	0.001*
	OPA1	2.6	1.2-5.6	0.01*
6p gain	*ECI2*	0.7	0.3-1.3	0.2
	DCDC2	0.7	0.4-1.3	0.3
	CDKN1A	0.5	0.3-1.0	0.06
	RUNX2	0.6	0.3-1.2	0.2
6q loss	*CTGF*	0.8	0.4-1.7	0.6
	IGF2R	0.8	0.4-1.5	0.4
8p loss	*LZTS1*	1.8	1.0-3.5	0.07
	NRG1	2.8	1.5-5.5	0.002*
8q+	*RP1*	5.3	2.5-11.0	< 0.001*
	MYC	6.6	0.9-48.1	0.06
	ASAP1	6.1	1.9-19.9	0.003*
Multivariate - final model				
NBL1 deletion	5.3	2.2-13.0	< 0.001*	
LZTS1 deletion	5.3	2.2-12.8	< 0.001*	
Monosomy 3	11.0	3.4-35.7	< 0.001*	
8q+	3.9	1.6-9.2	0.002*	

* $p \leq 0.05$ considered significant

Table S3. Predictive accuracies of Cox univariate and multivariate models

Variable	Cox PHA	AUC at fixed time points (months)					Integrated AUC (C^T) (months)					Harrell's C-index	SE
		12	24	36	48	64	12	24	36	48	64		
Univariate													
Immune infiltrate	0.77	0.662	0.653	0.628	0.551	0.502	0.678	0.666	0.661	0.657	0.647	0.653	0.03
Age[a]	0.03	0.535	0.537	0.583	0.607	0.7	0.561	0.548	0.553	0.558	0.566	0.502	0.04
Gender	0.34	0.56	0.555	0.572	0.561	0.539	0.555	0.559	0.56	0.559	0.558	0.578	0.04
Diameter	0.89	0.498	0.494	0.513	0.502	0.516	0.498	0.498	0.499	0.498	0.499	0.503	0.04
Thickness	0.22	0.505	0.497	0.518	0.511	0.515	0.5	0.504	0.505	0.506	0.507	0.501	0.04
Location	0.71	0.539	0.54	0.553	0.542	0.544	0.538	0.539	0.539	0.539	0.539	0.546	0.04
Stage	0.18	0.589	0.591	0.62	0.609	0.609	0.587	0.59	0.592	0.593	0.594	0.610	0.04
Extrascleral extension	0.80	0.565	0.54	0.533	0.5	0.502	0.571	0.566	0.561	0.557	0.553	0.559	0.02
Epithelioid	0.32	0.636	0.64	0.628	0.631	0.619	0.636	0.64	0.638	0.637	0.636	0.651	0.04
Mitotic activity[a]	0.03	0.719	0.631	0.56	0.572	0.584	0.733	0.717	0.694	0.679	0.671	0.690	0.04
Necrosis	0.97	0.591	0.575	0.569	0.535	0.551	0.595	0.584	0.581	0.581	0.579	0.579	0.03
Pigmentation	0.33	0.528	0.511	0.53	0.515	0.511	0.516	0.518	0.52	0.519	0.518	0.519	0.04
Monosomy 3	0.83	0.678	0.693	0.725	0.715	0.721	0.671	0.68	0.687	0.69	0.692	0.692	0.04
Isochromosome 8q	0.78	0.655	0.639	0.585	0.561	0.502	0.685	0.673	0.659	0.651	0.641	0.654	0.03
8q gain	0.42	0.685	0.686	0.711	0.695	0.707	0.681	0.686	0.69	0.69	0.691	0.699	0.04
8p loss	0.29	0.595	0.595	0.587	0.586	0.583	0.61	0.606	0.603	0.6	0.599	0.617	0.04
6p gain	0.34	0.56	0.558	0.577	0.568	0.549	0.559	0.559	0.561	0.561	0.56	0.576	0.04
1p loss	0.10	0.521	0.514	0.529	0.518	0.555	0.507	0.511	0.511	0.511	0.514	0.499	0.04
LZTS1 deletion	0.16	0.571	0.571	0.576	0.577	0.585	0.578	0.578	0.577	0.576	0.577	0.594	0.04
NBL1 deletion	0.09	0.52	0.514	0.53	0.52	0.542	0.512	0.515	0.516	0.516	0.518	0.502	0.04
Multivariate models													
Clinical	0.43	0.631	0.624	0.618	0.608	0.608	0.64	0.636	0.634	0.631	0.629	0.631	0.05
Histology	0.20	0.727	0.728	0.722	0.699	0.715	0.732	0.727	0.725	0.725	0.725	0.743	0.05
CNA	0.22	0.8	0.823	0.832	0.788	0.801	0.824	0.821	0.825	0.825	0.823	0.797	0.05
Immune-CNA	0.33	0.823	0.833	0.837	0.794	0.797	0.834	0.829	0.834	0.833	0.831	0.809	0.05
Combined	0.61	0.836	0.832	0.805	0.801	0.759	0.846	0.841	0.837	0.834	0.829	0.851	0.05
External model*													
M3/8q+	0.65	0.737	0.748	0.778	0.759	0.743	0.731	0.738	0.745	0.747	0.747	0.748	0.05

[a]Local Cox PHA: proportional hazards assumption; SE: standard error

*From Cassoux,et al. Br J Ophthalmol. 2013 Oct 29

Synopsis of publication III

(Manuscript in preparation)

Identification of an interferon-gamma induced gene signature associated with immune cell infiltration in uveal melanomas

Narasimhaiah D, Remark R, Legrand C, Damotte D, De Potter P, Coulie PG, Vikkula M, Godfraind C

In uveal melanoma (UM) infiltration by cytotoxic (CD8+) T-cells is associated with poor prognosis. This is unlike in most other solid tumors, where CD8+ T-cells is a marker of good prognosis. On the other hand, presence of tumor associated macrophages (TAM) is associated with poor outcome, both in UM and most other solid tumors.

When this work began, there was no data available concerning the immune profile of UM; genes and pathways involved in eliciting the immune infiltrate. Our analysis of the transcriptomic profiles using both unsupervised and supervised approaches led to the characterization of two molecular subgroups of UM based on a gene signature. The latter comprised of immune genes of IFNG/STAT1-IRF1 axis and its presence correlated with intra-tumoral infiltrate of lymphocytes and macrophages. It was also clinically relevant, being associated with poor clinical outcome; reinforced by validating on two external datasets. In addition, UM were stratified into three prognostic groups using combined densities of CD8+ T-cells and TAM. This again corroborates the presence of three risk-groups in UM.

New information from this work:

- Identification of a prognostically relevant interferon-gamma induced gene signature in UM
- Delineation of three UM risk-groups based on CD8+ T-cell and TAM infiltrate

The author carried out the vast majority of experiments and analyses in this study.

Identification of an interferon-gamma induced gene signature associated with immune cell infiltration in uveal melanomas

Narasimhaiah D[1], Remark R[2], Legrand C[3], Damotte D[2], De Potter P[4], Coulie PG[5], Vikkula M[1], Godfraind C[1,6]

[1]Laboratory of Human Molecular Genetics, de Duve Institute, [3]Institute of Statistics, Biostatistics and Actuarial Sciences, [4]Department of Ophthalmology, [5]de Duve Institute, Université catholique de Louvain, Belgium
[2] INSERM U1138, Team <Cancer, Immune control, and Escape>, Centre de Recherche des Cordeliers, 15 rue de l'Ecole de Médecine, 75006 Paris, France
[6]Département d'Anatomie et Cytologie Pathologiques DACP, Pôle de Biologie, Institut de Biologie et de Pathologie, CHU A Michallon, CS 10217, Grenoble 38043, France.

Running title: Immune signature and prognosis

Key words: melanoma, uveal, immune signature, interferon-gamma

Corresponding author:
Catherine Godfraind MD, PhD
Professor,
Département d'Anatomie et Cytologie Pathologiques DACP,
Pôle de Biologie, Institut de Biologie et de Pathologie
CHU A Michallon, CS 10217,
38043 Grenoble cedex 09
tel: 04 76 76 73 77- 06 63 71 48 42
fax: 04 76 76 59 49
email: cgodfraind@chu-grenoble.fr

Conflict of interest: None

Abstract

Background

Immune cell infiltration is emerging as a novel biomarker in cancer. Uveal melanomas (UM) also happen to be infiltrated by cytotoxic CD8+ T-lymphocytes and tumor-associated macrophages (TAM); but contrary to most solid tumors, this infiltrate is of poor prognosis. The objective of this work was to better understand the pathobiology of immune infiltration in UM.

Materials and methods

Primary, untreated, mainly large, retinal detached UM were analyzed (1) for gene expression using Affymetrix U133 Plus 2.0 array (n =15) and RT-qPCR (n = 36); (2) by immunohistochemistry (n = 89) and (3) by survival statistics.

Results

Two molecular subgroups of UM were identified based on a gene signature comprising of immune genes of interferon-gamma (IFNγ)/STAT1-IRF1 axis. This signature correlated with high degree of intra-tumoral CD8+ cytotoxic T-lymphocyte and macrophage infiltrate and poor clinical outcome. These findings were validated on two external datasets. In addition, survival analysis demonstrated UM to better stratify when using three prognostic groups defined according to the densities of cytotoxic T-cells and TAM.

Conclusion

To the best of our knowledge, this is the first *in vivo* description of an immune gene signature in UM bearing the footprint of IFNγ activation. Its presence correlated with poor clinical outcome. Also, its association with macrophage and cytotoxic T-cells demonstrated for the first time that co-analysis of these immune cells stratifies UM into three risk-groups.

Introduction

If the scientific developments over the last century have led to the notion of cancer being a genetic disease, the last two decades have highlighted the role of 'tumor microenvironment' (TME) in the multistep process of tumorigenesis {Hanahan et al, 2011}. It is diverse, encompassing different components like immune cells, fibroblasts, vasculature, cytokines, chemokines and extracellular matrix {Bindea et al, 2010}. With the emergence of cancer immunosurveillance and immunoediting concepts, {Shankaran et al, 2001; Dunn et al, 2004} the immune environment has received much attention. It is heterogeneous, comprising of cell types from both innate and adaptive systems {Pagès et al, 2009}. Also, in majority of solid tumors, high infiltrate of lymphocytes correlates with good clinical outcome {Fridman et al, 2012}.

Uveal melanomas (UM) arise in an immune-privileged site {Streilein 2003}, and a subgroup of them demonstrate an immune reaction {de la Cruz et al, 1990; Makitie et al, 2001}. Even though the cell types involved, lymphocytes and tumor-associated macrophages (TAM) have been defined, the pathways eliciting this immune reaction have not yet been unraveled *in vivo*. Elucidating the latter will facilitate a better understanding of the tumor biology.

This was done by first analyzing the transcriptomic profiles of 15 primary, untreated, large, retinal detached UM. In a variety of cancers, such analyses have led to the identification of immune gene signatures with common aspects between tumor types. Their annotation and validation has contributed not only to a better understanding of tumor biology, but has also highlighted their prognostic and predictive roles {Pages et al, 2009; Ascierto et al, 2011;

Ascierto et al, 2012; Carretero et al, 2012; Mann et al, 2013}. In UM, it resulted in identification of an interferon-gamma (IFNγ) induced gene signature associated with infiltration by cytotoxic T-cells and macrophages.

This molecular profile was subsequently translated into an immunohistochemistry one. The latter was tested on an additional 76 tumors, allowing the series to be large enough to allow correlation of immune infiltration with clinical outcome. Contrary to most cancers, high immune infiltration was associated with poor outcome. This was also validated on external datasets. In addition, three prognostic groups were defined through combined analysis of cytotoxic T-lymphocyte and macrophage infiltrate.

Materials and methods

Tumor series

The series included 91 choroidal and ciliochoroidal melanomas, 89 of which have been previously described (*Narasimhaiah, et al. Manuscript in preparation*). The patients underwent enucleation at Ophthalmology Department of Saint-Luc Hospital, Brussels, Belgium between 1997 and 2010 and were previously untreated. Age at operation varied from 35 years to 90 years with a mean of 64.6 years and a median of 67 years. The male to female ratio was 1.1. Snap-frozen (n=15), RNA later preserved (n=21) and formalin-fixed paraffin-embedded (FFPE; n=89) tumor material were available. The study was carried out according to our institutional ethics committee guidelines.

RNA extraction

For the 15 snap-frozen samples, total RNA was extracted using guanidine isothiocyanate/cesium chloride procedure. The first-strand cDNA was synthesized from 2µg of total RNA with M-MLV reverse transcriptase (catalog # 28025) (Invitrogen, Life Technologies) and random hexamer primer (Fermentas), as recommended by manufacturer {Cipponi et al, 2012}.

For 21 samples stored in RNA later (-80°C), RNA was extracted using NucleoSpin RNA (catalog # 740955) (Macherey-Nagel, Düren, Germany) and first strand cDNA was synthesized from 1µg of total RNA using RevertAid H minus first strand cDNA synthesis kit and random hexamer primer (catalog # K1632) (Fermentas, ThermoScientific), as per manufacturer's guidelines (**Supplementary methods**).

Array hybridization

The RNA samples were processed as described previously {Palm T 2009}. RNA was quantified using NanoDrop (ThermoScientific, Wilmington, DE) and samples with A_{260}/A_{280} ratio between 1.70-1.83 were included. Also, only samples with intact RNA indicated by sharp, clear bands for 18S and 28S rRNA on agarose gels were utilized. Human Genome U133 Plus 2.0 arrays (Affymetrix, Santa Clara, CA) were used to generate gene expression profiles from 5µg of total RNA following manufacturer's protocol. The intensity files were obtained by processing the images using Microarray suite 5.0 gene expression software. Probe sets present in <90% of the samples were excluded from analysis.

Array data analysis

Additional normalization was performed to reduce variation between individual hybridizations. Therefore, the mean intensity of each probe set was defined based on the intensity of all tumors. Then, individual intensities were divided by their respective mean intensity and converted to log2. The first 1500 probe sets with highest standard deviation (SD) were submitted for statistical analysis using TIGR MultiExperiment Viewer platform (MeV4.8.1, http://www.tm4.org/mev/){Saeed et al, 2003}. Subgroups of UM were unraveled by performing hierarchical clustering with Pearson's correlation. Estimation of sampling distribution was assessed by bootstrapping, using 100 iterations. Differentially expressed probe sets were identified by t-test applying high stringency (5000 permutations, p-value 0.001) and low stringency (1000 permutations, p-value 0.01) conditions, with adjusted Bonferroni method of p-value correction.

The annotation of statistically significant probe sets was performed using DAVID v6.7 {Dennis et al, 2003}, InnateDB {Lynn et al, 2008}, Gene Set Enrichment Analysis (GSEA v2.0.13) with Molecular Signatures Database (MSigDB v4.0) {Subramanian et al, 2005; Liberzon et al, 2011} and CluePedia v1.2.1 {Bindea et al, 2013} (**Supplementary methods**).

Immune genes

The immunologically relevant genes were compiled from three databases: 5998 genes from ImmPort (https://immport.niaid.nih.gov), 1773 genes related to "immune system process" from Gene Ontology database (http://amigo.geneontology.org) and 1326 immunologically important genes from Wiki for Immunology (http://wiki.geneontology.org/index.php/Immunology). There were a total of 6487 genes after accounting for common genes between databases and 4840 genes with available probe sets (n=11,103) were included for further analysis.

Immunohistochemistry

FFPE sections from 89 UM were immunolabeled with antibodies directed against CD3, CD4, CD8, CD163 and HLA-DRA using BenchMark XT (Ventana Medical Systems, Tuscon, AZ). CD3/DC-LAMP, NKp46 and GBP1 were tested on 63, 65 and 39 tumors, respectively. Immunolabeling for CD3/DC-LAMP and NKp46 was performed as described previously {Remark et al, 2013} and for GBP1 by manual method (**Supplementary methods and Table M1**).

The evaluation of CD3 and HLA-DRA staining was based on a semi-quantitative scoring of five tumoral regions: edges, apex, centre and base. For each area and for each antibody, a score of 0, 1 or 2 was assigned, resulting in a

total score of 20. The latter was referred as 'immune score'. For DC-LAMP and NKp46, all intra-tumoral positive cells per section were counted. GBP1 was quantified using an image analysis system with whole slide scanner, LeicaSCN400 (Leica Microsystems GmbH, Wetzlar, Germany) and analysis software, Tissue IA 2.0 (SlidePath, Leica) (**Supplementary methods**).

Quantitative real-time reverse transcription polymerase chain reaction (RT-qPCR)

The RT-qPCR was carried out using SYBR Green I master (catalog # 04 707 516 001) in a LightCycler 480 (both from Roche Diagnostics, Basel, Switzerland) (**Supplementary methods**). The target genes tested were: *CXCL9, GBP1*, *RARRES3, STAT1*-beta-transcript, and *PSMB9*. The reference gene was *CSNK2B*. The primer sequences have been provided in **Table M2**.

Statistics

To assess significance between groups, Chi-square or Fischer's exact tests were used for dichotomous variables and Mann-Whitney (two groups) or Kruskal-Wallis (> two groups) tests for continuous variables. Survival analyses (n =86) were based on disease-free survival (DFS), defined as time from enucleation to radiological diagnosis of metastases for patients developing metastases. Patients still alive and metastases-free at the time of the analysis were censored at the date of last follow-up {Tosolini et al, 2011}. For these latter patients, the inclusion criterion was availability of at least 24 months post-enucleation follow-up. DFS was estimated by Kaplan-Meier (KM) curves and compared using the log-rank test. A p-value of ≤ 0.05 was considered significant. Statistical analyses were performed using JMP v10 (SAS Institute Inc., Cary, NC) and IBM SPSS Statistics v20, v21 (IBM, Armonk, NY).

External validation

Two primary UM gene expression datasets on Affymetrix Human Genome U133 Plus 2.0 array platform: GSE22138 (n = 63) and GSE27831 (n = 29) were downloaded from GEO (http://www.ncbi.nlm.nih.gov/geo/). The raw data were normalized as described above. Failure to fulfill the clinical inclusion criterion of our series led to exclusion of two and seven cases from GSE22138 and GSE27831, respectively. The 83 remaining tumors were categorized as immune-high and immune-low based on the 44 significant probe sets identified as responsible for similar division of our UM series. Tumors with overexpression of ≥ 70% of 44 probe sets (mean+3SD) were considered as immune-high and ≤ 20% (mean-3SD) were considered as immune-low. The rest of the tumors were considered as intermediate and excluded from further analysis.

Supplementary methods

RNA extraction

For each tumor, 20 cryosections of 20µm thickness were used for extraction. Isolation of total RNA was performed using NucleoSpin RNA (catalog # 740955) (Macherey-Nagel, Düren, Germany) as per the manufacturer's guidelines. In brief, the cryosections were homogenized with RA1 buffer and beta-mercaptoethanol and filtered using NucleoSpin filters. The filtrate was mixed with 70% ethanol and bound to NucleoSpin RNA column. The column was washed and dried using buffers RAW2 and RA3, followed by elution using RNase-free water. Total RNA was treated with Turbo DNA-free^{TM} kit (catalog # AM1907) (Ambion, Life Technologies, Carlsbad, CA) to remove the residual DNA. RNA was quantified using NanoDrop (ThermoScientific, Wilmington, DE). The A_{260}/A_{280} ratio for the samples ranged from 1.88-1.99. The melanin concentration in RNA was assessed by measuring the absorbance at 320nm and samples with absorbance > 0.1 were re-purified on RNA column.

Bioinformatics

For annotation by DAVID and InnateDB, the recommended default criteria were applied. The false-discovery rate (FDR) cut-off was 0.05 and p-value was corrected by Benjamini-Hochberg method. For analysis by GSEA, the input probesets (n=26,493) were a combination of probesets from transcripts present in >90% of tumors and probesets from immune genes. The two phenotypes, immune-high and immune-low were analyzed by applying the GSEA recommended default criteria. For each of the phenotypes, the 100 top-ranked genes were used for further analysis.

GBP1 immunohistochemistry

4µm sections were deparaffinized, endogenous peroxidase activity was blocked with 3% hydrogen peroxide and heat-induced epitope retrieval was performed in 0.1M, pH 6.0 citrate buffer at 100°C for 75 minutes. Following blocking of aspecific binding with 10% normal goat serum for 30 minutes, endogenous biotins were neutralized with Avidin/Biotin blocking kit (catalog # SP-2001) (Vector Laboratories, Burlingame, CA) and the sections were incubated overnight with unlabeled GBP1 primary antibody. After washing, they were incubated with secondary antibody, 1:500 biotinylated anti-mouse IgG (catalog # BA-9200) (Vector laboratories), followed by incubation with 1% streptavidin-AP-conjugate (catalog # 11089161001) (Roche Diagnostics) for 30 minutes each. Revelation was performed using Sigma Fast Fast Red TR/Napthol AS–MX (catalog # F4648) (Sigma-Aldrich, St. Louis, MO) in dark for 30 minutes. The slides were counterstained with haematoxylin and coverslipped using an aqueous mounting medium. All reactions were carried out at room temperature.

GBP1 quantification

Digital images of GBP1-stained slides were obtained at 20x magnification using a whole slide scanner, LeicaSCN400 (Leica Microsystems GmbH, Wetzlar, Germany). The images were stored and managed using a web-enabled image server, Digital Image Hub (DIH) (SlidePath, Leica). Quantification of GBP1 was performed using the image analysis software, Tissue IA 2.0 (SlidePath, Leica) using ‘measure stained area’ algorithm. First, the total tumor area (reference area) to be analyzed was outlined manually using the annotation tool. Image segmentation was performed using two thresholds that were manually set. The first was a tissue

segmentation threshold to separate the tumor tissue from background. The second was a color definition threshold to define the positively stained pixels. In order to ensure that the latter adequately reflected all positive staining, it was tested on multiple areas within the same slide and on multiple different slides. The output results included: total area of the annotated tumor (reference area), positively stained tumor area, average staining intensity and concentration of the stain within the tissue sample. The ratio of the positive surface area with respect to the reference surface area was computed and was referred to as the GBP1 labeling index {Decaestecker et al, 2009}.

Quantitative real-time reverse transcription polymerase chain reaction (RT-qPCR)

The PCR mix was prepared as follows: PCR-grade water 3.4µl, forward and reverse primers 0.8µl each (5µM) and master mix 10µl. For one reaction, 15µl of PCR mix and 5µl of cDNA (2ng/µl concentration) template was used. The LightCycler experimental run protocol was: denaturation program (95°C for 10 min), amplification and quantification program repeated 50 times (95°C for 10s, annealing temperature primer-dependent for 15s, 72°C for 15s), melting curve program (65-97°C) and cooling step to 40°C. All samples were tested in triplicate, along with no-DNA controls. The specificity of the amplified PCR product was assessed by performing melt curve analysis for both target and reference genes. Standard curves were generated for each target and reference genes and were used for quantification by taking PCR efficiencies (E) into consideration. Crossing point (Cp) in an amplification reaction is the cycle at which the fluorescence

of a sample rises above the background fluorescence. The relative expression of target genes was determined using the E-method of relative quantification. The mean Cp for target and reference genes was obtained for all samples. The relative expression ratio of the target gene for each sample was calculated using the formula: $(E_{target})^{\Delta Cp\ target} / (E_{reference})^{\Delta Cp\ reference}$ {Uebelhoer et al, 2013}. *CSNK2B* was used as the reference gene for normalization.

Table M1. Details of antibodies used for immunohistochemistry

Primary antibody	Dilution	Incubation time	Clone	Product code	Company
CD3	1:250	120 minutes	-	A0452	Dako, Glostrup, Denmark
CD4	1:50	100 minutes	4B12	NCL-CD4-368	Novocastra, Newcastle upon Tyne, UK
CD8	1:24	48 minutes	CD8/144B	M7103	Dako
CD163	1:300	72 minutes	10D6	NCL-CD163	Novocastra
HLA-DRA	1:50	36 minutes	TAL1.B5	M0746	Dako
NKp46	1:100	60 minutes	195314	MAB1850	R &D Systems, Minneapolis, MN
CD3/ DC-LAMP	1:80 1:80	60 minutes 60 minutes	- 1010E1.01	A0452 DDX0191	Dako Dendritics, Lyon, France
GBP1	1:300 1:900	overnight	4D10	ab109995	Abcam, Cambridge, UK

Table M2. Primer sequences used for RT-qPCR

Gene	Orientation	Primer sequence	Product size	Annealing temperature	Company
CXCL9	F R	5'-GCACCAACCAAGGGACTATC-3' 5'-GCTTTTTCTTTTGGCTGACC-3'	192 bp	57°C	IDT Coralville, IA
GBP1	F R	5'-TGTTGCAGGAAATGCAAAGA-3' 5'-TCCCTCTTTTAGTAGTTGCTCCTG-3'	179 bp	57°C	IDT
RARRES3	F R	5'-TGGACCATGAGTACCAACCA-3' 5'-GCCACACCAACTTCAACCTT-3'	181 bp	57°C	IDT
STAT1-β-transcript	F R	5′-ATGGGTGGAGCGGTCCCAGAAC-3′* 5′-AGCATCTTCAACAGGCCCCAGCC-3′*	369 bp	60°C	IDT
PSMB9	F R	5'-CAGCTGCTGATGCCCAAG-3' 5'-CAGTTCATTGCCCAAGATGA-3'	437 bp	60°C	IDT
CSNK2B	F R	5'-GGCAATGAATTCTTCTGTGAA-3' 5'-AACCAAAGTCTCCTTGCTGGT-3'	271 bp	60°C	Eurogentec Seraing, Belgium

F: forward; R: reverse

*From: Ascierto ML, et al, Breast Cancer Res Treat 2012;131:871-80

IDT: Integrated DNA Technologies

Results

1. Identification of a uveal melanoma immune signature by gene expression analyses

1.1. Microarray hierarchical clustering analysis

Hierarchical clustering (HCL) spontaneously separated the 15 genome-wide profiled primary UM in two subgroups of five and ten tumors, with dendrogram node values of 96 and 59, respectively (**Figure 1a**). Forty-four probe sets, corresponding to 34 genes, identified by high-stringency t-test were responsible for this segregation (**Figure 1b, Table S1**). They were all relatively overexpressed in the subgroup with five uveal melanomas when compared to the rest. These genes were related to immune response in DAVID {Dennis et al, 2003}.

1.2. Immune gene analysis

A catalogue of immune response genes collated from various databases was constructed and subsequently submitted to new HCL analysis. It spontaneously separated the melanomas into same two subgroups. Low-stringency t-test identified 156 probe sets, corresponding to 122 genes as responsible for this partition. As before, one of the subgroups only predominantly overexpressed genes of the immune response (n=111), and underexpressed only few (n=11) (**Figure 1c, Table S1**). Therefore, tumors of this subgroup were referred as immune-high and those of other subgroup as immune-low.

1.3. Gene set enrichment analysis (GSEA)

The first 100 top-ranked genes, identified in GSEA, in both immune-high and immune-low subgroups were analyzed. In the former, genes were mainly involved in innate and adaptive immune responses; antigen processing and presentation; endocytosis and lymphocyte mediated immunity. In the latter, they were predominantly associated with regulation of transcription, cell adhesion and apoptosis (**Table S1**).

1.4. Composition of the immune signature

1.4.1. Overexpressed genes

The immune signature comprised of 245 overexpressed genes in immune-high UM. They were unraveled by HCL (n = 34), supervised analysis of genes of immune response (n = 111) and GSEA (n =100). They constituted seven subgroups when considering if genes overlap or not between these three analyses. They were named according to the analyses that identified them. So, the 18 genes common to all analyses were named "common". The 33 genes intersecting between immune response analysis and GSEA constituted the "immune-GSEA" subgroup. The eight genes overlapping between the immune and HCL corresponded to "immune-HCL". The four genes coinciding between HCL and GSEA were named "HCL-GSEA". The remaining genes were specific to each algorithm: 52 for immune response analysis, 45 for GSEA and four for HCL and corresponded to the "immune", "GSEA" and "HCL" subgroups, respectively (**Figures 1d and S1a**).

1.4.2. Underexpressed genes

The signature also comprised of 111 underexpressed genes in immune-high UM. They were identified by three methods: HCL (n = 0), supervised analysis of genes of immune response (immune; n = 11) and GSEA (n =100). *NRARP* was the only gene common between analyses.

2. Identification of a uveal melanoma immune signature by immunohistochemistry

2.1. IHC-based immune score definition

UM that classified according to array, also demonstrated dissimilarities when analyzing their immune infiltration by IHC. Immune-high tumors demonstrated a dense infiltrate of tumor-associated macrophages (HLA-DRA+CD163+) and cytotoxic T-lymphocytes (CD3+CD8+), in the absence of helper T-cells (CD3+CD4+) (**Figures 2a,b,c**). It mostly involved tumor edges, apex, center and base. A similar distribution was seen in immune-low tumors, but the infiltrate density varied: TAM being only mild to moderately abundant (**Figures 2d,e,g,h**) and T-cells occasional or absent (**Figures 2f,i**). These histological differences, observed on 13 UM, were transformed into a semi-quantitative "immune score" for which immune-high tumors had a mean score of 16.9 and a median of 17 (SD: 1.29). This defined a cut-off (mean-2SD) of 14 to discriminate immune subgroups.

2.2. Classification of additional UM by IHC-based immune score

An additional 76 UM, not previously tested by array, were defined as immune-high or immune-low using the IHC semi-quantitative immune score. Fourteen had a score $\geq$ 14 and 62 < 14. When added to the 13 initial tumors, the cut-off remained 14; meanwhile, the average immune score for immune-high UM

decreased from 16.9 to 16.7 with a median of 16.5 (SD: 1.5). In addition, the individual cut-off scores for HLA-DRA was seven, and for CD3 five, with HLA ≥7 and CD3 ≥5 in immune-high and HLA <7 and CD3 <5 in immune-low, respectively.

2.3. Validation of the IHC-based immune score by RT-qPCR.

UM immune-classification based on IHC was validated by RT-qPCR using *CXCL9*, *GBP1*, *RARRES3*, *PSMB9* and *STAT1*-beta. These genes were chosen because on microarray they had high fold differences between immune-high and immune-low UM (11.9 to 34.3) and high absolute expression values (693.5 to 1953) in immune-high tumors. RT-qPCR was performed on the 15 UM tested by microarray, as well as in five tumors categorized as immune-high and 16 as immune-low by IHC alone. Expression values of the five transcripts were higher in immune-high UM when compared to immune-low ones in either series: microarray, p-value = 0.002 (Mann-Whitney test; **Figure 2j**) and IHC, p-value = 0.05-0.002 (Mann-Whitney test; **Figure 3a**).

3. Histological characteristics related to immune signature

3.1. Cellular composition of the immune infiltrate

The analyses of additional UM confirmed the main immune cell types to be cytotoxic T-lymphocytes (CD3+CD8+) and TAM (CD163+HLA-DRA+). They were more abundant in immune-high than immune-low UM with scores of 7.9 and 1.3 for CD3 and 8.8 and 4 for HLA-DRA, respectively (for both, p <0.001, Mann-Whitney test). Their occurrence in the five tumoral regions analyzed per tumor, tested by the frequency of having a semi-quantitative score of more than 0.5 was: 78.9% and 2.9% for CD3, 99% and 22.9% for

HLA-DRA in immune-high and immune-low tumors, respectively (for both, p <0.001, Mann-Whitney test).

Analyses for additional immune cell types demonstrated T-helper cells (CD3+CD4+) to be very occasional. Zero to six natural killer cells (NK) was counted per immune-high UM, and zero to ten per immune-low, respectively. The count of mature dendritic cells (DC) ranged from zero to 13 in immune-high tumors, with two lesions containing 125 and 60 DC, respectively, and from zero to six in immune-low tumors, with one tumor showing 40 cells.

3.2. Topographic characteristics of the immune infiltrate

The distribution of T-lymphocytes and TAM appeared heterogeneous. Comparisons were made for immune score (combined HLA-DRA and CD3), HLA-DRA only and CD3 only. The mean immune scores in immune-low UM were: 0.7 for base, 1.0 for centre, 1.1 for apex and 1.2 for both edges ($p < 0.001$, Kruskal-Wallis test). The mean scores in these regions for HLA-DRA ranged from 0.6 to 0.9 ($p = 0.007$, Kruskal-Wallis test) and for CD3 from 0.1 to 0.3 ($p < 0.001$, Kruskal-Wallis test) (**Figure 3b**). Likewise, pair-wise comparisons between the regions indicated significant differences mostly between base and others for immune score, HLA-DRA only and CD3 only (**Table S2**).

In immune-high tumors, the mean immune scores were: 3.2 for base and edge; 3.4 for apex and 3.7 for centre ($p = 0.02$, Kruskal-Wallis test). The mean scores in these four regions for HLA-DRA ranged from 1.7 to 1.9 ($p = 0.03$, Kruskal-Wallis test) and for CD3 from 1.5 to 1.7 (p = not significant, Kruskal-Wallis test) (**Figure 3c**). Likewise, pair-wise comparisons between the regions indicated significant differences mostly between centre and others for immune score and HLA-DRA (**Table S2**).

3.3. Region-wise accuracy in prediction of immune category

The performance of each individual region was better than by random assignment ($p < 0.001$, Chi-square) as assessed by simple logistic regression. The receiver operating characteristic (ROC) curves demonstrated the area under the curve to be 0.96 for apex, 0.97 for edge and base and 0.99 for centre. The misclassification rates were: 3.3% for centre, 5.6% for apex and 6.7% for both edge and base, respectively. Of all the regions, centre had the highest sensitivity 100% (specificity 90%) in correctly predicting immune-high and immune-low groups.

4. Biological significance of immune signature

4.1. Overexpressed genes

4.1.1. Associated pathways

The seven subgroups of overexpressed genes were significantly associated with different pathways. Some were common between all of them: interferon-gamma signaling (*STAT1*, *IRF1*, *GBP1*, *GBP2*, *CCL4*, *CCL5)*; cell adhesion molecules (*CD2*, *CD8A*, *CD86*, *SIGLEC1*, *LGMN*, MHC class I and II molecules); allograft rejection and graft-versus host disease (*CD86*, *GZMB*, MHC class I and II molecules); antigen processing and presentation (*TAP1*, *TAPBP*, *PSME1*, *PSME2*, MHC class I and II molecules) and phagosome (*TAP1*, MHC class I and II molecules). Others were associated with specific subgroups: TCR (*CD2*, *CD8A*, *CD86*, *FYB*, *LCK*); natural-killer cell mediated cytotoxicity (*CD48*, *GZMB*, *TNFSF10*) and TCR signaling in naïve CD8+ and CD4+ T cells (*CD3D*, *CD8A*, *LCK*, *FYB*, *PTPN6*; **Figure 4a**). The complete list of pathways and associated genes has been provided in **Tables S3 and S4**.

4.1.2. Associated gene ontology terms

The gene ontology (GO) terms significantly associated with all subgroups were: immune response, interferon-gamma mediated signaling, cytokine-mediated signaling and innate immune response. Those specific to subgroups included: positive regulation of T-cell mediated cytotoxicity, T-helper 1 type immune response, immune response to tumor cell and positive regulation of phosphorylation of STAT protein (**Figure 4b and Table S5**).

4.1.3. Validation of IFN-gamma pathway implication by IHC

GBP1 is an end product of IFNγ signaling. It was tested for its expression by IHC in 18 immune-high and 21 immune-low tumors. Both tumor cells and immune cells expressed GBP1 in cytoplasm and membrane (**Figure 4c**). The staining intensity varied from weak to strong. The labeling index was: 18.6% in immune-high (SD = 12.6) and 9.9% in immune-low (SD = 8.9) ($p = 0.03$, Mann-Whitney test, **Figure 4d**).

4.1.4. Associated transcription factors

No transcription factors were common to the seven subgroups when computed from MSigDB {Liberzon et al, 2011}. Few were specific to some of them, such as: *IRF1*, *IRF2*, *IRF8*, *STAT1* and *RUNX1* (**Figure S1b**).

4.1.5. Associated cancer modules

The subgroups of UM overexpressed genes were compared to the cancer modules {Liberzon et al, 2011} which are gene groups with significant differential expression in diverse cancers. Of them, three or more subgroups were significantly associated to cancer modules 84, 46, 75, 45, 345, 436, 44

and 171; while, modules 143, 27, 119, 204 and 128 were specific to one or two subgroups (**Figure S1c**). The overexpressed UM genes happened to be predominantly underexpressed in lung and prostate carcinoma; medulloblastoma and hepatic metastases, but both under and overexpressed in those of breast and primary liver cancer (**Figure S1d**).

4.1.6. Relation between overexpressed genes

A network based on actions of overexpressed genes was constructed (**Figure S2**). It revealed three main gene groups. One was centred on transcription factors, *STAT1* and *IRF1*, comprising of IFNγ response genes (*CCL5*, *IDO1*, *IFIT3*, *PSMB9*, *XAF1*, *GBP1*, *GBP2*, *CXCL9*, *TAP1*, *TAPBP)* activated by them. The second one was T-lymphocyte associated such as, receptors (*TRAC*, *TRBC1*), cluster differentiation molecules (*CD2*, *CD3D*, *CD8A*) and signal transduction genes (*LCK*, *CD48*, *LY9*, *SLAMF7*, *SH2D1A*). The third group comprised of MHC class I (*B2M*; *HLA-B, C, E, G*) and II (*CD74*; *HLA-DRA*, *DPA1*) molecules.

4.1.7. Induction of immune signature

Cancer-testis antigens and melanocyte differentiation proteins are known to induce immune response in cancers. Comparison of their expression between immune-high and immune-low UM did not reveal any differentially expressed genes.

4.2. Underexpressed genes

Underexpressed genes were associated with pathways of prostate cancer, hepatitis C, integrin signaling, generic transcription pathway and regulators of bone mineralization.

The GO terms comprised: negative regulation of Wnt protein secretion, positive regulation of ERK1 and ERK2 cascade, cellular response to morphine and positive regulation of apoptotic process (**Tables S3 and S5**).

5. Clinical significance of immune signature

5.1. Immune infiltration and clinicopathological features

The series comprised of mainly large tumors (80%) with retinal detachment (97.5%) (**Table S6**). Between immune-high and immune-low groups, there were no significant differences with respect to patient age, tumor size, stage, location and extrascleral extension. With regard to pathological features, mitotic activity and necrosis were significantly increased in immune-high UM; but there were no differences with respect to epithelioid component and pigmentation (**Table 1**).

5.2. Immune infiltration and outcome

5.2.1. Based on gene signature

To attain statistical power, two external datasets, GSE22138 and GSE27831, were used to analyze the outcome associated with the unraveled immune signature. They differed from our series regarding tumor size and retinal detachment status (**Table S6**). In our series, 97.5% had retinal detachment (RD), in comparison with 62.5% in external dataset 1; where as its status was not available for dataset 2.

In external dataset 1, based on the expression profiles, nine tumors were classified as immune-high and 37 tumors as immune-low. The median DFS in immune-high was 17.6 months and in immune-low it was 64 months, but was not statistically different (log-rank test p = 0.3, **Figure 5a**). However, while considering only tumors with RD, this difference was significant (log-rank test p = 0.006, **Figure 5b**). Moreover, in external dataset 1, there was a significant difference in DFS between tumors having RD and those lacking it (log-rank test p = 0.01).

In external dataset 2**,** based on the expression patterns, four cases were classified as immune-high and nine as immune-low. The KM curves corroborated the relation between immune signature and DFS (log-rank test p = 0.03, **Figure 5c**).

5.5.2. Based on immunohistochemistry

Significant difference in DFS between immune-high and immune-low tumors (log-rank test p < 0.001) as defined by IHC was observed (*Narasimhaiah D, et al. Manuscript in preparation*). This was also true when HLA-DRA and CD3 were individually considered (**Figures 5d/e**). An additional stratification was performed considering combined densities of HLA-DRA and CD3. This identified three risk-groups (log-rank test p <0.001, **Figure 5f**). DFS at 36 months was: 26.3% [95% confidence interval (CI): 6.5-46.1] in CD3-high/HLA-high, 66.7% [95% CI: 35.9-97.5] in CD3-low/HLA-high and 76.3% [95% CI: 64.9-87.7] in CD3-low/HLA-low. The survival in CD3-high/HLA-low tumors could not be assessed as there were only two tumors.

Discussion

An interferon-gamma (IFNγ) induced gene signature was identified by analyzing the transcriptomic profiles of 15 primary, untreated large, retinal detached uveal melanomas (UM). This unraveled signature is characterized by IFNγ stimulated genes affiliated to STAT1-IRF1 pathway; also encompassing chemokine ligands which attract lymphocytes and macrophages and cytotoxic molecules. Moreover, the IFNγ molecular imprint was also corroborated by *in vivo* demonstration of CD3+CD8+ T-lymphocytes and GBP1, an interferon inducible protein {Cheng et al, 1983}. The signature correlation with infiltration by cytotoxic T-cells and tumor associated macrophages (TAMs) facilitated the translation of transcriptome-based signature into an IHC-based one on additional 76 UM. From a prognostic point of view, this signature was linked to poor clinical outcome as demonstrated in internal series and also by external validation.

Interestingly, the identified signature is similar to immune signatures described in cancers of breast, colorectum; cutaneous melanoma and ovary {Jonsson et al, 2010; Leffers et al, 2010; Mlecnik et al, 2011; Ascierto et al, 2012} indicating a redundancy, with IFNγ signaling/STAT1-IRF1 axis as the common denominator {Galon et al, 2013}. Furthermore, it is reinforced by the demonstration of increased interferon-gamma expression by activated T-cells co-cultured with UM cells *in vitro* {Jehs et al, 2014}. It is intriguing that even though UM and other cancers have common immunological profile, it has such contrasting influence on clinical outcome. This also indicates that the effect of the immune profile is tumor-specific and intrinsic to its biology.

Also, UM is unique, originating from an immune-privileged site; the latter also including brain, ovary, testis and pregnant uterus {Streilein 2003}. When one considers the impact of immune response in tumors originating from these organs, it is adverse in UM, but not in tumors of ovary and brain {Leffers et al, 2010; Lohr et al, 2011}. This too corroborates that the influence of immune cells is specific to tumor type.

Similar to the situation in other cancers {Pages et al, 2009; Jonsson et al, 2010}, the immune gene expression showed a positive correlation with infiltration by CD3+CD8+ T-cells and HLA-DRA+CD163+ macrophages. This facilitated the translation of the transcriptome-based signature into an IHC-based one by applying a semi-quantitative immune score. Moreover, the use of IHC helped appreciate the heterogeneity in immune cell distribution, which was not unexpected, as cancers *per se* are heterogeneous at genetic, epigenetic and microenvironmental levels {De Sousa et al, 2013}. The relevance of the topographic characteristics of immune infiltrate in solid tumors is only beginning to be analyzed, using colorectal cancer as the prototype {Pages et al, 2009; Mlecnik et al, 2011}.

In this series, the study of immune cell distribution demonstrated both quantitative and qualitative differences between immune-low and immune-high UM. The former displayed low to moderate numbers of macrophages and a sparse population of cytotoxic T-cells; whereas, the latter showed dense infiltrates of both cell types. Topographically, the immune cells localized the edges, apex, centre and base, with differences between the immune phenotypes. In immune-low tumors, the density of both macrophages and T-cells was highest at the edge and lowest at the base. However, this was not the

case with immune-high tumors, where the tumor centre was the region with highest density of macrophages and T-cells.

The reason for this immune cell distribution is not clear, but could be partly due to the orientation of vasculature in these tumors. They demonstrate neovessels at apex and centre and mature ones at base, with the former predisposing to hypoxia {Pina et al, 2009}. The latter increases the expression of pro-inflammatory chemokines such as, CCL2 involved in monocyte migration {Bronkhorst et al, 2014}. Also, one could speculate if the regional hypoxia levels may influence the degree of cytokine expression leading to intra-tumoral differences in immune infiltrate distribution. This may be the reason for higher expression of CCL2 in immune-high tumors (fold change 1.8) compared to immune-low ones.

Moreover, from a clinical point of view, this differential distribution may prove to be problematic for assessment of immune score on a biopsy sample, leading to misclassification. In this situation, the tumor site to be sampled becomes important. Our analyses of the accuracies of individual regions in predicting immune-high and immune-low status by IHC demonstrated ‘centre’ as the one with highest sensitivity and specificity making it the preferred area for a biopsy to minimize the false-negative rate. This correlates with that of colorectal cancers, where tumor centre is a significant region for assessment of immune infiltrate {Pagès et al, 2009}.

The impact of lymphocytes and macrophages on clinical outcome has been well-studied in cancer, {Pagès et al, 2009} {Zhang et al, 2012} with diametrically opposite effects; the former being good and the latter poor. In

case of UM, both cell types have been associated with adverse outcome {de la Cruz et al, 1990; Makitie et al, 2001; Bronkhorst et al, 2011}. Herein, the clinical relevance of the identified signature was assessed on two external datasets (GSE22138 and GSE27831) downloaded from GEO. Both of them demonstrated that overexpression of immune genes correlated with shorter disease-free survival. These results could also be reproduced on a larger internal dataset using immune score as a surrogate marker of gene signature.

Moreover, in our series, combined IHC analysis of TAM and T-lymphocyte densities delineated three risk-groups and improved prognostication. The risk of metastases was high for tumors with dense infiltrate of both cytotoxic T-cells and TAM; intermediate for those with low infiltrate of former and high infiltrate of latter and low for melanomas with low infiltrates of both. The relevance of high T-cell and low TAM infiltrate could not be assessed as there were only two tumors with this phenotype. This again reinforces the presence of three prognostic groups in UM (*Narasimhaiah D, et al, Manuscript in preparation*) {Cassoux et al, 2013}. In addition, this three-tier stratification could be a predictive biomarker to assess response to treatment like in other cancers {Ono et al, 2012; Seo et al, 2013} {Ayari et al, 2009; Deau et al, 2013}.

Besides, the prognostic and predictive role, the tumor immune response forms the basis of cancer immunotherapy. It is centered on identification of tumor-specific antigens that elicit T-cell responses. The former can be antigens resulting from mutations or rearrangements in exome; cancer-testis genes; differentiation and viral antigens {Coulie et al, 2014}. In the present series, there were no significant differences in the expression profiles of cancer-testis

antigens and melanocyte differentiation proteins between immune-high and immune-low tumors. The immunogenicity may be due to mutations and interrogation of immune-high UM at exome level may shed some light on the origin of T-cell response.

In conclusion, this is the first *in vivo* identification of an immune gene signature in large, retinal detached UM which is IFNγ/STAT1-IRF1 axis induced providing an insight into the immune profile of these tumors. The elucidated network of immune genes and pathways leads to a better understanding of the underlying immunological processes. Its association with poor prognosis could have implications for identification of novel therapeutic targets. In addition, this is the first study in UM to propose three immune-based prognostic groups on combined evaluation of intra-tumoral lymphocytes and macrophages. Its role as a predictive biomarker and therapeutic target warrants further exploration.

Acknowledgements

The authors thank Ludwig Institute of Cancer Research (LICR), Brussels branch for snap-frozen samples; Professor van Baren N, Ms. Mercier M and Ms. Daumerie A, LICR, Brussels branch for RNA extraction protocol and cDNA; Prof Limaye N, Dr Uebelhoer M and Miss Soblet J, GEHU, de Duve Institute for assistance with RT-qPCR; and Ms. Liliana Niculescu for secretarial assistance.

Funding support

This project was supported by Fonds Maisin (Université catholique de Louvain), F.R.S -FNRS (CDR J.0049.13) and Télévie (7.4607.10), all to CG.

ND was supported by fellowship from le Centre du Cancer, Cliniques Universitaires Saint-Luc, Université catholique de Louvain, Brussels, Belgium and grants from Télévie (7.4607.10 and 7.4585.12F).

1a

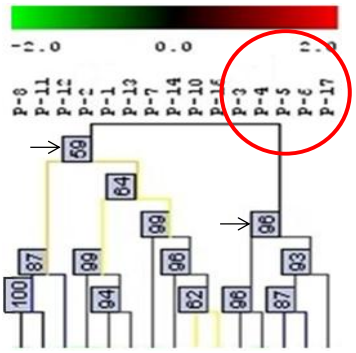

1b

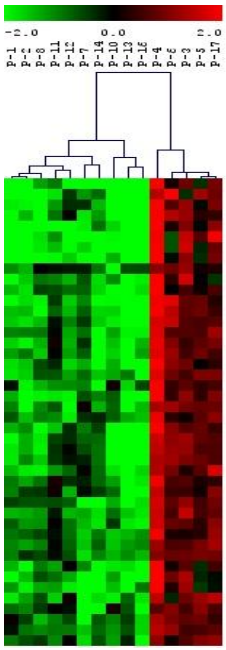

1c

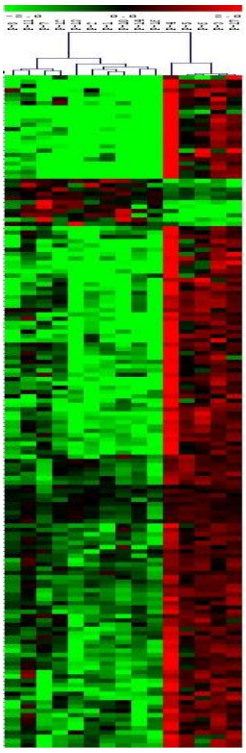

1d

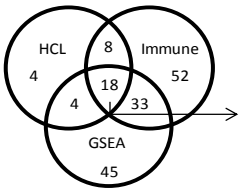

Common genes	
BATF2	*HLA-E*
C1QA	*HLA-G*
C1QB	*IRF1*
C1QC	*MPEG1*
CCL5	*PSMB10*
CD74	*PSMB9*
HLA-DPA1	*STAT1*
HLA-DRA	*TAPBPL*
HLA-DRB6	*UBE2L6*

Figure1. Unsupervised and supervised analyses

1a. Organization of tumors into two groups of ten and five (red circle) based on hierarchical clustering. The node values (black arrows) denote the number of times the tumors clustered together during resampling.
1b & 1c. Heat maps of 44 significant probe sets isolated from HCL analysis (1b) and 156 probe sets isolated from immune gene analysis (red and green indicate over and underexpression, respectively)
1d. Venn diagram indicating the significant genes unraveled by HCL, immune gene analysis and GSEA and list of 18 genes common between all algorithms

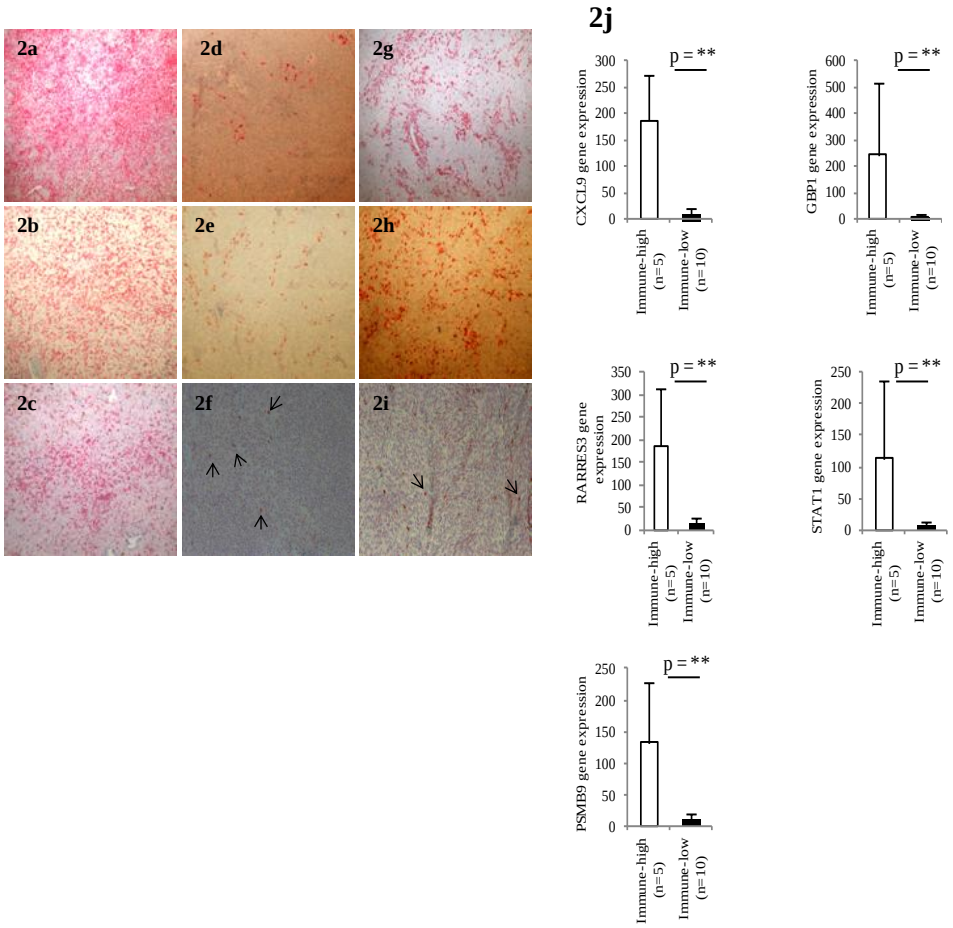

Figure2. Validation of significant genes

2a-2i. Comparison of macrophage and T-lymphocyte infiltrates in immune-high and immune-low melanomas. Immune-high uveal melanoma with dense infiltrates of HLA-DRA+ (2a) and CD163+ (2b) macrophages and CD3+ (2c) T-lymphocytes. Immune-low uveal melanomas with mild and moderate infiltrates of HLA-DRA+ (2d/g) and CD163+ (2e/h) macrophages and sparse CD3+ (2f/i, black arrows) T-lymphocytes (Original magnification: 50x and 100x)

*2j. Expression of significant genes in immune-high and immune-low uveal melanomas on microarray measured by RT-qPCR (p-value: * ≤ 0.05, ** < 0.01)*

3a

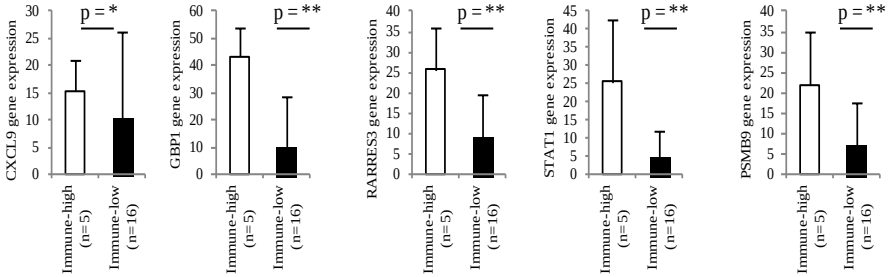

3b

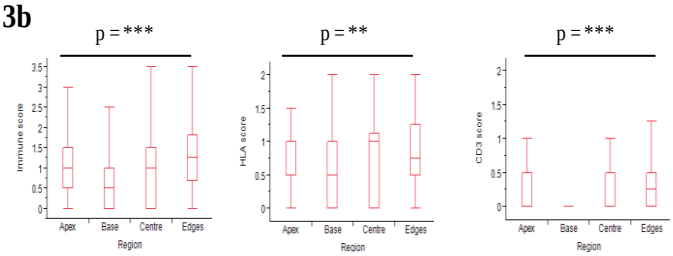

3c

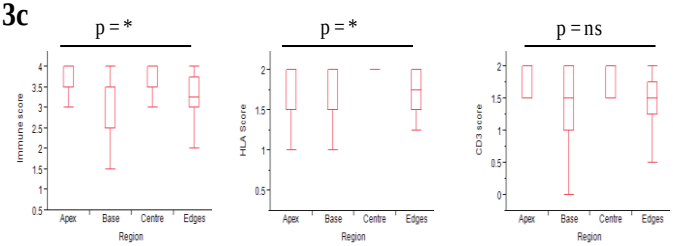

Figure 3. Validation of immune score and immune infiltrate topography

3a. Expression of significant genes in IHC categorized immune-high and immune-low uveal melanomas measured by RT-qPCR

3b and 3c. Box-plots comparing the mean values in tumor apex, base, centre and both edges for immune score, HLA-DRA only and CD3 only in immune-low (3b) and immune-high (3c) uveal melanomas

*(p-value: * ≤ 0.05, ** < 0.01, *** < 0.001, ns : not significant)*

Pathway	Common	I - GSEA	GSEA	Immune	I - HCL
Interferon-gamma signaling	x	x	x		x
Cell adhesion molecules (CAMs)	x	x	x	x	
Allograft rejection	x	x	x	x	
Graft-versus-host disease	x	x	x	x	
Type I diabetes mellitus	x	x	x	x	
Antigen processing and presentation	x	x	x		
Phagosome	x	x	x		
Interferon alpha/beta signaling	x	x	x		
Autoimmune thyroid disease	x	x	x		
Leishmaniasis	x	x	x		
Systemic lupus erythematosus	x	x	x		
Staphylococcus aureus infection	x	x	x		
ER-Phagosome pathway	x	x			
Viral myocarditis	x	x			
Translocation of ZAP-70 to Immunological synapse	x		x		
IR interactions between a lymphoid and a non-lymphoid cell		x	x		
Intestinal immune network for IgA production		x	x		
Asthma		x	x		
PD-1 signaling			x	x	
Generation of second messenger molecules			x	x	
MHC class II antigen presentation	x				
Classical antibody-mediated complement activation	x				
Antigen presentation: Folding, assembly and peptide loading of class I MHC		x			
Endosomal/Vacuolar pathway		x			
Phosphorylation of CD3 and TCR zeta chains			x		
TCR				x	
Natural killer cell mediated cytotoxicity				x	
TCR signaling in naïve CD8+ T cells				x	
TCR signaling in naïve CD4+ T cells				x	
PECAM1 interactions				x	
Downstream signaling in naïve CD8+ T cells				x	
The co-stimulatory signal during t-cell activation				x	
IL12-mediated signaling events				x	
Cytokine-cytokine receptor interaction					x

I: Immune; IR: Immunoregulatory interaction

Figure 4a. Pathways associated with various gene subgroups

Gene Ontology term	Common	I - GSEA	GSEA	I - HCL	Immune
Biological process					
Immune response	x	x	x	x	x
Interferon-gamma-mediated signaling pathway	x	x	x	x	
Cytokine-mediated signaling pathway	x	x	x	x	
Antigen processing and presentation	x	x	x		
Type I interferon-mediated signaling pathway	x	x	x		
Innate immune response	x	x			x
Immunoglobulin mediated immune response	x			x	
APP of exogenous peptide antigen via MHC class I, TAP-dependent		x	x		
T-cell receptor signaling pathway			x		x
Defense response			x		x
Defense response to virus				x	x
Complement activation	x				
Positive regulation of T cell mediated cytotoxicity		x			
T-helper 1 type immune response			x		
Immune response to tumor cell				x	
Positive regulation of tyrosine phosphorylation of STAT protein				x	
Positive regulation of immune system process					x
Lymphocyte activation					x
Cellular component					
Integral to lumenal side of endoplasmic reticulum membrane	x	x	x		
ER to Golgi transport vesicle membrane	x		x		
MHC class II protein complex	x		x		
Clathrin-coated endocytic vesicle membrane	x		x		
Intrinsic to membrane		x	x		
TAP complex		x			
Cytolytic granule				x	
Immunological synapse					x
Molecular function					
MHC class II receptor activity	x		x		
MHC protein binding		x			
CCR5 chemokine receptor binding				x	

I: Immune; APP: antigen processing and presentation

Figure 4b. Gene ontology terms associated with various gene subgroups

4c

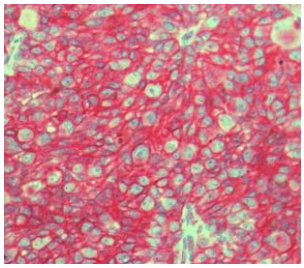

4d

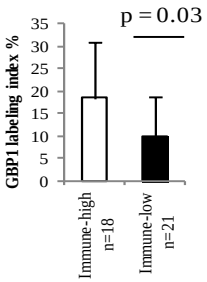

Figure 4c. GBP1 protein expression in an immune-high uveal melanoma

Figure 4d. GBP1 labeling indices in immune-high and immune-low tumors

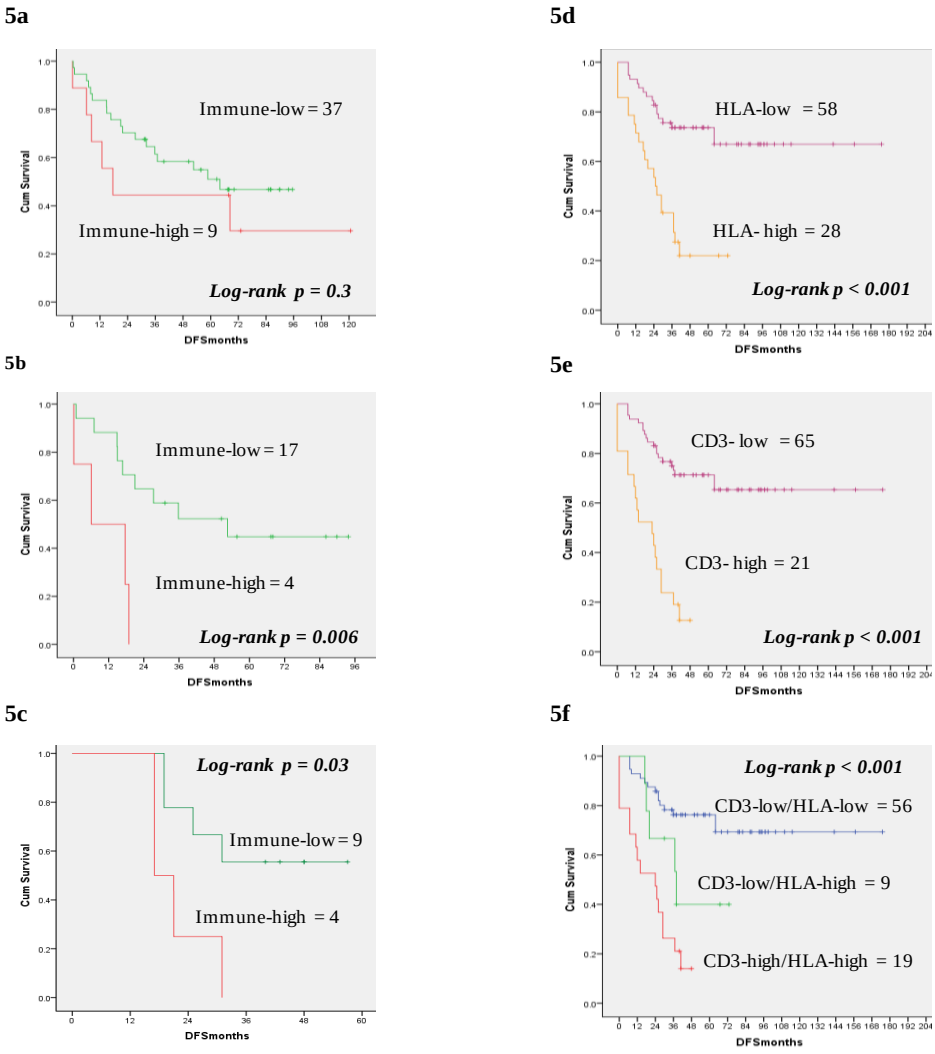

Figure5. Clinical significance of immune signature

5a and 5b. Kaplan-Meier (KM) plots for the duration of DFS between immune-high and immune-low uveal melanomas in external dataset 1 for all tumors (5a) and retinal detached alone (5b)

5c. KM plots for the duration of DFS between immune-high and immune-low uveal melanomas in external dataset 2

5d – 5f. KM plots for the duration of DFS in present series between HLA-high and HLA-low (5d); CD3-high and CD3-low uveal melanomas (5e) and for combined densities of CD3 and HLA-DRA infiltrate (5f)

Table1. Comparison of clinicopathological variables between immune-high and immune-low uveal melanomas

Clinical variables		**Valid N**	**Immune-low (n=70)**	**Immune-high (n=19)**	**p-value**
Age at diagnosis	upto 60 years	89	22(31.4%)	10(52.6%)	0.09
	> 60 years		48(68.6%)	9(47.4%)	
Gender	female	89	35(50%)	8(42.1%)	0.54
	male		35(50%)	11(57.9%)	
Stage	II	78	22(37.3%)	4(21.1%)	0.19
	III & IV		37(62.7%)	15(78.9%)	
T category	T1-T3	77	32(54.2%)	7(38.9%)	0.25
	T4		27(45.8%)	11(61.1%)	
Diameter	upto 15mm	77	11(18.6%)	5(37.8%)	0.51
	>15mm		48(81.4%)	13(72.2%)	
Thickness	upto 8mm	84	13(20%)	3(15.8%)	1.00
	> 8mm		52(80%)	16(84.2%)	
Location	choroid only	89	28(40%)	9(47.4%)	0.56
	choroid & ciliary body		42(60%)	10(52.6%)	
Extrascleral extension	absent	89	65(92.9%)	17(89.5%)	0.64
	present		5(7.1%)	2(10.5%)	
Pathologic variables					
Epithelioid component	upto 25%	88	43(62.3%)	8(42.1%)	0.11
	>25%		26(37.7%)	11(57.9%)	
Mitoses	upto 10/40hpf	88	38(55.1%)	5(26.3%)	0.03$
	>10/40hpf		31(44.9%)	14(73.7%)	
Pigmentation	upto 25%	89	54(77.1%)	15(78.9%)	1.00
	>25%		16(22.9%)	4(21.1%)	
Necrosis	absent	89	64(91.4%)	14(73.7%)	0.05$
	present		6(8.6%)	5(26.3%)	

$ Significant

S1a

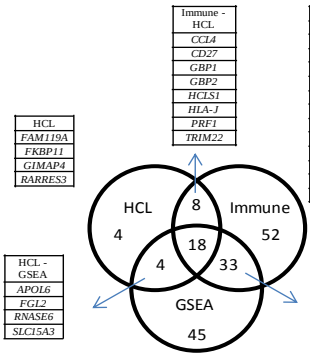

Immune - HCL
CCL4
CD27
GBP1
GBP2
HCLS1
HLA-J
PRF1
TRIM22

HCL
FAM119A
FKBP11
GIMAP4
RARRES3

Immune			
AIF1	DOCK8	IL21R	PTPRCAP
C1S	EHD1	IL32	RASSF5
CARD16	ERAP1	INPP5D	SH2D1A
CASP1	FPR3	LAIR1	SIGLEC1
CD2	FYB	LCK	SLAMF7
CD38	GZMB	LILRB1	SNX1
CD3D	HLA-DOA	LY9	SP110
CD48	IDO1	NFATC2	THEMIS
CD86	IFIT3	NKG7	TLR8
CD8A	IGHM	NLK	TMSB4X
CORO1A	IGSF6	NLRC5	TNFSF10
CXCL9	IKZF3	PSMC2	TRAC
CYTIP	IL10RA	PTPN6	TRBC1

HCL - GSEA
APOL6
FGL2
RNASE6
SLC15A3

Immune - GSEA		
ADAMDEC1	HLA-C	NCF4
AMICA1	HLA-DMA	OAS3
APOL1	HLA-DMB	PSME2
B2M	IL12RB1	SECTM1
BTN3A3	IL15RA	TAP1
C2	ITGAL	TAPBP
CAPN10	LAG3	TNFRSF1B
CD14	LGMN	TRIM69
CD68	LILRB2	XAF1
CLEC4A	LST1	IRF9
HLA-B	LYZ	CD70

GSEA			
BAT5	HCK	LGALS9	PQLC3
BTN3A3 /// BTN3A2	HLA-DPB1	LILRB5	PSMB8
C22ORF13	HLA-DQA1 /// HLA-DQA	LOC116236	PSME1
CCR5 /// LOC653725	HLA-DQB1	LOC133874	SEPP1
CD163L1	HLA-DRB1	LOC286076	STK17B
CRIP1	HLA-DRB4	LOC648998 /// LOC653	TMEM176B
CSF1R	HLA-F	LOC93349	TMSB4X /// TMSL3
CST3	IFI27	LYZ /// LILRB1	TYROBP
DHRS7B	IFI35	MBOAT5	UCP2
FOLR2	IFITM1	NAGK	
GIMAP5	IL18BP	NCKAP1L	
GNLY	LAT1-3TM	PILRA	

S1b

Transcription factor	Common	GSEA	Immune	I - GSEA
IRF1	x	x		x
IRF8	x			x
Unknown	x			
REL			x	
RUNX1			x	
LEF1			x	
IRF2				x
STAT1				x
ETS2				x

I: Immune

S1c

Cancer Module	Common	I - GSEA	GSEA	Immune	I - HCL
MODULE_84	x	x	x	x	x
MODULE_46	x	x	x	x	x
MODULE_75	x	x	x	x	x
MODULE_45	x	x	x	x	x
MODULE_345	x	x	x		
MODULE_436	x	x	x		
MODULE_44	x		x	x	
MODULE_171			x	x	x
MODULE_293	x	x			
MODULE_5	x	x			
MODULE_292			x	x	
MODULE_208			x	x	
MODULE_64		x		x	
MODULE_143	x				
MODULE_27		x			
MODULE_119				x	
MODULE_204					x
MODULE_128					x
MODULE_79					x
MODULE_170					x
MODULE_177					x

I: Immune

S1d

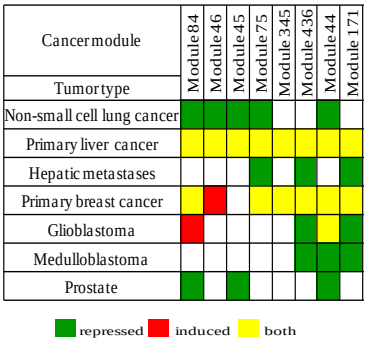

Figure S1. Annotation of significant genes

S1a. Genes associated with each of the subgroups identified through HCL, immune gene analysis and GSEA algorithms

S1b. Transcription factors associated with gene subgroups

S1c. Cancer modules associated with gene subgroups

S1d. Expression profiles of tumor types in cancer modules common to gene subgroups

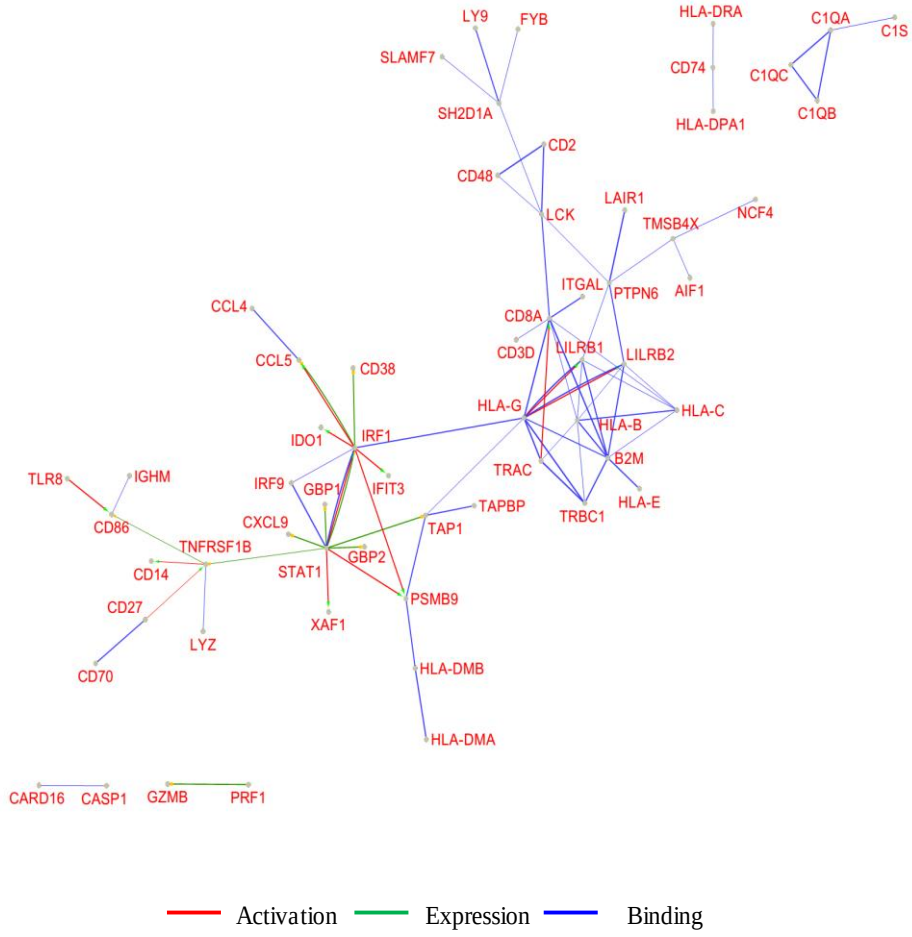

Figure S2. Action-based network of significant genes

Table S1. Overexpressed and underexpressed significant probe sets identified from different algorithms

For each probe set, the associated gene symbol; mean expression in immune-high and immune-low uveal melanoma; and fold change with respect to immune-high have been indicated

Genes overexpressed in immune-high

HCL significant genes				
		Average expression		
Gene symbol	**Probeset ID**	**Immune-high**	**Immune-low**	**Fold change**
GBP1	202269_x_at	1259.56	87.36	14.4
CCL5	204655_at	498.46	36.78	13.6
RARRES3	204070_at	1792.2	147.55	12.1
PSMB9	204279_at	1214.04	101.88	11.9
PRF1	214617_at	306.26	27.53	11.1
CD74	1567628_at	2516.48	299.4	8.4
FGL2	227265_at	628.62	76.89	8.2
C1QA	218232_at	2589.12	323	8.0
CCL4	204103_at	195.66	26.99	7.2
HLA-DQA1 /// HLA-DQA2 /// LOC100507718 /// LOC100509457	212671_s_at	2340.42	333.85	7.0
HLA-DRA	210982_s_at	3599.94	518.12	6.9
C1QB	202953_at	2988.62	440.41	6.8
UBE2L6	201649_at	1520.18	224.7	6.8
GIMAP4	219243_at	324.84	51.61	6.3
FGL2	204834_at	363.92	60.81	6.0
CD27	206150_at	250.24	43.21	5.8
HLA-DPA1	211991_s_at	4409.98	768.5	5.7
GBP2	202748_at	409.06	72.98	5.6
C1QC	225353_s_at	3381.78	615.82	5.5
HLA-DRB1 /// HLA-DRB3 /// HLA-DRB4 /// LOC100507709 /// LOC100507714	215193_x_at	5288	990.45	5.3
IRF1	202531_at	408.84	79.3	5.2
SLC15A3	219593_at	529.42	104.63	5.1
APOL6	219716_at	305.32	60.83	5.0
HLA-G	211530_x_at	4790.08	958.17	5.0
MPEG1	226818_at	767.9	156.33	4.9
MPEG1	226841_at	394.5	81.08	4.9
APOL6	1557116_at	391.02	82.45	4.7
HLA-DRB1 /// HLA-DRB4 /// HLA-DRB5 /// LOC100507709 /// LOC100507714	209312_x_at	6458.72	1366.29	4.7
STAT1	200887_s_at	3630.14	784.04	4.6
HLA-DRB6	217362_x_at	511.58	113.56	4.5

HLA-DRB1 /// HLA-DRB4 /// LOC100507709 /// LOC100507714	204670_x_at	5147.34	1174.07	4.4
APOL6	241869_at	333.38	83.13	4.0
HLA-E	200904_at	4159.3	1080.39	3.8
BATF2	228439_at	225.46	58.8	3.8
TRIM22	213293_s_at	950	252.46	3.8
PSMB10	202659_at	647.56	173.88	3.7
TAPBPL	218747_s_at	283.64	76.73	3.7
HLA-E	200905_x_at	7782.54	2237.12	3.5
HCLS1	202957_at	365.9	109.9	3.3
TAPBPL	218746_at	257.84	78.95	3.3
HLA-J	217436_x_at	3100.42	986.82	3.1
RNASE6	213566_at	405.34	136.83	3.0
FKBP11	219118_at	1039.04	360.55	2.9
FAM119A	235931_at	87.98	32.66	2.7
Significant genes from immune response gene analysis				
CXCL9	203915_at	1262.9	36.8	34.3
IDO1	210029_at	610.8	18.0	33.9
IL32	203828_s_at	191.0	6.2	30.9
IGHM	216491_x_at	263.3	9.5	27.8
NKG7	213915_at	283.9	12.3	23.1
GBP1	202270_at	859.6	37.3	23.1
GBP1	231577_s_at	1953.0	96.4	20.3
CCL5	1405_i_at	648.5	32.9	19.7
GABBR1 /// UBD	205890_s_at	609.9	33.6	18.1
TRBC1	211796_s_at	569.3	32.9	17.3
TRAC	209671_x_at	468.1	28.8	16.2
TRAC /// TRAJ17 /// TRAV20	210972_x_at	617.4	38.5	16.0
IKZF3	227030_at	122.7	7.8	15.7
GBP1	202269_x_at	1259.6	87.4	14.4
CCL5	1555759_a_at	727.4	52.9	13.7
APOL1	209546_s_at	200.6	14.7	13.7
ADAMDEC1	206134_at	409.4	30.0	13.6
CCL5	204655_at	498.5	36.8	13.6
LCK	204891_s_at	127.0	10.5	12.1
STAT1	209969_s_at	693.5	57.9	12.0
PSMB9	204279_at	1214.0	101.9	11.9
CD8A	205758_at	277.4	24.6	11.3
PRF1	214617_at	306.3	27.5	11.1
LYZ	1555745_a_at	687.2	63.1	10.9
LAG3	206486_at	106.3	10.0	10.6
PTPRCAP	204960_at	91.1	8.7	10.4
NFATC2	226991_at	67.7	7.0	9.7
TRBC1	210915_x_at	486.1	51.8	9.4
CD2	205831_at	367.9	39.3	9.4
C1S	1555229_a_at	240.2	27.6	8.7
CD74	1567628_at	2516.5	299.4	8.4
ERAP1	214012_at	84.1	10.1	8.3
IL12RB1	1552584_at	214.1	25.8	8.3
CD38	205692_s_at	115.8	14.3	8.1

C1QA	218232_at	2589.1	323.0	8.0
AIF1	209901_x_at	329.5	41.2	8.0
IL21R	219971_at	28.3	3.6	8.0
INPP5D	203331_s_at	18.5	2.4	7.9
LCK	204890_s_at	71.5	9.4	7.6
SH2D1A	210116_at	56.5	7.7	7.4
CORO1A	209083_at	185.4	25.6	7.2
CCL4	204103_at	195.7	27.0	7.2
HLA-DQA1 /// HLA-DQA2 /// LOC100507718 /// LOC100509457	212671_s_at	2340.4	333.9	7.0
SLAMF7	222838_at	192.6	27.6	7.0
HLA-DRA	210982_s_at	3599.9	518.1	6.9
GZMB	210164_at	100.6	14.5	6.9
C1QB	202953_at	2988.6	440.4	6.8
UBE2L6	201649_at	1520.2	224.7	6.8
CD3D	213539_at	236.7	36.3	6.5
THEMIS	1558971_at	21.8	3.7	5.9
CD27	206150_at	250.2	43.2	5.8
TRBC1	213193_x_at	532.1	92.4	5.8
HLA-DPA1	211991_s_at	4410.0	768.5	5.7
FYB	227266_s_at	199.8	35.6	5.6
GBP2	202748_at	409.1	73.0	5.6
C1QC	225353_s_at	3381.8	615.8	5.5
TLR8	229560_at	121.7	22.5	5.4
TAP1	202307_s_at	1536.4	284.2	5.4
HLA-DRB1 /// HLA-DRB3 /// HLA-DRB4 /// LOC100507709 /// LOC100507714	215193_x_at	5288.0	990.5	5.3
IRF1	202531_at	408.8	79.3	5.2
TNFSF10	202688_at	196.9	38.4	5.1
HLA-G	211530_x_at	4790.1	958.2	5.0
C1S	208747_s_at	843.3	170.3	5.0
MPEG1	226818_at	767.9	156.3	4.9
MPEG1	226841_at	394.5	81.1	4.9
FYB	205285_s_at	144.7	29.9	4.8
ITGAL	1554240_a_at	152.2	31.9	4.8
IGSF6	206420_at	216.2	45.4	4.8
HLA-DRB1 /// HLA-DRB4 /// HLA-DRB5 /// LOC100507709 /// LOC100507714	209312_x_at	6458.7	1366.3	4.7
LY9	210370_s_at	21.9	4.7	4.7
STAT1	200887_s_at	3630.1	784.0	4.6
HLA-DMA	217478_s_at	1423.4	312.0	4.6
NLRC5	226474_at	289.8	64.1	4.5
HLA-DRB6	217362_x_at	511.6	113.6	4.5
SIGLEC1	219519_s_at	137.8	30.8	4.5
CYTIP	209606_at	96.5	21.9	4.4
HLA-DRB1 /// HLA-DRB4 /// LOC100507709 /// LOC100507714	204670_x_at	5147.3	1174.1	4.4
AIF1	213095_x_at	258.0	58.9	4.4
BTN3A3	204821_at	895.4	205.2	4.4

BTN3A3	38241_at	756.8	182.4	4.2
LST1	215633_x_at	77.5	19.1	4.1
NCF4	207677_s_at	53.9	13.5	4.0
AIF1	215051_x_at	329.7	83.2	4.0
XAF1	228617_at	369.9	93.9	3.9
IL10RA	204912_at	265.9	68.1	3.9
HLA-E	200904_at	4159.3	1080.4	3.8
BATF2	228439_at	225.5	58.8	3.8
TRIM22	213293_s_at	950.0	252.5	3.8
CARD16 /// CASP1	1552703_s_at	248.9	66.2	3.8
PSMB10	202659_at	647.6	173.9	3.7
TAPBPL	218747_s_at	283.6	76.7	3.7
RASSF5	223322_at	174.5	47.7	3.7
LST1	214181_x_at	103.2	28.3	3.6
FPR3	230422_at	165.9	46.7	3.6
HLA-DMB	203932_at	646.5	183.3	3.5
LILRB2	207697_x_at	102.3	29.1	3.5
IFIT3	229450_at	847.5	242.6	3.5
HLA-E	200905_x_at	7782.5	2237.1	3.5
CD86	210895_s_at	161.7	46.9	3.4
CD48	204118_at	116.7	34.6	3.4
XAF1	206133_at	153.8	45.9	3.4
HLA-DOA	206313_at	45.3	13.6	3.3
HCLS1	202957_at	365.9	109.9	3.3
CARD16	1552701_a_at	224.3	67.4	3.3
SECTM1	213716_s_at	191.9	58.1	3.3
TAPBPL	218746_at	257.8	79.0	3.3
TNFRSF1B	203508_at	166.2	51.3	3.2
AMICA1	228094_at	54.7	17.1	3.2
HLA-J	217436_x_at	3100.4	986.8	3.1
ITGAL	213475_s_at	90.3	29.4	3.1
PSME2	201762_s_at	2069.5	681.6	3.0
PRF1	1553681_a_at	155.0	51.3	3.0
CD70	206508_at	80.5	27.2	3.0
HLA-E	217456_x_at	2502.3	863.9	2.9
TMSB4X	216438_s_at	5518.4	1915.0	2.9
IL15RA	207375_s_at	70.4	25.2	2.8
TRIM69	1568592_at	610.6	218.5	2.8
TAPBP	208829_at	1997.4	723.2	2.8
LILRB1	211336_x_at	86.2	31.4	2.7
HLA-B	211911_x_at	10442.8	3816.9	2.7
LAIR1	208071_s_at	60.1	22.8	2.6
CAPN10	219333_s_at	38.4	14.6	2.6
PTPN6	206687_s_at	159.8	61.1	2.6
IRF9	203882_at	798.8	312.4	2.6
CASP1	206011_at	87.3	34.7	2.5
LGMN	201212_at	1406.5	561.7	2.5
CLEC4A	219947_at	39.8	16.2	2.5
HLA-B	208729_x_at	7820.4	3272.1	2.4
CD68	203507_at	123.7	51.9	2.4

C2	203052_at	1113.0	473.4	2.4
CD14	201743_at	1008.3	431.3	2.3
DOCK8	225502_at	253.0	109.3	2.3
HLA-G	211528_x_at	6898.4	3124.2	2.2
OAS3	218400_at	258.5	129.1	2.0
NCF4	205147_x_at	71.9	36.6	2.0
SP110	209761_s_at	388.0	225.8	1.7
ABHD16A /// LY6G6E	224756_s_at	466.5	271.7	1.7
HLA-C	216526_x_at	9153.9	5455.3	1.7
NLK	222590_s_at	118.8	72.1	1.6
B2M	216231_s_at	12216.2	7478.4	1.6
HLA-C	208812_x_at	9160.0	5746.7	1.6
SNX1	214531_s_at	358.3	227.6	1.6
EHD1	209039_x_at	203.1	132.4	1.5
PSMC2	201067_at	340.9	242.1	1.4
B2M	201891_s_at	10258.1	7539.3	1.4
Significant genes from GSEA (100 genes corresponding to 175 probesets)				
CCL5	1405_i_at	648.5	32.9	19.7
IFI27	202411_at	2466.7	138.1	17.9
IRF1	238725_at	308.4	20.7	14.9
HLA-DRB4 /// LOC100509582	209728_at	916.3	64.1	14.3
CCL5	1555759_a_at	727.4	52.9	13.7
APOL1	209546_s_at	200.6	14.7	13.7
ADAMDEC1	206134_at	409.4	30.0	13.6
CCL5	204655_at	498.5	36.8	13.6
STAT1	209969_s_at	693.5	57.9	12.0
PSMB9	204279_at	1214.0	101.9	11.9
LYZ	1555745_a_at	687.2	63.1	10.9
LAG3	206486_at	106.3	10.0	10.6
HLA-DQB1	209480_at	203.8	20.5	9.9
CD74	1567628_at	2516.5	299.4	8.4
IL12RB1	1552584_at	214.1	25.8	8.3
FGL2	227265_at	628.6	76.9	8.2
C1QA	218232_at	2589.1	323.0	8.0
HLA-DPA1	213537_at	444.9	58.4	7.6
APOL6	1557236_at	155.6	22.3	7.0
HLA-DRA	210982_s_at	3599.9	518.1	6.9
C1QB	202953_at	2988.6	440.4	6.8
UBE2L6	201649_at	1520.2	224.7	6.8
LYZ	213975_s_at	2293.3	375.2	6.1
FGL2	204834_at	363.9	60.8	6.0
HLA-DRB1 /// HLA-DRB3 /// HLA-DRB4 /// HLA-DRB5 /// LOC100507709 /// LOC100507714	238900_at	45.5	7.9	5.8
HLA-DRA	208894_at	5337.1	926.5	5.8
HLA-DPA1	211991_s_at	4410.0	768.5	5.7
C1QC	225353_s_at	3381.8	615.8	5.5
TAP1	202307_s_at	1536.4	284.2	5.4
HLA-DRB1 /// HLA-DRB3 /// HLA-DRB4 /// LOC100507709 /// LOC100507714	215193_x_at	5288.0	990.5	5.3

HLA-DQB1 /// LOC100293977	212998_x_at	1598.1	301.0	5.3
IRF1	202531_at	408.8	79.3	5.2
SLC15A3	219593_at	529.4	104.6	5.1
APOL6	219716_at	305.3	60.8	5.0
NCKAP1L	209734_at	112.4	22.4	5.0
HLA-G	211530_x_at	4790.1	958.2	5.0
HLA-DQB1 /// LOC100293977	212999_x_at	172.3	34.8	4.9
MPEG1	226818_at	767.9	156.3	4.9
MPEG1	226841_at	394.5	81.1	4.9
LILRB2	210146_x_at	65.8	13.7	4.8
ITGAL	1554240_a_at	152.2	31.9	4.8
HLA-DQB1	211654_x_at	1134.9	239.1	4.7
APOL6	1557116_at	391.0	82.5	4.7
HLA-DRB1 /// HLA-DRB4 /// HLA-DRB5 /// LOC100507709 /// LOC100507714	209312_x_at	6458.7	1366.3	4.7
STAT1	200887_s_at	3630.1	784.0	4.6
CD163L1	223655_at	143.2	31.0	4.6
CRIP1	205081_at	114.7	24.9	4.6
HLA-DMA	217478_s_at	1423.4	312.0	4.6
HLA-DRB6	217362_x_at	511.6	113.6	4.5
HLA-DRB1 /// HLA-DRB4 /// LOC100507709 /// LOC100507714	204670_x_at	5147.3	1174.1	4.4
BTN3A3	204821_at	895.4	205.2	4.4
CD74	209619_at	10505.6	2418.8	4.3
BTN3A3	38241_at	756.8	182.4	4.2
HLA-DQB1 /// LOC100293977	209823_x_at	1086.0	263.1	4.1
LST1	215633_x_at	77.5	19.1	4.1
HLA-DQB1 /// LOC100293977	211656_x_at	1054.3	261.9	4.0
APOL6	241869_at	333.4	83.1	4.0
NCF4	207677_s_at	53.9	13.5	4.0
IL18BP	222868_s_at	385.6	98.2	3.9
HLA-E	200904_at	4159.3	1080.4	3.8
BATF2	228439_at	225.5	58.8	3.8
HLA-DPB1	201137_s_at	3564.4	940.0	3.8
PSMB10	202659_at	647.6	173.9	3.7
TAPBPL	218747_s_at	283.6	76.7	3.7
HLA-DRB1 /// LOC100507709 /// LOC100507714	208306_x_at	6100.7	1652.3	3.7
GNLY	205495_s_at	38.6	10.6	3.7
LST1	214181_x_at	103.2	28.3	3.6
LILRB5	206856_at	77.0	21.2	3.6
TYROBP	204122_at	853.8	235.5	3.6
HLA-C	211799_x_at	4756.5	1335.0	3.6
PSMB8	209040_s_at	687.6	193.6	3.6
GNLY	37145_at	44.6	12.6	3.5
HLA-DMB	203932_at	646.5	183.3	3.5
LILRB2	207697_x_at	102.3	29.1	3.5

HLA-E	200905_x_at	7782.5	2237.1	3.5
GIMAP1-GIMAP5 /// GIMAP5	218805_at	230.7	68.3	3.4
BREA2(LOC28076)	241475_at	16.1	4.8	3.3
SECTM1	213716_s_at	191.9	58.1	3.3
TAPBPL	218746_at	257.8	79.0	3.3
TNFRSF1B	203508_at	166.2	51.3	3.2
UCP2	208998_at	634.4	196.5	3.2
AMICA1	228094_at	54.7	17.1	3.2
IFITM1	214022_s_at	4393.5	1377.7	3.2
ITGAL	213475_s_at	90.3	29.4	3.1
PSME2	201762_s_at	2069.5	681.6	3.0
B2M	232311_at	29.4	9.7	3.0
STK17B	226525_at	180.0	59.6	3.0
IFI35	209417_s_at	498.4	167.3	3.0
RNASE6	213566_at	405.3	136.8	3.0
STK17B	205214_at	18.4	6.3	2.9
TMEM176B	220532_s_at	661.1	226.2	2.9
LST1	211582_x_at	102.7	35.4	2.9
HLA-E	217456_x_at	2502.3	863.9	2.9
HCK	208018_s_at	150.9	52.7	2.9
PILRA	219788_at	45.6	16.0	2.9
LST1	210629_x_at	96.9	34.6	2.8
IL15RA	207375_s_at	70.4	25.2	2.8
HLA-F	204806_x_at	3684.5	1316.9	2.8
TRIM69	1568592_at	610.6	218.5	2.8
CLEC4A	221724_s_at	24.7	8.9	2.8
TAPBP	208829_at	1997.4	723.2	2.8
HLA-B	211911_x_at	10442.8	3816.9	2.7
PILRA	222218_s_at	128.2	46.9	2.7
HLA-F	221875_x_at	4346.3	1619.4	2.7
BTN3A2 /// BTN3A3	204820_s_at	2370.2	887.8	2.7
CAPN10	219333_s_at	38.4	14.6	2.6
IFITM1 /// IFITM2	201601_x_at	3520.5	1338.5	2.6
HLA-DRB1 /// HLA-DRB3 /// HLA-DRB4 /// HLA-DRB5 /// LOC100507709 /// LOC100507714 /// LOC100509582	221491_x_at	125.3	47.7	2.6
IRF9 (ISGF3G)	203882_at	798.8	312.4	2.6
LGALS9	203236_s_at	120.7	47.3	2.6
UCP2	208997_s_at	280.5	110.2	2.5
LGMN	201212_at	1406.5	561.7	2.5
CLEC4A	219947_at	39.8	16.2	2.5
CSF1R	203104_at	472.7	196.9	2.4
HLA-B	208729_x_at	7820.4	3272.1	2.4
CD68	203507_at	123.7	51.9	2.4
GIMAP1-GIMAP5 /// GIMAP5	64064_at	227.9	95.7	2.4
SEPP1	201427_s_at	4509.9	1897.6	2.4
C2	203052_at	1113.0	473.4	2.4
CD14	201743_at	1008.3	431.3	2.3

TRIM69	232792_at	14.5	6.2	2.3
FOLR2	204829_s_at	212.4	91.9	2.3
HLA-DPA1	211990_at	6245.2	2706.1	2.3
LST1	211581_x_at	73.0	31.8	2.3
LST1	214574_x_at	123.2	53.7	2.3
HLA-DPB1	244485_at	49.1	21.8	2.3
PQLC3	225579_at	584.0	260.0	2.2
HLA-G	211528_x_at	6898.4	3124.2	2.2
HLA-G	211529_x_at	6473.5	2981.4	2.2
CST3	201360_at	3779.9	1821.1	2.1
IL18BP	224283_x_at	53.2	26.2	2.0
HLA-DRB4	215666_at	8.0	3.9	2.0
HLA-DQB1	210747_at	13.6	6.8	2.0
OAS3	218400_at	258.5	129.1	2.0
DHRS7B	220690_s_at	571.9	289.3	2.0
NCF4	205147_x_at	71.9	36.6	2.0
HLA-F	221978_at	70.2	36.1	1.9
PSME1	200814_at	1492.0	780.3	1.9
SEPP1	231669_at	51.8	27.2	1.9
HLA-C	214459_x_at	10606.1	5782.9	1.8
ABHD15 (LOC116236)	226796_at	109.2	62.5	1.7
LPCAT3 (LPCAT3)	202793_at	96.9	55.6	1.7
STK17B	243797_at	7.3	4.2	1.7
NAGK	218231_at	490.1	290.0	1.7
HLA-B	209140_x_at	9578.5	5674.2	1.7
HLA-C	216526_x_at	9153.9	5455.3	1.7
STK17B	217503_at	19.1	11.6	1.7
TAPBP	1555565_s_at	167.1	101.1	1.7
B2M	216231_s_at	12216.2	7478.4	1.6
HLA-C	208812_x_at	9160.0	5746.7	1.6
CST3	237623_at	23.9	15.2	1.6
C22orf13	223039_at	750.0	487.3	1.5
C2	1554533_at	106.2	70.5	1.5
IL12RB1	206890_at	19.5	13.0	1.5
HLA-G	210514_x_at	1289.6	871.0	1.5
GIMAP1-GIMAP5 /// GIMAP5	215352_at	5.1	3.5	1.5
B2M	201891_s_at	10258.1	7539.3	1.4
C5orf58 (LOC133874)	1554115_at	30.4	23.0	1.3
TRIM69	229037_at	25.5	19.4	1.3
OAS3	232666_at	17.2	14.2	1.2
SEPP1	229620_at	34.3	28.9	1.2
HLA-DRB4	215669_at	10.9	9.8	1.1
IL12RB1	239522_at	33.8	31.9	1.1
IRF9 /// RNF31	220788_s_at	106.6	100.7	1.1
TMEM176B	236348_at	4.1	3.9	1.1
IL18BP	219323_s_at	11.2	11.6	1.0
LPCAT3 (LPCAT3)	213615_at	36.7	49.3	0.7

CD74	1567627_at	4.9	7.4	0.7
C5orf58 (LOC133874)	237956_s_at	3.5	5.7	0.6
CAPN10	221040_at	5.0	8.5	0.6
TAPBP	210294_at	7.5	12.6	0.6
PQLC3	216458_at	5.4	9.7	0.6
HLA-DRB6	217323_at	3.2	7.7	0.4
C5orf58 (LOC133874)	237955_at	4.5	11.1	0.4
FOLR2	229619_at	5.2	14.2	0.4

Table S1. continued

Genes underexpressed in immune-high

Significant genes from immune response gene analysis				
		Average expression		
Gene symbol	**Probeset ID**	**Immune-high**	**Immune-low**	**Fold change**
ANTXR1	220093_at	2.1	14.3	0.1
RBM15	232971_at	1.5	9.9	0.2
CFHR3	1570228_at	2.1	12.0	0.2
OCLN	209925_at	3.0	16.5	0.2
OPRM1	207994_s_at	1.2	5.9	0.2
PDGFD	219304_s_at	41.2	199.7	0.2
SLC5A8	237503_at	2.0	7.1	0.3
SCARA5	1554705_at	1.4	4.8	0.3
CD44	217523_at	134.9	269.5	0.5
SOS2	217644_s_at	20.2	38.1	0.5
NRARP	226499_at	53.1	96.7	0.5
Significant genes from GSEA (100 genes corresponding to 216 probesets)				
SPP1	209875_s_at	218.9	2883.4	0.1
IFNA8	207932_at	1.0	6.9	0.1
GPR37	209631_s_at	151.9	1058.3	0.1
KDM4C	1556493_a_at	4.0	27.0	0.1
GPR37	214586_at	23.5	149.9	0.2
AMFR	202203_s_at	31.1	197.4	0.2
MCOLN3	242308_at	6.9	39.6	0.2
CDH20	210913_at	1.3	6.8	0.2
CYP11B1	214610_at	2.5	12.5	0.2
ZNF544	244466_at	1.5	7.1	0.2
ETV1	221911_at	89.2	399.3	0.2
CLDN17	221328_at	4.2	18.7	0.2
CSRNP3	220462_at	5.3	21.5	0.2
KIAA1609	233423_at	2.7	10.7	0.2
LRIG2	242164_s_at	3.5	13.9	0.3
RETN	220570_at	9.3	34.7	0.3
NUDT7	215818_at	4.7	16.9	0.3
SPP1	1568574_x_at	9.7	34.2	0.3
MAGI1	206144_at	5.0	16.6	0.3
PCDHGA4	1552735_at	24.9	81.3	0.3
ZNF532	220617_s_at	78.4	254.1	0.3
FHL3	218818_at	29.2	93.8	0.3
RPS6KA6	228503_at	5.7	18.2	0.3
CSRNP3	235355_at	7.5	23.5	0.3
IL1RAP	205227_at	30.7	96.0	0.3

ETV1	217053_x_at	32.6	95.5	0.3
RPS6KA6	220737_at	8.2	24.0	0.3
ETV1	217061_s_at	27.9	81.2	0.3
PDIA2	206691_s_at	4.1	11.9	0.3
ETV1	221910_at	10.0	28.6	0.3
HLF	204753_s_at	9.8	27.1	0.4
LOC400590	1560992_at	1.6	4.5	0.4
TP53AIP1	220402_at	4.1	11.3	0.4
SSH2	1555425_x_at	8.5	23.2	0.4
HLF	204754_at	13.3	34.9	0.4
MCOLN3	220484_at	14.1	36.6	0.4
COL4A5	213110_s_at	44.4	113.4	0.4
MAP3K5	203836_s_at	148.3	370.3	0.4
MCOLN3	229797_at	41.1	102.3	0.4
IGFBP3	212143_s_at	27.9	68.7	0.4
ZNF532	225021_at	72.7	177.5	0.4
CENPV	226611_s_at	42.2	102.0	0.4
TP53AIP1	223920_s_at	3.4	8.1	0.4
CSRNP3	1558122_s_at	7.9	18.6	0.4
ZNF544	218735_s_at	86.7	198.8	0.4
CENPV	226610_at	16.2	37.1	0.4
LRIG2	242165_at	3.7	8.5	0.4
ZNF19	240836_at	7.8	17.6	0.4
ENAH	222434_at	52.5	118.6	0.4
ADCY10	214547_at	4.0	8.9	0.4
ETV1	206501_x_at	52.5	116.2	0.5
SUPT3H	206506_s_at	65.2	144.0	0.5
ADCY10	217305_s_at	6.8	14.9	0.5
IER3	201631_s_at	188.7	411.8	0.5
MEF2C	209199_s_at	398.7	869.2	0.5
MAP3K5	203837_at	186.4	405.5	0.5
IGFBP3	210095_s_at	61.3	130.0	0.5
MAGI1	225474_at	21.2	45.0	0.5
CAND2	213547_at	89.9	188.7	0.5
KDM4C	209984_at	47.9	100.2	0.5
MEF2C	207968_s_at	73.3	152.3	0.5
CCL22	207861_at	3.0	6.3	0.5
C15orf41	232507_at	4.6	9.5	0.5
SSH2	1554114_s_at	11.2	23.0	0.5
HECW1	215584_at	25.4	51.5	0.5
MCOLN3	1557292_a_at	14.9	30.0	0.5
MEF2C	209200_at	260.9	515.9	0.5
ENAH	222433_at	208.3	409.9	0.5
PDIA2	206889_at	5.7	11.1	0.5
ZNF496	225335_at	204.7	398.9	0.5
MAGI1	1563881_at	3.4	6.7	0.5
CDON	227526_at	37.1	72.2	0.5
HECW1	210331_at	14.1	27.4	0.5
UACA	238868_at	11.4	22.2	0.5
TMEM192	226589_at	187.8	363.6	0.5

SLC7A6	203580_s_at	101.4	194.5	0.5
HLF	204755_x_at	13.3	25.2	0.5
CSRNP3	1558121_at	3.2	6.0	0.5
ASB7	219996_at	24.8	46.5	0.5
AMFR	202204_s_at	100.6	187.3	0.5
THNSL1	222931_s_at	67.9	126.3	0.5
FUBP3	212824_at	237.4	441.8	0.5
PGM5-AS1	231024_at	32.7	60.7	0.5
SRPX	204955_at	436.3	807.8	0.5
KIAA1609	221843_s_at	33.8	62.2	0.5
ACAT1	1559239_s_at	6.7	12.4	0.5
ENAH	228310_at	48.5	89.2	0.5
TP53AIP1	220403_s_at	3.8	7.1	0.5
PDIA2	216127_at	3.9	7.2	0.5
MAGI1	225465_at	25.7	47.2	0.5
SSH2	1555423_at	7.4	13.5	0.5
NRARP	226499_at	53.1	96.7	0.5
PDP2	226855_at	90.8	165.0	0.6
HOXA7	206847_s_at	8.6	15.5	0.6
ARL4A	205020_s_at	68.6	120.3	0.6
KLHL23	241682_at	14.3	25.1	0.6
CSRNP3	235017_s_at	24.2	42.3	0.6
KIAA1919	242851_at	55.4	95.9	0.6
KIAA2026	236306_at	6.0	10.3	0.6
ZNF692	220661_s_at	54.9	94.1	0.6
SRSF6	208804_s_at	382.4	655.3	0.6
KIAA1609	236078_at	25.7	43.7	0.6
LOC440944	1555860_x_at	30.2	51.2	0.6
MYO19	225947_at	68.2	115.1	0.6
ZNF496	1557616_at	8.5	14.4	0.6
ENAH	228553_at	12.6	21.0	0.6
NOA1	223157_at	525.1	871.6	0.6
TOP3A	204946_s_at	44.2	73.1	0.6
ZNF496	225333_at	21.9	36.1	0.6
SSH2	226080_at	267.2	439.1	0.6
TRIM66	229466_at	33.7	55.4	0.6
SRSF6	206108_s_at	81.3	133.2	0.6
THG1L	219122_s_at	95.1	155.3	0.6
ZNF354C	234409_at	5.8	9.4	0.6
ZP4	231756_at	17.7	28.8	0.6
SAFB	201747_s_at	68.6	111.2	0.6
ZNF19	228958_at	36.1	58.4	0.6
UACA	223279_s_at	87.3	141.3	0.6
SLC7A1	212295_s_at	1166.8	1872.7	0.6
PEX1	215023_s_at	49.1	78.8	0.6
CDON	207230_at	11.4	18.2	0.6
SLC7A1	212292_at	44.8	71.4	0.6
UBN2	225445_at	135.0	215.3	0.6
ZNF354C	228208_x_at	45.3	72.2	0.6
ACAT1	205412_at	451.1	717.4	0.6

HOXB9	226461_at	19.7	31.2	0.6
UACA	1558356_at	8.3	13.2	0.6
PFKM	210976_s_at	1113.8	1748.3	0.6
CYP11B1	1552493_s_at	2.7	4.3	0.6
BLMH	202179_at	137.6	214.5	0.6
ZNF407	227768_at	122.8	190.8	0.6
UBN2	225444_at	49.3	76.1	0.6
C15orf41	224486_s_at	64.8	100.1	0.6
KIAA2026	228446_at	143.8	220.0	0.7
ENAH	217820_s_at	147.1	225.0	0.7
ACAT1	1554947_at	5.5	8.4	0.7
UACA	236715_x_at	128.0	193.9	0.7
SAFB	201748_s_at	220.1	333.0	0.7
UBN2	238349_at	18.3	27.5	0.7
ZNF19	234953_x_at	37.9	57.1	0.7
RPP25L	225403_at	187.1	280.3	0.7
KCTD15	222668_at	403.6	603.4	0.7
MYO19	219320_at	38.1	56.6	0.7
SLC7A1	212290_at	274.1	402.4	0.7
SLC7A1	206566_at	25.5	37.2	0.7
LRIG2	205953_at	51.7	74.7	0.7
ZNF266	214686_at	171.6	247.4	0.7
ZNF786	239083_at	52.2	75.1	0.7
AIMP2	202138_x_at	495.7	710.9	0.7
HOXB9	216417_x_at	8.6	12.3	0.7
C17orf85	229342_at	124.2	176.6	0.7
AIMP2	209971_x_at	597.7	849.2	0.7
SUPT3H	211106_at	30.8	43.7	0.7
KIAA1609	65438_at	20.7	29.2	0.7
C17orf85	218896_s_at	62.5	88.0	0.7
FUBP3	239193_at	30.8	43.4	0.7
PEX1	204873_at	49.9	70.0	0.7
LOC440944	1555858_at	23.0	32.2	0.7
IL1RAP	210233_at	7.1	9.9	0.7
KIAA2026	238490_at	89.9	125.6	0.7
SAFB	213635_s_at	29.8	41.5	0.7
SLC7A6	203579_s_at	40.8	55.3	0.7
KCTD15	222664_at	280.7	371.9	0.8
KIAA1609	222261_at	3.4	4.5	0.8
C15orf41	232506_s_at	20.4	26.8	0.8
C17orf85	236384_at	54.5	70.8	0.8
C17orf85	222779_s_at	55.4	72.0	0.8
SLC7A6	203578_s_at	23.5	30.0	0.8
GAS5	1560402_at	30.1	38.4	0.8
TRIM66	213748_at	52.5	66.3	0.8
KIAA1919	238828_at	26.9	33.4	0.8
NUDT7	228855_at	82.5	102.3	0.8
TP53AIP1	223919_at	33.3	41.1	0.8
KCTD15	218553_s_at	111.8	137.5	0.8
CENPV	230436_s_at	12.2	14.8	0.8

ZNF496	238145_at	13.3	16.1	0.8
LOC647859 /// OCLN	227492_at	45.02	53.63	0.8
ZNF407	220836_at	6.8	8.0	0.8
ENAH	1553672_at	20.3	23.1	0.9
CSRNP3	235018_at	10.5	11.9	0.9
LOC440944	1557357_at	12.9	14.5	0.9
LOC400590	1560994_x_at	6.0	6.7	0.9
KCTD15	229683_s_at	9.5	10.3	0.9
ZNF407	220835_s_at	15.7	16.9	0.9
LOC389634	240002_at	15.2	16.2	0.9
ZNF407	234844_at	7.6	8.0	0.9
KIAA2026	235021_at	35.8	37.8	0.9
KDM4C	214861_at	23.4	24.5	1.0
ASB7	226513_at	175.8	183.2	1.0
LOC389634	1560119_at	2.8	2.9	1.0
UBN2	240932_at	6.9	7.0	1.0
RPS6KA6	220738_s_at	7.6	7.7	1.0
CAND2	234404_at	3.6	3.7	1.0
PDP2	232861_at	79.1	79.9	1.0
AIMP2	209972_s_at	67.0	67.1	1.0
THNSL1	219800_s_at	23.4	23.3	1.0
MAGI1	1559257_a_at	12.2	12.1	1.0
UBN2	238350_at	51.8	50.6	1.0
MAGI1	1559256_at	15.1	14.6	1.0
LOC440944	232052_at	25.8	24.6	1.0
HOXA7	235753_at	19.1	18.0	1.1
TOP3A	214300_s_at	33.5	28.6	1.2
MAGI1	232859_s_at	22.8	18.7	1.2
TOP3A	214299_at	39.3	32.2	1.2
SLC7A1	215979_s_at	13.0	10.5	1.2
KIAA1919	232139_s_at	32.5	26.0	1.3
COL4A5	234387_at	7.7	6.1	1.3
ZNF496	225349_at	42.7	33.2	1.3
TRIM66	237679_at	6.7	5.2	1.3
WASH3P	233929_x_at	204.3	156.7	1.3
KCTD15	228683_s_at	30.0	20.5	1.5
MYO19	236022_at	24.2	13.8	1.7
KDM4C	244385_at	16.8	9.5	1.8
CDON	1563677_at	13.9	7.9	1.8
RPS6KA6	228502_at	5.3	2.8	1.9
MAGI1	1555262_a_at	9.1	4.0	2.3

Table S2. Pair-wise comparison of immune score; HLA-DRA score and CD3 score between topographic regions (both edges, apex, centre and base) in immune-high and immune-low uveal melanomas

	Level	Level	Score mean diff	SE diff	Z	p-value $	HL Median	Confidence limit	
								Lower	Upper
Immune-low tumors									
Immune score	Edge	Apex	7.7	6.8	1.1	0.7	0.25	-0.25	0.5
	Edge	Centre	11.8	6.8	1.7	0.3	0.25	0	0.75
	Edge	Base	29.5	6.8	4.3	<.0001*	0.5	0.25	0.75
	Centre	Apex	-4.5	6.7	-0.7	0.9	0	-0.5	0.5
	Centre	Base	14.6	6.7	2.2	0.1	0.5	0	0.5
	Base	Apex	-21.2	6.7	-3.2	0.009*	-0.5	-1	0
HLA-DRA	Edge	Apex	6.6	6.8	1.0	0.8	0	-0.25	0.25
	Edge	Centre	8.5	6.8	1.3	0.6	0.25	-0.25	0.5
	Edge	Base	24.5	6.8	3.6	0.002*	0.25	0	0.75
	Centre	Apex	-2.7	6.6	-0.4	1.0	0	-0.5	0
	Centre	Base	11.0	6.6	1.7	0.3	0	0	0.5
	Base	Apex	-16.2	6.6	-2.4	0.07	-0.5	-0.5	0
CD3	Edge	Apex	10.5	6.3	1.7	0.3	0	0	0.25
	Edge	Centre	14.6	6.3	2.3	0.09	0	0	0.25
	Edge	Base	30.6	5.9	5.2	<.0001*	0.25	0	0.25
	Centre	Apex	-3.3	5.8	-0.6	0.9	0	0	0
	Centre	Base	12.8	5.0	2.5	0.05*	0	0	0
	Base	Apex	-16.6	5.2	-3.2	0.008*	0	0	0
Immune-high tumors									
Immune score	Edge	Apex	-5.9	3.5	-1.7	0.3	-0.25	-0.75	0.25
	Edge	Centre	-9.8	3.5	-2.8	0.03*	-0.5	-1	0
	Edge	Base	-0.3	3.6	-0.1	1.0	0	-0.5	0.5
	Centre	Apex	3.7	3.3	1.1	0.7	0	0	0.5
	Centre	Base	8.5	3.4	2.5	0.06	0.5	0	1
	Base	Apex	-4.7	3.4	-1.4	0.5	0	-1	0
HLA-DRA	Edge	Apex	-2.6	3.3	-0.8	0.9	0	-0.5	0.25
	Edge	Centre	-8.9	3.0	-2.9	0.02*	-0.25	-0.5	0
	Edge	Base	0.1	3.4	0.0	1.0	0	-0.25	0.5
	Centre	Apex	4.4	2.6	1.7	0.3	0	0	0.5
	Centre	Base	8.2	2.9	2.8	0.03*	0	0	0.5
	Base	Apex	-2.4	3.2	-0.7	0.9	0	-0.5	0
CD3	Edge	Apex	-6.5	3.4	-1.9	0.2	-0.25	-0.5	0
	Edge	Centre	-7.3	3.4	-2.1	0.1	-0.25	-0.5	0
	Edge	Base	-0.9	3.5	-0.3	1.0	0	-0.5	0.5
	Centre	Apex	0.9	3.2	0.3	1.0	0	0	0.5
	Centre	Base	4.7	3.3	1.4	0.5	0	0	0.5
	Base	Apex	-4.1	3.3	-1.2	0.6	0	-0.5	0

$ Steel-Dwass method * Significant
diff: difference, SE: standard error, HL: Hodges-Lehmann

Table S3. Pathways associated with overexpressed and underexpressed genes in each subgroup

Overexpressed genes			
Pathway	**Genes**	**Genes ratio**	**p-value**
Common			
Interferon gamma signaling	5	9%	6.70E-07
Antigen processing and presentation	5	8%	9.36E-07
Classical antibody-mediated complement activation	3	60%	1.00E-06
Staphylococcus aureus infection	5	9%	1.22E-06
Graft-versus-host disease	4	11%	2.74E-06
Allograft rejection	4	11%	2.78E-06
Prion diseases	4	12%	2.88E-06
Systemic lupus erythematosus	5	6%	3.22E-06
Type I diabetes mellitus	4	10%	3.75E-06
Autoimmune thyroid disease	4	8%	7.04E-06
Classical complement pathway	3	21%	8.36E-06
Viral myocarditis	4	6%	2.10E-05
Chagas disease (American trypanosomiasis)	4	4%	9.91E-05
Cell adhesion molecules (CAMs)	4	3%	2.28E-04
Interferon alpha/beta signaling	3	7%	2.59E-04
Phagosome	4	3%	3.30E-04
ER-Phagosome pathway	3	5%	5.96E-04
Leishmaniasis	3	4%	7.04E-04
MHC class II antigen presentation	3	4%	7.04E-04
Translocation of ZAP-70 to Immunological synapse	2	13%	9.83E-04
Immune- GSEA			
Antigen processing and presentation	9	14%	7.71E-13
Antigen Presentation: Folding, assembly and peptide loading of class I MHC	5	22%	3.61E-08
ER-Phagosome pathway	6	10%	8.97E-08
Immunoregulatory interactions between a Lymphoid and a non-Lymphoid cell	6	9%	1.08E-07
Phagosome	7	5%	3.00E-07
Viral myocarditis	5	7%	3.46E-06
Endosomal/Vacuolar pathway	3	38%	3.84E-06
Graft-versus-host disease	4	11%	6.59E-06
Allograft rejection	4	11%	6.60E-06
Type I diabetes mellitus	4	10%	1.01E-05
Interferon alpha/beta signaling	4	9%	1.47E-05
Autoimmune thyroid disease	4	8%	1.89E-05
Staphylococcus aureus infection	4	8%	2.20E-05
Interferon gamma signaling	4	7%	2.21E-05
Cell adhesion molecules (CAMs)	5	4%	3.18E-05
Intestinal immune network for IgA production	3	7%	4.00E-04
Leishmaniasis	3	4%	1.32E-03
Systemic lupus erythematosus	3	3%	2.43E-03
Asthma	2	7%	3.80E-03

Alpha4 beta1 integrin signaling events	2	6%	3.10E-03
Immune			
TCR	10	4%	1.12E-06
Natural killer cell mediated cytotoxicity	7	5%	1.51E-05
TCR signaling in naïve CD8+ T cells	5	11%	1.64E-05
TCR signaling in naïve CD4+ T cells	5	8%	3.89E-05
PECAM1 interactions	3	27%	1.07E-04
Downstream signaling in naïve CD8+ T cells	4	9%	2.06E-04
T cell receptor signaling pathway	5	5%	3.64E-04
The co-stimulatory signal during t-cell activation	3	17%	3.70E-04
PD-1 signaling	3	15%	4.01E-04
IL12-mediated signaling events	4	7%	4.08E-04
Cell adhesion molecules (CAMs)	5	4%	6.24E-04
Generation of second messenger molecules	3	11%	8.46E-04
Hematopoietic cell lineage	4	5%	1.22E-03
Allograft rejection	3	9%	1.25E-03
Primary immunodeficiency	3	9%	1.25E-03
Graft-versus-host disease	3	8%	1.28E-03
Interleukin receptor SHC signaling	2	29%	1.41E-03
Downstream TCR signaling	3	8%	1.42E-03
Type I diabetes mellitus	3	7%	1.68E-03
CD28 co-stimulation	2	22%	1.69E-03
GSEA			
Antigen processing and presentation	6	9%	1.08E-07
Graft-versus-host disease	5	14%	1.11E-07
Allograft rejection	5	14%	1.44E-07
Type I diabetes mellitus	5	12%	1.65E-07
Interferon alpha/beta signaling	5	11%	2.39E-07
Autoimmune thyroid disease	5	10%	3.07E-07
Viral myocarditis	5	7%	1.27E-06
Asthma	4	14%	1.52E-06
Intestinal immune network for IgA production	4	9%	9.61E-06
Cell adhesion molecules (CAMs)	5	4%	1.50E-05
Toxoplasmosis	5	4%	1.50E-05
Interferon gamma signaling	4	7%	1.51E-05
Translocation of ZAP-70 to Immunological synapse	3	20%	1.54E-05
Phosphorylation of CD3 and TCR zeta chains	3	18%	1.68E-05
Staphylococcus aureus infection	4	8%	1.68E-05
Phagosome	5	3%	2.42E-05
PD-1 signaling	3	15%	2.48E-05
Immunoregulatory interactions between a Lymphoid and a non-Lymphoid cell	4	6%	2.55E-05
Leishmaniasis	4	6%	2.72E-05
Generation of second messenger molecules	3	11%	5.99E-05
Immune-HCL			
Interferon gamma signaling	2	4%	1.13E-03
BCR	2	1%	4.83E-03
Cytokine-cytokine receptor interaction	2	1%	8.82E-03

Table S3 continued

Underexpressed genes			
Pathway	**Genes**	**Genes ratio**	**p-value**
Immune			
Prostate cancer	2	2%	3.49E-03
Hepatitis C	2	1%	4.02E-03
Integrin signaling pathway	2	2%	4.46E-03
Regulation of actin cytoskeleton	2	1%	6.55E-03
Gap junction	2	2%	6.68E-03
Focal adhesion	2	1%	7.08E-03
EGFR1	2	0%	2.65E-02
GSEA			
Generic transcription pathway	6	2%	2.15E-02
Regulators of bone mineralization	2	18%	2.56E-02
Amino acid transport across the plasma membrane	2	7%	3.23E-02
P38 mapk signaling pathway	2	7%	4.23E-02
CDO in myogenesis	2	7%	5.25E-02

In italics: terms common to DAVID and InnateDB (databases used for annotation);
rest: terms from InnateDB only

Table S4. Genes associated with significant pathways

Common

Pathway	C1QA	C1QB	C1QC	CCL5	CD74	HLA-E	HLA-G	HLA-DPA1	HLA-DRA	IRF1	PSMB9	PSMB10	STAT1
Interferon-gamma signaling							x	x	x	x			x
Antigen processing and presentation					x	x	x	x	x				
Classical antibody-mediated complement activation	x	x	x										
Staphylococcus aureus infection	x	x	x					x	x				
Graft-versus-host disease						x	x	x	x				
Allograft rejection						x	x	x	x				
Prion diseases	x	x	x	x									
Systemic lupus erythematosus	x	x	x					x	x				
Type I diabetes mellitus						x	x	x	x				
Autoimmune thyroid disease						x	x	x	x				
Classical complement pathway	x	x	x										
Viral myocarditis						x	x	x	x				
Chagas disease (American trypanosomiasis)	x	x	x	x									
Cell adhesion molecules (CAMs)						x	x	x	x				
Interferon alpha/beta signaling							x			x			x
Phagosome						x	x	x	x				
ER-phagosome pathway							x				x	x	
Leishmaniasis								x	x				x
MHC class II antigen presentation					x			x	x				
Translocation of ZAP-70 to Immunological synapse								x	x				
Antigen presentation: folding, assembly and peptide loading of class I MHC													
Immunoregulatory interactions between a lymphoid and a non-lymphoid cell													
Endosomal/Vacuolar pathway													
Intestinal immune network for IgA production													
Asthma													
Alpha4 beta1 integrin signaling events													
Toxoplasmosis													
Phosphorylation of CD3 and TCR zeta chains													
TCR													
Natural killer cell mediated cytotoxicity													
TCR signaling in naive CD8+ T cells													
TCR signaling in naive CD4+ T cells													
PECAM1 interactions													
Downstream signaling in naive CD8+ T cells													
T-cell receptor signaling pathway													
The co-stimulatory signal during T-cell activation													
PD-1 signaling													
IL2-mediated signaling events													
Generation of second messenger molecules													
Hematopoietic cell lineage													
Primary immunodeficiency													
Interleukin receptor SHC signaling													
Downstream TCR signaling													
CD28 co-stimulation													
BCR													
Cytokine-cytokine receptor interaction													

Immune - GSEA

Pathway	AMICA1	B2M	C2	CD14	HLA-B	HLA-C	HLA-DMA	HLA-DMB	IL15RA	ITGAL	LGMN	LILRB2	NCF4	OAS3	PSME2	TAP1	TAPBP	XAF1
Interferon-gamma signaling		x			x	x								x				
Antigen processing and presentation		x			x	x	x				x				x	x	x	
Classical antibody-mediated complement activation																		
Staphylococcus aureus infection			x				x	x		x								
Graft-versus-host disease					x	x	x	x										
Allograft rejection					x	x	x	x										
Prion diseases																		
Systemic lupus erythematosus			x				x	x										
Type I diabetes mellitus					x	x	x	x										
Autoimmune thyroid disease					x	x	x	x										
Classical complement pathway																		
Viral myocarditis					x	x	x	x		x								
Chagas disease (American trypanosomiasis)																		
Cell adhesion molecules (CAMs)					x	x	x	x		x								
Interferon alpha/beta signaling					x	x								x				x
Phagosome				x	x	x	x	x								x		
ER-phagosome pathway		x			x	x									x	x	x	
Leishmaniasis							x	x					x					
MHC class II antigen presentation																		
Translocation of ZAP-70 to Immunological synapse																		
Antigen presentation: folding, assembly and peptide loading of class I MHC		x			x	x										x	x	
Immunoregulatory interactions between a lymphoid and a non-lymphoid cell	x	x			x	x				x		x						
Endosomal/Vacuolar pathway		x			x	x												
Intestinal immune network for IgA production							x	x	x									
Asthma							x	x										
Alpha4 beta1 integrin signaling events	x			x														
Toxoplasmosis																		
Phosphorylation of CD3 and TCR zeta chains																		
TCR																		
Natural killer cell mediated cytotoxicity																		
TCR signaling in naive CD8+ T cells																		
TCR signaling in naive CD4+ T cells																		
PECAM1 interactions																		
Downstream signaling in naive CD8+ T cells																		
T-cell receptor signaling pathway																		
The co-stimulatory signal during T-cell activation																		
PD-1 signaling																		
IL2-mediated signaling events																		
Generation of second messenger molecules																		
Hematopoietic cell lineage																		
Primary immunodeficiency																		
Interleukin receptor SHC signaling																		
Downstream TCR signaling																		
CD28 co-stimulation																		
BCR																		
Cytokine-cytokine receptor interaction																		

GSEA

Pathway	CCR5	HLA-DPB1	HLA-DQA1	HLA-DQB1	HLA-DRB1	HLA-F	IFI27	IFI35	IFITM1	LILRB5	PSMB8	PSME1	TYROBP
Interferon-gamma signaling		x	x		x	x							
Antigen processing and presentation		x	x	x	x	x						x	
Classical antibody-mediated complement activation													
Staphylococcus aureus infection		x	x	x	x								
Graft-versus-host disease		x	x	x	x	x							
Allograft rejection		x	x	x	x	x							
Prion diseases													
Systemic lupus erythematosus													
Type I diabetes mellitus		x	x	x	x	x							
Autoimmune thyroid disease		x	x	x	x	x							
Classical complement pathway													
Viral myocarditis		x	x	x	x	x							
Chagas disease (American trypanosomiasis)													
Cell adhesion molecules (CAMs)		x	x	x	x	x							
Interferon alpha/beta signaling						x	x	x	x		x		
Phagosome		x	x	x	x	x							
ER-phagosome pathway													
Leishmaniasis		x	x	x	x								
MHC class II antigen presentation													
Translocation of ZAP-70 to Immunological synapse		x	x		x								
Antigen presentation: folding, assembly and peptide loading of class I MHC													
Immunoregulatory interactions between a lymphoid and a non-lymphoid cell						x			x	x			x
Endosomal/Vacuolar pathway													
Intestinal immune network for IgA production		x	x	x	x								
Asthma		x	x	x	x								
Alpha4 beta1 integrin signaling events													
Toxoplasmosis	x	x	x	x	x								
Phosphorylation of CD3 and TCR zeta chains		x	x		x								
TCR													
Natural killer cell mediated cytotoxicity													
TCR signaling in naive CD8+ T cells													
TCR signaling in naive CD4+ T cells													
PECAM1 interactions													
Downstream signaling in naive CD8+ T cells													
T-cell receptor signaling pathway													
The co-stimulatory signal during T-cell activation													
PD-1 signaling		x	x		x								
IL2-mediated signaling events													
Generation of second messenger molecules		x	x		x								
Hematopoietic cell lineage													
Primary immunodeficiency													
Interleukin receptor SHC signaling													
Downstream TCR signaling													
CD28 co-stimulation													
BCR													
Cytokine-cytokine receptor interaction													

Immune and **Immune - HCL**

Pathway	CD2	CD3D	CD8A	CD38	CD48	CD86	FYB	GZMB	HLA-DOA	INPP5D	LCK	LY9	NFATC2	PTPN6	RASSF5	SH2D1A	SIGLEC1	TNFSF10	CCL4	CD27	GBP1	GBP2	HCLS1
Interferon-gamma signaling																					x	x	
Antigen processing and presentation																							
Classical antibody-mediated complement activation																							
Staphylococcus aureus infection																							
Graft-versus-host disease						x		x	x														
Allograft rejection						x		x	x														
Prion diseases																							
Systemic lupus erythematosus																							
Type I diabetes mellitus						x		x	x														
Autoimmune thyroid disease																							
Classical complement pathway																							
Viral myocarditis																							
Chagas disease (American trypanosomiasis)																							
Cell adhesion molecules (CAMs)	x		x			x			x								x						
Interferon alpha/beta signaling																							
Phagosome																							
ER-phagosome pathway																							
Leishmaniasis																							
MHC class II antigen presentation																							
Translocation of ZAP-70 to Immunological synapse																							
Antigen presentation: folding, assembly and peptide loading of class I MHC																							
Immunoregulatory interactions between a lymphoid and a non-lymphoid cell																							
Endosomal/Vacuolar pathway																							
Intestinal immune network for IgA production																							
Asthma																							
Alpha4 beta1 integrin signaling events																							
Toxoplasmosis																							
Phosphorylation of CD3 and TCR zeta chains																							
TCR	x	x	x			x	x			x	x	x	x	x									
Natural killer cell mediated cytotoxicity					x			x			x		x	x		x		x					
TCR signaling in naive CD8+ T cells		x	x								x			x	x								
TCR signaling in naive CD4+ T cells		x					x				x			x	x								
PECAM1 interactions										x	x			x									
Downstream signaling in naive CD8+ T cells		x	x					x					x										
T-cell receptor signaling pathway		x	x								x		x	x									
The co-stimulatory signal during T-cell activation		x				x					x												
PD-1 signaling		x									x			x									
IL2-mediated signaling events		x	x					x			x												
Generation of second messenger molecules		x					x				x												
Hematopoietic cell lineage	x	x	x	x																			
Primary immunodeficiency		x	x								x												
Interleukin receptor SHC signaling										x				x									
Downstream TCR signaling		x								x	x												
CD28 co-stimulation						x					x												
BCR																			x				x
Cytokine-cytokine receptor interaction																			x	x			

Table S5. Gene ontology terms associated with overexpressed and underexpressed genes in each subgroup

Overexpressed genes				
Term	**GO ID**	**Count**	**Genes Ratio**	**p-value**
Common				
Biological process				
Antigen processing and presentation	GO:0019882	6	12%	1.23E-09
Interferon-gamma-mediated signaling pathway	GO:0060333	5	8%	2.54E-07
Immune response	GO:0006955	7	2%	1.07E-06
Cytokine-mediated signaling pathway	GO:0019221	6	3%	1.39E-06
Antigen processing and presentation of peptide antigen*	GO:0048002	5	27.8%	2.15E-06
B cell mediated immunity*	GO:0019724	5	27.8%	2.27E-05
Immunoglobulin mediated immune response*	GO:0016064	5	27.8%	2.45E-05
Complement activation	GO:0006956	3	9%	8.21E-05
Complement activation, classical pathway	GO:0006958	3	8%	1.08E-04
Innate immune response	GO:0045087	7	1%	4.10E-04
Type I interferon-mediated signaling pathway	GO:0060337	3	5%	4.35E-04
Cellular component				
Integral to lumenal side of endoplasmic reticulum membrane	GO:0071556	4	18%	3.32E-07
ER to Golgi transport vesicle membrane	GO:0012507	4	14%	8.06E-07
MHC class II protein complex	GO:0042613	3	19%	1.46E-05
Complement component C1 complex	GO:0005602	2	100%	2.54E-05
Clathrin-coated endocytic vesicle membrane	GO:0030669	3	15%	2.59E-05
Trans-Golgi network membrane	GO:0032588	3	11%	5.30E-05
Transport vesicle membrane	GO:0030658	3	10%	6.01E-05
Endocytic vesicle membrane	GO:0030666	3	7%	1.37E-04
MHC protein complex*	GO:0042611	4	22.2%	1.07E-03
Molecular function				
MHC class II receptor activity	GO:0032395	2	25%	3.99E-04
Immune- GSEA				
Biological process				
Immune response	GO:0006955	14	4%	1.10E-13
APP of exogenous peptide antigen via MHC class I	GO:0042590	7	9%	5.69E-09
APP of exogenous peptide antigen via MHC class I, TAP-dependent	GO:0002479	7	9%	5.87E-09
APP of peptide antigen via MHC class I	GO:0002474	7	7%	1.60E-08
Regulation of immune response	GO:0050776	6	7%	4.84E-07
Cytokine-mediated signaling pathway	GO:0019221	7	3%	3.85E-06
APP of exogenous peptide antigen via MHC class I, TAP-independent	GO:0002480	3	38%	1.09E-05

Positive regulation of T cell mediated cytotoxicity	GO:0001916	3	25%	3.72E-05
Innate immune response	GO:0045087	11	1%	3.73E-05
Antigen processing and presentation	GO:0019882	4	8%	4.93E-05
Regulation of dendritic cell differentiation	GO:2001198	2	100%	6.54E-05
Cell surface receptor signaling pathway	GO:0007166	6	3%	6.71E-05
Interferon-gamma-mediated signaling pathway	GO:0060333	4	7%	6.91E-05
Type I interferon-mediated signaling pathway	GO:0060337	4	6%	8.36E-05
Defense response*	GO:0006952	10	31.3%	5.46E-04
Cellular component				
MHC class I protein complex	GO:0042612	3	14%	1.11E-04
Integral to lumenal side of endoplasmic reticulum membrane	GO:0071556	3	14%	1.21E-04
Extracellular space	GO:0005615	9	1%	1.43E-04
TAP complex	GO:0042825	2	50%	2.31E-04
Insoluble fraction*	GO:0005626	8	25%	2.45E-02
Plasma membrane part*	GO:0044459	13	40.6%	2.74E-02
Intrinsic to membrane*	GO:0031224	22	68.8%	2.93E-02
Plasma membrane*	GO:0005886	18	56.3%	3.10E-02
Membrane fraction*	GO:0005624	8	25%	3.17E-02
Integral to membrane*	GO:0016021	21	65.6%	3.63E-02
Molecular function				
TAP1 binding	GO:0046978	2	50%	2.31E-04
MHC protein binding*	GO:0042287	4	12.5%	1.37E-03
GSEA				
Biological process				
Cytokine-mediated signaling pathway	GO:0019221	10	5%	2.27E-09
Antigen processing and presentation	GO:0019882	6	12%	9.63E-08
Interferon-gamma-mediated signaling pathway	GO:0060333	5	8%	6.35E-06
Type I interferon-mediated signaling pathway	GO:0060337	5	8%	7.35E-06
APP of peptide or polysaccharide antigen via MHC class II	GO:0002504	3	27%	4.49E-05
Immune response	GO:0006955	7	2%	1.88E-04
Positive regulation of gamma-delta T cell differentiation	GO:0045588	2	29%	1.86E-03
Cellular defense response	GO:0006968	3	5%	3.75E-03
T-helper 1 type immune response	GO:0042088	2	18%	3.99E-03
T cell costimulation	GO:0031295	3	5%	4.71E-03
APP of exogenous peptide antigen via MHC class I, TAP-dependent	GO:0002479	3	4%	7.13E-03
T cell receptor signaling pathway	GO:0050852	3	4%	7.52E-03
Cellular component				
MHC class II protein complex	GO:0042613	4	25%	2.25E-06
Integral to lumenal side of endoplasmic reticulum membrane	GO:0071556	4	18%	6.73E-06
ER to Golgi transport vesicle membrane	GO:0012507	4	14%	1.24E-05
Clathrin-coated endocytic vesicle membrane	GO:0030669	3	15%	2.45E-04
Trans-Golgi network membrane	GO:0032588	3	11%	5.67E-04
Transport vesicle membrane	GO:0030658	3	10%	6.48E-04
Endocytic vesicle membrane	GO:0030666	3	7%	1.72E-03

Intrinsic to membrane*	GO:0031224	25	62.5%	5.44E-02
Molecular function				
MHC class II receptor activity	GO:0032395	2	25%	2.31E-03
Immune-HCL				
Biological process				
Defense response to virus	GO:0051607	3	2%	1.09E-03
Immune response to tumor cell	GO:0002418	1	100%	6.30E-03
Immune response	GO:0006955	3	1%	7.07E-03
Response to virus	GO:0009615	2	2%	7.10E-03
Defense response to tumor cell	GO:0002357	1	50%	7.87E-03
Interferon-gamma-mediated signaling pathway	GO:0060333	2	3%	8.86E-03
Response to ethanol	GO:0045471	2	2%	1.01E-02
Positive regulation of natural killer cell chemotaxis	GO:2000503	1	20%	1.05E-02
Positive regulation of tyrosine phosphorylation of STAT protein	GO:0042531	1	20%	1.05E-02
Release of cytoplasmic sequestered NF-kappaB	GO:0008588	1	25%	1.26E-02
Cytokine-mediated signaling pathway	GO:0019221	2	1%	1.39E-02
Positive regulation of B cell differentiation	GO:0045579	1	10%	1.65E-02
Protein trimerization	GO:0070206	1	10%	1.65E-02
Immunoglobulin mediated immune response	GO:0016064	1	8%	1.86E-02
Cellular component				
Cytolytic granule	GO:0044194	1	50%	7.87E-03
Endosome lumen	GO:0031904	1	20%	1.05E-02
Extracellular region	GO:0005576	4	0%	1.16E-02
Molecular function				
Wide pore channel activity	GO:0022829	1	100%	6.30E-03
CCR5 chemokine receptor binding	GO:0031730	1	20%	1.05E-02
CCR1 chemokine receptor binding	GO:0031726	1	17%	1.18E-02
Immune				
Biological process				
Innate immune response	GO:0045087	21	2%	1.70E-11
Positive regulation of immune system process*	GO:0002684	11	21.1%	1.72E-06
Defense response to virus	GO:0051607	7	5%	7.71E-06
Lymphocyte activation*	GO:0046649	9	17.3%	6.42E-05
Defense response*	GO:0006952	13	25%	8.24E-05
Regulation of lymphocyte activation*	GO:0051249	8	15.4%	9.54E-05
B cell receptor signaling pathway	GO:0050853	4	13%	1.16E-04
Leukocyte activation*	GO:0045321	9	17.3%	1.21E-04
T cell receptor signaling pathway	GO:0050852	5	6%	1.34E-04
Regulation of leukocyte activation*	GO:0002694	8	15.4%	1.38E-04
Regulation of cell activation*	GO:0050865	8	15.4%	1.47E-04
Immunoglobulin mediated immune response	GO:0016064	3	23%	2.12E-04
Natural killer cell activation	GO:0030101	3	23%	2.12E-04
Immune response	GO:0006955	8	2%	2.18E-04
T cell activation	GO:0042110	4	9%	2.44E-04
Lymphocyte mediated immunity*	GO:0002449	6	11.5%	2.59E-04
Leukocyte migration	GO:0050900	5	4%	3.60E-04
Blood coagulation	GO:0007596	8	2%	7.19E-04

T cell costimulation	GO:0031295	4	6%	7.21E-04
Negative regulation of T cell proliferation	GO:0042130	3	11%	1.24E-03
Microglial cell activation	GO:0001774	2	40%	1.64E-03
Regulation of T cell differentiation	GO:0045580	2	33%	2.33E-03
Cellular component				
External side of plasma membrane	GO:0009897	6	3%	2.80E-04
Immunological synapse	GO:0001772	3	14%	7.01E-04
Alpha-beta T cell receptor complex	GO:0042105	2	40%	1.64E-03
Plasma membrane	GO:0005886	25	48.1%	2.31E-02
Molecular function				
Protein binding	GO:0005515	41	0%	3.60E-06
Receptor activity	GO:0004872	7	3%	2.09E-04
SH2 domain binding	GO:0042169	4	12%	1.38E-04
HCL				
Biological process				
Protein methylation	GO:0006479	1	4%	1.67E-02
Protein peptidyl-prolyl isomerization	GO:0000413	1	5%	1.92E-02
Lipid catabolic process	GO:0016042	1	1%	3.97E-02
Peptidyl-proline modification	GO:0018208	1	7%	5.39E-02
Molecular function				
Phospholipase A2 activity	GO:0004623	1	4%	1.67E-02
Protein methyltransferase activity	GO:0008276	1	5%	1.92E-02
Peptidyl-prolyl cis-trans isomerase activity	GO:0003755	1	2%	2.25E-02
FK506 binding	GO:0005528	1	7%	2.89E-02
Methyltransferase activity	GO:0008168	1	1%	5.09E-02

Table S5 continued

Underexpressed genes				
Term	**GO ID**	**Count**	**Gene ratio**	**p-value**
Immune				
Biological process				
Negative regulation of Wnt protein secretion	GO:0061358	1	100%	1.46E-02
Positive regulation of ERK1 and ERK2 cascade	GO:0070374	2	2%	1.63E-02
Cellular response to morphine	GO:0071315	1	50%	1.75E-02
Positive regulation of monocyte aggregation	GO:1900625	1	50%	1.75E-02
Wound healing involved in inflammatory response	GO:0002246	1	50%	1.75E-02
Blood vessel endothelial cell proliferation involved in sprouting angiogenesis	GO:0002043	1	25%	2.19E-02
Iron ion transmembrane transport	GO:0034755	1	25%	2.19E-02
Positive regulation of heterotypic cell-cell adhesion	GO:0034116	1	25%	2.19E-02
Positive regulation of transcription of Notch receptor target	GO:0007221	1	25%	2.19E-02
Monocyte aggregation	GO:0070487	1	33%	2.19E-02
Cellular component				
Apicolateral plasma membrane	GO:0016327	1	9%	2.41E-02
Membrane	GO:0016020	5	0%	2.55E-02
Apical plasma membrane	GO:0016324	2	1%	2.59E-02
Lamellipodium membrane	GO:0031258	1	7%	2.61E-02
Filopodium membrane	GO:0031527	1	8%	2.64E-02
Molecular function				
Beta-endorphin receptor activity	GO:0004979	1	100%	1.46E-02
Ferritin receptor activity	GO:0070287	1	100%	1.46E-02
Morphine receptor activity	GO:0038047	1	100%	1.46E-02
Thiopurine S-methyltransferase activity	GO:0008119	1	50%	1.75E-02
Hyalurononglucosaminidase activity	GO:0004415	1	14%	2.27E-02
GSEA				
Biological process				
Positive regulation of apoptotic process	GO:0043065	7	3%	3.38E-02

Table S6. Baseline data in present series, external dataset 1 and external dataset 2

Parameter		Present series (n = 91)	External dataset 1 (n = 61)	External dataset 2 (n = 22)
Age	Range	35-90 years	28.6-85 years	42-85 years
	Median	67 years	61.8 years	65.5 years
	Mean	64.7 years	60.6 years	65.7 years
	NA	2 (2.2%)	–	–
	≤ 60 years	32 (36%)	28 (45.9%)	7 (31.8%)
	> 60 years	57 (64%)	33 (54.1%)	15 (68.2%)
Gender	Male	46 (51.7%)	37 (60.7%)	8 (36.4%)
	Female	43 (48.3%)	24 (39.3%)	14 (63.6%)
	NA	2 (2.2%)	–	–
Diameter	Range	7-25 mm	9-23 mm	6-25 mm
	Median	18 mm	15 mm	13.5 mm
	Mean	17.8 mm	15.3 mm	14 mm
	NA	14 (15.4%)	10 (16.4%)	–
	≤15 mm	16 (20.8%)	27 (52.9%)	15 (68.2%)
	>15 mm	61 (79.2%)	24 (47.1%)	7 (31.8%)
Thickness	Range	1.6-18 mm	6-17 mm	4-16 mm
	Median	11.1 mm	11.7 mm	8.5 mm
	Mean	10.5 mm	11.6 mm	9.4 mm
	NA	7 (7.7%)	–	2 (9.1%)
	≤ 8mm	16 (19%)	3 (4.9%)	10 (60%)
	>8mm	68 (81%)	58 (95.1%)	10 (40%)
Retinal detachment	Present	79 (97.5%)	35 (62.5%)	NA
	Absent	2 (2.5%)	21 (37.5%)	NA
	NA	10 (11%)	5 (8.2%)	–
Extrascleral extension	Absent	82 (92.1%)	46 (90.2%)	11 (50%)
	Present	7 (7.9%)	5 (9.8%)	11 (50%)
	NA	2 (2.2%)	10 (16.4%)	–
Histology	Epithelioid	–	21 (47.7%)	5 (23.8%)
	Mixed	–	23 (52.3%)	10 (47.6%)
	Spindle	–	–	6 (28.6%)
	NA	–	17 (27.9%)	1 (4.5%)
Metastases	Present	38 (44.2%)	35 (57.4%)	10 (45.5%)
	Absent	48 (55.8%)	26 (42.6%)	12 (54.5%)
	no follow-up	5 (5.5%)	–	–

NA: not available

DISCUSSION

Uveal melanomas (UM) are the most common, malignant, primary intra-ocular tumors in adults. Their karyotypic features have been well-characterized since a decade and over the last few years some of the driver mutations have been identified. Nevertheless, none of this, as yet has translated into improved survival. About 50% of them metastasize, with a limited survival of about one to two years after that. This indicates a need for better identification of patient-groups at high-risk for metastases so that they can receive adjuvant therapies tailor-made to their risk status.

I. Immune-high and immune-low phenotypes of uveal melanomas

The transcriptomic profiles of 15 uveal melanomas were analyzed by both unsupervised and supervised approaches. The former indicated the existence of two sub-groups of primary tumors and the latter unraveled a gene signature comprising of genes of immune response. These two phenotypes had over-expression (immune-high) and under-expression (immune-low) of the signature genes. These phenotypes are similar to other cancers where gene signatures that bear the footprint of immune activation have been described {Pages et al, 2009; Ascierto et al, 2011; Ascierto et al, 2012; Carretero et al, 2012; Mann et al, 2013}.

The signature in uveal melanomas was characterized by: IFNG stimulated genes of STAT1-IRF1 axis with Th1 orientation, chemokine ligands which attract lymphocytes and macrophages and cytotoxic effectors. In this aspect also, it is comparable to solid tumors of breast, colorectum and cutaneous melanoma {Jonsson et al, 2010; Mlecnik et al, 2011; Ascierto et al, 2012}. These results indicate IFNG signaling/STAT1-IRF1 axis to be the common denominator in immune phenotypes of different cancers {Galon et al, 2013}. It is intriguing that such redundancy exists between uveal melanomas which arise

in an immune-privileged milieu and other cancer types. Yet, their influence on behavior of uveal melanomas is different from those of other cancers as discussed below.

II. Correlation of immune phenotypes with immune cell infiltration

In view of technological advances, the present trend is to categorize tumors into sub-groups based on gene expression signatures, rather than the conventional histologic subtypes. If these molecular subtypes are to become part of day-to-day clinical practice, there is a need for their translation into routinely used techniques such as immunohistochemistry (IHC).

In order to test the identified immune phenotypes in additional samples, the transcriptome-based signature was converted to an IHC-based one. This was possible since immune-high tumors demonstrated dense infiltrates of cytotoxic T-cells and macrophages; whereas, immune-low tumors had occasional T-cells and mild to moderate numbers of macrophages.

By utilizing routinely used antibodies and application of a semi-quantitative scoring method (immune score), the melanoma phenotypes could be recognized, indicating that immune score can be used as a surrogate marker for gene signature. The advantages of this approach were: expansion of cohort size, visualization of intra-tumoral heterogeneity in immune cell distribution and better understanding of topography. The latter indicated that ‘tumor centre’ would be the site of choice for a biopsy in order to assess the immune status as it minimizes the false-negative rate associated with heterogeneity.

III. Prognostic and therapeutic relevance of immune phenotypes

Uveal melanomas were stratified into three prognostic groups based on the degree of infiltration by tumor-associated macrophages and cytotoxic T-cells.

The combination of TAM and CD8+ T-cells was a marker of prognosis. The risk of metastases was highest for tumors with dense infiltrate of both cytotoxic T-cells and TAM; intermediate for those with low infiltrate of former and high infiltrate of latter and low for melanomas with sparse infiltrates of both.

A predictive biomarker in cancer is useful for assessment of therapeutic response. The predictive role of immune infiltrate has been demonstrated in other cancers {Ono et al, 2012; Seo et al, 2013} {Ayari et al, 2009; Deau et al, 2013}. In addition, drugs which target immune cells have been shown to be beneficial in sarcomas and ovarian cancer {Grosso et al, 2007; Monk et al, 2010}.

The proposed risk-groups based on TAM and cytotoxic T-cells is a potential predictive biomarker. Moreover, the groups with high macrophage infiltrate could benefit from strategies targeting macrophages. In short, this proposed biomarker could be useful for design of adjuvant therapy, selection of the recipient risk-group and assessment of therapeutic response. These aspects need to be explored through clinical trials.

IV. Chromosomal alterations associated with immune phenotypes

The two phenotypes were associated with distinct chromosomal anomalies. Majority of immune-high melanomas were characterized by monosomy 3 (M3) and isochromosome 8q. This combination can be considered to be a marker of this phenotype. The immune-low tumors could be dichotomized further based on presence or absence of M3. The characteristic alterations in this group were 6p gain mostly isochromosome 6p and 1p loss. The alterations in chromosome 6 can be considered to be a marker of this phenotype.

They appear to follow the two proposed temporal sequence of chromosomal alterations associated with uveal melanoma progression previously described in

the introduction {Hoglund et al, 2004; Ehlers et al, 2008}. The immune-high tumors demonstrate the M3-8q gain-8p loss sequence. On the other hand, the immune-low tumors lacking M3 appear to follow the 6p gain-6q loss sequence. The immune-low tumors with M3 are in between, sharing alterations of both sequences.

V. Identification of risk-groups and their therapeutic relevance

In uveal melanomas, there is a need for better definition of prognostic groups as survival rates have not improved in over three decades {Singh et al, 2003}. To identify risk-groups, Cox multivariate models were constructed using clinical, pathologic, genetic and immune parameters. They were: copy number alteration (CNA), immune and CNA (immune-CNA) and combined (immune-CNA-pathology) models.

Each of these models independently stratified the patients into three groups with high-, intermediate- and low-risk for development of metastasis. This correlates with the results of other groups {Cassoux et al, 2013} {Field et al, 2014}. In addition, further refinement of the intermediate group indicated the possibility of an additional risk category. These results could have an impact on design of future clinical trials. Treating them with risk relevant adjuvant therapies in future clinical trials could improve the outcome.

The CNA model based on four copy number alterations is most suitable for clinical use as it is applicable to fine needle aspiration biopsy (FNAB) samples {Cassoux et al, 2013} and is cost-effective. Assessment of the risk-category of the tumor soon after diagnosis would help with further patient management decisions.

The immune-CNA model compared the relative prognostic impact of immune infiltrate and karyotype. Immune-high tumors were distributed in all risk-

groups, but 70% belonged to high-risk category. This could be another reason for the paradoxical relation between high lymphocytic infiltration and poor outcome, besides the immune evasion mechanisms {Niederkorn 2009} described in the introduction.

In addition, the clinical impact of immune phenotype varied with risk-group. In high-risk group, there was no survival difference between immune-high and -low tumors. In intermediate group, immune-high tumors had shorter survival than their immune-low counterparts. This indicates that the effect of immune infiltrate on survival depends on the associated karyotype. If one considers the previously described temporal sequence of CNA in uveal melanomas, M3 is an early alteration, followed by 8q alterations; whereas, 8p and 1p changes occur later. It can be considered that uveal melanomas show genetic progression as we move from low to high-risk group. This progression is probably associated with modulation of impact of immune infiltrate. This is analogous to the evolution of immune response in colorectal cancer as tumors progress from stage T1 to T4 {Bindea et al, 2013}.

These findings could have therapeutic implications. The high risk-group may benefit from targeting the DNA alterations on chromosome 3 (*BAP1*) {Landreville et al, 2012} by using histone deacetylase inhibitors as they have been shown to reverse the stem-like phenotype of mutated cells to differentiated ones. In the intermediate group perhaps it would be beneficial to target the immune infiltrate using macrophage cytotoxic agents such as trabectedine and anti PD-L1 and IDO inhibitors for lymphocytes.

VI. Summary

It is a known fact that in uveal melanomas infiltration by T-cells is associated with poor clinical outcome. In the light of our results this contrary observation can be surmised in two ways:

- *Epiphenomenon secondary to genetic alterations*

This argument is favored by the fact that uveal melanomas with a high infiltrate of cytotoxic T-cells have increased aneuploidy. Moreover, immune-high and immune-low tumors with same CNA have similar outcome. In other words, in presence of aneuploidy, there is no prognostic role for the co-existent T-cell response. Even though it has not been demonstrated, it would be logical to hypothesize that aneuploidy leads to genetic instability resulting in increased mutation load. The latter in turn, may lead to new antigenic peptides which elicit a spontaneous T-cell response. However, this is either not sufficient enough to effect tumor rejection or is being overwhelmed by immune escape mechanisms mounted by the tumor or both. One of the reasons may be due to interferon-gamma mediated upregulation of *IDO1* and *PD-L1* leading to inhibition of T-cell proliferation and activation as has been demonstrated in uveal melanoma {Chen et al, 2007; Yang et al, 2008}.

- *T-cell response per se is responsible for poor outcome*

An alternate explanation is that the T-cell response itself is somehow facilitating uveal melanoma progression. It may be related to production of cytokines and chemokines by T-cells such as TNF-α and CCL5 which can facilitate EMT and tumor cell motility {Balkwill 2009; Chuang et al, 2009}. Even IFN-γ in low doses has been shown to enhance the metastatic potential of tumor cells in murine models {Kelly et al, 1991; He et al, 2005}. Even though our results are more in favor of the first option, there is still the unresolved

situation in intermediate risk-group uveal melanomas. In the latter, the immune-high tumors had worse outcome than their immune-low counterparts. As this was based on very small number of tumors, it is not possible to conclude anything at this point. Nevertheless, it can be speculated that perhaps the impact of T-cell response is CNA dependent. High-risk CNA are such a dominant influence that most melanomas tend to progress, irrespective of T-cell response. On the other hand, the intermediate-risk CNA needs some help to promote tumor advancement which is provided by T-cells. In this situation, T-cells may be responsible for the poor outcome, provided this can be confirmed on larger series.

Therefore, at present it can only be concluded that in uveal melanomas T-cell response is an epiphenomenon secondary to genetic alterations.

These questions can be addressed to a certain extent through whole-exome and transcriptome profiling (discussed in detail below) of immune-high and immune-low uveal melanomas. This will give an idea regarding the mutation load in the respective immune phenotypes. In addition, combining sequencing with functional studies would enable identification of immunogenic mutations and candidate tumor antigens {Segal et al, 2008; Castle et al, 2012}. An alternate approach would be to establish cell lines from immune-high uveal melanomas and derive from peripheral blood lymphocytes autologous cytolytic T-lymphocyte (CTL) clones directed against autologous tumor cell line and use gene transfection method to identify the antigens {Van den Eynde et al, 1989}. This method would also help in identification of resistance or sensitivity of tumor cell variants to CTL clones.

VI. Future perspectives

VI.1. Next-generation sequencing (NGS)

This is a high-throughput technology available since 2004 that can be considered an evolution of sequencing and microarray technology. The depth and breadth of genomic interrogation made possible by this technology is unprecedented. Different types of input material: DNA, RNA and chromatin can be analyzed. The analysis of NGS data requires powerful computational tools which can align the billions of output sequences to a reference genome {Metzker 2010; MacConaill 2013; Mori et al, 2013}.

Major caveats for the use of this technology are: cost, consumption of computational resources and time required for analysis {Yoshida et al, 2013}. Even though the cost has been steadily decreasing since its advent, it still remains expensive (as of January 2014 the cost per genome was $4,008) {Wetterstrand }. The analysis of massive amounts of data generated can be challenging from statistical and computational point of view. The main difficulty is in efficient separation of causative alterations from noise {Meyerson et al, 2010}. In general, germline whole exome sequencing generates about 20000 single nucleotide variants which need be filtered through application of algorithms followed by annotation of the remaining 'rare variants', the ones which are probably causative {Chang et al, 2013}. Even though there are different software available for data analysis, they have their limitations {Chang et al, 2013}. In addition, the biological relevance of the identified variants has to be assessed through their links to pathways and functional studies {Meyerson et al, 2010}.

Whole-genome sequencing

This provides full-range information about multiple genomic alterations such as, mutations, insertions and deletions (indels), copy number alterations and rearrangements {Mori et al, 2013}.

Exome sequencing

This targets the coding regions which are of interest and at lower cost. However, compared to whole-genome sequencing, the sensitivity is decreased and structural alterations cannot be detected {Yoshida et al, 2013}.

Transcriptome (RNA-seq)

This captures the expressed genome (transcriptome) of tumor samples and enables detection of fusion genes, the result of translocation between chromosomes {Palanisamy et al, 2010; Ma et al, 2014}; analysis of expression profiles and identification of novel transcripts {Concha et al, 2012} {Meyerson et al, 2010; MacConaill 2013}.

Epigenome (Methyl-seq)

This enables DNA methylation, post-translational modification of histone proteins and chromatin remodeling to be studied at a global level {Pinto et al, 2014}.

VI.2. NGS in cancer immunology

Whole-genome and exome sequencing are being applied to unravel different aspects of the tumor immunome which can facilitate design of effective cancer vaccines {Kroemer et al, 2012}. Some of the applications include:

- Identification of potential immunogenic mutations

Mutanome is a comprehensive map of somatic mutations in a tumor. Combination of whole-exome and transcriptome profiling facilitates the

discovery of ‘protein coding mutanome’. Analysis of the latter allows for identification of potential immunogenic mutations {Castle et al, 2012}.

- Identification of candidate tumor antigens

Epitope refers to the part of the antigen recognized by the immune system. NGS can be used to identify candidate tumor antigens through epitope mapping {Segal et al, 2008}. The tumor of each patient bears its own individual antigenic signature with 95% of it being unique and patient specific, indicating the need for individualized cancer vaccines.

All these approaches require that the tumor of each patient be sequenced which is still expensive at the present time, but could be feasible in near future {Segal et al, 2008}.

Relevance to present study

From the point of view of the identified immune phenotypes, it would be informative to perform exome and transcriptome sequencing of immune-high and immune-low melanomas matched for risk-category, copy number alterations and survival. This may lead to identification of certain genetic alterations characteristic of each sub-group, though not necessarily immune-related. They may be common mutations, mutations in genes implicated in the same pathway or mutations that may lead to similar downstream signaling changes. These approaches could contribute to a better understanding of their biology and to identification of novel therapeutic targets. Moreover, it will give an idea regarding the mutation load in the respective phenotypes.

In addition, analysis of the protein coding mutanome of immune-high tumors would help identify potential immunogenic mutations and candidate tumor antigens. Their comparison may indicate some common aspect. However, in view of the uniqueness of antigenic signatures of individual tumors {Segal et

al, 2008} this would be unlikely. Further validation of candidate mutations could lead to improved vaccine design.

VI.3. Exosomes

Exosomes are small, 30-100nm membrane vesicles shed from tissues under both normal and pathological states {Henderson et al, 2012; Sun et al, 2014}. They contain certain exosome specific proteins; as well as, mRNA, miRNA and proteins from the target cell. In short, their molecular content is fingerprint of the cell of origin. Cancer cell-derived exosomes act as oncogenic messengers transmitting information through mRNA, miRNA and protein They have the potential to be used for diagnostic, prognostic and therapeutic purposes in cancer {Sun et al, 2014}.

Relevance to present study

The objective of analyzing the exosomal profiles of immune phenotypes would be to identify a non-invasive prognostic biomarker.

This requires the exosomal profile of each sub-group to be established by analyzing the exosomes extracted from melanoma culture supernatant. Comparison of their mRNA, microRNA and protein profiles could identify exosomal signature characteristic of each sub-group. Following this, these signatures have to be assessed in peripheral blood exosomes of uveal melanoma patients in a prospective study. The exosomal levels have to be estimated pre- and post-therapy, the latter at intervals (every 3-6 months) and correlated with metastatic status at the end of the study period. The pattern of alteration of exosomal profiles may provide a clue as to clinical outcome and their utility as a prognostic biomarker.

VI.4. Characterization of pro-metastatic role of signature genes

Amongst the two phenotypes identified, the immune-high group of tumors metastasized earlier than their immune-low counterparts. For some of the over-expressed genes such as, *GBP1*, chemokine *CCL5*, MHC class II invariant chain, *CD74* there is evidence in other cancers for their role in mediating tumor invasion {Li et al, 2011; Yu et al, 2011; Johnson et al, 2012; Aldinucci et al, 2014; Kindt et al, 2014; Zhang et al, 2014}and in addition, they are druggable targets {Kaufman et al, 2013; Aldinucci et al, 2014}. Elucidating their role in uveal melanoma dissemination could facilitate a better understanding of the biology and help identify novel therapeutic targets.

Amongst them, *GBP1* would be an interesting candidate as it is an IFNG response gene, highly inducible by it. Though its function is largely unknown, recently, its role in cancer has been explored. Increased GBP1 serum levels, as well as its expression by tumor cells have been correlated with poor survival in oral cancer {Yu et al, 2011}. In addition, *in vitro* studies in oral cancer have demonstrated that *GBP1* overexpression increases motility and invasion by tumor cells {Yu et al, 2011}. Likewise, *GBP1* also facilitates invasion by glioblastoma {Li et al, 2011; Johnson et al, 2012}.

Relevance to present study

The genes most relevant to metastases-free survival can be selected from the list of over-expressed genes using *in silico* approaches. The effect of their over-expression and knock-down on tumor cell proliferation, motility and invasiveness can be performed using *in vitro* models. In addition, study of transcriptomic profiles of uveal melanoma cell lines over-expressing the gene/s of interest can help identify the downstream signaling pathways for further validation.

Conclusion

A comprehensive analysis of genetic and immune parameters, alongside clinical and pathological factors led to the delineation of three groups of uveal melanoma with risk of metastases ranging from high to low. In addition, inclusion of immune as a marker highlighted the relation between immune infiltrate and chromosomal alterations; with the latter modifying the immune associated clinical impact. Identification of the interferon-gamma induced gene signature and elucidation of associated pathways contribute towards a better understanding of uveal melanoma immune profile. Likewise, the work on gliomatosis cerebri emphasized the prognostic importance of *IDH* mutation testing in these tumors.

These findings could be the first step towards improved survival through application of risk-tailored adjuvant therapies and identification of novel therapeutic targets.

References

(2013). Selumetinib shows promise in metastatic uveal melanoma. Cancer Discov **3**(7): OF8.

Aalto Y, Eriksson L, Seregard S, *et al.* (2001). Concomitant loss of chromosome 3 and whole arm losses and gains of chromosome 1, 6, or 8 in metastasizing primary uveal melanoma. Invest Ophthalmol Vis Sci **42**(2): 313-317.

Abdel-Rahman MH, Cebulla CM, Verma V, *et al.* (2012). Monosomy 3 status of uveal melanoma metastases is associated with rapidly progressive tumors and short survival. Exp Eye Res **100**: 26-31.

Abdel-Rahman MH, Christopher BN, Faramawi MF, *et al.* (2011). Frequency, molecular pathology and potential clinical significance of partial chromosome 3 aberrations in uveal melanoma. Mod Pathol **24**(7): 954-962.

Abdel-Rahman MH, Pilarski R, Cebulla CM, *et al.* (2011). Germline BAP1 mutation predisposes to uveal melanoma, lung adenocarcinoma, meningioma, and other cancers. J Med Genet **48**(12): 856-859.

Abdel-Rahman MH, Pilarski R, Ezzat S, *et al.* (2010). Cancer family history characterization in an unselected cohort of 121 patients with uveal melanoma. Fam Cancer **9**(3): 431-438.

Abi-Hanna D, Wakefield D &Watkins S (1988). HLA antigens in ocular tissues. I. In vivo expression in human eyes. Transplantation **45**(3): 610-613.

Achberger S, Aldrich W, Tubbs R, *et al.* (2014). Circulating immune cell and microRNA in patients with uveal melanoma developing metastatic disease. Mol Immunol **58**(2): 182-186.

Adams SF, Levine DA, Cadungog MG, *et al.* (2009). Intraepithelial T cells and tumor proliferation: impact on the benefit from surgical cytoreduction in advanced serous ovarian cancer. Cancer **115**(13): 2891-2902.

Aghili M, Zahedi F &Rafiee E (2009). Hydroxyglutaric aciduria and malignant brain tumor: a case report and literature review. J Neurooncol **91**(2): 233-236.

Ahmadi R, Stockhammer F, Becker N, *et al.* (2012). No prognostic value of IDH1 mutations in a series of 100 WHO grade II astrocytomas. J Neurooncol **109**(1): 15-22.

Ajili F, Kourda N, Darouiche A, *et al.* (2013). Prognostic value of tumor-associated macrophages count in human non-muscle-invasive bladder cancer treated by BCG immunotherapy. Ultrastruct Pathol **37**(1): 56-61.

Akao Y, Nakagawa Y &Naoe T (2006). MicroRNAs 143 and 145 are possible common onco-microRNAs in human cancers. Oncol Rep **16**(4): 845-850.

Al-Attar A, Shehata M, Durrant L, *et al.* (2010). T cell density and location can influence the prognosis of ovarian cancer. Pathol Oncol Res **16**(3): 361-370.

Al-Shibli KI, Donnem T, Al-Saad S, *et al.* (2008). Prognostic effect of epithelial and stromal lymphocyte infiltration in non-small cell lung cancer. Clin Cancer Res **14**(16): 5220-5227.

Albert DM, Diener-West M, Robinson NL, *et al.* (1998). Histopathologic characteristics of uveal melanomas in eyes enucleated from the Collaborative Ocular Melanoma Study. COMS report no. 6. Am J Ophthalmol **125**(6): 745-766.

Aldinucci D &Colombatti A (2014). The inflammatory chemokine CCL5 and cancer progression. Mediators Inflamm **2014**: 292376.

Allavena P &Mantovani A (2012). Immunology in the clinic review series; focus on cancer: tumour-associated macrophages: undisputed stars of the inflammatory tumour microenvironment. Clin Exp Immunol **167**(2): 195-205.

Amary MF, Bacsi K, Maggiani F, *et al.* (2011). IDH1 and IDH2 mutations are frequent events in central chondrosarcoma and central and periosteal chondromas but not in other mesenchymal tumours. J Pathol **224**(3): 334-343.

An J, Wan H, Zhou X, *et al.* (2011). A comparative transcriptomic analysis of uveal melanoma and normal uveal melanocyte. PLoS One **6**(1): e16516.

Ananiev J, Gulubova MV &Manolova IM (2011). Prognostic significance of CD83 positive tumor-infiltrating dendritic cells and expression of TGF-beta 1 in human gastric cancer. Hepatogastroenterology **58**(110-111): 1834-1840.

Anastassiou G, Coupland SE, Stang A, *et al.* (2001). Expression of Fas and Fas ligand in uveal melanoma: biological implication and prognostic value. J Pathol **194**(4): 466-472.

Anastassiou G, Rebmann V, Wagner S, *et al.* (2003). Expression of classic and nonclassic HLA class I antigens in uveal melanoma. Invest Ophthalmol Vis Sci **44**(5): 2016-2019.

Anichini A, Mortarini R, Nonaka D, *et al.* (2006). Association of antigen-processing machinery and HLA antigen phenotype of melanoma cells with survival in American Joint Committee on Cancer stage III and IV melanoma patients. Cancer Res **66**(12): 6405-6411.

Aoude LG, Vajdic CM, Kricker A, *et al.* (2013). Prevalence of germline BAP1 mutation in a population-based sample of uveal melanoma cases. Pigment Cell Melanoma Res **26**(2): 278-279.

Ascierto ML, De Giorgi V, Liu Q, *et al.* (2011). An immunologic portrait of cancer. J Transl Med **9**: 146.

Ascierto ML, Idowu MO, Zhao Y, *et al.* (2013). Molecular signatures mostly associated with NK cells are predictive of relapse free survival in breast cancer patients. J Transl Med **11**(1): 145.

Ascierto ML, Kmieciak M, Idowu MO, *et al.* (2012). A signature of immune function genes associated with recurrence-free survival in breast cancer patients. Breast Cancer Res Treat **131**(3): 871-880.

Atkins D, Breuckmann A, Schmahl GE, *et al.* (2004). MHC class I antigen processing pathway defects, ras mutations and disease stage in colorectal carcinoma. Int J Cancer **109**(2): 265-273.

Atreya R &Neurath MF (2005). Involvement of IL-6 in the pathogenesis of inflammatory bowel disease and colon cancer. Clin Rev Allergy Immunol **28**(3): 187-196.

Avadanei ER, Wierzbicki PM, Giusca SE, *et al.* (2014). Macrophage profile in primary versus secondary liver tumors. Folia Histochem Cytobiol **52**(2): 112-123.

Ayari C, LaRue H, Hovington H, *et al.* (2013). High level of mature tumor-infiltrating dendritic cells predicts progression to muscle invasion in bladder cancer. Hum Pathol **44**(8): 1630-1637.

Ayari C, LaRue H, Hovington H, *et al.* (2009). Bladder tumor infiltrating mature dendritic cells and macrophages as predictors of response to bacillus Calmette-Guerin immunotherapy. Eur Urol **55**(6): 1386-1395.

Babchia N, Calipel A, Mouriaux F, *et al.* (2010). The PI3K/Akt and mTOR/P70S6K signaling pathways in human uveal melanoma cells: interaction with B-Raf/ERK. Invest Ophthalmol Vis Sci **51**(1): 421-429.

Bachmayr-Heyda A, Aust S, Heinze G, *et al.* (2013). Prognostic impact of tumor infiltrating CD8+ T cells in association with cell proliferation in ovarian cancer patients--a study of the OVCAD consortium. BMC Cancer **13**: 422.
Badoual C, Hans S, Rodriguez J, *et al.* (2006). Prognostic value of tumor-infiltrating CD4+ T-cell subpopulations in head and neck cancers. Clin Cancer Res **12**(2): 465-472.
Balermpas P, Michel Y, Wagenblast J, *et al.* (2014). Tumour-infiltrating lymphocytes predict response to definitive chemoradiotherapy in head and neck cancer. Br J Cancer **110**(2): 501-509.
Balkwill F (2009). Tumour necrosis factor and cancer. Nat Rev Cancer **9**(5): 361-371.
Barbieri G, Rimini E &Costa MA (2011). Effects of human leukocyte antigen (HLA)-DR engagement on melanoma cells. Int J Oncol **38**(6): 1589-1595.
Battaglia A (2014). The Importance of Multidisciplinary Approach in Early Detection of BAP1 Tumor Predisposition Syndrome: Clinical Management and Risk Assessment. Clin Med Insights Oncol **8**: 37-47.
Bauer J, Kilic E, Vaarwater J, *et al.* (2009). Oncogenic GNAQ mutations are not correlated with disease-free survival in uveal melanoma. Br J Cancer **101**(5): 813-815.
Baurain J-F &De Potter P (2013). Practice guidelines in the management of uveal melanoma Belgian Journal of medical oncology **7**: 20-26.
Becker C, Fantini MC, Schramm C, *et al.* (2004). TGF-beta suppresses tumor progression in colon cancer by inhibition of IL-6 trans-signaling. Immunity **21**(4): 491-501.
Bellmann C, Lumbroso-Le Rouic L, Levy C, *et al.* (2010). Uveal melanoma: management and outcome of patients with extraocular spread. Br J Ophthalmol **94**(5): 569-574.
Bello DM, Ariyan CE &Carvajal RD (2013). Melanoma mutagenesis and aberrant cell signaling. Cancer Control **20**(4): 261-281.
Benhar I, London A &Schwartz M (2012). The privileged immunity of immune privileged organs: the case of the eye. Front Immunol **3**: 296.
Bergeron MA, Champagne S, Gaudreault M, *et al.* (2012). Repression of genes involved in melanocyte differentiation in uveal melanoma. Mol Vis **18**: 1813-1822.
Bethwaite PB, Holloway LJ, Thornton A, *et al.* (1996). Infiltration by immunocompetent cells in early stage invasive carcinoma of the uterine cervix: a prognostic study. Pathology **28**(4): 321-327.
Beutel J, Wegner J, Wegner R, *et al.* (2009). Possible implications of MCAM expression in metastasis and non-metastatic of primary uveal melanoma patients. Curr Eye Res **34**(11): 1004-1009.
Bindea G, Galon J &Mlecnik B (2013). CluePedia Cytoscape plugin: pathway insights using integrated experimental and in silico data. Bioinformatics **29**(5): 661-663.
Bindea G, Mlecnik B, Fridman W-H, *et al.* (2010). Natural immunity to cancer in humans. Current Opinion in Immunology **22**(2): 215-222.
Bindea G, Mlecnik B, Tosolini M, *et al.* (2013). Spatiotemporal dynamics of intratumoral immune cells reveal the immune landscape in human cancer. Immunity **39**(4): 782-795.
Bishop KD &Olszewski AJ (2013). Epidemiology and survival outcomes of ocular and mucosal melanomas: A population-based analysis. Int J Cancer.
Biswas SK &Mantovani A (2012). Orchestration of metabolism by macrophages. Cell Metab **15**(4): 432-437.
Blasi MA, Roccella F, Balestrazzi E, *et al.* (1999). 3p13 region: a possible location of a tumor suppressor gene involved in uveal melanoma. Cancer Genet Cytogenet **108**(1): 81-83.

Blom DJ, Luyten GP, Mooy C, *et al.* (1997). Human leukocyte antigen class I expression. Marker of poor prognosis in uveal melanoma. Invest Ophthalmol Vis Sci **38**(9): 1865-1872.

Boel P, Wildmann C, Sensi ML, *et al.* (1995). BAGE: a new gene encoding an antigen recognized on human melanomas by cytolytic T lymphocytes. Immunity **2**(2): 167-175.

Bolouri H (2014). Network dynamics in the tumor microenvironment. Semin Cancer Biol.

Bonaldi L, Midena E, Filippi B, *et al.* (2008). FISH analysis of chromosomes 3 and 6 on fine needle aspiration biopsy samples identifies distinct subgroups of uveal melanomas. J Cancer Res Clin Oncol **134**(10): 1123-1127.

Borodovsky A, Salmasi V, Turcan S, *et al.* (2013). 5-azacytidine reduces methylation, promotes differentiation and induces tumor regression in a patient-derived IDH1 mutant glioma xenograft. Oncotarget **4**(10): 1737-1747.

Borthwick NJ, Thombs J, Polak M, *et al.* (2011). The biology of micrometastases from uveal melanoma. J Clin Pathol **64**(8): 666-671.

Brantley MA, Jr. &Harbour JW (2000). Deregulation of the Rb and p53 pathways in uveal melanoma. Am J Pathol **157**(6): 1795-1801.

Brantley MA, Jr. &Harbour JW (2000). Inactivation of retinoblastoma protein in uveal melanoma by phosphorylation of sites in the COOH-terminal region. Cancer Res **60**(16): 4320-4323.

Bromwich EJ, McArdle PA, Canna K, *et al.* (2003). The relationship between T-lymphocyte infiltration, stage, tumour grade and survival in patients undergoing curative surgery for renal cell cancer. Br J Cancer **89**(10): 1906-1908.

Bron L, Jandus C, Andrejevic-Blant S, *et al.* (2013). Prognostic value of arginase-II expression and regulatory T-cell infiltration in head and neck squamous cell carcinoma. Int J Cancer **132**(3): E85-93.

Bronkhorst IH, Jehs TM, Dijkgraaf EM, *et al.* (2014). Effect of hypoxic stress on migration and characteristics of monocytes in uveal melanoma. JAMA Ophthalmol **132**(5): 614-621.

Bronkhorst IH, Ly LV, Jordanova ES, *et al.* (2011). Detection of M2-macrophages in uveal melanoma and relation with survival. Invest Ophthalmol Vis Sci **52**(2): 643-650.

Bronkhorst IH, Vu TH, Jordanova ES, *et al.* (2012). Different subsets of tumor-infiltrating lymphocytes correlate with macrophage influx and monosomy 3 in uveal melanoma. Invest Ophthalmol Vis Sci.

Buccoliero AM, Castiglione F, Degl'Innocenti DR, *et al.* (2012). IDH1 mutation in pediatric gliomas: has it a diagnostic and prognostic value? Fetal Pediatr Pathol **31**(5): 278-282.

Budhu S, Wolchok J &Merghoub T (2014). The importance of animal models in tumor immunity and immunotherapy. Curr Opin Genet Dev **24**: 46-51.

Buecher B, Gauthier-Villars M, Desjardins L, *et al.* (2010). Contribution of CDKN2A/P16 (INK4A), P14 (ARF), CDK4 and BRCA1/2 germline mutations in individuals with suspected genetic predisposition to uveal melanoma. Fam Cancer **9**(4): 663-667.

Bukur J, Jasinski S &Seliger B (2012). The role of classical and non-classical HLA class I antigens in human tumors. Semin Cancer Biol **22**(4): 350-358.

Bulian P, Rossi D, Forconi F, *et al.* (2012). IGHV gene mutational status and 17p deletion are independent molecular predictors in a comprehensive clinical-biological

prognostic model for overall survival prediction in chronic lymphocytic leukemia. J Transl Med **10**: 18.

Burkholder B, Huang RY, Burgess R, *et al.* (2014). Tumor-induced perturbations of cytokines and immune cell networks. Biochim Biophys Acta **1845**(2): 182-201.

Burnet FM (1970). The concept of immunological surveillance. Prog Exp Tumor Res **13**: 1-27.

Burton AL, Roach BA, Mays MP, *et al.* (2011). Prognostic significance of tumor infiltrating lymphocytes in melanoma. Am Surg **77**(2): 188-192.

Cai XY, Gao Q, Qiu SJ, *et al.* (2006). Dendritic cell infiltration and prognosis of human hepatocellular carcinoma. J Cancer Res Clin Oncol **132**(5): 293-301.

Cairncross JG, Wang M, Jenkins RB, *et al.* (2014). Benefit from procarbazine, lomustine, and vincristine in oligodendroglial tumors is associated with mutation of IDH. J Clin Oncol **32**(8): 783-790.

Cairns RA, Harris IS &Mak TW (2011). Regulation of cancer cell metabolism. Nat Rev Cancer **11**(2): 85-95.

Cairns RA &Mak TW (2013). Oncogenic isocitrate dehydrogenase mutations: mechanisms, models, and clinical opportunities. Cancer Discov **3**(7): 730-741.

Calin GA &Croce CM (2006). MicroRNA signatures in human cancers. Nat Rev Cancer **6**(11): 857-866.

Calipel A, Abonnet V, Nicole O, *et al.* (2011). Status of RASSF1A in uveal melanocytes and melanoma cells. Mol Cancer Res **9**(9): 1187-1198.

Callahan MJ, Nagymanyoki Z, Bonome T, *et al.* (2008). Increased HLA-DMB expression in the tumor epithelium is associated with increased CTL infiltration and improved prognosis in advanced-stage serous ovarian cancer. Clin Cancer Res **14**(23): 7667-7673.

Callender G (1931). Malignant melanotic tumors of the eye. A study of histologic types in 111 cases. Trans. Am. Acad. Ophthalmol. Otolaryngol. **36**: 131-140.

Campregher C, Luciani MG &Gasche C (2008). Activated neutrophils induce an hMSH2-dependent G2/M checkpoint arrest and replication errors at a (CA)13-repeat in colon epithelial cells. Gut **57**(6): 780-787.

Canning CR &Hungerford J (1988). Familial uveal melanoma. Br J Ophthalmol **72**(4): 241-243.

Carbone M, Ferris LK, Baumann F, *et al.* (2012). BAP1 cancer syndrome: malignant mesothelioma, uveal and cutaneous melanoma, and MBAITs. J Transl Med **10**: 179.

Cariani E, Pilli M, Zerbini A, *et al.* (2012). Immunological and molecular correlates of disease recurrence after liver resection for hepatocellular carcinoma. PLoS One **7**(3): e32493.

Carretero R, Wang E, Rodriguez AI, *et al.* (2012). Regression of melanoma metastases after immunotherapy is associated with activation of antigen presentation and interferon-mediated rejection genes. Int J Cancer **131**(2): 387-395.

Carus A, Ladekarl M, Hager H, *et al.* (2013). Tumour-associated CD66b+ neutrophil count is an independent prognostic factor for recurrence in localised cervical cancer. Br J Cancer **108**(10): 2116-2122.

Carus A, Ladekarl M, Hager H, *et al.* (2013). Tumor-associated neutrophils and macrophages in non-small cell lung cancer: no immediate impact on patient outcome. Lung Cancer **81**(1): 130-137.

Cassoux N, Rodrigues MJ, Plancher C, *et al.* (2013). Genome-wide profiling is a clinically relevant and affordable prognostic test in posterior uveal melanoma. Br J Ophthalmol.

Castle JC, Kreiter S, Diekmann J, *et al.* (2012). Exploiting the mutanome for tumor vaccination. Cancer Res **72**(5): 1081-1091.

Chamuleau ME, Ossenkoppele GJ &van de Loosdrecht AA (2006). MHC class II molecules in tumour immunology: prognostic marker and target for immune modulation. Immunobiology **211**(6-8): 619-625.

Chang F &Li MM (2013). Clinical application of amplicon-based next-generation sequencing in cancer. Cancer Genet **206**(12): 413-419.

Chen HC, Kodell RL, Cheng KF, *et al.* (2012). Assessment of performance of survival prediction models for cancer prognosis. BMC Med Res Methodol **12**: 102.

Chen KJ, Zhou L, Xie HY, *et al.* (2012). Intratumoral regulatory T cells alone or in combination with cytotoxic T cells predict prognosis of hepatocellular carcinoma after resection. Med Oncol **29**(3): 1817-1826.

Chen L (2009). Ocular lymphatics: state-of-the-art review. Lymphology **42**(2): 66-76.

Chen LJ, Sun J, Wu HY, *et al.* (2011). B7-H4 expression associates with cancer progression and predicts patient's survival in human esophageal squamous cell carcinoma. Cancer Immunol Immunother **60**(7): 1047-1055.

Chen LS, Balakrishnan K &Gandhi V (2010). Inflammation and survival pathways: chronic lymphocytic leukemia as a model system. Biochem Pharmacol **80**(12): 1936-1945.

Chen PW, Mellon JK, Mayhew E, *et al.* (2007). Uveal melanoma expression of indoleamine 2,3-deoxygenase: establishment of an immune privileged environment by tryptophan depletion. Exp Eye Res **85**(5): 617-625.

Chen S, Tanaka S, Giannini C, *et al.* (2013). Gliomatosis cerebri: clinical characteristics, management, and outcomes. J Neurooncol **112**(2): 267-275.

Chen W, Peace DJ, Rovira DK, *et al.* (1992). T-cell immunity to the joining region of p210BCR-ABL protein. Proc Natl Acad Sci U S A **89**(4): 1468-1472.

Chen X, He D, Dong XD, *et al.* (2013). MicroRNA-124a is epigenetically regulated and acts as a tumor suppressor by controlling multiple targets in uveal melanoma. Invest Ophthalmol Vis Sci **54**(3): 2248-2256.

Chen X, Wu Q, Tan L, *et al.* (2013). Combined PKC and MEK inhibition in uveal melanoma with GNAQ and GNA11 mutations. Oncogene.

Cheng YS, Colonno RJ &Yin FH (1983). Interferon induction of fibroblast proteins with guanylate binding activity. J Biol Chem **258**(12): 7746-7750.

Chew A, Salama P, Robbshaw A, *et al.* (2011). SPARC, FOXP3, CD8 and CD45 correlation with disease recurrence and long-term disease-free survival in colorectal cancer. PLoS One **6**(7): e22047.

Chew V, Chen J, Lee D, *et al.* (2012). Chemokine-driven lymphocyte infiltration: an early intratumoural event determining long-term survival in resectable hepatocellular carcinoma. Gut **61**(3): 427-438.

Chiaravalli AM, Feltri M, Bertolini V, *et al.* (2006). Intratumour T cells, their activation status and survival in gastric carcinomas characterised for microsatellite instability and Epstein-Barr virus infection. Virchows Arch **448**(3): 344-353.

Chiba T, Ohtani H, Mizoi T, *et al.* (2004). Intraepithelial CD8+ T-cell-count becomes a prognostic factor after a longer follow-up period in human colorectal carcinoma: possible association with suppression of micrometastasis. Br J Cancer **91**(9): 1711-1717.

Cho WCS (2010). An Omics Perspective on Cancer Research, Springer.
Cho Y, Miyamoto M, Kato K, *et al.* (2003). CD4+ and CD8+ T cells cooperate to improve prognosis of patients with esophageal squamous cell carcinoma. Cancer Res **63**(7): 1555-1559.
Choi C, Ganji SK, DeBerardinis RJ, *et al.* (2012). 2-hydroxyglutarate detection by magnetic resonance spectroscopy in IDH-mutated patients with gliomas. Nat Med **18**(4): 624-629.
Chowdhury R, Yeoh KK, Tian YM, *et al.* (2011). The oncometabolite 2-hydroxyglutarate inhibits histone lysine demethylases. EMBO Rep **12**(5): 463-469.
Chuang JY, Yang WH, Chen HT, *et al.* (2009). CCL5/CCR5 axis promotes the motility of human oral cancer cells. J Cell Physiol **220**(2): 418-426.
Cimino-Mathews A, Ye X, Meeker A, *et al.* (2013). Metastatic triple-negative breast cancers at first relapse have fewer tumor-infiltrating lymphocytes than their matched primary breast tumors: a pilot study. Hum Pathol **44**(10): 2055-2063.
Cipponi A, Mercier M, Seremet T, *et al.* (2012). Neogenesis of lymphoid structures and antibody responses occur in human melanoma metastases. Cancer Res **72**(16): 3997-4007.
Clarke B, Tinker AV, Lee CH, *et al.* (2009). Intraepithelial T cells and prognosis in ovarian carcinoma: novel associations with stage, tumor type, and BRCA1 loss. Mod Pathol **22**(3): 393-402.
Coleman K, Baak JP, van Diest PJ, *et al.* (1995). DNA ploidy status in 84 ocular melanomas: a study of DNA quantitation in ocular melanomas by flow cytometry and automatic and interactive static image analysis. Hum Pathol **26**(1): 99-105.
Colotta F, Allavena P, Sica A, *et al.* (2009). Cancer-related inflammation, the seventh hallmark of cancer: links to genetic instability. Carcinogenesis **30**(7): 1073-1081.
Concha M, Wang X, Cao S, *et al.* (2012). Identification of new viral genes and transcript isoforms during Epstein-Barr virus reactivation using RNA-Seq. J Virol **86**(3): 1458-1467.
Costa NL, Valadares MC, Souza PP, *et al.* (2013). Tumor-associated macrophages and the profile of inflammatory cytokines in oral squamous cell carcinoma. Oral Oncol **49**(3): 216-223.
Coulie PG, Van den Eynde BJ, van der Bruggen P, *et al.* (2014). Tumour antigens recognized by T lymphocytes: at the core of cancer immunotherapy. Nat Rev Cancer **14**(2): 135-146.
Coupland SE, Anastassiou G, Stang A, *et al.* (2000). The prognostic value of cyclin D1, p53, and MDM2 protein expression in uveal melanoma. J Pathol **191**(2): 120-126.
Coupland SE, Campbell I &Damato B (2008). Routes of extraocular extension of uveal melanoma: risk factors and influence on survival probability. Ophthalmology **115**(10): 1778-1785.
Coussens LM &Werb Z (2002). Inflammation and cancer. Nature **420**(6917): 860-867.
Cunha LL, Morari EC, Guihen AC, *et al.* (2012). Infiltration of a mixture of immune cells may be related to good prognosis in patients with differentiated thyroid carcinoma. Clin Endocrinol (Oxf) **77**(6): 918-925.
Curiel TJ, Coukos G, Zou L, *et al.* (2004). Specific recruitment of regulatory T cells in ovarian carcinoma fosters immune privilege and predicts reduced survival. Nat Med **10**(9): 942-949.
Curtin JA, Busam K, Pinkel D, *et al.* (2006). Somatic activation of KIT in distinct subtypes of melanoma. J Clin Oncol **24**(26): 4340-4346.

Curtin JA, Fridlyand J, Kageshita T, *et al.* (2005). Distinct sets of genetic alterations in melanoma. N Engl J Med **353**(20): 2135-2147.
Curtis C, Shah SP, Chin SF, *et al.* (2012). The genomic and transcriptomic architecture of 2,000 breast tumours reveals novel subgroups. Nature **486**(7403): 346-352.
D'Urso OF, D'Urso PI, Marsigliante S, *et al.* (2009). Correlative analysis of gene expression profile and prognosis in patients with gliomatosis cerebri. Cancer **115**(16): 3749-3757.
Dahlin AM, Henriksson ML, Van Guelpen B, *et al.* (2011). Colorectal cancer prognosis depends on T-cell infiltration and molecular characteristics of the tumor. Mod Pathol **24**(5): 671-682.
Dai F, Liu L, Che G, *et al.* (2010). The number and microlocalization of tumor-associated immune cells are associated with patient's survival time in non-small cell lung cancer. BMC Cancer **10**: 220.
Damato B (2010). Does ocular treatment of uveal melanoma influence survival? Br J Cancer **103**(3): 285-290.
Damato B, Dopierala JA &Coupland SE (2010). Genotypic profiling of 452 choroidal melanomas with multiplex ligation-dependent probe amplification. Clin Cancer Res **16**(24): 6083-6092.
Dang L, White DW, Gross S, *et al.* (2009). Cancer-associated IDH1 mutations produce 2-hydroxyglutarate. Nature **462**(7274): 739-744.
Davies H, Bignell GR, Cox C, *et al.* (2002). Mutations of the BRAF gene in human cancer. Nature **417**(6892): 949-954.
de Jong AE, van Puijenbroek M, Hendriks Y, *et al.* (2004). Microsatellite instability, immunohistochemistry, and additional PMS2 staining in suspected hereditary nonpolyposis colorectal cancer. Clin Cancer Res **10**(3): 972-980.
de Jong RA, Kema IP, Boerma A, *et al.* (2012). Prognostic role of indoleamine 2,3-dioxygenase in endometrial carcinoma. Gynecol Oncol **126**(3): 474-480.
de Jong RA, Leffers N, Boezen HM, *et al.* (2009). Presence of tumor-infiltrating lymphocytes is an independent prognostic factor in type I and II endometrial cancer. Gynecol Oncol **114**(1): 105-110.
de la Cruz PO, Jr., Specht CS &McLean IW (1990). Lymphocytic infiltration in uveal malignant melanoma. Cancer **65**(1): 112-115.
De Sousa EMF, Vermeulen L, Fessler E, *et al.* (2013). Cancer heterogeneity--a multifaceted view. EMBO Rep **14**(8): 686-695.
de Vos van Steenwijk PJ, Ramwadhdoebe TH, Goedemans R, *et al.* (2013). Tumor-infiltrating CD14-positive myeloid cells and CD8-positive T-cells prolong survival in patients with cervical carcinoma. Int J Cancer **133**(12): 2884-2894.
Deau B, Bachy E, Ribrag V, *et al.* (2013). Macrophage, mast cell and T lymphocyte infiltrations are independent predictive biomarkers of primary refractoriness or early relapse in classical Hodgkin lymphoma. Leuk Lymphoma **54**(1): 41-45.
Decaestecker C, Lopez XM, D'Haene N, *et al.* (2009). Requirements for the valid quantification of immunostains on tissue microarray materials using image analysis. Proteomics **9**(19): 4478-4494.
Demir L, Yigit S, Ellidokuz H, *et al.* (2013). Predictive and prognostic factors in locally advanced breast cancer: effect of intratumoral FOXP3+ Tregs. Clin Exp Metastasis **30**(8): 1047-1062.

DeNardo DG, Brennan DJ, Rexhepaj E, *et al.* (2011). Leukocyte complexity predicts breast cancer survival and functionally regulates response to chemotherapy. Cancer Discov **1**(1): 54-67.

Dennis G, Jr., Sherman BT, Hosack DA, *et al.* (2003). DAVID: Database for Annotation, Visualization, and Integrated Discovery. Genome Biol **4**(5): P3.

Deschoolmeester V, Baay M, Van Marck E, *et al.* (2010). Tumor infiltrating lymphocytes: an intriguing player in the survival of colorectal cancer patients. BMC Immunol **11**: 19.

Desclee P, Rommel D, Hernalsteen D, *et al.* (2010). Gliomatosis cerebri, imaging findings of 12 cases. J Neuroradiol **37**(3): 148-158.

Desestret V, Ciccarino P, Ducray F, *et al.* (2011). Prognostic stratification of gliomatosis cerebri by IDH1 R132H and INA expression. J Neurooncol **105**(2): 219-224.

Di Tomaso T, Mazzoleni S, Wang E, *et al.* (2010). Immunobiological characterization of cancer stem cells isolated from glioblastoma patients. Clin Cancer Res **16**(3): 800-813.

Diaz-Montero CM, Finke J &Montero AJ (2014). Myeloid-derived suppressor cells in cancer: therapeutic, predictive, and prognostic implications. Semin Oncol **41**(2): 174-184.

Diener-West M, Hawkins BS, Markowitz JA, *et al.* (1992). A review of mortality from choroidal melanoma. II. A meta-analysis of 5-year mortality rates following enucleation, 1966 through 1988. Arch Ophthalmol **110**(2): 245-250.

Diener-West M, Reynolds SM, Agugliaro DJ, *et al.* (2005). Development of metastatic disease after enrollment in the COMS trials for treatment of choroidal melanoma: Collaborative Ocular Melanoma Study Group Report No. 26. Arch Ophthalmol **123**(12): 1639-1643.

Dieu-Nosjean MC, Antoine M, Danel C, *et al.* (2008). Long-Term Survival for Patients With Non-Small-Cell Lung Cancer With Intratumoral Lymphoid Structures. Journal of Clinical Oncology **26**(27): 4410-4417.

Dillhoff M, Liu J, Frankel W, *et al.* (2008). MicroRNA-21 is overexpressed in pancreatic cancer and a potential predictor of survival. J Gastrointest Surg **12**(12): 2171-2176.

Ding T, Xu J, Wang F, *et al.* (2009). High tumor-infiltrating macrophage density predicts poor prognosis in patients with primary hepatocellular carcinoma after resection. Hum Pathol **40**(3): 381-389.

Distel LV, Fickenscher R, Dietel K, *et al.* (2009). Tumour infiltrating lymphocytes in squamous cell carcinoma of the oro- and hypopharynx: prognostic impact may depend on type of treatment and stage of disease. Oral Oncol **45**(10): e167-174.

Dobner BC, Riechardt AI, Joussen AM, *et al.* (2012). Expression of haematogenous and lymphogenous chemokine receptors and their ligands on uveal melanoma in association with liver metastasis. Acta Ophthalmol **90**(8): e638-644.

Dogan Y, Erdogan G, Pestereli HE, *et al.* (2009). Effect of intratumoral lymphocyte density on the disease-free survival and overall survival in malignant epithelial tumors of the ovary. Eur J Gynaecol Oncol **30**(5): 523-526.

Dong F &Lou D (2012). MicroRNA-34b/c suppresses uveal melanoma cell proliferation and migration through multiple targets. Mol Vis **18**: 537-546.

Dong J, Li J, Liu SM, *et al.* (2013). CD33(+)/p-STAT1(+) double-positive cell as a prognostic factor for stage IIIa gastric cancer. Med Oncol **30**(1): 442.

Donnem T, Al-Shibli K, Andersen S, *et al.* (2010). Combination of low vascular endothelial growth factor A (VEGF-A)/VEGF receptor 2 expression and high lymphocyte infiltration is a strong and independent favorable prognostic factor in patients with nonsmall cell lung cancer. Cancer **116**(18): 4318-4325.

Dono M, Angelini G, Cecconi M, *et al.* (2014). Mutation frequencies of GNAQ, GNA11, BAP1, SF3B1, EIF1AX and TERT in uveal melanoma: detection of an activating mutation in the TERT gene promoter in a single case of uveal melanoma. Br J Cancer **110**(4): 1058-1065.

Donson AM, Birks DK, Schittone SA, *et al.* (2012). Increased immune gene expression and immune cell infiltration in high-grade astrocytoma distinguish long-term from short-term survivors. J Immunol **189**(4): 1920-1927.

Dratviman-Storobinsky O, Cohen Y, Frenkel S, *et al.* (2010). Lack of oncogenic GNAQ mutations in melanocytic lesions of the conjunctiva as compared to uveal melanoma. Invest Ophthalmol Vis Sci **51**(12): 6180-6182.

Du L, Xiao X, Wang C, *et al.* (2011). Human leukocyte antigen-G is closely associated with tumor immune escape in gastric cancer by increasing local regulatory T cells. Cancer Sci **102**(7): 1272-1280.

Duan F, Lin M, Li C, *et al.* (2014). Effects of inhibition of hedgehog signaling on cell growth and migration of uveal melanoma cells. Cancer Biol Ther **15**(5): 544-559.

Dudley ME, Yang JC, Sherry R, *et al.* (2008). Adoptive cell therapy for patients with metastatic melanoma: evaluation of intensive myeloablative chemoradiation preparative regimens. J Clin Oncol **26**(32): 5233-5239.

Dunn GP, Koebel CM &Schreiber RD (2006). Interferons, immunity and cancer immunoediting. Nat Rev Immunol **6**(11): 836-848.

Dunn GP, Old LJ &Schreiber RD (2004). The immunobiology of cancer immunosurveillance and immunoediting. Immunity **21**(2): 137-148.

Durie FH, Campbell AM, Lee WR, *et al.* (1990). Analysis of lymphocytic infiltration in uveal melanoma. Invest Ophthalmol Vis Sci **31**(10): 2106-2110.

Dutta S, Going JJ, Crumley AB, *et al.* (2012). The relationship between tumour necrosis, tumour proliferation, local and systemic inflammation, microvessel density and survival in patients undergoing potentially curative resection of oesophageal adenocarcinoma. Br J Cancer **106**(4): 702-710.

Edin S, Wikberg ML, Dahlin AM, *et al.* (2012). The distribution of macrophages with a M1 or M2 phenotype in relation to prognosis and the molecular characteristics of colorectal cancer. PLoS One **7**(10): e47045.

Edmunds SC, Kelsell DP, Hungerford JL, *et al.* (2002). Mutational analysis of selected genes in the TGFbeta, Wnt, pRb, and p53 pathways in primary uveal melanoma. Invest Ophthalmol Vis Sci **43**(9): 2845-2851.

Ehlers JP &Harbour JW (2005). NBS1 expression as a prognostic marker in uveal melanoma. Clin Cancer Res **11**(5): 1849-1853.

Ehlers JP, Worley L, Onken MD, *et al.* (2005). DDEF1 is located in an amplified region of chromosome 8q and is overexpressed in uveal melanoma. Clin Cancer Res **11**(10): 3609-3613.

Ehlers JP, Worley L, Onken MD, *et al.* (2008). Integrative genomic analysis of aneuploidy in uveal melanoma. Clin Cancer Res **14**(1): 115-122.

Eiro N, Pidal I, Fernandez-Garcia B, *et al.* (2012). Impact of CD68/(CD3+CD20) ratio at the invasive front of primary tumors on distant metastasis development in breast cancer. PLoS One **7**(12): e52796.

Eletr ZM &Wilkinson KD (2011). An emerging model for BAP1's role in regulating cell cycle progression. Cell Biochem Biophys **60**(1-2): 3-11.

Enomoto K, Sho M, Wakatsuki K, *et al.* (2012). Prognostic importance of tumour-infiltrating memory T cells in oesophageal squamous cell carcinoma. Clin Exp Immunol **168**(2): 186-191.

Ericsson C, Seregard S, Bartolazzi A, *et al.* (2001). Association of HLA class I and class II antigen expression and mortality in uveal melanoma. Invest Ophthalmol Vis Sci **42**(10): 2153-2156.

Errington JA, Conway RM, Walsh-Conway N, *et al.* (2012). Expression of cancer-testis antigens (MAGE-A1, MAGE-A3/6, MAGE-A4, MAGE-C1 and NY-ESO-1) in primary human uveal and conjunctival melanoma. Br J Ophthalmol **96**(3): 451-458.

Esser P, Grisanti S &Bartz-Schmidt K (2001). TGF-beta in uveal melanoma. Microsc Res Tech **52**(4): 396-400.

Esteller M (2007). Cancer epigenomics: DNA methylomes and histone-modification maps. Nat Rev Genet **8**(4): 286-298.

Ewens KG, Kanetsky PA, Richards-Yutz J, *et al.* (2013). Genomic profile of 320 uveal melanoma cases: chromosome 8p-loss and metastatic outcome. Invest Ophthalmol Vis Sci **54**(8): 5721-5729.

Eyles J, Puaux AL, Wang X, *et al.* (2010). Tumor cells disseminate early, but immunosurveillance limits metastatic outgrowth, in a mouse model of melanoma. J Clin Invest **120**(6): 2030-2039.

Facciabene A, Peng X, Hagemann IS, *et al.* (2011). Tumour hypoxia promotes tolerance and angiogenesis via CCL28 and T(reg) cells. Nature **475**(7355): 226-230.

Fan QM, Jing YY, Yu GF, *et al.* (2014). Tumor-associated macrophages promote cancer stem cell-like properties via transforming growth factor-beta1-induced epithelial-mesenchymal transition in hepatocellular carcinoma. Cancer Lett.

Farazi TA, Hoell JI, Morozov P, *et al.* (2013). MicroRNAs in human cancer. Adv Exp Med Biol **774**: 1-20.

Ferrarelli LK (2014). Focus issue: refining the war on cancer. Sci Signal **7**(318): eg2.

Field MG &Harbour JW (2014). Recent developments in prognostic and predictive testing in uveal melanoma. Curr Opin Ophthalmol **25**(3): 234-239.

Fisk B, Blevins TL, Wharton JT, *et al.* (1995). Identification of an immunodominant peptide of HER-2/neu protooncogene recognized by ovarian tumor-specific cytotoxic T lymphocyte lines. J Exp Med **181**(6): 2109-2117.

Flammiger A, Bayer F, Cirugeda-Kuhnert A, *et al.* (2012). Intratumoral T but not B lymphocytes are related to clinical outcome in prostate cancer. APMIS **120**(11): 901-908.

Flammiger A, Weisbach L, Huland H, *et al.* (2013). High tissue density of FOXP3+ T cells is associated with clinical outcome in prostate cancer. Eur J Cancer **49**(6): 1273-1279.

Folberg R, Pe'er J, Gruman LM, *et al.* (1992). The morphologic characteristics of tumor blood vessels as a marker of tumor progression in primary human uveal melanoma: a matched case-control study. Hum Pathol **23**(11): 1298-1305.

Folberg R, Rummelt V, Parys-Van Ginderdeuren R, *et al.* (1993). The prognostic value of tumor blood vessel morphology in primary uveal melanoma. Ophthalmology **100**(9): 1389-1398.

Font R, Croxatto J &Rao N (2006). Tumors of the eye and ocular adnexa. Washington DC, American Registry of Pathology.
Francisco LM, Sage PT &Sharpe AH (2010). The PD-1 pathway in tolerance and autoimmunity. Immunol Rev **236**: 219-242.
Franco R, Botti G, Mascolo M, *et al.* (2010). "CXCR4-CXCL12 and VEGF correlate to uveal melanoma progression". Front Biosci (Elite Ed) **2**: 13-21.
Franco R, Cantile M, Scala S, *et al.* (2010). Histomorphologic parameters and CXCR4 mRNA and protein expression in sentinel node melanoma metastasis are correlated to clinical outcome. Cancer Biol Ther **9**(6): 423-429.
Freund M, Hahnel S, Sommer C, *et al.* (2001). CT and MRI findings in gliomatosis cerebri: a neuroradiologic and neuropathologic review of diffuse infiltrating brain neoplasms. Eur Radiol **11**(2): 309-316.
Fridman WH, Pagès F, Sautès-Fridman C, *et al.* (2012). The immune contexture in human tumours: impact on clinical outcome. Nature Reviews Cancer **12**(4): 298-306.
Fu J, Xu D, Liu Z, *et al.* (2007). Increased regulatory T cells correlate with CD8 T-cell impairment and poor survival in hepatocellular carcinoma patients. Gastroenterology **132**(7): 2328-2339.
Fu J, Zhang Z, Zhou L, *et al.* (2013). Impairment of CD4+ cytotoxic T cells predicts poor survival and high recurrence rates in patients with hepatocellular carcinoma. Hepatology **58**(1): 139-149.
Fujii N, Shomori K, Shiomi T, *et al.* (2012). Cancer-associated fibroblasts and CD163-positive macrophages in oral squamous cell carcinoma: their clinicopathological and prognostic significance. J Oral Pathol Med **41**(6): 444-451.
Fukunaga A, Miyamoto M, Cho Y, *et al.* (2004). CD8+ tumor-infiltrating lymphocytes together with CD4+ tumor-infiltrating lymphocytes and dendritic cells improve the prognosis of patients with pancreatic adenocarcinoma. Pancreas **28**(1): e26-31.
Furney SJ, Pedersen M, Gentien D, *et al.* (2013). SF3B1 mutations are associated with alternative splicing in uveal melanoma. Cancer Discov **3**(10): 1122-1129.
Gajewski TF (2012). Cancer immunotherapy. Mol Oncol **6**(2): 242-250.
Gallagher RP, Elwood JM, Rootman J, *et al.* (1985). Risk factors for ocular melanoma: Western Canada Melanoma Study. J Natl Cancer Inst **74**(4): 775-778.
Galon J, Angell HK, Bedognetti D, *et al.* (2013). The continuum of cancer immunosurveillance: prognostic, predictive, and mechanistic signatures. Immunity **39**(1): 11-26.
Gangemi R, Mirisola V, Barisione G, *et al.* (2012). Mda-9/syntenin is expressed in uveal melanoma and correlates with metastatic progression. PLoS One **7**(1): e29989.
Gao Q, Qiu SJ, Fan J, *et al.* (2007). Intratumoral balance of regulatory and cytotoxic T cells is associated with prognosis of hepatocellular carcinoma after resection. J Clin Oncol **25**(18): 2586-2593.
Gao Q, Wang XY, Qiu SJ, *et al.* (2009). Overexpression of PD-L1 significantly associates with tumor aggressiveness and postoperative recurrence in human hepatocellular carcinoma. Clin Cancer Res **15**(3): 971-979.
Gao Q, Zhou J, Wang XY, *et al.* (2012). Infiltrating memory/senescent T cell ratio predicts extrahepatic metastasis of hepatocellular carcinoma. Ann Surg Oncol **19**(2): 455-466.
Garraway LA &Lander ES (2013). Lessons from the cancer genome. Cell **153**(1): 17-37.

Germain C, Gnjatic S, Tamzalit F, *et al.* (2014). Presence of B cells in tertiary lymphoid structures is associated with a protective immunity in patients with lung cancer. Am J Respir Crit Care Med **189**(7): 832-844.

Giatromanolaki A, Bates GJ, Koukourakis MI, *et al.* (2008). The presence of tumor-infiltrating FOXP3+ lymphocytes correlates with intratumoral angiogenesis in endometrial cancer. Gynecol Oncol **110**(2): 216-221.

Glas M, Bahr O, Felsberg J, *et al.* (2011). NOA-05 phase 2 trial of procarbazine and lomustine therapy in gliomatosis cerebri. Ann Neurol **70**(3): 445-453.

Glondu M, Liaudet-Coopman E, Derocq D, *et al.* (2002). Down-regulation of cathepsin-D expression by antisense gene transfer inhibits tumor growth and experimental lung metastasis of human breast cancer cells. Oncogene **21**(33): 5127-5134.

Goc J, Germain C, Vo-Bourgais TK, *et al.* (2014). Dendritic cells in tumor-associated tertiary lymphoid structures signal a Th1 cytotoxic immune contexture and license the positive prognostic value of infiltrating CD8+ T cells. Cancer Res **74**(3): 705-715.

Goeppert B, Frauenschuh L, Zucknick M, *et al.* (2013). Prognostic impact of tumour-infiltrating immune cells on biliary tract cancer. Br J Cancer **109**(10): 2665-2674.

Goldstein AM, Chan M, Harland M, *et al.* (2006). High-risk melanoma susceptibility genes and pancreatic cancer, neural system tumors, and uveal melanoma across GenoMEL. Cancer Res **66**(20): 9818-9828.

Gonzalez-Martin A, Gomez L, Lustgarten J, *et al.* (2011). Maximal T cell-mediated antitumor responses rely upon CCR5 expression in both CD4(+) and CD8(+) T cells. Cancer Res **71**(16): 5455-5466.

Goslings WR, Blom DJ, de Waard-Siebinga I, *et al.* (1996). Membrane-bound regulators of complement activation in uveal melanomas. CD46, CD55, and CD59 in uveal melanomas. Invest Ophthalmol Vis Sci **37**(9): 1884-1891.

Griewank KG, Murali R, Schilling B, *et al.* (2013). TERT promoter mutations in ocular melanoma distinguish between conjunctival and uveal tumours. Br J Cancer **109**(2): 497-501.

Griewank KG, van de Nes J, Schilling B, *et al.* (2014). Genetic and clinico-pathologic analysis of metastatic uveal melanoma. Mod Pathol **27**(2): 175-183.

Griewank KG, Westekemper H, Murali R, *et al.* (2013). Conjunctival melanomas harbor BRAF and NRAS mutations and copy number changes similar to cutaneous and mucosal melanomas. Clin Cancer Res **19**(12): 3143-3152.

Griffith TS, Brunner T, Fletcher SM, *et al.* (1995). Fas ligand-induced apoptosis as a mechanism of immune privilege. Science **270**(5239): 1189-1192.

Grivennikov SI, Greten FR &Karin M (2010). Immunity, inflammation, and cancer. Cell **140**(6): 883-899.

Grosso F, Jones RL, Demetri GD, *et al.* (2007). Efficacy of trabectedin (ecteinascidin-743) in advanced pretreated myxoid liposarcomas: a retrospective study. Lancet Oncol **8**(7): 595-602.

Grotz TE, Vaince F &Hieken TJ (2013). Tumor-infiltrating lymphocyte response in cutaneous melanoma in the elderly predicts clinical outcomes. Melanoma Res **23**(2): 132-137.

Gu-Trantien C, Loi S, Garaud S, *et al.* (2013). CD4(+) follicular helper T cell infiltration predicts breast cancer survival. J Clin Invest **123**(7): 2873-2892.

Guidoboni M, Gafa R, Viel A, *et al.* (2001). Microsatellite instability and high content of activated cytotoxic lymphocytes identify colon cancer patients with a favorable prognosis. Am J Pathol **159**(1): 297-304.
Gulubova MV, Ananiev JR, Vlaykova TI, *et al.* (2012). Role of dendritic cells in progression and clinical outcome of colon cancer. Int J Colorectal Dis **27**(2): 159-169.
Halama N, Spille A, Lerchl T, *et al.* (2013). Hepatic metastases of colorectal cancer are rather homogeneous but differ from primary lesions in terms of immune cell infiltration. Oncoimmunology **2**(4): e24116.
Hallermalm K, Seki K, De Geer A, *et al.* (2008). Modulation of the tumor cell phenotype by IFN-gamma results in resistance of uveal melanoma cells to granule-mediated lysis by cytotoxic lymphocytes. J Immunol **180**(6): 3766-3774.
Hamanishi J, Mandai M, Iwasaki M, *et al.* (2007). Programmed cell death 1 ligand 1 and tumor-infiltrating CD8+ T lymphocytes are prognostic factors of human ovarian cancer. Proc Natl Acad Sci U S A **104**(9): 3360-3365.
Hammer H, Olah J &Toth-Molnar E (1996). Dysplastic nevi are a risk factor for uveal melanoma. Eur J Ophthalmol **6**(4): 472-474.
Han LY, Fletcher MS, Urbauer DL, *et al.* (2008). HLA class I antigen processing machinery component expression and intratumoral T-Cell infiltrate as independent prognostic markers in ovarian carcinoma. Clin Cancer Res **14**(11): 3372-3379.
Hanada T, Nakagawa M, Emoto A, *et al.* (2000). Prognostic value of tumor-associated macrophage count in human bladder cancer. Int J Urol **7**(7): 263-269.
Hanahan D &Coussens LM (2012). Accessories to the crime: functions of cells recruited to the tumor microenvironment. Cancer Cell **21**(3): 309-322.
Hanahan D &Weinberg RA (2000). The hallmarks of cancer. Cell **100**(1): 57-70.
Hanahan D &Weinberg Robert A (2011). Hallmarks of Cancer: The Next Generation. Cell **144**(5): 646-674.
Hanaoka E, Ozaki T, Nakamura Y, *et al.* (2000). Overexpression of DAN causes a growth suppression in p53-deficient SAOS-2 cells. Biochem Biophys Res Commun **278**(1): 20-26.
Harbeck N, Sotlar K, Wuerstlein R, *et al.* (2014). Molecular and protein markers for clinical decision making in breast cancer: today and tomorrow. Cancer Treat Rev **40**(3): 434-444.
Harbour JW (2012). The genetics of uveal melanoma: an emerging framework for targeted therapy. Pigment Cell Melanoma Res **25**(2): 171-181.
Harbour JW &Chao DL (2014). A Molecular Revolution in Uveal Melanoma: Implications for Patient Care and Targeted Therapy. Ophthalmology.
Harbour JW &Chen R (2013). The DecisionDx-UM Gene Expression Profile Test Provides Risk Stratification and Individualized Patient Care in Uveal Melanoma. PLoS Curr **5**.
Harbour JW, Onken MD, Roberson ED, *et al.* (2010). Frequent mutation of BAP1 in metastasizing uveal melanomas. Science **330**(6009): 1410-1413.
Harbour JW, Roberson ED, Anbunathan H, *et al.* (2013). Recurrent mutations at codon 625 of the splicing factor SF3B1 in uveal melanoma. Nat Genet **45**(2): 133-135.
Harbour JW, Wilson D, Finger PT, *et al.* (2013). Gene expressing profiling of iris melanomas. Ophthalmology **120**(1): 213, 213 e211-213.
Harrell FE (2001). Regression modeling strategies : with applications to linear models, logistic regression, and survival analysis. New York, Springer.

Hasita H, Komohara Y, Okabe H, *et al.* (2010). Significance of alternatively activated macrophages in patients with intrahepatic cholangiocarcinoma. Cancer Sci **101**(8): 1913-1919.

Hasmim M, Badoual C, Vielh P, *et al.* (2013). Expression of EPHRIN-A1, SCINDERIN and MHC class I molecules in head and neck cancers and relationship with the prognostic value of intratumoral CD8+ T cells. BMC Cancer **13**: 592.

Hausler T, Stang A, Anastassiou G, *et al.* (2005). Loss of heterozygosity of 1p in uveal melanomas with monosomy 3. Int J Cancer **116**(6): 909-913.

Hawkes JE, Campbell J, Garvin D, *et al.* (2013). Lack of GNAQ and GNA11 Germ-Line Mutations in Familial Melanoma Pedigrees with Uveal Melanoma or Blue Nevi. Front Oncol **3**: 160.

Hayashi T, Sentani K, Oue N, *et al.* (2013). The search for secreted proteins in prostate cancer by the Escherichia coli ampicillin secretion trap: expression of NBL1 is highly restricted to the prostate and is related to cancer progression. Pathobiology **80**(2): 60-69.

He KF, Zhang L, Huang CF, *et al.* (2014). CD163+ tumor-associated macrophages correlated with poor prognosis and cancer stem cells in oral squamous cell carcinoma. Biomed Res Int **2014**: 838632.

He L, Thomson JM, Hemann MT, *et al.* (2005). A microRNA polycistron as a potential human oncogene. Nature **435**(7043): 828-833.

He YF, Wang XH, Zhang GM, *et al.* (2005). Sustained low-level expression of interferon-gamma promotes tumor development: potential insights in tumor prevention and tumor immunotherapy. Cancer Immunol Immunother **54**(9): 891-897.

He YF, Zhang MY, Wu X, *et al.* (2013). High MUC2 expression in ovarian cancer is inversely associated with the M1/M2 ratio of tumor-associated macrophages and patient survival time. PLoS One **8**(12): e79769.

Heagerty PJ &Zheng Y (2005). Survival model predictive accuracy and ROC curves. Biometrics **61**(1): 92-105.

Hecht BK, Turc-Carel C, Chatel M, *et al.* (1995). Chromosomes in gliomatosis cerebri. Genes Chromosomes Cancer **14**(2): 149-153.

Hegi ME, Diserens AC, Gorlia T, *et al.* (2005). MGMT gene silencing and benefit from temozolomide in glioblastoma. N Engl J Med **352**(10): 997-1003.

Heimberger AB, Abou-Ghazal M, Reina-Ortiz C, *et al.* (2008). Incidence and prognostic impact of FoxP3+ regulatory T cells in human gliomas. Clin Cancer Res **14**(16): 5166-5172.

Heine B, Coupland SE, Kneiff S, *et al.* (2000). Telomerase expression in uveal melanoma. Br J Ophthalmol **84**(2): 217-223.

Henderson MC &Azorsa DO (2012). The genomic and proteomic content of cancer cell-derived exosomes. Front Oncol **2**: 38.

Henriquez F, Janssen C, Kemp EG, *et al.* (2007). The T1799A BRAF mutation is present in iris melanoma. Invest Ophthalmol Vis Sci **48**(11): 4897-4900.

Herrera M, Herrera A, Dominguez G, *et al.* (2013). Cancer-associated fibroblast and M2 macrophage markers together predict outcome in colorectal cancer patients. Cancer Sci **104**(4): 437-444.

Herrlinger U, Felsberg J, Kuker W, *et al.* (2002). Gliomatosis cerebri: molecular pathology and clinical course. Ann Neurol **52**(4): 390-399.

Herwig MC, Bergstrom C, Wells JR, *et al.* (2013). M2/M1 ratio of tumor associated macrophages and PPAR-gamma expression in uveal melanomas with class 1 and class 2 molecular profiles. Exp Eye Res **107**: 52-58.

Hill VK, Gartner JJ, Samuels Y, *et al.* (2013). The genetics of melanoma: recent advances. Annu Rev Genomics Hum Genet **14**: 257-279.

Hillen F, Baeten CI, van de Winkel A, *et al.* (2008). Leukocyte infiltration and tumor cell plasticity are parameters of aggressiveness in primary cutaneous melanoma. Cancer Immunol Immunother **57**(1): 97-106.

Hilly O, Koren R, Raz R, *et al.* (2013). The role of s100-positive dendritic cells in the prognosis of papillary thyroid carcinoma. Am J Clin Pathol **139**(1): 87-92.

Hilmy M, Campbell R, Bartlett JM, *et al.* (2006). The relationship between the systemic inflammatory response, tumour proliferative activity, T-lymphocytic infiltration and COX-2 expression and survival in patients with transitional cell carcinoma of the urinary bladder. Br J Cancer **95**(9): 1234-1238.

Hiraoka N, Onozato K, Kosuge T, *et al.* (2006). Prevalence of FOXP3+ regulatory T cells increases during the progression of pancreatic ductal adenocarcinoma and its premalignant lesions. Clin Cancer Res **12**(18): 5423-5434.

Hodi FS, O'Day SJ, McDermott DF, *et al.* (2010). Improved survival with ipilimumab in patients with metastatic melanoma. N Engl J Med **363**(8): 711-723.

Hodis E, Watson IR, Kryukov GV, *et al.* (2012). A landscape of driver mutations in melanoma. Cell **150**(2): 251-263.

Hoglund M, Gisselsson D, Hansen GB, *et al.* (2004). Dissecting karyotypic patterns in malignant melanomas: temporal clustering of losses and gains in melanoma karyotypic evolution. Int J Cancer **108**(1): 57-65.

Holland AJ &Cleveland DW (2012). Losing balance: the origin and impact of aneuploidy in cancer. EMBO Rep **13**(6): 501-514.

Holly EA, Aston DA, Char DH, *et al.* (1990). Uveal melanoma in relation to ultraviolet light exposure and host factors. Cancer Res **50**(18): 5773-5777.

Horbinski C (2013). What do we know about IDH1/2 mutations so far, and how do we use it? Acta Neuropathol **125**(5): 621-636.

Horsman DE, Sroka H, Rootman J, *et al.* (1990). Monosomy 3 and isochromosome 8q in a uveal melanoma. Cancer Genet Cytogenet **45**(2): 249-253.

Hosch SB, Meyer AJ, Schneider C, *et al.* (1997). Expression and prognostic significance of HLA class I, ICAM-1, and tumor-infiltrating lymphocytes in esophageal cancer. J Gastrointest Surg **1**(4): 316-323.

Hotta K, Sho M, Fujimoto K, *et al.* (2011). Prognostic significance of CD45RO+ memory T cells in renal cell carcinoma. Br J Cancer **105**(8): 1191-1196.

Hou J, Yu Z, Xiang R, *et al.* (2014). Correlation between infiltration of FOXP3+ regulatory T cells and expression of B7-H1 in the tumor tissues of gastric cancer. Exp Mol Pathol **96**(3): 284-291.

Houillier C, Wang X, Kaloshi G, *et al.* (2010). IDH1 or IDH2 mutations predict longer survival and response to temozolomide in low-grade gliomas. Neurology **75**(17): 1560-1566.

Hsia JY, Chen JT, Chen CY, *et al.* (2005). Prognostic significance of intratumoral natural killer cells in primary resected esophageal squamous cell carcinoma. Chang Gung Med J **28**(5): 335-340.

Hsu MM, Hsu HC &Lui LT (1989). Local immune reaction in nasopharyngeal carcinoma, with special reference to its prognostic evaluation. Head Neck **11**(6): 505-510.

http://cancer.sanger.ac.uk/cancergenome/projects/cosmic.
Hua H, Li M, Luo T, *et al.* (2011). Matrix metalloproteinases in tumorigenesis: an evolving paradigm. Cell Mol Life Sci **68**(23): 3853-3868.
Huang A, Zhang B, Wang B, *et al.* (2013). Increased CD14(+)HLA-DR (-/low) myeloid-derived suppressor cells correlate with extrathoracic metastasis and poor response to chemotherapy in non-small cell lung cancer patients. Cancer Immunol Immunother **62**(9): 1439-1451.
Huang Y, Wang F, Wang Y, *et al.* (2014). Intrahepatic interleukin-17+ T cells and FoxP3+ regulatory T cells cooperate to promote development and affect the prognosis of hepatocellular carcinoma. J Gastroenterol Hepatol **29**(4): 851-859.
Huang Y, Wang FM, Wang T, *et al.* (2012). Tumor-infiltrating FoxP3+ Tregs and CD8+ T cells affect the prognosis of hepatocellular carcinoma patients. Digestion **86**(4): 329-337.
Hubbard KB &Hepler JR (2006). Cell signalling diversity of the Gqalpha family of heterotrimeric G proteins. Cell Signal **18**(2): 135-150.
Hurks HM, Valter MM, Wilson L, *et al.* (2001). Uveal melanoma: no expression of HLA-G. Invest Ophthalmol Vis Sci **42**(13): 3081-3084.
Hyakudomi M, Matsubara T, Hyakudomi R, *et al.* (2008). Increased expression of fractalkine is correlated with a better prognosis and an increased number of both CD8+ T cells and natural killer cells in gastric adenocarcinoma. Ann Surg Oncol **15**(6): 1775-1782.
Iasonos A, Schrag D, Raj GV, *et al.* (2008). How to build and interpret a nomogram for cancer prognosis. J Clin Oncol **26**(8): 1364-1370.
Ido E, Furihata M, Ohtsuki Y, *et al.* (1994). S-100 protein-positive dendritic cells detected in hepatocellular-carcinoma in relation to tumor progression and prognosis. Int J Oncol **5**(2): 231-236.
Ijland SA, Jager MJ, Heijdra BM, *et al.* (1999). Expression of angiogenic and immunosuppressive factors by uveal melanoma cell lines. Melanoma Res **9**(5): 445-450.
Infanger DW, Lynch ME &Fischbach C (2013). Engineered culture models for studies of tumor-microenvironment interactions. Annu Rev Biomed Eng **15**: 29-53.
Ino Y, Yamazaki-Itoh R, Shimada K, *et al.* (2013). Immune cell infiltration as an indicator of the immune microenvironment of pancreatic cancer. Br J Cancer **108**(4): 914-923.
Ishigami S, Arigami T, Uenosono Y, *et al.* (2012). Cancerous HLA class I expression and regulatory T cell infiltration in gastric cancer. Cancer Immunol Immunother **61**(10): 1663-1669.
Ishigami S, Natsugoe S, Matsumoto M, *et al.* (2003). Clinical implications of intratumoral dendritic cell infiltration in esophageal squamous cell carcinoma. Oncol Rep **10**(5): 1237-1240.
Ishigami S, Natsugoe S, Tokuda K, *et al.* (2000). Prognostic value of intratumoral natural killer cells in gastric carcinoma. Cancer **88**(3): 577-583.
Ishigami S, Natsugoe S, Tokuda K, *et al.* (2003). Tumor-associated macrophage (TAM) infiltration in gastric cancer. Anticancer Res **23**(5A): 4079-4083.
Italiano A (2011). Prognostic or predictive? It's time to get back to definitions! J Clin Oncol **29**(35): 4718; author reply 4718-4719.

Iwamoto M, Shinohara H, Miyamoto A, *et al.* (2003). Prognostic value of tumor-infiltrating dendritic cells expressing CD83 in human breast carcinomas. Int J Cancer **104**(1): 92-97.

Jacobs JF, Idema AJ, Bol KF, *et al.* (2010). Prognostic significance and mechanism of Treg infiltration in human brain tumors. J Neuroimmunol **225**(1-2): 195-199.

Jager MJ, van der Pol JP, de Wolff-Rouendaal D, *et al.* (1988). Decreased expression of HLA class II antigens on human uveal melanoma cells after in vivo X-ray irradiation. Am J Ophthalmol **105**(1): 78-86.

Jannie KM, Stipp CS &Weiner JA (2012). ALCAM regulates motility, invasiveness, and adherens junction formation in uveal melanoma cells. PLoS One **7**(6): e39330.

Jehs T, Faber C, Juel HB, *et al.* (2014). Inflammation-induced chemokine expression in uveal melanoma cell lines stimulates monocyte chemotaxis. Invest Ophthalmol Vis Sci **55**(8): 5169-5175.

Jenkins RB, Xiao Y, Sicotte H, *et al.* (2012). A low-frequency variant at 8q24.21 is strongly associated with risk of oligodendroglial tumors and astrocytomas with IDH1 or IDH2 mutation. Nat Genet **44**(10): 1122-1125.

Jensen HK, Donskov F, Marcussen N, *et al.* (2009). Presence of intratumoral neutrophils is an independent prognostic factor in localized renal cell carcinoma. J Clin Oncol **27**(28): 4709-4717.

Jensen TO, Schmidt H, Moller HJ, *et al.* (2012). Intratumoral neutrophils and plasmacytoid dendritic cells indicate poor prognosis and are associated with pSTAT3 expression in AJCC stage I/II melanoma. Cancer **118**(9): 2476-2485.

Jensen TO, Schmidt H, Moller HJ, *et al.* (2009). Macrophage markers in serum and tumor have prognostic impact in American Joint Committee on Cancer stage I/II melanoma. J Clin Oncol **27**(20): 3330-3337.

Ji RR, Chasalow SD, Wang L, *et al.* (2012). An immune-active tumor microenvironment favors clinical response to ipilimumab. Cancer Immunol Immunother **61**(7): 1019-1031.

Jiang XF, Tang QL, Shen XM, *et al.* (2012). Tumor-associated macrophages, epidermal growth factor receptor correlated with the triple negative phenotype in endometrial endometrioid adenocarcinoma. Pathol Res Pract **208**(12): 730-735.

Jiang YP, Wu XH, Shi B, *et al.* (2006). Expression of chemokine CXCL12 and its receptor CXCR4 in human epithelial ovarian cancer: an independent prognostic factor for tumor progression. Gynecol Oncol **103**(1): 226-233.

Jiao Y, Killela PJ, Reitman ZJ, *et al.* (2012). Frequent ATRX, CIC, FUBP1 and IDH1 mutations refine the classification of malignant gliomas. Oncotarget **3**(7): 709-722.

Jin SA, Chun SM, Choi YD, *et al.* (2013). BRAF mutations and KIT aberrations and their clinicopathological correlation in 202 Korean melanomas. J Invest Dermatol **133**(2): 579-582.

Johnson H, Del Rosario AM, Bryson BD, *et al.* (2012). Molecular characterization of EGFR and EGFRvIII signaling networks in human glioblastoma tumor xenografts. Mol Cell Proteomics **11**(12): 1724-1740.

Johnson SK, Kerr KM, Chapman AD, *et al.* (2000). Immune cell infiltrates and prognosis in primary carcinoma of the lung. Lung Cancer **27**(1): 27-35.

Jonsson G, Busch C, Knappskog S, *et al.* (2010). Gene expression profiling-based identification of molecular subtypes in stage IV melanomas with different clinical outcome. Clin Cancer Res **16**(13): 3356-3367.

Jordanova ES, Gorter A, Ayachi O, *et al.* (2008). Human leukocyte antigen class I, MHC class I chain-related molecule A, and CD8+/regulatory T-cell ratio: which variable determines survival of cervical cancer patients? Clin Cancer Res **14**(7): 2028-2035.

Jung AC, Guihard S, Krugell S, *et al.* (2013). CD8-alpha T-cell infiltration in human papillomavirus-related oropharyngeal carcinoma correlates with improved patient prognosis. Int J Cancer **132**(2): E26-36.

Jung JI, Cho HJ, Jung YJ, *et al.* (2014). High-fat diet-induced obesity increases lymphangiogenesis and lymph node metastasis in the B16F10 melanoma allograft model: Roles of adipocytes and M2-macrophages. Int J Cancer.

Juratli TA, Kirsch M, Robel K, *et al.* (2012). IDH mutations as an early and consistent marker in low-grade astrocytomas WHO grade II and their consecutive secondary high-grade gliomas. J Neurooncol **108**(3): 403-410.

Kageshita T, Hirai S, Ono T, *et al.* (1999). Down-regulation of HLA class I antigen-processing molecules in malignant melanoma: association with disease progression. Am J Pathol **154**(3): 745-754.

Kajiyama H, Shibata K, Terauchi M, *et al.* (2008). Involvement of SDF-1alpha/CXCR4 axis in the enhanced peritoneal metastasis of epithelial ovarian carcinoma. Int J Cancer **122**(1): 91-99.

Kang MJ, Kim KM, Bae JS, *et al.* (2013). Tumor-infiltrating PD1-Positive Lymphocytes and FoxP3-Positive Regulatory T Cells Predict Distant Metastatic Relapse and Survival of Clear Cell Renal Cell Carcinoma. Transl Oncol **6**(3): 282-289.

Kantoff PW, Higano CS, Shore ND, *et al.* (2010). Sipuleucel-T immunotherapy for castration-resistant prostate cancer. N Engl J Med **363**(5): 411-422.

Karlsson M, Boeryd B, Carstensen J, *et al.* (1995). DNA ploidy and S-phase fraction as prognostic factors in patients with uveal melanomas. Br J Cancer **71**(1): 177-181.

Kashimura S, Saze Z, Terashima M, *et al.* (2012). CD83(+) dendritic cells and Foxp3(+) regulatory T cells in primary lesions and regional lymph nodes are inversely correlated with prognosis of gastric cancer. Gastric Cancer **15**(2): 144-153.

Kaufman JL, Niesvizky R, Stadtmauer EA, *et al.* (2013). Phase I, multicentre, dose-escalation trial of monotherapy with milatuzumab (humanized anti-CD74 monoclonal antibody) in relapsed or refractory multiple myeloma. Br J Haematol **163**(4): 478-486.

Kawai O, Ishii G, Kubota K, *et al.* (2008). Predominant infiltration of macrophages and CD8(+) T Cells in cancer nests is a significant predictor of survival in stage IV nonsmall cell lung cancer. Cancer **113**(6): 1387-1395.

Kelly SA, Gschmeissner S, East N, *et al.* (1991). Enhancement of metastatic potential by gamma-interferon. Cancer Res **51**(15): 4020-4027.

Kenawy N, Lake SL, Coupland SE, *et al.* (2013). Conjunctival melanoma and melanocytic intra-epithelial neoplasia. Eye (Lond) **27**(2): 142-152.

Keyes M, Macaulay C, Hayes M, *et al.* (2013). DNA ploidy measured on archived pretreatment biopsy material may correlate with prostate-specific antigen recurrence after prostate brachytherapy. Int J Radiat Oncol Biol Phys **86**(5): 829-834.

Khanh do T, Mekata E, Mukaisho K, *et al.* (2011). Prognostic role of CD10(+) myeloid cells in association with tumor budding at the invasion front of colorectal cancer. Cancer Sci **102**(9): 1724-1733.

Kilic E, Bruggenwirth HT, Meier M, *et al.* (2008). Increased expression of p73Deltaex2 transcript in uveal melanoma with loss of chromosome 1p. Melanoma Res **18**(3): 208-213.

Kilic E, Naus NC, van Gils W, *et al.* (2005). Concurrent loss of chromosome arm 1p and chromosome 3 predicts a decreased disease-free survival in uveal melanoma patients. Invest Ophthalmol Vis Sci **46**(7): 2253-2257.

Killela PJ, Pirozzi CJ, Healy P, *et al.* (2014). Mutations in IDH1, IDH2, and in the TERT promoter define clinically distinct subgroups of adult malignant gliomas. Oncotarget **5**(6): 1515-1525.

Kim HI, Kim H, Cho HW, *et al.* (2011). The ratio of intra-tumoral regulatory T cells (Foxp3+)/helper T cells (CD4+) is a prognostic factor and associated with recurrence pattern in gastric cardia cancer. J Surg Oncol **104**(7): 728-733.

Kim J, Mori T, Chen SL, *et al.* (2006). Chemokine receptor CXCR4 expression in patients with melanoma and colorectal cancer liver metastases and the association with disease outcome. Ann Surg **244**(1): 113-120.

Kim KJ, Lee KS, Cho HJ, *et al.* (2014). Prognostic implications of tumor-infiltrating FoxP3+ regulatory T cells and CD8+ cytotoxic T cells in microsatellite-unstable gastric cancers. Hum Pathol **45**(2): 285-293.

Kim YH, Jung TY, Jung S, *et al.* (2012). Tumour-infiltrating T-cell subpopulations in glioblastomas. Br J Neurosurg **26**(1): 21-27.

Kindt N, Lechien JR, Nonclercq D, *et al.* (2014). Involvement of CD74 in head and neck squamous cell carcinomas. J Cancer Res Clin Oncol **140**(6): 937-947.

Kivela T, Eskelin S, Makitie T, *et al.* (2001). Exudative retinal detachment from malignant uveal melanoma: predictors and prognostic significance. Invest Ophthalmol Vis Sci **42**(9): 2085-2093.

Kmiecik J, Poli A, Brons NH, *et al.* (2013). Elevated CD3+ and CD8+ tumor-infiltrating immune cells correlate with prolonged survival in glioblastoma patients despite integrated immunosuppressive mechanisms in the tumor microenvironment and at the systemic level. J Neuroimmunol **264**(1-2): 71-83.

Kobayashi N, Hiraoka N, Yamagami W, *et al.* (2007). FOXP3+ regulatory T cells affect the development and progression of hepatocarcinogenesis. Clin Cancer Res **13**(3): 902-911.

Kochan G, Escors D, Breckpot K, *et al.* (2013). Role of non-classical MHC class I molecules in cancer immunosuppression. Oncoimmunology **2**(11): e26491.

Koelsche C, Sahm F, Capper D, *et al.* (2013). Distribution of TERT promoter mutations in pediatric and adult tumors of the nervous system. Acta Neuropathol **126**(6): 907-915.

Koivunen P, Lee S, Duncan CG, *et al.* (2012). Transformation by the (R)-enantiomer of 2-hydroxyglutarate linked to EGLN activation. Nature **483**(7390): 484-488.

Kondratiev S, Sabo E, Yakirevich E, *et al.* (2004). Intratumoral CD8+ T lymphocytes as a prognostic factor of survival in endometrial carcinoma. Clin Cancer Res **10**(13): 4450-4456.

Kong LQ, Zhu XD, Xu HX, *et al.* (2013). The clinical significance of the CD163+ and CD68+ macrophages in patients with hepatocellular carcinoma. PLoS One **8**(3): e59771.

Kono K, Kawaida H, Takahashi A, *et al.* (2006). CD4(+)CD25high regulatory T cells increase with tumor stage in patients with gastric and esophageal cancers. Cancer Immunol Immunother **55**(9): 1064-1071.

Kranendijk M, Struys EA, van Schaftingen E, *et al.* (2010). IDH2 mutations in patients with D-2-hydroxyglutaric aciduria. Science **330**(6002): 336.
Krauthammer M, Kong Y, Ha BH, *et al.* (2012). Exome sequencing identifies recurrent somatic RAC1 mutations in melanoma. Nat Genet **44**(9): 1006-1014.
Krieg AM (2006). Therapeutic potential of Toll-like receptor 9 activation. Nat Rev Drug Discov **5**(6): 471-484.
Krishnakumar S, Abhyankar D, Lakshmi SA, *et al.* (2004). HLA expression in choroidal melanomas: correlation with clinicopathological features. Curr Eye Res **28**(6): 409-416.
Krishnakumar S, Abhyankar D, Lakshmi SA, *et al.* (2003). HLA class II antigen expression in uveal melanoma: correlation with clinicopathological features. Exp Eye Res **77**(2): 175-180.
Krishnakumar S, Abhyankar D, Sundaram AL, *et al.* (2003). Major histocompatibility antigens and antigen-processing molecules in uveal melanoma. Clin Cancer Res **9**(11): 4159-4164.
Krishnakumar S, Lakshmi SA, Abhyankar D, *et al.* (2004). Transporter associated protein expression in uveal melanoma. Br J Ophthalmol **88**(7): 925-928.
Kroemer G &Zitvogel L (2012). Can the exome and the immunome converge on the design of efficient cancer vaccines? Oncoimmunology **1**(5): 579-580.
Kros JM, Zheng P, Dinjens WN, *et al.* (2002). Genetic aberrations in gliomatosis cerebri support monoclonal tumorigenesis. J Neuropathol Exp Neurol **61**(9): 806-814.
Kuang DM, Zhao Q, Wu Y, *et al.* (2011). Peritumoral neutrophils link inflammatory response to disease progression by fostering angiogenesis in hepatocellular carcinoma. J Hepatol **54**(5): 948-955.
Kujala E, Damato B, Coupland SE, *et al.* (2013). Staging of ciliary body and choroidal melanomas based on anatomic extent. J Clin Oncol **31**(22): 2825-2831.
Kurahara H, Shinchi H, Mataki Y, *et al.* (2011). Significance of M2-polarized tumor-associated macrophage in pancreatic cancer. J Surg Res **167**(2): e211-219.
Kurahara H, Takao S, Kuwahata T, *et al.* (2012). Clinical significance of folate receptor beta-expressing tumor-associated macrophages in pancreatic cancer. Ann Surg Oncol **19**(7): 2264-2271.
Kwon MJ, Kim ST, Kong DS, *et al.* (2012). Mutated IDH1 is a favorable prognostic factor for type 2 gliomatosis cerebri. Brain Pathol **22**(3): 307-317.
Lackner C, Jukic Z, Tsybrovskyy O, *et al.* (2004). Prognostic relevance of tumour-associated macrophages and von Willebrand factor-positive microvessels in colorectal cancer. Virchows Arch **445**(2): 160-167.
Ladanyi A, Kiss J, Mohos A, *et al.* (2011). Prognostic impact of B-cell density in cutaneous melanoma. Cancer Immunol Immunother **60**(12): 1729-1738.
Ladanyi A, Kiss J, Somlai B, *et al.* (2007). Density of DC-LAMP(+) mature dendritic cells in combination with activated T lymphocytes infiltrating primary cutaneous melanoma is a strong independent prognostic factor. Cancer Immunol Immunother **56**(9): 1459-1469.
Ladanyi A, Mohos A, Somlai B, *et al.* (2010). FOXP3+ cell density in primary tumor has no prognostic impact in patients with cutaneous malignant melanoma. Pathol Oncol Res **16**(3): 303-309.
Lagouros E, Salomao D, Thorland E, *et al.* (2009). Infiltrative T regulatory cells in enucleated uveal melanomas. Trans Am Ophthalmol Soc **107**: 223-228.

Lai K, Conway RM, Crouch R, *et al.* (2008). Expression and distribution of MMPs and TIMPs in human uveal melanoma. Exp Eye Res **86**(6): 936-941.
Lake SL, Jmor F, Dopierala J, *et al.* (2011). Multiplex ligation-dependent probe amplification of conjunctival melanoma reveals common BRAF V600E gene mutation and gene copy number changes. Invest Ophthalmol Vis Sci **52**(8): 5598-5604.
Lakshmi Narendra B, Eshvendar Reddy K, Shantikumar S, *et al.* (2013). Immune system: a double-edged sword in cancer. Inflamm Res **62**(9): 823-834.
Lamb GW, McArdle PA, Ramsey S, *et al.* (2008). The relationship between the local and systemic inflammatory responses and survival in patients undergoing resection for localized renal cancer. BJU Int **102**(6): 756-761.
Lamperska K, Mackiewicz K, Kaczmarek A, *et al.* (2002). Expression of p16 in sporadic primary uveal melanoma. Acta Biochim Pol **49**(2): 377-385.
Lan C, Huang X, Lin S, *et al.* (2013). Expression of M2-polarized macrophages is associated with poor prognosis for advanced epithelial ovarian cancer. Technol Cancer Res Treat **12**(3): 259-267.
Lanciotti M, Masieri L, Raspollini MR, *et al.* (2014). The role of M1 and M2 macrophages in prostate cancer in relation to extracapsular tumor extension and biochemical recurrence after radical prostatectomy. Biomed Res Int **2014**: 486798.
Landreville S, Agapova OA, Matatall KA, *et al.* (2012). Histone deacetylase inhibitors induce growth arrest and differentiation in uveal melanoma. Clin Cancer Res **18**(2): 408-416.
Landreville S, Lupien CB, Vigneault F, *et al.* (2011). Identification of differentially expressed genes in uveal melanoma using suppressive subtractive hybridization. Mol Vis **17**: 1324-1333.
Lang JR, Davidorf FH &Baba N (1977). The prognostic significance of lymphocytic infiltration in malignant melanoma of the choroid. Cancer **40**(5): 2388-2394.
Larsen AC, Holst L, Kaczkowski B, *et al.* (2013). MicroRNA expression analysis and Multiplex ligation-dependent probe amplification in metastatic and non-metastatic uveal melanoma. Acta Ophthalmol.
Lassus H, Staff S, Leminen A, *et al.* (2011). Aurora-A overexpression and aneuploidy predict poor outcome in serous ovarian carcinoma. Gynecol Oncol **120**(1): 11-17.
Lattanzio L, Tonissi F, Torta I, *et al.* (2013). Role of IL-8 induced angiogenesis in uveal melanoma. Invest New Drugs **31**(5): 1107-1114.
Laurent C, Valet F, Planque N, *et al.* (2011). High PTP4A3 phosphatase expression correlates with metastatic risk in uveal melanoma patients. Cancer Res **71**(3): 666-674.
Le Discorde M, Moreau P, Sabatier P, *et al.* (2003). Expression of HLA-G in human cornea, an immune-privileged tissue. Hum Immunol **64**(11): 1039-1044.
Le Page C, Marineau A, Bonza PK, *et al.* (2012). BTN3A2 expression in epithelial ovarian cancer is associated with higher tumor infiltrating T cells and a better prognosis. PLoS One **7**(6): e38541.
Lee CG, Das B, Lin TL, *et al.* (2012). A rare fraction of drug-resistant follicular lymphoma cancer stem cells interacts with follicular dendritic cells to maintain tumourigenic potential. Br J Haematol **158**(1): 79-90.
Lee WS, Kang M, Baek JH, *et al.* (2013). Clinical impact of tumor-infiltrating lymphocytes for survival in curatively resected stage IV colon cancer with isolated liver or lung metastasis. Ann Surg Oncol **20**(2): 697-702.

Leffers N, Fehrmann RS, Gooden MJ, *et al.* (2010). Identification of genes and pathways associated with cytotoxic T lymphocyte infiltration of serous ovarian cancer. Br J Cancer **103**(5): 685-692.

Leffers N, Gooden MJ, de Jong RA, *et al.* (2009). Prognostic significance of tumor-infiltrating T-lymphocytes in primary and metastatic lesions of advanced stage ovarian cancer. Cancer Immunol Immunother **58**(3): 449-459.

Leiter U, Meier F, Schittek B, *et al.* (2004). The natural course of cutaneous melanoma. J Surg Oncol **86**(4): 172-178.

Li H, Yang W, Chen PW, *et al.* (2009). Inhibition of chemokine receptor expression on uveal melanomas by CXCR4 siRNA and its effect on uveal melanoma liver metastases. Invest Ophthalmol Vis Sci **50**(12): 5522-5528.

Li J, Cui Y, Wang Q, *et al.* (2014). The proliferation of malignant melanoma cells could be inhibited by ranibizumab via antagonizing VEGF through VEGFR1. Mol Vis **20**: 649-660.

Li M, Mukasa A, Inda MM, *et al.* (2011). Guanylate binding protein 1 is a novel effector of EGFR-driven invasion in glioblastoma. J Exp Med **208**(13): 2657-2673.

Li Y, Huang Q, Shi X, *et al.* (2014). MicroRNA 145 may play an important role in uveal melanoma cell growth by potentially targeting insulin receptor substrate-1. Chin Med J (Engl) **127**(8): 1410-1416.

Li YW, Qiu SJ, Fan J, *et al.* (2009). Tumor-infiltrating macrophages can predict favorable prognosis in hepatocellular carcinoma after resection. J Cancer Res Clin Oncol **135**(3): 439-449.

Li YW, Qiu SJ, Fan J, *et al.* (2011). Intratumoral neutrophils: a poor prognostic factor for hepatocellular carcinoma following resection. J Hepatol **54**(3): 497-505.

Liberzon A, Subramanian A, Pinchback R, *et al.* (2011). Molecular signatures database (MSigDB) 3.0. Bioinformatics **27**(12): 1739-1740.

Lin EY, Li JF, Gnatovskiy L, *et al.* (2006). Macrophages regulate the angiogenic switch in a mouse model of breast cancer. Cancer Res **66**(23): 11238-11246.

Lin GH, Wang J, Li SH, *et al.* (2010). Relationship and clinical significance of TGF-beta1 expression with Treg cell infiltration in hepatocellular carcinoma. Chin J Cancer **29**(4): 403-407.

Lin JY, Li XY, Tadashi N, *et al.* (2011). Clinical significance of tumor-associated macrophage infiltration in supraglottic laryngeal carcinoma. Chin J Cancer **30**(4): 280-286.

Lin SZ, Chen KJ, Xu ZY, *et al.* (2013). Prediction of recurrence and survival in hepatocellular carcinoma based on two Cox models mainly determined by FoxP3+ regulatory T cells. Cancer Prev Res (Phila) **6**(6): 594-602.

Ling A, Edin S, Wikberg ML, *et al.* (2014). The intratumoural subsite and relation of CD8(+) and FOXP3(+) T lymphocytes in colorectal cancer provide important prognostic clues. Br J Cancer **110**(10): 2551-2559.

Liu F, Lang R, Zhao J, *et al.* (2011). CD8(+) cytotoxic T cell and FOXP3(+) regulatory T cell infiltration in relation to breast cancer survival and molecular subtypes. Breast Cancer Res Treat **130**(2): 645-655.

Liu H, Zhang T, Ye J, *et al.* (2012). Tumor-infiltrating lymphocytes predict response to chemotherapy in patients with advance non-small cell lung cancer. Cancer Immunol Immunother **61**(10): 1849-1856.

Liu M, Matsumura N, Mandai M, *et al.* (2009). Classification using hierarchical clustering of tumor-infiltrating immune cells identifies poor prognostic ovarian cancers with high levels of COX expression. Mod Pathol **22**(3): 373-384.

Liu S, Lachapelle J, Leung S, *et al.* (2012). CD8+ lymphocyte infiltration is an independent favorable prognostic indicator in basal-like breast cancer. Breast Cancer Res **14**(2): R48.

Liu XY, Gerges N, Korshunov A, *et al.* (2012). Frequent ATRX mutations and loss of expression in adult diffuse astrocytic tumors carrying IDH1/IDH2 and TP53 mutations. Acta Neuropathol **124**(5): 615-625.

Liu Y, Li PK, Li C, *et al.* (2010). Inhibition of STAT3 signaling blocks the anti-apoptotic activity of IL-6 in human liver cancer cells. J Biol Chem **285**(35): 27429-27439.

Liu Y, Saeter T, Vlatkovic L, *et al.* (2013). Dendritic and lymphocytic cell infiltration in prostate carcinoma. Histol Histopathol **28**(12): 1621-1628.

Logan P, Burnier J &Burnier MN, Jr. (2013). Vascular endothelial growth factor expression and inhibition in uveal melanoma cell lines. Ecancermedicalscience **7**: 336.

Lohr J, Ratliff T, Huppertz A, *et al.* (2011). Effector T-cell infiltration positively impacts survival of glioblastoma patients and is impaired by tumor-derived TGF-beta. Clin Cancer Res **17**(13): 4296-4308.

Louis DN (2007). WHO classification of tumours of the central nervous system. Lyon, International Agency for Research on Cancer.

Lu C, Ward PS, Kapoor GS, *et al.* (2012). IDH mutation impairs histone demethylation and results in a block to cell differentiation. Nature **483**(7390): 474-478.

Lu L, Pan K, Zheng HX, *et al.* (2013). IL-17A promotes immune cell recruitment in human esophageal cancers and the infiltrating dendritic cells represent a positive prognostic marker for patient survival. J Immunother **36**(8): 451-458.

Lu P, Takai K, Weaver VM, *et al.* (2011). Extracellular matrix degradation and remodeling in development and disease. Cold Spring Harb Perspect Biol **3**(12).

Luke JJ, Callahan MK, Postow MA, *et al.* (2013). Clinical activity of ipilimumab for metastatic uveal melanoma: a retrospective review of the Dana-Farber Cancer Institute, Massachusetts General Hospital, Memorial Sloan-Kettering Cancer Center, and University Hospital of Lausanne experience. Cancer **119**(20): 3687-3695.

Lv L, Pan K, Li XD, *et al.* (2011). The accumulation and prognosis value of tumor infiltrating IL-17 producing cells in esophageal squamous cell carcinoma. PLoS One **6**(3): e18219.

Ly LV, Bronkhorst IH, van Beelen E, *et al.* (2010). Inflammatory cytokines in eyes with uveal melanoma and relation with macrophage infiltration. Invest Ophthalmol Vis Sci **51**(11): 5445-5451.

Lynn DJ, Winsor GL, Chan C, *et al.* (2008). InnateDB: facilitating systems-level analyses of the mammalian innate immune response. Mol Syst Biol **4**: 218.

Ma C, Zhang Q, Ye J, *et al.* (2012). Tumor-infiltrating gammadelta T lymphocytes predict clinical outcome in human breast cancer. J Immunol **189**(10): 5029-5036.

Ma GF, Miao Q, Liu YM, *et al.* (2014). High FoxP3 expression in tumour cells predicts better survival in gastric cancer and its role in tumour microenvironment. Br J Cancer **110**(6): 1552-1560.

Ma Y, Ambannavar R, Stephans J, *et al.* (2014). Fusion transcript discovery in formalin-fixed paraffin-embedded human breast cancer tissues reveals a link to tumor progression. PLoS One **9**(4): e94202.

Maat W, Beiboer SH, Jager MJ, *et al.* (2008). Epigenetic regulation identifies RASEF as a tumor-suppressor gene in uveal melanoma. Invest Ophthalmol Vis Sci **49**(4): 1291-1298.

Maat W, Haasnoot GW, Claas FH, *et al.* (2006). HLA Class I and II genotype in uveal melanoma: relation to occurrence and prognosis. Invest Ophthalmol Vis Sci **47**(1): 3-6.

Maat W, Ly LV, Jordanova ES, *et al.* (2008). Monosomy of chromosome 3 and an inflammatory phenotype occur together in uveal melanoma. Invest Ophthalmol Vis Sci **49**(2): 505-510.

Maat W, van der Velden PA, Out-Luiting C, *et al.* (2007). Epigenetic inactivation of RASSF1a in uveal melanoma. Invest Ophthalmol Vis Sci **48**(2): 486-490.

Maccalli C, Volonte A, Cimminiello C, *et al.* (2014). Immunology of cancer stem cells in solid tumours. A review. Eur J Cancer **50**(3): 649-655.

MacConaill LE (2013). Existing and emerging technologies for tumor genomic profiling. J Clin Oncol **31**(15): 1815-1824.

Machida YJ, Machida Y, Vashisht AA, *et al.* (2009). The deubiquitinating enzyme BAP1 regulates cell growth via interaction with HCF-1. J Biol Chem **284**(49): 34179-34188.

Maeda N, Yoshimura K, Yamamoto S, *et al.* (2014). Expression of B7-H3, a Potential Factor of Tumor Immune Evasion in Combination with the Number of Regulatory T Cells, Affects Against Recurrence-Free Survival in Breast Cancer Patients. Ann Surg Oncol.

Mahmoud SM, Paish EC, Powe DG, *et al.* (2011). Tumor-infiltrating CD8+ lymphocytes predict clinical outcome in breast cancer. J Clin Oncol **29**(15): 1949-1955.

Mahmoud SM, Paish EC, Powe DG, *et al.* (2011). An evaluation of the clinical significance of FOXP3+ infiltrating cells in human breast cancer. Breast Cancer Res Treat **127**(1): 99-108.

Makitie T, Summanen P, Tarkkanen A, *et al.* (1999). Microvascular density in predicting survival of patients with choroidal and ciliary body melanoma. Invest Ophthalmol Vis Sci **40**(11): 2471-2480.

Makitie T, Summanen P, Tarkkanen A, *et al.* (2001). Tumor-infiltrating macrophages (CD68(+) cells) and prognosis in malignant uveal melanoma. Invest Ophthalmol Vis Sci **42**(7): 1414-1421.

Malina HZ &Martin XD (1996). Indoleamine 2,3-dioxygenase: antioxidant enzyme in the human eye. Graefes Arch Clin Exp Ophthalmol **234**(7): 457-462.

Mallett S, Royston P, Waters R, *et al.* (2010). Reporting performance of prognostic models in cancer: a review. BMC Med **8**: 21.

Mallone S, De Vries E, Guzzo M, *et al.* (2012). Descriptive epidemiology of malignant mucosal and uveal melanomas and adnexal skin carcinomas in Europe. Eur J Cancer **48**(8): 1167-1175.

Mann GJ, Pupo GM, Campain AE, *et al.* (2013). BRAF mutation, NRAS mutation, and the absence of an immune-related expressed gene profile predict poor outcome in patients with stage III melanoma. J Invest Dermatol **133**(2): 509-517.

Mantovani A, Savino B, Locati M, *et al.* (2010). The chemokine system in cancer biology and therapy. Cytokine Growth Factor Rev **21**(1): 27-39.

Martin M, Masshofer L, Temming P, *et al.* (2013). Exome sequencing identifies recurrent somatic mutations in EIF1AX and SF3B1 in uveal melanoma with disomy 3. Nat Genet **45**(8): 933-936.

Martinez-Rodriguez M, Thompson AK &Monteagudo C (2014). A significant percentage of CD20-positive TIL correlates with poor prognosis in patients with primary cutaneous malignant melanoma. Histopathology.

Matatall KA, Agapova OA, Onken MD, *et al.* (2013). BAP1 deficiency causes loss of melanocytic cell identity in uveal melanoma. BMC Cancer **13**: 371.

Matkowski R, Gisterek I, Halon A, *et al.* (2009). The prognostic role of tumor-infiltrating CD4 and CD8 T lymphocytes in breast cancer. Anticancer Res **29**(7): 2445-2451.

Matsushita K, Takenouchi T, Shimada H, *et al.* (2006). Strong HLA-DR antigen expression on cancer cells relates to better prognosis of colorectal cancer patients: Possible involvement of c-myc suppression by interferon-gamma in situ. Cancer Sci **97**(1): 57-63.

Matsushita N, Ghazizadeh M, Konishi H, *et al.* (2003). Association of ovarian tumor epithelium coexpressing HLA-DR and CA-125 antigens with tumor infiltrating cytotoxic T lymphocytes. J Nippon Med Sch **70**(1): 40-44.

Mawrin C, Kirches E, Schneider-Stock R, *et al.* (2003). Analysis of TP53 and PTEN in gliomatosis cerebri. Acta Neuropathol **105**(6): 529-536.

Mawrin C, Schneider T, Firsching R, *et al.* (2005). Assessment of tumor cell invasion factors in gliomatosis cerebri. J Neurooncol **73**(2): 109-115.

McArdle PA, Canna K, McMillan DC, *et al.* (2004). The relationship between T-lymphocyte subset infiltration and survival in patients with prostate cancer. Br J Cancer **91**(3): 541-543.

McGranahan N, Burrell RA, Endesfelder D, *et al.* (2012). Cancer chromosomal instability: therapeutic and diagnostic challenges. EMBO Rep **13**(6): 528-538.

McLaughlin CC, Wu XC, Jemal A, *et al.* (2005). Incidence of noncutaneous melanomas in the U.S. Cancer **103**(5): 1000-1007.

McLean IW, Foster WD, Zimmerman LE, *et al.* (1983). Modifications of Callender's classification of uveal melanoma at the Armed Forces Institute of Pathology. Am J Ophthalmol **96**(4): 502-509.

Meecham WJ &Char DH (1986). DNA content abnormalities and prognosis in uveal melanoma. Arch Ophthalmol **104**(11): 1626-1629.

Mensink HW, Vaarwater J, de Keizer RJ, *et al.* (2011). Chromosomal aberrations in iris melanomas. Br J Ophthalmol **95**(3): 424-428.

Merbs SL &Sidransky D (1999). Analysis of p16 (CDKN2/MTS-1/INK4A) alterations in primary sporadic uveal melanoma. Invest Ophthalmol Vis Sci **40**(3): 779-783.

Merhavi E, Cohen Y, Avraham BC, *et al.* (2007). Promoter methylation status of multiple genes in uveal melanoma. Invest Ophthalmol Vis Sci **48**(10): 4403-4406.

Metellus P, Coulibaly B, Colin C, *et al.* (2010). Absence of IDH mutation identifies a novel radiologic and molecular subtype of WHO grade II gliomas with dismal prognosis. Acta Neuropathol **120**(6): 719-729.

Metzelaar-Blok JA, Hurks HM, Naipal A, *et al.* (2005). Normal HLA class I, II, and MICA gene distribution in uveal melanoma. Mol Vis **11**: 1166-1172.

Metzker ML (2010). Sequencing technologies - the next generation. Nat Rev Genet **11**(1): 31-46.

Meyerson M, Gabriel S &Getz G (2010). Advances in understanding cancer genomes through second-generation sequencing. Nat Rev Genet **11**(10): 685-696.

Mhawech-Fauceglia P, Wang D, Ali L, *et al.* (2013). Intraepithelial T cells and tumor-associated macrophages in ovarian cancer patients. Cancer Immun **13**: 1.

Milne K, Kobel M, Kalloger SE, *et al.* (2009). Systematic analysis of immune infiltrates in high-grade serous ovarian cancer reveals CD20, FoxP3 and TIA-1 as positive prognostic factors. PLoS One **4**(7): e6412.
Min HS, Kim B &Park SH (2008). Array-based comparative genomic hybridization and immunohistochemical studies in gliomatosis cerebri. J Neurooncol **90**(3): 259-266.
Miracco C, Mourmouras V, Biagioli M, *et al.* (2007). Utility of tumour-infiltrating CD25+FOXP3+ regulatory T cell evaluation in predicting local recurrence in vertical growth phase cutaneous melanoma. Oncol Rep **18**(5): 1115-1122.
Mittal D, Gubin MM, Schreiber RD, *et al.* (2014). New insights into cancer immunoediting and its three component phases--elimination, equilibrium and escape. Curr Opin Immunol **27**: 16-25.
Mittal K, Ebos J &Rini B (2014). Angiogenesis and the tumor microenvironment: vascular endothelial growth factor and beyond. Semin Oncol **41**(2): 235-251.
Mlecnik B, Tosolini M, Kirilovsky A, *et al.* (2011). Histopathologic-Based Prognostic Factors of Colorectal Cancers Are Associated With the State of the Local Immune Reaction. Journal of Clinical Oncology **29**(6): 610-618.
Mohamed MM &Sloane BF (2006). Cysteine cathepsins: multifunctional enzymes in cancer. Nat Rev Cancer **6**(10): 764-775.
Molenaar RJ, Radivoyevitch T, Maciejewski JP, *et al.* (2014). The driver and passenger effects of isocitrate dehydrogenase 1 and 2 mutations in oncogenesis and survival prolongation. Biochim Biophys Acta.
Monk BJ, Herzog TJ, Kaye SB, *et al.* (2010). Trabectedin plus pegylated liposomal Doxorubicin in recurrent ovarian cancer. J Clin Oncol **28**(19): 3107-3114.
Mori A, Deola S, Xumerle L, *et al.* (2013). Next generation sequencing: new tools in immunology and hematology. Blood Res **48**(4): 242-249.
Mougiakakos D, Johansson CC, Trocme E, *et al.* (2010). Intratumoral forkhead box P3-positive regulatory T cells predict poor survival in cyclooxygenase-2-positive uveal melanoma. Cancer **116**(9): 2224-2233.
Moulin AP, Clement G, Bosman FT, *et al.* (2008). Methylation of CpG island promoters in uveal melanoma. Br J Ophthalmol **92**(2): 281-285.
Mouriaux F, Sanschagrin F, Diorio C, *et al.* (2014). Increased HIF-1alpha expression correlates with cell proliferation and vascular markers CD31 and VEGF-A in uveal melanoma. Invest Ophthalmol Vis Sci **55**(3): 1277-1283.
Mukaida N &Baba T (2012). Chemokines in tumor development and progression. Exp Cell Res **318**(2): 95-102.
Mulcahy KA, Rimoldi D, Brasseur F, *et al.* (1996). Infrequent expression of the MAGE gene family in uveal melanomas. Int J Cancer **66**(6): 738-742.
Mullen AR &DeBerardinis RJ (2012). Genetically-defined metabolic reprogramming in cancer. Trends Endocrinol Metab **23**(11): 552-559.
Musi E, Ambrosini G, De Stanchina E, *et al.* (2014). The Phosphoinositide 3-Kinasealpha Selective Inhibitor, BYL719, Enhances the Effect of the Protein Kinase C Inhibitor, AEB071, in GNAQ/GNA11 Mutant Uveal Melanoma Cells. Mol Cancer Ther.
Nagarkatti-Gude N, Bronkhorst IH, van Duinen SG, *et al.* (2012). Cytokines and chemokines in the vitreous fluid of eyes with uveal melanoma. Invest Ophthalmol Vis Sci **53**(11): 6748-6755.
Nagtegaal ID, Marijnen CA, Kranenbarg EK, *et al.* (2001). Local and distant recurrences in rectal cancer patients are predicted by the nonspecific immune response; specific

immune response has only a systemic effect--a histopathological and immunohistochemical study. BMC Cancer **1**: 7.
Nakakubo Y, Miyamoto M, Cho Y, *et al.* (2003). Clinical significance of immune cell infiltration within gallbladder cancer. Br J Cancer **89**(9): 1736-1742.
Nakano O, Sato M, Naito Y, *et al.* (2001). Proliferative activity of intratumoral CD8(+) T-lymphocytes as a prognostic factor in human renal cell carcinoma: clinicopathologic demonstration of antitumor immunity. Cancer Res **61**(13): 5132-5136.
Nasman A, Romanitan M, Nordfors C, *et al.* (2012). Tumor infiltrating CD8+ and Foxp3+ lymphocytes correlate to clinical outcome and human papillomavirus (HPV) status in tonsillar cancer. PLoS One **7**(6): e38711.
Naumov GN, Akslen LA &Folkman J (2006). Role of angiogenesis in human tumor dormancy: animal models of the angiogenic switch. Cell Cycle **5**(16): 1779-1787.
Nedergaard BS, Ladekarl M, Thomsen HF, *et al.* (2007). Low density of CD3+, CD4+ and CD8+ cells is associated with increased risk of relapse in squamous cell cervical cancer. Br J Cancer **97**(8): 1135-1138.
Neefjes J, Jongsma ML, Paul P, *et al.* (2011). Towards a systems understanding of MHC class I and MHC class II antigen presentation. Nat Rev Immunol **11**(12): 823-836.
Nelson CM &Bissell MJ (2006). Of extracellular matrix, scaffolds, and signaling: tissue architecture regulates development, homeostasis, and cancer. Annu Rev Cell Dev Biol **22**: 287-309.
Neves SR, Ram PT &Iyengar R (2002). G protein pathways. Science **296**(5573): 1636-1639.
Nevin S (1938). Gliomatosis cerebri. Brain **61**: 170-191.
Niederkorn JY (2009). Immune escape mechanisms of intraocular tumors. Prog Retin Eye Res **28**(5): 329-347.
Niederkorn JY (2012). Ocular immune privilege and ocular melanoma: parallel universes or immunological plagiarism? Front Immunol **3**: 148.
Nielsen HJ, Hansen U, Christensen IJ, *et al.* (1999). Independent prognostic value of eosinophil and mast cell infiltration in colorectal cancer tissue. J Pathol **189**(4): 487-495.
Nielsen JS, Sahota RA, Milne K, *et al.* (2012). CD20+ tumor-infiltrating lymphocytes have an atypical CD27- memory phenotype and together with CD8+ T cells promote favorable prognosis in ovarian cancer. Clin Cancer Res **18**(12): 3281-3292.
Nishikawa H &Sakaguchi S (2010). Regulatory T cells in tumor immunity. Int J Cancer **127**(4): 759-767.
Njauw CN, Kim I, Piris A, *et al.* (2012). Germline BAP1 inactivation is preferentially associated with metastatic ocular melanoma and cutaneous-ocular melanoma families. PLoS One **7**(4): e35295.
Nobusawa S, Watanabe T, Kleihues P, *et al.* (2009). IDH1 mutations as molecular signature and predictive factor of secondary glioblastomas. Clin Cancer Res **15**(19): 6002-6007.
Nonomura N, Takayama H, Nishimura K, *et al.* (2007). Decreased number of mast cells infiltrating into needle biopsy specimens leads to a better prognosis of prostate cancer. Br J Cancer **97**(7): 952-956.
Nordfors C, Grun N, Tertipis N, *et al.* (2013). CD8+ and CD4+ tumour infiltrating lymphocytes in relation to human papillomavirus status and clinical outcome in

tonsillar and base of tongue squamous cell carcinoma. Eur J Cancer **49**(11): 2522-2530.

Nozawa H, Chiu C &Hanahan D (2006). Infiltrating neutrophils mediate the initial angiogenic switch in a mouse model of multistage carcinogenesis. Proc Natl Acad Sci U S A **103**(33): 12493-12498.

O'Donnell RK, Mick R, Feldman M, *et al.* (2007). Distribution of dendritic cell subtypes in primary oral squamous cell carcinoma is inconsistent with a functional response. Cancer Lett **255**(1): 145-152.

Oda N, Shimazu K, Naoi Y, *et al.* (2012). Intratumoral regulatory T cells as an independent predictive factor for pathological complete response to neoadjuvant paclitaxel followed by 5-FU/epirubicin/cyclophosphamide in breast cancer patients. Breast Cancer Res Treat **136**(1): 107-116.

Ogino S, Nosho K, Irahara N, *et al.* (2009). Lymphocytic reaction to colorectal cancer is associated with longer survival, independent of lymph node count, microsatellite instability, and CpG island methylator phenotype. Clin Cancer Res **15**(20): 6412-6420.

Ohgaki H &Kleihues P (2009). Genetic alterations and signaling pathways in the evolution of gliomas. Cancer Sci **100**(12): 2235-2241.

Ohno S, Inagawa H, Dhar DK, *et al.* (2003). The degree of macrophage infiltration into the cancer cell nest is a significant predictor of survival in gastric cancer patients. Anticancer Res **23**(6D): 5015-5022.

Onken MD, Worley LA, Char DH, *et al.* (2012). Collaborative Ocular Oncology Group report number 1: prospective validation of a multi-gene prognostic assay in uveal melanoma. Ophthalmology **119**(8): 1596-1603.

Onken MD, Worley LA, Ehlers JP, *et al.* (2004). Gene expression profiling in uveal melanoma reveals two molecular classes and predicts metastatic death. Cancer Res **64**(20): 7205-7209.

Onken MD, Worley LA &Harbour JW (2008). A metastasis modifier locus on human chromosome 8p in uveal melanoma identified by integrative genomic analysis. Clin Cancer Res **14**(12): 3737-3745.

Onken MD, Worley LA, Long MD, *et al.* (2008). Oncogenic mutations in GNAQ occur early in uveal melanoma. Invest Ophthalmol Vis Sci **49**(12): 5230-5234.

Onken MD, Worley LA, Tuscan MD, *et al.* (2010). An accurate, clinically feasible multi-gene expression assay for predicting metastasis in uveal melanoma. J Mol Diagn **12**(4): 461-468.

Ono M, Tsuda H, Shimizu C, *et al.* (2012). Tumor-infiltrating lymphocytes are correlated with response to neoadjuvant chemotherapy in triple-negative breast cancer. Breast Cancer Res Treat **132**(3): 793-805.

Oshikiri T, Miyamoto M, Shichinohe T, *et al.* (2003). Prognostic value of intratumoral CD8+ T lymphocyte in extrahepatic bile duct carcinoma as essential immune response. J Surg Oncol **84**(4): 224-228.

Ossowski L &Aguirre-Ghiso JA (2010). Dormancy of metastatic melanoma. Pigment Cell Melanoma Res **23**(1): 41-56.

Ostrand-Rosenberg S (2008). Immune surveillance: a balance between protumor and antitumor immunity. Curr Opin Genet Dev **18**(1): 11-18.

Ostrom QT, Gittleman H, Farah P, *et al.* (2013). CBTRUS statistical report: Primary brain and central nervous system tumors diagnosed in the United States in 2006-2010. Neuro Oncol **15 Suppl 2**: ii1-56.

Otto W, Denzinger S, Wieland WF, *et al.* (2012). First analysis of immune cell infiltration in stage pT1 urothelial bladder carcinoma: CD3 positivity as a prognostic marker for cancer-specific survival. World J Urol **30**(6): 875-877.
Paez D, Labonte MJ, Bohanes P, *et al.* (2012). Cancer dormancy: a model of early dissemination and late cancer recurrence. Clin Cancer Res **18**(3): 645-653.
Pagès F, Galon J, Dieu-Nosjean MC, *et al.* (2009). Immune infiltration in human tumors: a prognostic factor that should not be ignored. Oncogene **29**(8): 1093-1102.
Pages F, Kirilovsky A, Mlecnik B, *et al.* (2009). In situ cytotoxic and memory T cells predict outcome in patients with early-stage colorectal cancer. J Clin Oncol **27**(35): 5944-5951.
Palanisamy N, Ateeq B, Kalyana-Sundaram S, *et al.* (2010). Rearrangements of the RAF kinase pathway in prostate cancer, gastric cancer and melanoma. Nat Med **16**(7): 793-798.
Palena C, Hamilton DH &Fernando RI (2012). Influence of IL-8 on the epithelial-mesenchymal transition and the tumor microenvironment. Future Oncol **8**(6): 713-722.
Palm T F-BD, Chapon F, Lacroix C, Gray F, Scaravilli F, Ellison DW, Salmon I, Vikkula M, Godfraind C (2009). Expression profiling of ependymomas unravels localization and tumor grade-specific tumorigenesis. Cancer **115**(17): 3955-3968.
Park MH, Lee JS &Yoon JH (2012). High expression of CX3CL1 by tumor cells correlates with a good prognosis and increased tumor-infiltrating CD8+ T cells, natural killer cells, and dendritic cells in breast carcinoma. J Surg Oncol **106**(4): 386-392.
Park TS, Donnenberg VS, Donnenberg AD, *et al.* (2014). Dynamic Interactions Between Cancer Stem Cells And Their Stromal Partners. Curr Pathobiol Rep **2**(1): 41-52.
Parrella P, Caballero OL, Sidransky D, *et al.* (2001). Detection of c-myc amplification in uveal melanoma by fluorescent in situ hybridization. Invest Ophthalmol Vis Sci **42**(8): 1679-1684.
Parrella P, Fazio VM, Gallo AP, *et al.* (2003). Fine mapping of chromosome 3 in uveal melanoma: identification of a minimal region of deletion on chromosomal arm 3p25.1-p25.2. Cancer Res **63**(23): 8507-8510.
Parsons DW, Jones S, Zhang X, *et al.* (2008). An integrated genomic analysis of human glioblastoma multiforme. Science **321**(5897): 1807-1812.
Patel M, Smyth E, Chapman PB, *et al.* (2011). Therapeutic implications of the emerging molecular biology of uveal melanoma. Clin Cancer Res **17**(8): 2087-2100.
Patel P &Chen EI (2012). Cancer stem cells, tumor dormancy, and metastasis. Front Endocrinol (Lausanne) **3**: 125.
Pe'er J, Stefani FH, Seregard S, *et al.* (2001). Cell proliferation activity in posterior uveal melanoma after Ru-106 brachytherapy: an EORTC ocular oncology group study. Br J Ophthalmol **85**(10): 1208-1212.
Peng RQ, Chen YB, Ding Y, *et al.* (2010). Expression of calreticulin is associated with infiltration of T-cells in stage IIIB colon cancer. World J Gastroenterol **16**(19): 2428-2434.
Peng RQ, Wu XJ, Ding Y, *et al.* (2010). Co-expression of nuclear and cytoplasmic HMGB1 is inversely associated with infiltration of CD45RO+ T cells and prognosis in patients with stage IIIB colon cancer. BMC Cancer **10**: 496.
Perrone G, Ruffini PA, Catalano V, *et al.* (2008). Intratumoural FOXP3-positive regulatory T cells are associated with adverse prognosis in radically resected gastric cancer. Eur J Cancer **44**(13): 1875-1882.

Petrausch U, Martus P, Tonnies H, *et al.* (2008). Significance of gene expression analysis in uveal melanoma in comparison to standard risk factors for risk assessment of subsequent metastases. Eye (Lond) **22**(8): 997-1007.

Phan LM, Yeung SC &Lee MH (2014). Cancer metabolic reprogramming: importance, main features, and potentials for precise targeted anti-cancer therapies. Cancer Biol Med **11**(1): 1-19.

Pilarski R, Cebulla CM, Massengill JB, *et al.* (2014). Expanding the clinical phenotype of hereditary BAP1 cancer predisposition syndrome, reporting three new cases. Genes Chromosomes Cancer **53**(2): 177-182.

Pina Y, Cebulla CM, Murray TG, *et al.* (2009). Blood vessel maturation in human uveal melanoma: spatial distribution of neovessels and mature vasculature. Ophthalmic Res **41**(3): 160-169.

Pinto R, De Summa S, Petriella D, *et al.* (2014). The value of new high-throughput technologies for diagnosis and prognosis in solid tumors. Cancer Biomark **14**(2): 103-117.

Piras F, Colombari R, Minerba L, *et al.* (2005). The predictive value of CD8, CD4, CD68, and human leukocyte antigen-D-related cells in the prognosis of cutaneous malignant melanoma with vertical growth phase. Cancer **104**(6): 1246-1254.

Polak ME, Borthwick NJ, Johnson P, *et al.* (2007). Presence and phenotype of dendritic cells in uveal melanoma. Br J Ophthalmol **91**(7): 971-976.

Porta C, Larghi P, Rimoldi M, *et al.* (2009). Cellular and molecular pathways linking inflammation and cancer. Immunobiology **214**(9-10): 761-777.

Prall F, Duhrkop T, Weirich V, *et al.* (2004). Prognostic role of CD8+ tumor-infiltrating lymphocytes in stage III colorectal cancer with and without microsatellite instability. Hum Pathol **35**(7): 808-816.

Pretscher D, Distel LV, Grabenbauer GG, *et al.* (2009). Distribution of immune cells in head and neck cancer: CD8+ T-cells and CD20+ B-cells in metastatic lymph nodes are associated with favourable outcome in patients with oro- and hypopharyngeal carcinoma. BMC Cancer **9**: 292.

Prosniak M, Harshyne LA, Andrews DW, *et al.* (2013). Glioma grade is associated with the accumulation and activity of cells bearing M2 monocyte markers. Clin Cancer Res **19**(14): 3776-3786.

Psaila B &Lyden D (2009). The metastatic niche: adapting the foreign soil. Nat Rev Cancer **9**(4): 285-293.

Pusch S, Sahm F, Meyer J, *et al.* (2011). Glioma IDH1 mutation patterns off the beaten track. Neuropathol Appl Neurobiol **37**(4): 428-430.

Qin L, Gong C, Chen AM, *et al.* (2014). Peroxisome proliferatoractivated receptor gamma agonist rosiglitazone inhibits migration and invasion of prostate cancer cells through inhibition of the CXCR4/CXCL12 axis. Mol Med Rep.

Radhakrishnan A, Badhrinarayanan N, Biswas J, *et al.* (2009). Analysis of chromosomal aberration (1, 3, and 8) and association of microRNAs in uveal melanoma. Mol Vis **15**: 2146-2154.

Ramnath N, Tan D, Li Q, *et al.* (2006). Is downregulation of MHC class I antigen expression in human non-small cell lung cancer associated with prolonged survival? Cancer Immunol Immunother **55**(8): 891-899.

Raspollini MR, Castiglione F, Rossi Degl'innocenti D, *et al.* (2005). Tumour-infiltrating gamma/delta T-lymphocytes are correlated with a brief disease-free interval in advanced ovarian serous carcinoma. Ann Oncol **16**(4): 590-596.

Rauser S, Langer R, Tschernitz S, *et al.* (2010). High number of CD45RO+ tumor infiltrating lymphocytes is an independent prognostic factor in non-metastasized (stage I-IIA) esophageal adenocarcinoma. BMC Cancer **10**: 608.

Rees RC &Mian S (1999). Selective MHC expression in tumours modulates adaptive and innate antitumour responses. Cancer Immunol Immunother **48**(7): 374-381.

Reichert TE, Scheuer C, Day R, *et al.* (2001). The number of intratumoral dendritic cells and zeta-chain expression in T cells as prognostic and survival biomarkers in patients with oral carcinoma. Cancer **91**(11): 2136-2147.

Remark R, Alifano M, Cremer I, *et al.* (2013). Characteristics and clinical impacts of the immune environments in colorectal and renal cell carcinoma lung metastases: influence of tumor origin. Clin Cancer Res.

Repp AC, Mayhew ES, Apte S, *et al.* (2000). Human uveal melanoma cells produce macrophage migration-inhibitory factor to prevent lysis by NK cells. J Immunol **165**(2): 710-715.

Ribatti D, Ennas MG, Vacca A, *et al.* (2003). Tumor vascularity and tryptase-positive mast cells correlate with a poor prognosis in melanoma. Eur J Clin Invest **33**(5): 420-425.

Rice T, Zheng S, Decker PA, *et al.* (2013). Inherited variant on chromosome 11q23 increases susceptibility to IDH-mutated but not IDH-normal gliomas regardless of grade or histology. Neuro Oncol **15**(5): 535-541.

Richtig E, Langmann G, Mullner K, *et al.* (2004). Ocular melanoma: epidemiology, clinical presentation and relationship with dysplastic nevi. Ophthalmologica **218**(2): 111-114.

Riether C, Schurch C &Ochsenbein AF (2013). From "magic bullets" to specific cancer immunotherapy. Swiss Med Wkly **143**: w13734.

Rimsza LM, Roberts RA, Miller TP, *et al.* (2004). Loss of MHC class II gene and protein expression in diffuse large B-cell lymphoma is related to decreased tumor immunosurveillance and poor patient survival regardless of other prognostic factors: a follow-up study from the Leukemia and Lymphoma Molecular Profiling Project. Blood **103**(11): 4251-4258.

Romeike B &Mawrin C (2008). Gliomatosis cerebri: growing evidence for diffuse gliomas with wide invasion. Expert Rev Neurother **8**(4): 587-597.

Rosenberg SA, Restifo NP, Yang JC, *et al.* (2008). Adoptive cell transfer: a clinical path to effective cancer immunotherapy. Nat Rev Cancer **8**(4): 299-308.

Rutledge WC, Kong J, Gao J, *et al.* (2013). Tumor-infiltrating lymphocytes in glioblastoma are associated with specific genomic alterations and related to transcriptional class. Clin Cancer Res **19**(18): 4951-4960.

Ryder M, Ghossein RA, Ricarte-Filho JC, *et al.* (2008). Increased density of tumor-associated macrophages is associated with decreased survival in advanced thyroid cancer. Endocr Relat Cancer **15**(4): 1069-1074.

Saeed AI, Sharov V, White J, *et al.* (2003). TM4: a free, open-source system for microarray data management and analysis. Biotechniques **34**(2): 374-378.

Salama P, Phillips M, Grieu F, *et al.* (2009). Tumor-infiltrating FOXP3+ T regulatory cells show strong prognostic significance in colorectal cancer. J Clin Oncol **27**(2): 186-192.

Salama P, Stewart C, Forrest C, *et al.* (2012). FOXP3+ cell density in lymphoid follicles from histologically normal mucosa is a strong prognostic factor in early stage colon cancer. Cancer Immunol Immunother **61**(8): 1183-1190.

Sanchez-Fernandez G, Cabezudo S, Garcia-Hoz C, *et al.* (2014). Galphaq signalling: The new and the old. Cell Signal **26**(5): 833-848.
Sandel MH, Dadabayev AR, Menon AG, *et al.* (2005). Prognostic value of tumor-infiltrating dendritic cells in colorectal cancer: role of maturation status and intratumoral localization. Clin Cancer Res **11**(7): 2576-2582.
Sanson M, Marie Y, Paris S, *et al.* (2009). Isocitrate dehydrogenase 1 codon 132 mutation is an important prognostic biomarker in gliomas. J Clin Oncol **27**(25): 4150-4154.
Saraiva VS, Caissie AL, Segal L, *et al.* (2005). Immunohistochemical expression of phospho-Akt in uveal melanoma. Melanoma Res **15**(4): 245-250.
Sasaki A, Tanaka F, Mimori K, *et al.* (2008). Prognostic value of tumor-infiltrating FOXP3+ regulatory T cells in patients with hepatocellular carcinoma. Eur J Surg Oncol **34**(2): 173-179.
Sasaki M, Knobbe CB, Itsumi M, *et al.* (2012). D-2-hydroxyglutarate produced by mutant IDH1 perturbs collagen maturation and basement membrane function. Genes Dev **26**(18): 2038-2049.
Sato E, Olson SH, Ahn J, *et al.* (2005). Intraepithelial CD8+ tumor-infiltrating lymphocytes and a high CD8+/regulatory T cell ratio are associated with favorable prognosis in ovarian cancer. Proc Natl Acad Sci U S A **102**(51): 18538-18543.
Sawanobori Y, Ueha S, Kurachi M, *et al.* (2008). Chemokine-mediated rapid turnover of myeloid-derived suppressor cells in tumor-bearing mice. Blood **111**(12): 5457-5466.
Schadendorf D, Kohlmus C, Gawlik C, *et al.* (1995). Mast cells in melanocytic tumours. Arch Dermatol Res **287**(5): 452-456.
Schatton T, Schutte U, Frank NY, *et al.* (2010). Modulation of T-cell activation by malignant melanoma initiating cells. Cancer Res **70**(2): 697-708.
Schmidt M, Bohm D, von Torne C, *et al.* (2008). The humoral immune system has a key prognostic impact in node-negative breast cancer. Cancer Res **68**(13): 5405-5413.
Schumacher K, Haensch W, Roefzaad C, *et al.* (2001). Prognostic significance of activated CD8(+) T cell infiltrations within esophageal carcinomas. Cancer Res **61**(10): 3932-3936.
Schwartzentruber DJ, Lawson DH, Richards JM, *et al.* (2011). gp100 peptide vaccine and interleukin-2 in patients with advanced melanoma. N Engl J Med **364**(22): 2119-2127.
Seddon JM, Gragoudas ES, Glynn RJ, *et al.* (1990). Host factors, UV radiation, and risk of uveal melanoma. A case-control study. Arch Ophthalmol **108**(9): 1274-1280.
Segal NH, Parsons DW, Peggs KS, *et al.* (2008). Epitope landscape in breast and colorectal cancer. Cancer Res **68**(3): 889-892.
Seiz M, Tuettenberg J, Meyer J, *et al.* (2010). Detection of IDH1 mutations in gliomatosis cerebri, but only in tumors with additional solid component: evidence for molecular subtypes. Acta Neuropathol **120**(2): 261-267.
Seltzer MJ, Bennett BD, Joshi AD, *et al.* (2010). Inhibition of glutaminase preferentially slows growth of glioma cells with mutant IDH1. Cancer Res **70**(22): 8981-8987.
Seo AN, Lee HJ, Kim EJ, *et al.* (2013). Tumour-infiltrating CD8+ lymphocytes as an independent predictive factor for pathological complete response to primary systemic therapy in breast cancer. Br J Cancer **109**(10): 2705-2713.
Shah W, Yan X, Jing L, *et al.* (2011). A reversed CD4/CD8 ratio of tumor-infiltrating lymphocytes and a high percentage of CD4(+)FOXP3(+) regulatory T cells are

significantly associated with clinical outcome in squamous cell carcinoma of the cervix. Cell Mol Immunol **8**(1): 59-66.

Shankaran V, Ikeda H, Bruce AT, *et al.* (2001). IFNgamma and lymphocytes prevent primary tumour development and shape tumour immunogenicity. Nature **410**(6832): 1107-1111.

Sharma D, Brummel-Ziedins KE, Bouchard BA, *et al.* (2014). Platelets in tumor progression: a host factor that offers multiple potential targets in the treatment of cancer. J Cell Physiol **229**(8): 1005-1015.

Sharma P, Shen Y, Wen S, *et al.* (2007). CD8 tumor-infiltrating lymphocytes are predictive of survival in muscle-invasive urothelial carcinoma. Proc Natl Acad Sci U S A **104**(10): 3967-3972.

Shechter R, London A &Schwartz M (2013). Orchestrated leukocyte recruitment to immune-privileged sites: absolute barriers versus educational gates. Nat Rev Immunol **13**(3): 206-218.

Shen SL, Liang LJ, Peng BG, *et al.* (2011). Foxp3+ regulatory T cells and the formation of portal vein tumour thrombus in patients with hepatocellular carcinoma. Can J Surg **54**(2): 89-94.

Shen Z, Zhou S, Wang Y, *et al.* (2010). Higher intratumoral infiltrated Foxp3+ Treg numbers and Foxp3+/CD8+ ratio are associated with adverse prognosis in resectable gastric cancer. J Cancer Res Clin Oncol **136**(10): 1585-1595.

Shields CL, Furuta M, Thangappan A, *et al.* (2009). Metastasis of uveal melanoma millimeter-by-millimeter in 8033 consecutive eyes. Arch Ophthalmol **127**(8): 989-998.

Shields CL, Kaliki S, Furuta M, *et al.* (2012). Clinical spectrum and prognosis of uveal melanoma based on age at presentation in 8,033 cases. Retina **32**(7): 1363-1372.

Shields CL, Kaliki S, Livesey M, *et al.* (2013). Association of ocular and oculodermal melanocytosis with the rate of uveal melanoma metastasis: analysis of 7872 consecutive eyes. JAMA Ophthalmol **131**(8): 993-1003.

Shields CL, Ramasubramanian A, Ganguly A, *et al.* (2011). Cytogenetic testing of iris melanoma using fine needle aspiration biopsy in 17 patients. Retina **31**(3): 574-580.

Shields CL, Shields JA, Gunduz K, *et al.* (2000). Conjunctival melanoma: risk factors for recurrence, exenteration, metastasis, and death in 150 consecutive patients. Arch Ophthalmol **118**(11): 1497-1507.

Shigeoka M, Urakawa N, Nakamura T, *et al.* (2013). Tumor associated macrophage expressing CD204 is associated with tumor aggressiveness of esophageal squamous cell carcinoma. Cancer Sci **104**(8): 1112-1119.

Shimura S, Yang G, Ebara S, *et al.* (2000). Reduced infiltration of tumor-associated macrophages in human prostate cancer: association with cancer progression. Cancer Res **60**(20): 5857-5861.

Siddiqui SA, Frigola X, Bonne-Annee S, *et al.* (2007). Tumor-infiltrating Foxp3-CD4+CD25+ T cells predict poor survival in renal cell carcinoma. Clin Cancer Res **13**(7): 2075-2081.

Simpson JA, Al-Attar A, Watson NF, *et al.* (2010). Intratumoral T cell infiltration, MHC class I and STAT1 as biomarkers of good prognosis in colorectal cancer. Gut **59**(7): 926-933.

Singh AD, De Potter P, Fijal BA, *et al.* (1998). Lifetime prevalence of uveal melanoma in white patients with oculo(dermal) melanocytosis. Ophthalmology **105**(1): 195-198.
Singh AD, Kalyani P &Topham A (2005). Estimating the risk of malignant transformation of a choroidal nevus. Ophthalmology **112**(10): 1784-1789.
Singh AD, Rennie IG, Seregard S, *et al.* (2004). Sunlight exposure and pathogenesis of uveal melanoma. Surv Ophthalmol **49**(4): 419-428.
Singh AD, Sisley K, Xu Y, *et al.* (2007). Reduced expression of autotaxin predicts survival in uveal melanoma. Br J Ophthalmol **91**(10): 1385-1392.
Singh AD &Topham A (2003). Survival rates with uveal melanoma in the United States: 1973-1997. Ophthalmology **110**(5): 962-965.
Singh AD, Turell ME &Topham AK (2011). Uveal melanoma: trends in incidence, treatment, and survival. Ophthalmology **118**(9): 1881-1885.
Sinicrope FA, Rego RL, Ansell SM, *et al.* (2009). Intraepithelial effector (CD3+)/regulatory (FoxP3+) T-cell ratio predicts a clinical outcome of human colon carcinoma. Gastroenterology **137**(4): 1270-1279.
Sisley K, Brand C, Parsons MA, *et al.* (1998). Cytogenetics of iris melanomas: disparity with other uveal tract melanomas. Cancer Genet Cytogenet **101**(2): 128-133.
Sisley K, Rennie IG, Parsons MA, *et al.* (1997). Abnormalities of chromosomes 3 and 8 in posterior uveal melanoma correlate with prognosis. Genes Chromosomes Cancer **19**(1): 22-28.
Sjodahl G, Lovgren K, Lauss M, *et al.* (2014). Infiltration of CD3 and CD68 cells in bladder cancer is subtype specific and affects the outcome of patients with muscle-invasive tumors. Urol Oncol.
Smith HA &Kang Y (2013). The metastasis-promoting roles of tumor-associated immune cells. J Mol Med (Berl) **91**(4): 411-429.
Sobin LH, Gospodarowicz MK &Wittekind C (2010). TNM classification of malignant tumours. Oxford, Wiley-Blackwell.
Sohn JH, Kaplan HJ, Suk HJ, *et al.* (2000). Chronic low level complement activation within the eye is controlled by intraocular complement regulatory proteins. Invest Ophthalmol Vis Sci **41**(11): 3492-3502.
Sosa MS, Bragado P, Debnath J, *et al.* (2013). Regulation of tumor cell dormancy by tissue microenvironments and autophagy. Adv Exp Med Biol **734**: 73-89.
Speicher MR, Prescher G, du Manoir S, *et al.* (1994). Chromosomal gains and losses in uveal melanomas detected by comparative genomic hybridization. Cancer Res **54**(14): 3817-3823.
Sperveslage J, Frank S, Heneweer C, *et al.* (2012). Lack of CCR7 expression is rate limiting for lymphatic spread of pancreatic ductal adenocarcinoma. Int J Cancer **131**(4): E371-381.
Spurrell EL &Lockley M (2014). Adaptive immunity in cancer immunology and therapeutics. Ecancermedicalscience **8**: 441.
Staibano S, Mascolo M, Tranfa F, *et al.* (2006). Tumor infiltrating lymphocytes in uveal melanoma: a link with clinical behavior? Int J Immunopathol Pharmacol **19**(1): 171-179.
Stark MS, Tyagi S, Nancarrow DJ, *et al.* (2010). Characterization of the Melanoma miRNAome by Deep Sequencing. PLoS One **5**(3): e9685.
Stewart TJ &Smyth MJ (2011). Improving cancer immunotherapy by targeting tumor-induced immune suppression. Cancer Metastasis Rev **30**(1): 125-140.

Steyerberg EW, Vickers AJ, Cook NR, *et al.* (2010). Assessing the performance of prediction models: a framework for traditional and novel measures. Epidemiology **21**(1): 128-138.
Storr SJ, Safuan S, Mitra A, *et al.* (2012). Objective assessment of blood and lymphatic vessel invasion and association with macrophage infiltration in cutaneous melanoma. Mod Pathol **25**(4): 493-504.
Straetemans T, van Brakel M, van Steenbergen S, *et al.* (2012). TCR gene transfer: MAGE-C2/HLA-A2 and MAGE-A3/HLA-DP4 epitopes as melanoma-specific immune targets. Clin Dev Immunol **2012**: 586314.
Stratton MR, Campbell PJ &Futreal PA (2009). The cancer genome. Nature **458**(7239): 719-724.
Streilein JW (2003). Ocular immune privilege: therapeutic opportunities from an experiment of nature. Nat Rev Immunol **3**(11): 879-889.
Stumpf M, Hasenburg A, Riener MO, *et al.* (2009). Intraepithelial CD8-positive T lymphocytes predict survival for patients with serous stage III ovarian carcinomas: relevance of clonal selection of T lymphocytes. Br J Cancer **101**(9): 1513-1521.
Sturm D, Witt H, Hovestadt V, *et al.* (2012). Hotspot mutations in H3F3A and IDH1 define distinct epigenetic and biological subgroups of glioblastoma. Cancer Cell **22**(4): 425-437.
Subramanian A, Tamayo P, Mootha VK, *et al.* (2005). Gene set enrichment analysis: a knowledge-based approach for interpreting genome-wide expression profiles. Proc Natl Acad Sci U S A **102**(43): 15545-15550.
Sudhakar A (2009). History of Cancer, Ancient and Modern Treatment Methods. J Cancer Sci Ther **1**(2): 1-4.
Sun S, Fei X, Mao Y, *et al.* (2014). PD-1(+) immune cell infiltration inversely correlates with survival of operable breast cancer patients. Cancer Immunol Immunother **63**(4): 395-406.
Sun Y &Liu J (2014). Potential of Cancer Cell-Derived Exosomes in Clinical Application: A Review of Recent Research Advances. Clin Ther.
Sun Y, Mao X, Fan C, *et al.* (2014). CXCL12-CXCR4 axis promotes the natural selection of breast cancer cell metastasis. Tumour Biol.
Swartling FJ, Hede SM &Weiss WA (2013). What underlies the diversity of brain tumors? Cancer Metastasis Rev **32**(1-2): 5-24.
Taillibert S, Chodkiewicz C, Laigle-Donadey F, *et al.* (2006). Gliomatosis cerebri: a review of 296 cases from the ANOCEF database and the literature. J Neurooncol **76**(2): 201-205.
Takanami I, Takeuchi K &Giga M (2001). The prognostic value of natural killer cell infiltration in resected pulmonary adenocarcinoma. J Thorac Cardiovasc Surg **121**(6): 1058-1063.
Takenaka M, Seki N, Toh U, *et al.* (2013). FOXP3 expression in tumor cells and tumor-infiltrating lymphocytes is associated with breast cancer prognosis. Mol Clin Oncol **1**(4): 625-632.
Tandon RSR (2011). Parsons' Diseases of the Eye, Elsevier India.
Tang X, Mo C, Wang Y, *et al.* (2013). Anti-tumour strategies aiming to target tumour-associated macrophages. Immunology **138**(2): 93-104.
Testa JR, Cheung M, Pei J, *et al.* (2011). Germline BAP1 mutations predispose to malignant mesothelioma. Nat Genet **43**(10): 1022-1025.

Thomas L (1982). On immunosurveillance in human cancer. Yale J Biol Med **55**(3-4): 329-333.

Thomas NE, Busam KJ, From L, *et al.* (2013). Tumor-Infiltrating Lymphocyte Grade in Primary Melanomas Is Independently Associated With Melanoma-Specific Survival in the Population-Based Genes, Environment and Melanoma Study. J Clin Oncol.

Tinge B, Molin D, Bergqvist M, *et al.* (2010). Mast cells in squamous cell esophageal carcinoma and clinical parameters. Cancer Genomics Proteomics **7**(1): 25-29.

Tomsova M, Melichar B, Sedlakova I, *et al.* (2008). Prognostic significance of CD3+ tumor-infiltrating lymphocytes in ovarian carcinoma. Gynecol Oncol **108**(2): 415-420.

Topalian SL, Weiner GJ &Pardoll DM (2011). Cancer immunotherapy comes of age. J Clin Oncol **29**(36): 4828-4836.

Torres-Cabala CA, Wang WL, Trent J, *et al.* (2009). Correlation between KIT expression and KIT mutation in melanoma: a study of 173 cases with emphasis on the acral-lentiginous/mucosal type. Mod Pathol **22**(11): 1446-1456.

Tosolini M, Kirilovsky A, Mlecnik B, *et al.* (2011). Clinical Impact of Different Classes of Infiltrating T Cytotoxic and Helper Cells (Th1, Th2, Treg, Th17) in Patients with Colorectal Cancer. Cancer Research **71**(4): 1263-1271.

Traversari C, van der Bruggen P, Luescher IF, *et al.* (1992). A nonapeptide encoded by human gene MAGE-1 is recognized on HLA-A1 by cytolytic T lymphocytes directed against tumor antigen MZ2-E. J Exp Med **176**(5): 1453-1457.

Treilleux I, Blay JY, Bendriss-Vermare N, *et al.* (2004). Dendritic cell infiltration and prognosis of early stage breast cancer. Clin Cancer Res **10**(22): 7466-7474.

Trellakis S, Bruderek K, Dumitru CA, *et al.* (2011). Polymorphonuclear granulocytes in human head and neck cancer: enhanced inflammatory activity, modulation by cancer cells and expansion in advanced disease. Int J Cancer **129**(9): 2183-2193.

Trolet J, Hupe P, Huon I, *et al.* (2009). Genomic profiling and identification of high-risk uveal melanoma by array CGH analysis of primary tumors and liver metastases. Invest Ophthalmol Vis Sci **50**(6): 2572-2580.

Tschentscher F, Husing J, Holter T, *et al.* (2003). Tumor classification based on gene expression profiling shows that uveal melanomas with and without monosomy 3 represent two distinct entities. Cancer Res **63**(10): 2578-2584.

Tschentscher F, Prescher G, Horsman DE, *et al.* (2001). Partial deletions of the long and short arm of chromosome 3 point to two tumor suppressor genes in uveal melanoma. Cancer Res **61**(8): 3439-3442.

Tsitsiou E &Lindsay MA (2009). microRNAs and the immune response. Curr Opin Pharmacol **9**(4): 514-520.

Tsuchikawa T, Ikeda H, Cho Y, *et al.* (2011). Association of CD8+ T cell infiltration in oesophageal carcinoma lesions with human leucocyte antigen (HLA) class I antigen expression and survival. Clin Exp Immunol **164**(1): 50-56.

Turcan S, Fabius AW, Borodovsky A, *et al.* (2013). Efficient induction of differentiation and growth inhibition in IDH1 mutant glioma cells by the DNMT Inhibitor Decitabine. Oncotarget **4**(10): 1729-1736.

Turjanski AG, Vaque JP &Gutkind JS (2007). MAP kinases and the control of nuclear events. Oncogene **26**(22): 3240-3253.

Tymoszuk P, Charoentong P, Hackl H, *et al.* (2014). High STAT1 mRNA levels but not its tyrosine phosphorylation are associated with macrophage infiltration and bad prognosis in breast cancer. BMC Cancer **14**: 257.

Uebelhoer M, Natynki M, Kangas J, *et al.* (2013). Venous malformation-causative TIE2 mutations mediate an AKT-dependent decrease in PDGFB. Hum Mol Genet **22**(17): 3438-3448.

Urteaga O &Pack GT (1966). On the antiquity of melanoma. Cancer **19**(5): 607-610.

Vajdic CM, Kricker A, Giblin M, *et al.* (2001). Eye color and cutaneous nevi predict risk of ocular melanoma in Australia. Int J Cancer **92**(6): 906-912.

Vajdic CM, Kricker A, Giblin M, *et al.* (2002). Sun exposure predicts risk of ocular melanoma in Australia. Int J Cancer **101**(2): 175-182.

van den Bent MJ, Dubbink HJ, Marie Y, *et al.* (2010). IDH1 and IDH2 mutations are prognostic but not predictive for outcome in anaplastic oligodendroglial tumors: a report of the European Organization for Research and Treatment of Cancer Brain Tumor Group. Clin Cancer Res **16**(5): 1597-1604.

van den Bosch T, Koopmans AE, Vaarwater J, *et al.* (2013). Chemokine receptor CCR7 expression predicts poor outcome in uveal melanoma and relates to liver metastasis whereas expression of CXCR4 is not of clinical relevance. Invest Ophthalmol Vis Sci **54**(12): 7354-7361.

van den Bosch T, van Beek JG, Vaarwater J, *et al.* (2012). Higher percentage of FISH-determined monosomy 3 and 8q amplification in uveal melanoma cells relate to poor patient prognosis. Invest Ophthalmol Vis Sci **53**(6): 2668-2674.

Van den Eynde B, Hainaut P, Herin M, *et al.* (1989). Presence on a human melanoma of multiple antigens recognized by autologous CTL. Int J Cancer **44**(4): 634-640.

Van den Eynde B, Peeters O, De Backer O, *et al.* (1995). A new family of genes coding for an antigen recognized by autologous cytolytic T lymphocytes on a human melanoma. J Exp Med **182**(3): 689-698.

van der Velden PA, Metzelaar-Blok JA, Bergman W, *et al.* (2001). Promoter hypermethylation: a common cause of reduced p16(INK4a) expression in uveal melanoma. Cancer Res **61**(13): 5303-5306.

van Gils W, Lodder EM, Mensink HW, *et al.* (2008). Gene expression profiling in uveal melanoma: two regions on 3p related to prognosis. Invest Ophthalmol Vis Sci **49**(10): 4254-4262.

van Houdt IS, Sluijter BJ, Moesbergen LM, *et al.* (2008). Favorable outcome in clinically stage II melanoma patients is associated with the presence of activated tumor infiltrating T-lymphocytes and preserved MHC class I antigen expression. Int J Cancer **123**(3): 609-615.

Van Raamsdonk CD, Bezrookove V, Green G, *et al.* (2009). Frequent somatic mutations of GNAQ in uveal melanoma and blue naevi. Nature **457**(7229): 599-602.

Van Raamsdonk CD, Griewank KG, Crosby MB, *et al.* (2010). Mutations in GNA11 in uveal melanoma. N Engl J Med **363**(23): 2191-2199.

Vanneman M &Dranoff G (2012). Combining immunotherapy and targeted therapies in cancer treatment. Nat Rev Cancer **12**(4): 237-251.

Vauleon E, Tony A, Hamlat A, *et al.* (2012). Immune genes are associated with human glioblastoma pathology and patient survival. BMC Med Genomics **5**: 41.

Ventii KH, Devi NS, Friedrich KL, *et al.* (2008). BRCA1-associated protein-1 is a tumor suppressor that requires deubiquitinating activity and nuclear localization. Cancer Res **68**(17): 6953-6962.

Verhaak RG, Hoadley KA, Purdom E, *et al.* (2010). Integrated genomic analysis identifies clinically relevant subtypes of glioblastoma characterized by abnormalities in PDGFRA, IDH1, EGFR, and NF1. Cancer Cell **17**(1): 98-110.

Vermeij R, de Bock GH, Leffers N, *et al.* (2011). Tumor-infiltrating cytotoxic T lymphocytes as independent prognostic factor in epithelial ovarian cancer with wilms tumor protein 1 overexpression. J Immunother **34**(6): 516-523.

Villegas FR, Coca S, Villarrubia VG, *et al.* (2002). Prognostic significance of tumor infiltrating natural killer cells subset CD57 in patients with squamous cell lung cancer. Lung Cancer **35**(1): 23-28.

Viola A, Sarukhan A, Bronte V, *et al.* (2012). The pros and cons of chemokines in tumor immunology. Trends Immunol **33**(10): 496-504.

Vitale M, Rezzani R, Rodella L, *et al.* (1998). HLA class I antigen and transporter associated with antigen processing (TAP1 and TAP2) down-regulation in high-grade primary breast carcinoma lesions. Cancer Res **58**(4): 737-742.

Voelter V, Diserens AC, Moulin A, *et al.* (2008). Infrequent promoter methylation of the MGMT gene in liver metastases from uveal melanoma. Int J Cancer **123**(5): 1215-1218.

von Deimling A, Korshunov A &Hartmann C (2011). The next generation of glioma biomarkers: MGMT methylation, BRAF fusions and IDH1 mutations. Brain Pathol **21**(1): 74-87.

Voskoboynik M &Arkenau HT (2014). Combination Therapies for the Treatment of Advanced Melanoma: A Review of Current Evidence. Biochem Res Int **2014**: 307059.

Wakatsuki K, Sho M, Yamato I, *et al.* (2013). Clinical impact of tumor-infiltrating CD45RO(+) memory T cells on human gastric cancer. Oncol Rep **29**(5): 1756-1762.

Wallander ML, Layfield LJ, Emerson LL, *et al.* (2011). KIT mutations in ocular melanoma: frequency and anatomic distribution. Mod Pathol **24**(8): 1031-1035.

Walrath JC, Hawes JJ, Van Dyke T, *et al.* (2010). Genetically engineered mouse models in cancer research. Adv Cancer Res **106**: 113-164.

Wang B, Xu D, Yu X, *et al.* (2011). Association of intra-tumoral infiltrating macrophages and regulatory T cells is an independent prognostic factor in gastric cancer after radical resection. Ann Surg Oncol **18**(9): 2585-2593.

Wang F, Jing X, Li G, *et al.* (2012). Foxp3+ regulatory T cells are associated with the natural history of chronic hepatitis B and poor prognosis of hepatocellular carcinoma. Liver Int **32**(4): 644-655.

Wang S, Sun M, Gu C, *et al.* (2014). Expression of CD163, interleukin-10, and interferon-gamma in oral squamous cell carcinoma: mutual relationships and prognostic implications. Eur J Oral Sci **122**(3): 202-209.

Wansom D, Light E, Thomas D, *et al.* (2012). Infiltrating lymphocytes and human papillomavirus-16--associated oropharyngeal cancer. Laryngoscope **122**(1): 121-127.

Ward PS, Cross JR, Lu C, *et al.* (2012). Identification of additional IDH mutations associated with oncometabolite R(-)-2-hydroxyglutarate production. Oncogene **31**(19): 2491-2498.

Ware ML, Hirose Y, Scheithauer BW, *et al.* (2007). Genetic aberrations in gliomatosis cerebri. Neurosurgery **60**(1): 150-158; discussion 158.

Watanabe Y, Katou F, Ohtani H, *et al.* (2010). Tumor-infiltrating lymphocytes, particularly the balance between CD8(+) T cells and CCR4(+) regulatory T cells, affect the survival of patients with oral squamous cell carcinoma. Oral Surg Oral Med Oral Pathol Oral Radiol Endod **109**(5): 744-752.

Webb JR, Milne K, Watson P, *et al.* (2014). Tumor-infiltrating lymphocytes expressing the tissue resident memory marker CD103 are associated with increased survival in high-grade serous ovarian cancer. Clin Cancer Res **20**(2): 434-444.

Weis E, Shah CP, Lajous M, *et al.* (2006). The association between host susceptibility factors and uveal melanoma: a meta-analysis. Arch Ophthalmol **124**(1): 54-60.

Weis SM &Cheresh DA (2011). Tumor angiogenesis: molecular pathways and therapeutic targets. Nat Med **17**(11): 1359-1370.

Weiss GR, Grosh WW, Chianese-Bullock KA, *et al.* (2011). Molecular insights on the peripheral and intratumoral effects of systemic high-dose rIL-2 (aldesleukin) administration for the treatment of metastatic melanoma. Clin Cancer Res **17**(23): 7440-7450.

Weller M, Felsberg J, Hartmann C, *et al.* (2009). Molecular predictors of progression-free and overall survival in patients with newly diagnosed glioblastoma: a prospective translational study of the German Glioma Network. J Clin Oncol **27**(34): 5743-5750.

Weller M, Wick W &von Deimling A (2011). Isocitrate dehydrogenase mutations: a challenge to traditional views on the genesis and malignant progression of gliomas. Glia **59**(8): 1200-1204.

Weller P, Bankfalvi A, Gu X, *et al.* (2014). The role of tumour FoxP3 as prognostic marker in different subtypes of head and neck cancer. Eur J Cancer **50**(7): 1291-1300.

Welsh TJ, Green RH, Richardson D, *et al.* (2005). Macrophage and mast-cell invasion of tumor cell islets confers a marked survival advantage in non-small-cell lung cancer. J Clin Oncol **23**(35): 8959-8967.

West NR, Kost SE, Martin SD, *et al.* (2013). Tumour-infiltrating FOXP3(+) lymphocytes are associated with cytotoxic immune responses and good clinical outcome in oestrogen receptor-negative breast cancer. Br J Cancer **108**(1): 155-162.

Wetterstrand K. "DNA Sequencing Costs: Data from the NHGRI Genome Sequencing Program (GSP) Available at: www.genome.gov/sequencingcosts. Accessed 23-05-2014." Retrieved 23-05-2014.

Whelchel JC, Farah SE, McLean IW, *et al.* (1993). Immunohistochemistry of infiltrating lymphocytes in uveal malignant melanoma. Invest Ophthalmol Vis Sci **34**(8): 2603-2606.

White AE &Harper JW (2012). Cancer. Emerging anatomy of the BAP1 tumor suppressor system. Science **337**(6101): 1463-1464.

White VA, Horsman DE &Rootman J (1995). Cytogenetic characterization of an iris melanoma. Cancer Genet Cytogenet **82**(1): 85-87.

White VA, McNeil BK &Horsman DE (1998). Acquired homozygosity (isodisomy) of chromosome 3 in uveal melanoma. Cancer Genet Cytogenet **102**(1): 40-45.

Wick W, Hartmann C, Engel C, *et al.* (2009). NOA-04 randomized phase III trial of sequential radiochemotherapy of anaplastic glioma with procarbazine, lomustine, and vincristine or temozolomide. J Clin Oncol **27**(35): 5874-5880.

Wiesner T, Obenauf AC, Murali R, *et al.* (2011). Germline mutations in BAP1 predispose to melanocytic tumors. Nat Genet **43**(10): 1018-1021.

Will CL &Luhrmann R (2011). Spliceosome structure and function. Cold Spring Harb Perspect Biol **3**(7).
Williams PL &Warwick R (1980). Gray's Anatomy. Edinburgh, Churchill Livingstone.
Winerdal ME, Marits P, Winerdal M, *et al.* (2011). FOXP3 and survival in urinary bladder cancer. BJU Int **108**(10): 1672-1678.
Worley LA, Long MD, Onken MD, *et al.* (2008). Micro-RNAs associated with metastasis in uveal melanoma identified by multiplexed microarray profiling. Melanoma Res **18**(3): 184-190.
Wu Y, Antony S, Meitzler JL, *et al.* (2014). Molecular mechanisms underlying chronic inflammation-associated cancers. Cancer Lett **345**(2): 164-173.
Wu Y, Kuang DM, Pan WD, *et al.* (2013). Monocyte/macrophage-elicited natural killer cell dysfunction in hepatocellular carcinoma is mediated by CD48/2B4 interactions. Hepatology **57**(3): 1107-1116.
Xiao B, Guo J, Miao Y, *et al.* (2009). Detection of miR-106a in gastric carcinoma and its clinical significance. Clin Chim Acta **400**(1-2): 97-102.
Xu L, Zhu Y, Chen L, *et al.* (2014). Prognostic Value of Diametrically Polarized Tumor-Associated Macrophages in Renal Cell Carcinoma. Ann Surg Oncol.
Xu W, Liu H, Song J, *et al.* (2013). The appearance of Tregs in cancer nest is a promising independent risk factor in colon cancer. J Cancer Res Clin Oncol **139**(11): 1845-1852.
Xu W, Yang H, Liu Y, *et al.* (2011). Oncometabolite 2-hydroxyglutarate is a competitive inhibitor of alpha-ketoglutarate-dependent dioxygenases. Cancer Cell **19**(1): 17-30.
Yamagami W, Susumu N, Tanaka H, *et al.* (2011). Immunofluorescence-detected infiltration of CD4+FOXP3+ regulatory T cells is relevant to the prognosis of patients with endometrial cancer. Int J Gynecol Cancer **21**(9): 1628-1634.
Yan D, Dong XD, Chen X, *et al.* (2012). Role of microRNA-182 in posterior uveal melanoma: regulation of tumor development through MITF, BCL2 and cyclin D2. PLoS One **7**(7): e40967.
Yan M, Jene N, Byrne D, *et al.* (2011). Recruitment of regulatory T cells is correlated with hypoxia-induced CXCR4 expression, and is associated with poor prognosis in basal-like breast cancers. Breast Cancer Res **13**(2): R47.
Yang C, Lee H, Jove V, *et al.* (2013). Prognostic significance of B-cells and pSTAT3 in patients with ovarian cancer. PLoS One **8**(1): e54029.
Yang C &Wei W (2011). The miRNA expression profile of the uveal melanoma. Sci China Life Sci **54**(4): 351-358.
Yang W, Chen PW, Li H, *et al.* (2008). PD-L1: PD-1 interaction contributes to the functional suppression of T-cell responses to human uveal melanoma cells in vitro. Invest Ophthalmol Vis Sci **49**(6): 2518-2525.
Ye M, Hu D, Tu L, *et al.* (2008). Involvement of PI3K/Akt signaling pathway in hepatocyte growth factor-induced migration of uveal melanoma cells. Invest Ophthalmol Vis Sci **49**(2): 497-504.
Ye XZ, Xu SL, Xin YH, *et al.* (2012). Tumor-associated microglia/macrophages enhance the invasion of glioma stem-like cells via TGF-beta1 signaling pathway. J Immunol **189**(1): 444-453.
Yoon HH, Orrock JM, Foster NR, *et al.* (2012). Prognostic impact of FoxP3+ regulatory T cells in relation to CD8+ T lymphocyte density in human colon carcinomas. PLoS One **7**(8): e42274.

Yoshida K, Sanada M &Ogawa S (2013). Deep sequencing in cancer research. Jpn J Clin Oncol **43**(2): 110-115.
Yoshioka T, Miyamoto M, Cho Y, *et al.* (2008). Infiltrating regulatory T cell numbers is not a factor to predict patient's survival in oesophageal squamous cell carcinoma. Br J Cancer **98**(7): 1258-1263.
Yu CJ, Chang KP, Chang YJ, *et al.* (2011). Identification of guanylate-binding protein 1 as a potential oral cancer marker involved in cell invasion using omics-based analysis. J Proteome Res **10**(8): 3778-3788.
Yu HM, Yang JL, Jiao SC, *et al.* (2014). TGF-beta1 precursor and CD8 are potential prognostic and predictive markers in operated breast cancer. J Huazhong Univ Sci Technolog Med Sci **34**(1): 51-58.
Yu P &Fu YX (2006). Tumor-infiltrating T lymphocytes: friends or foes? Lab Invest **86**(3): 231-245.
Zack TI, Schumacher SE, Carter SL, *et al.* (2013). Pan-cancer patterns of somatic copy number alteration. Nat Genet **45**(10): 1134-1140.
Zeschnigk M, Tschentscher F, Lich C, *et al.* (2003). Methylation analysis of several tumour suppressor genes shows a low frequency of methylation of CDKN2A and RARB in uveal melanomas. Comp Funct Genomics **4**(3): 329-336.
Zhan HL, Gao X, Zhou XF, *et al.* (2012). Presence of tumour-infiltrating FOXP3+ lymphocytes correlates with immature tumour angiogenesis in renal cell carcinomas. Asian Pac J Cancer Prev **13**(3): 867-872.
Zhang CB, Bao ZS, Wang HJ, *et al.* (2014). Correlation of IDH1/2 mutation with clinicopathologic factors and prognosis in anaplastic gliomas: a report of 203 patients from China. J Cancer Res Clin Oncol **140**(1): 45-51.
Zhang G, Liu WL, Zhang L, *et al.* (2011). Involvement of indoleamine 2,3-dioxygenase in impairing tumor-infiltrating CD8 T-cell functions in esophageal squamous cell carcinoma. Clin Dev Immunol **2011**: 384726.
Zhang JF, Hua R, Liu DJ, *et al.* (2014). Effect of CD74 on the prognosis of patients with resectable pancreatic cancer. Hepatobiliary Pancreat Dis Int **13**(1): 81-86.
Zhang M, He Y, Sun X, *et al.* (2014). A high M1/M2 ratio of tumor-associated macrophages is associated with extended survival in ovarian cancer patients. J Ovarian Res **7**(1): 19.
Zhang QW, Liu L, Gong CY, *et al.* (2012). Prognostic significance of tumor-associated macrophages in solid tumor: a meta-analysis of the literature. PLoS One **7**(12): e50946.
Zhang W, Zhu XD, Sun HC, *et al.* (2010). Depletion of tumor-associated macrophages enhances the effect of sorafenib in metastatic liver cancer models by antimetastatic and antiangiogenic effects. Clin Cancer Res **16**(13): 3420-3430.
Zhang Y, Huang Y &Qin M (2013). Tumour-infiltrating FoxP3+ and IL-17-producing T cells affect the progression and prognosis of gallbladder carcinoma after surgery. Scand J Immunol **78**(6): 516-522.
Zhang Y, Ren H, Wang L, *et al.* (2014). Clinical impact of tumor-infiltrating inflammatory cells in primary small cell esophageal carcinoma. Int J Mol Sci **15**(6): 9718-9734.
Zhang Y, Yang Y, Chen L, *et al.* (2014). Expression analysis of genes and pathways associated with liver metastases of the uveal melanoma. BMC Med Genet **15**: 29.
Zhang YL, Li J, Mo HY, *et al.* (2010). Different subsets of tumor infiltrating lymphocytes correlate with NPC progression in different ways. Mol Cancer **9**: 4.

Zhou J, Ding T, Pan W, *et al.* (2009). Increased intratumoral regulatory T cells are related to intratumoral macrophages and poor prognosis in hepatocellular carcinoma patients. Int J Cancer **125**(7): 1640-1648.

Zhou S, Shen Z, Wang Y, *et al.* (2013). CCR7 expression and intratumoral FOXP3+ regulatory T cells are correlated with overall survival and lymph node metastasis in gastric cancer. PLoS One **8**(9): e74430.

Zhu W, Guo L, Zhang B, *et al.* (2014). Combination of osteopontin with peritumoral infiltrating macrophages is associated with poor prognosis of early-stage hepatocellular carcinoma after curative resection. Ann Surg Oncol **21**(4): 1304-1313.

Zhu XD, Zhang JB, Zhuang PY, *et al.* (2008). High expression of macrophage colony-stimulating factor in peritumoral liver tissue is associated with poor survival after curative resection of hepatocellular carcinoma. J Clin Oncol **26**(16): 2707-2716.

Zigler M, Shir A &Levitzki A (2013). Targeted cancer immunotherapy. Curr Opin Pharmacol **13**(4): 504-510.

Zingg U, Montani M, Frey DM, *et al.* (2010). Tumour-infiltrating lymphocytes and survival in patients with adenocarcinoma of the oesophagus. Eur J Surg Oncol **36**(7): 670-677.

Zlobec I, Lugli A, Baker K, *et al.* (2007). Role of APAF-1, E-cadherin and peritumoral lymphocytic infiltration in tumour budding in colorectal cancer. J Pathol **212**(3): 260-268.

Zlotnik A, Burkhardt AM &Homey B (2011). Homeostatic chemokine receptors and organ-specific metastasis. Nat Rev Immunol **11**(9): 597-606.

Zuidervaart W, van der Velden PA, Hurks MH, *et al.* (2003). Gene expression profiling identifies tumour markers potentially playing a role in uveal melanoma development. Br J Cancer **89**(10): 1914-1919.